



Universiteit
Leiden
The Netherlands

Discovery of reversible monoacylglycerol lipase inhibitors

Jiang, M.

Citation

Jiang, M. (2022, March 17). *Discovery of reversible monoacylglycerol lipase inhibitors*. Retrieved from <https://hdl.handle.net/1887/3279133>

Version: Publisher's Version

License: [Licence agreement concerning inclusion of doctoral thesis in the Institutional Repository of the University of Leiden](#)

Downloaded from: <https://hdl.handle.net/1887/3279133>

Note: To cite this publication please use the final published version (if applicable).

Discovery of Reversible Monoacylglycerol Lipase Inhibitors

PROEFSCHRIFT

ter verkrijging van

de graad van doctor aan de Universiteit Leiden,

op gezag van rector magnificus prof.dr.ir. H. Bijl,

volgens besluit van het college voor promoties

te verdedigen op donderdag 17 maart 2022

klokke 15:00 uur

door

Ming Jiang

geboren te Nanchang, China in 1990

Promotiecommissie

Promotor: Prof. Dr. M. van der Stelt

Prof. Dr. C.A.A. van Boeckel

Co-promotor: Dr. R.J.B.H.N. van den Berg

Overige leden Prof.dr. H.S. Overkleeft

Prof.dr. N.I. Martin

Prof.dr. L.H. Heitman

Prof.dr. G.J.P. van Westen

Dr. M.P. Baggelaar

(Universiteit Utrecht)

Prof.dr. R.F. Witkamp

(Wageningen University and Research)

Cover design: Ming Jiang

Printed by: PrintSupport4U

A single spark can start a prairie fire

星星之火，可以燎原

Mao Zedong

Table of Contents

Chapter 1

General Introduction7

Chapter 2

Hit Optimization of β -Sulfinyl Esters as Highly Potent
and Selective MAGL Inhibitors.....25

Chapter 3

Development of α -Aryl Ketones as Monoacylglycerol
Lipase Inhibitors107

Chapter 4

Discovery of LEI-515 as a Novel Ultrapotent, Reversible
MAGL Inhibitor with Improved Metabolic Stability129

Chapter 5

LEI-515 is an Orally Available and Peripherally
Restricted MAGL Inhibitor.....163

Chapter 6

Summary and future prospects195

List of publications205

中文总结.....207

Curriculum Vitae.....210

Chapter 1

General Introduction

1.1 The endocannabinoid system

The endocannabinoid system (ECS), well known as the target of Δ^9 -tetrahydrocannabinol (THC), the psychoactive component of marijuana, is a signaling network that modulates a diverse range of physiological processes including nociception, behavior, cognitive function, appetite, metabolism, motor control, memory formation, and inflammation.¹⁻³ There are two main endocannabinoids, 2-arachidonoylglycerol (2-AG) and *N*-arachidonylethanolamine (anandamide), which act through membrane-bound G-coupled protein receptors (mainly CB₁ and CB₂) to alter these varied aspects of mammalian physiology.^{4, 5} As shown in figure 1, the endogenous signaling lipid 2-AG is synthesized by diacylglycerol lipases (DAGL α and DAGL β) which catalyze the *sn*-1-specific hydrolysis of diacylglycerol (DAG)^{6, 7}, while anandamide is synthesized by initial generation of *N*-arachidonoyl phosphatidylethanolamine followed by several postulated routes, such as *N*-acylphosphatidylethanolaminephospholipase D (NAPE-PLD) or α/β -hydrolase 4 (ABHD4)⁸ mediated pathways. The main degradation enzyme for 2-AG is

monoacylglycerol lipase (MAGL), which hydrolyzes around 85% of 2-AG in the brain to give arachidonic acid (AA) and glycerol.⁹ Together with ABHD6 and ABHD12, those enzymes response for 98% of the 2-AG hydrolysis. The key enzyme for the hydrolysis of anandamide is fatty acid amide hydrolase (FAAH).¹⁰

Initial drug development targeting the ECS led to several marketed drugs, such as Marinol[®] (Δ^9 -tetrahydrocannabinol, THC), Epidiolex[®] (cannabidiol, CBD) and Cesamet[®] (Nabilone). These cannabinoid-based drugs directly activate cannabinoid receptors and, however, can also produce central side effects. Rimonabant[®], a non-cannabinoid-based inverse agonist for CB₁ receptor which was marketed as anorectic anti-obesity drug, was withdrawn from the market due to psychological side effects.¹¹ Increasing the levels of endocannabinoids 2-AG or anandamide through inhibiting the metabolic enzymes MAGL or FAAH provides an alternative way to activate CB receptors. To date, several selective MAGL and FAAH inhibitors have entered clinical trials, however, none reached the market yet.¹²⁻¹⁵

1.2 Monoacylglycerol lipase (MAGL)

Monoacylglycerol lipase (MAGL or MGLL) is a serine hydrolase that catalyzes the hydrolysis of saturated or unsaturated monoacylglycerides to give free fatty acid and glycerol.^{16, 17} It was initially discovered in the intestine and adipose tissue of rats.^{18, 19} Later on, it was found to be the principal degradative enzyme for the endocannabinoid 2-AG in the brain.²⁰ The endogenous signaling lipid 2-AG is a full agonist for the cannabinoid receptors CB₁ and CB₂, which are the main receptors through which 2-AG exerts its physiological effects.^{5, 21, 22} Besides this, 2-AG is also an important intermediate in lipid metabolism. Degradation of 2-AG leads to a major release of arachidonic acid (AA), which is the precursor of pro-inflammatory prostaglandins in the brain, liver and lung.²³ Therefore, MAGL is recognized as a critical player for regulating both the endocannabinoid and eicosanoid signaling pathways.

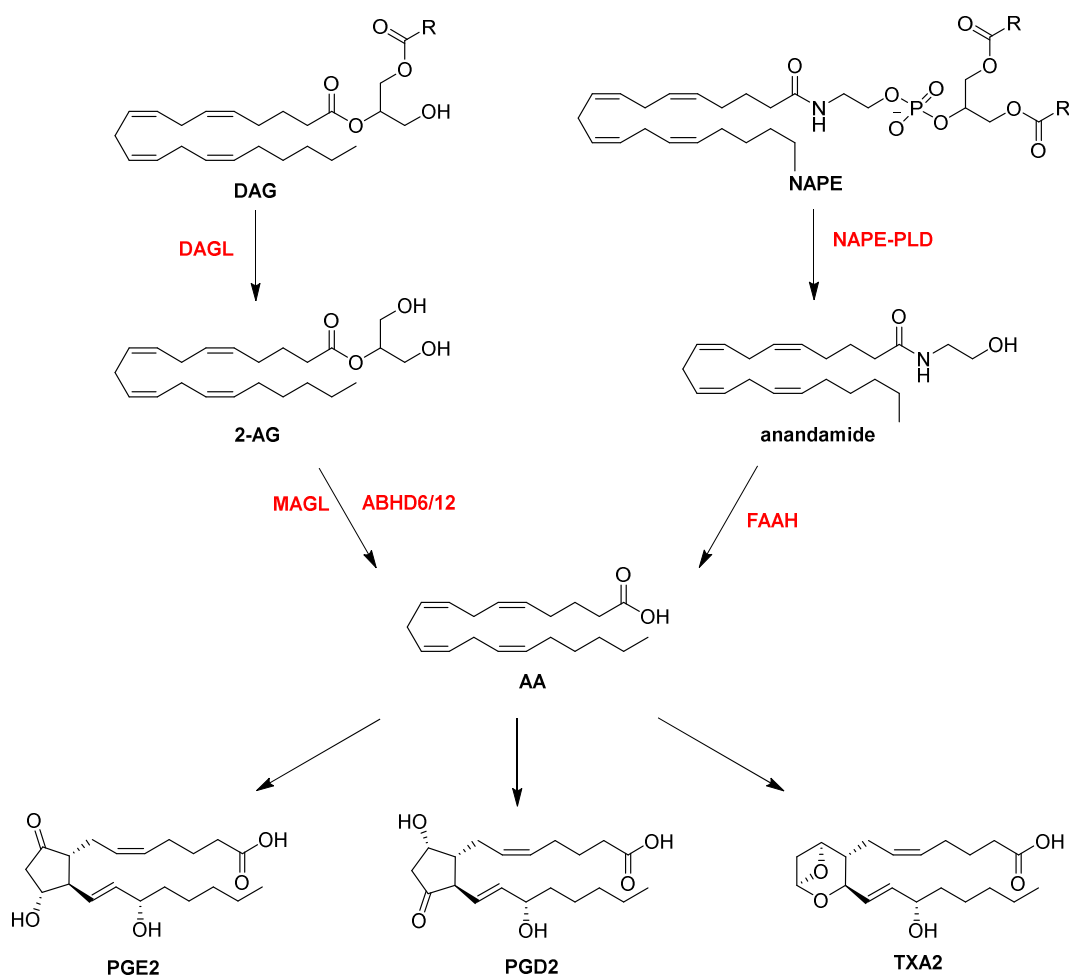


Figure 1. Biosynthesis and degradation of endocannabinoids 2-AG and anandamide. DAG: diacylglycerol; NAPE: N-acylphosphatidylethanolamine; 2-AG: 2-arachidonoylglycerol; AA: arachidonic acid; PGE2: prostaglandin E2; PGD2: prostaglandin D2; TXA2: thromboxane A2; DAGL: diacylglycerol lipases; NAPE-PLD: N-acylphosphatidylethanolaminephospholipase D; MAGL: monoacylglycerol lipase; ABHD6/12: α/β -hydrolase-domain containing protein 6/12; FAAH: fatty acid amide hydrolase.

MAGL is a membrane-associated enzyme which exists in two splicing forms with molecular weight of 33 and 35 kDa.²⁴ Several MAGL crystal structures have been reported and it has been described as a dimer.^{14, 25-27} The catalytic triad of MAGL is formed by a Ser-Asp-His commonly found in the serine hydrolase family, which in the human ortholog is constituted by Ser122, Asp239 and His269.²⁸ The His activates Ser122, which functions as a nucleophile to attack the carbonyl of the substrate. Besides the catalytic triad, the substrate binding site comprises a large hydrophobic tunnel (ACB pocket) in which the acyl chain binds and cytoplasmic access channel (CA channel), which functions as the exit channel for the hydrophilic glyceryl moiety.¹⁴

The MAGL catalytic mechanism consists of two different phases: the hydrolysis of the substrate and the reactivation of the enzyme (Figure 2).²⁹ First, the substrate binds into the active site of MAGL and the carbonyl of the substrate is anchored to the proper position by forming two hydrogen bonds with MAGL (Michaelis-Menten Complex). Next, the carbonyl of the ester is attacked by the catalytic serine residue of MAGL, which results in a tetrahedral transition state with an anion. Next, the glycerol will be released and a covalent acyl-enzyme adduct (ester) is formed. Finally, the enzyme will be reactivated by hydrolysis of the ester by an activated water molecule. AA will be released and free MAGL.

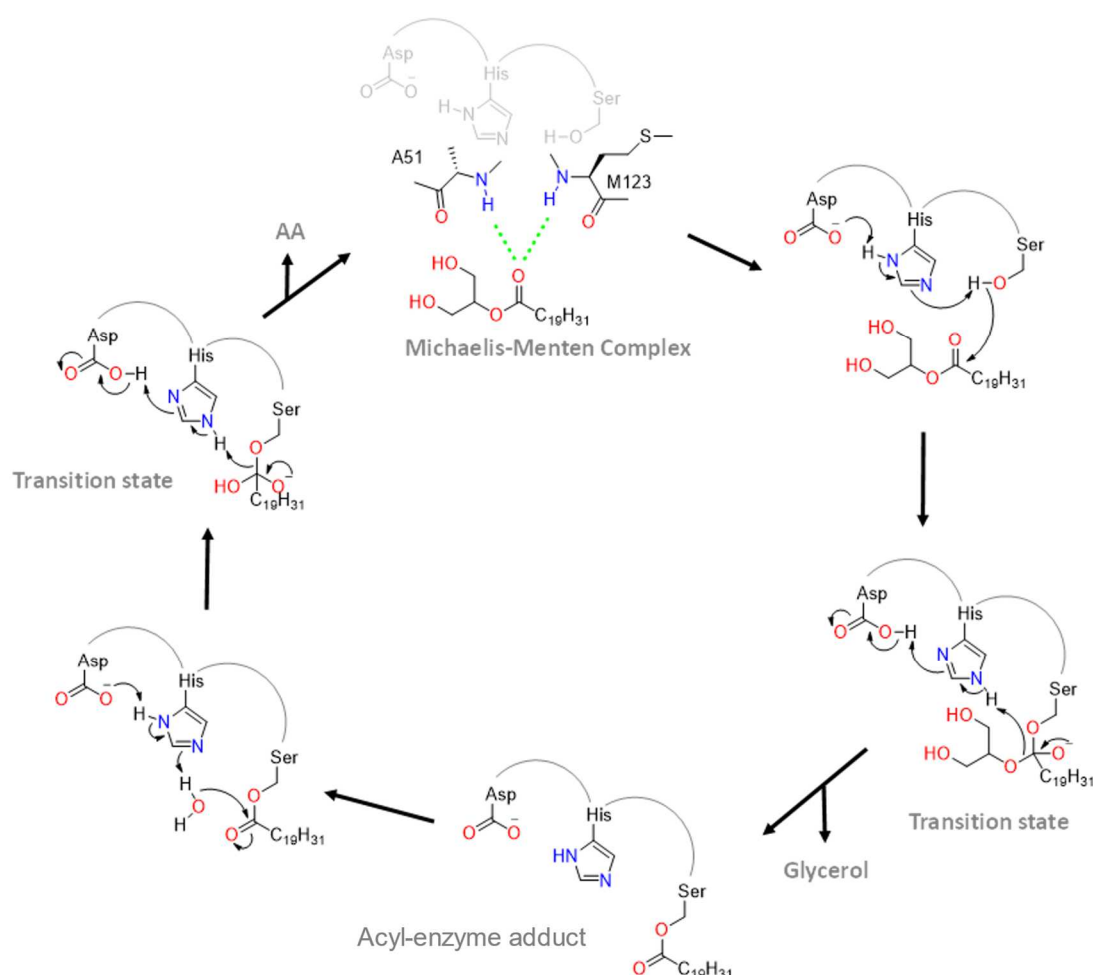


Figure 2. Catalytic mechanism of MAGL-mediated hydrolysis of 2-AG.

1.3 Therapeutic applications of MAGL inhibition

MAGL is considered as a promising drug target for a number of diseases due to its important roles in regulating both endocannabinoid and eicosanoid signaling pathways.

Acute MAGL inhibition with the selective inhibitor JZL184 (**1**, Figure 3) has been shown to exhibit a wide range of beneficial effects in various animal models of pain, inflammation, emesis, anxiety, opiate-induced withdrawal symptoms, colitis, neurodegeneration, inflammation-induced lung and liver injury, and cancer pathogenicity.³⁰⁻³⁴

1.3.1 Pain

Cannabinoids have analgesic effects due to their activation of the CB1 receptor. MAGL inhibition indirectly activates the CB1 receptor by increasing 2-AG levels. Not surprisingly, MAGL inhibition elicits also CB1-dependent antinociceptive effects in various mouse models of pain, including noxious chemical, inflammatory, thermal, and neuropathic pain.³⁵⁻³⁷ Of note, MAGL inhibition by covalent irreversible inhibitors desensitized the CB1 receptor, which may lead to a loss of analgesia upon chronic administration.^{38, 39} Using a lower dose of an irreversible inhibitor or a reversible inhibitor may prevent the induction of tolerance. Alternatively, administration of MAGL inhibitor JZL184 in combination with diclofenac (a cyclooxygenase inhibitor) has shown to reduce neuropathic pain with minimal adverse effects.⁴⁰

1.3.2 Neuroinflammation and neurodegenerative diseases

During neuroinflammation, activated microglia and astrocytes produce proinflammatory cytokines and chemokines, and the blood–brain barrier is deteriorated. Persistent neuroinflammation can result in neuronal death and ultimately contribute to neurodegeneration.⁴¹ MAGL inhibition has been shown to have beneficial effects in multiple neuroinflammatory processes. It was shown that MAGL hydrolysis of 2-AG provides the major pool of AA for the generation of neuroinflammatory eicosanoids in the brain. Pharmacological inhibition or genetic ablation of MAGL activity decreased lipopolysaccharide (LPS)-induced pro-inflammatory eicosanoid production, such as prostaglandin E₂ (PGE₂), PGD₂, PGF₂ and thromboxane B₂ (TXB₂), through CB receptor-independent mechanism.³¹ Abolishment of MAGL activity also provided neuroprotective effects against 1-methyl-4-phenyl-1,2,3,6-tetrahydropyridine (MPTP)-

induced dopaminergic neurodegeneration, a model of Parkinson's disease. MAGL inhibition reduced dopamine loss and lowered pro-inflammatory eicosanoids and suppressing neuroinflammation.⁴² In addition, inactivation of MAGL suppresses proinflammatory response and reduces production and accumulation of β -amyloid ($A\beta$) and improves cognitive function in the in a PS1/APP⁺ mouse model and 5XFAD mouse models of Alzheimer's disease.^{33, 43}

1.3.3 Inflammatory tissue injury

Several studies have revealed that MAGL inhibition may have therapeutic effects in peripheral inflammatory tissue injury. MAGL inactivation lowered hepatic inflammation caused by ischemia-reperfusion (I/R) injury through reducing neutrophil infiltration, inflammatory cytokines, and reactive oxygen stress, and this hepatoprotective effect appeared to be due to a combination of enhanced CB2 signaling and lower eicosanoid levels. MAGL inhibition was also protective in the carbon tetrachloride and galactosamine/LPS models of liver injury in mice.⁴⁴ In addition, protective effects were also observed in LPS-induced acute lung injury model where MAGL inhibition reduced leukocyte migration into the lungs, vascular permeability, and inflammatory cytokine and chemokine levels in bronchoalveolar lavage fluid.³⁴

1.4 Drug discovery of MAGL inhibitors

1.4.1 ABX-1431

Drug discovery for disorders of the central nervous system (CNS) is hard. Several factors contribute to the daunting task to discover novel therapies for brain diseases. First and foremost, there is a lack of validated therapeutic targets largely because of our limited understanding of the function of the brain in health and disease. Once a potential suitable target has been identified, the optimization of small molecules into drug candidates is complicated by the strict physicochemical properties required to pass the blood–brain barrier and to minimize efflux by membrane transporters. Furthermore, the determination of the target-interaction landscape (i.e., its selectivity profile) of the drug

in human brain is essential to avoid disasters as recently witnessed with fatal phase 1 clinical trial of BIA 10-2474. A volunteer died due to an overdose of BIA 10-2474. Thus, studies enabling target and off-target engagement in the brain are essential to guide drug discovery and development.⁴⁵⁻⁴⁸

Several academic groups and pharmaceutical companies have developed MAGL inhibitors that have a reversible or irreversible mode-of-action.⁴⁹⁻⁵¹ Irreversible inhibitors that covalently interact with the catalytic serine (Ser122) of MAGL, may achieve higher potency and sustained inactivation of the enzyme, thereby putting less demand on the pharmacokinetic properties. Determination of the selectivity profile of mechanism-based covalent inhibitors is, however, essential because other proteins from the same enzyme family of the primary target may also react with the warhead of the experimental drug in the same fashion. This could lead to unwanted side effects or toxicity. Thus, assessment of the interaction profile of the covalent inhibitor in human cells and brain is important.

ABX-1431 (**3**, Figure 3) is an irreversible MAGL inhibitor and was initially discovered by Abide Therapeutics which was acquired by Lundbeck B.V.. During the drug discovery process, activity-based protein profiling (ABPP) was utilized as the central technology for the discovery, optimization, and profiling of drug candidates. Competitive ABPP is an efficient chemical biology approach to study target engagement and interaction-landscape of covalent irreversible inhibitors in living systems.^{47, 48} It makes use of broad-spectrum chemical probes that report on the abundance of active enzymes in lysates, (human) cells, or even intact animals. The interaction of a small molecule with endogenously expressed enzymes, including all post-translational modifications, protein–protein interactions in the presence of endogenous substrates, can be assessed in one single experiment. ABPP makes use of activity-based probes consisting of warhead, recognition element, and reporter group. A fluorescent reporter group is used for gel-based ABPP, whereas a biotin reporter allows mass spectrometry (MS)-based identification of the interacting proteins.

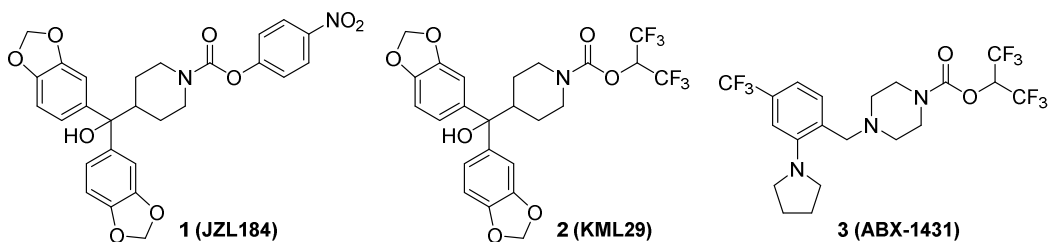


Figure 3. Chemical structure of MAGL inhibitors JZL184, KML29 and ABX-1431.

Cisar et al. used the prototypical fluorophosphonate (FP)-based probes to assess the interaction of their MAGL inhibitors on the serine hydrolase family.¹³ JZL184 and KML29 (**1** and **2**, Figure 3) were used as a starting point for the rational design of novel MAGL inhibitors. Careful optimization of the activity and selectivity using gel-based ABPP with multiple human proteomes and rodent brain homogenates led to the discovery of ABX-1431, which was selected as the lead compound for clinical evaluation. ABX-1431 is a potent human MAGL inhibitor with an average IC_{50} of 14 nM that only cross-reacts to a minor extent with ABHD6, PLA2G7, and some carboxyl esterases. The compound maintained activity and selectivity in human cellular assays and in human prefrontal cortex proteomes was determined by MS-based ABPP. ABX-1431 is a lipophilic molecule and has a basic amine, yet it has only weak hERG channel activity with an IC_{20} of 7 μ M. The compound did not display any significant activity against a panel of common off-targets and has low propensity to CYP-inhibition. ABX-1431 demonstrated acceptable pharmacokinetics in rodents and dogs. It inhibited MAGL activity with an ED_{50} of 0.5–1.4 mg/kg (po) and dose dependently increased brain 2-AG levels in mouse brain. A rat inflammatory pain model was used to assess the pharmacodynamics effect. ABX-1431 demonstrated potent antinociceptive effects in a formalin paw test at a dose that produced near complete MAGL inhibition and maximal elevation of 2-AG. Other pharmacological effects were not (yet) described. Currently, ABX-1431 is being tested in different clinical trials (www.clinicaltrials.gov). Notably, it has successfully completed phase 1 clinical trials. The compound was generally well-tolerated and safe. The most commonly observed adverse effects were headache, somnolence, and fatigue. It inhibited MAGL in the brain in a dose-dependent manner as demonstrated with a PET study. Importantly, in a randomized, double-blind,

placebo-controlled crossover, exploratory phase 1b study, ABX-1431 was able to show a positive impact on key measures of symptoms in adult patients with the syndrome of Gilles de la Tourette. It has now entered another phase 1b clinical trial for posttraumatic stress disorder (NCT04597450). The compound will also be tested in neuromyelitis optica, multiple sclerosis and as an add-on therapy in patients suffering from central neuropathic pain (NCT03138421). It will be interesting to see whether MAGL inhibitors mimic some of the psychoactive effects of cannabinoid CB1 receptor agonists, such as Δ^9 -THC, the psychoactive component in marijuana, or whether chronic dosing leads to functional antagonism of the CB1 receptor.^{35, 38}

1.4.2 PF-06795071

PF-06795071 is a potent and selective irreversible MAGL inhibitor which was reported by Pfizer.¹⁴ This compound contains a carbamate warhead, [3.1.0] pyrazole core system and unique trifluoromethyl glycol leaving group (Figure 4). PF-06795071 showed high MAGL inhibitory activity (with an IC_{50} of 3 nM) without significant inhibition of other serine hydrolases and CB receptors, with the exception of carboxylesterase 1 (CES1), which is inhibited at 80% when tested at 10 μ M. Moreover, it showed absence of binding at the hERG channel ($IC_{50} > 30 \mu$ M), suggesting a low risk of cardiovascular QT prolongation. PK/PD studies showed that administration of PF-06795071 (1 mg/kg, subcutaneous) increased in brain 2-AG levels, which persisted for 8 h post-dose, and decreased in brain AA level over a similar period. PF-06795071 demonstrated potent anti-neuroinflammation effects in LPS-induced sepsis or encephalitis-like state where it significantly reduced levels of brain inflammatory markers (PGE2, IL-1 β and TNF- α). So far, clinical trial studies have not been performed for this compound.

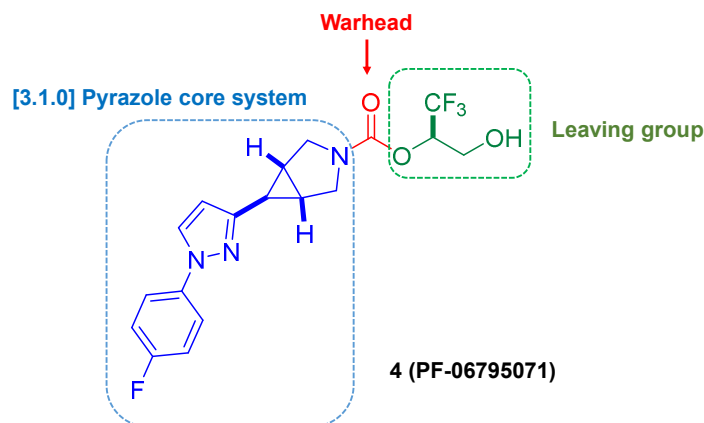


Figure 4. Chemical structure of PF-06795071.

1.4.3 Reversible MAGL inhibitors

Irreversible inhibitors may have several disadvantages to act as therapeutics. The reactive warhead might reduce the selectivity and induce idiosyncratic drug-related toxicity. In the case of MAGL inhibition, chronic exposure to irreversible MAGL inhibitor resulted in pharmacological tolerance.^{52, 53} Reversible inhibitors may provide a chance to avoid these undesirable side-effects. Several series of reversible MAGL inhibitors have been patented or published by different pharmaceutical companies.^{27, 50} All those compounds are amide-based MAGL inhibitors. In 2010, Johnson & Johnson patented a series of azetidines derivatives as reversible MAGL inhibitors⁵⁴ and crystallography studies demonstrated the reversible binding mode for one of those compounds (compound **5**, Figure 5).⁵⁵ The amide moiety of compound **5** formed two hydrogen bonds with Ala51 and Met123 of MAGL and no covalent bond between MAGL and the ligand was observed. The subsequent development led to the discovery of compound **6**. Compound **6** showed an $IC_{50} < 5$ nM. Mice administered with compound **6** (30 mg/kg, p.o.) showed less food consumption than control mice over a period of 30 min. Moreover, oral administration of this compound at doses of 0, 15, and 50 mg/kg/day for five consecutive days resulted in a decrease of mean body weight at the maximum tested concentration. Finally, *in vivo* studies were performed in dogs, which were subjected to a similar treatment, with doses of 0, 5, 15, and 45 mg/kg/day for five consecutive days. Treated dogs showed a decrease in body weight and food consumption, thus confirming the experimental results observed in mice.⁵⁰ In 2013, the

same company filed another patent reporting a series of compounds with similar structure of compound **6**, mainly differing for the presence of a piperidine instead of the piperazine ring.⁵⁴ The representative compounds **8a** and **8b** showed IC₅₀ values on MAGL lower than 5 nM.

In recent years, Takeda Pharmaceutical company reported piperazinyl pyrrolidin-2-one derivatives as reversible MAGL inhibitors. The best compound (compound **9**, Figure 5) in this series was developed starting from pyrrolidinone hit compounds using a structure-based drug design (SBDD) approach.²⁷ Compound **9** showed high MAGL inhibitory activity with an IC₅₀ of 3.6 nM. It showed high selective over FAAH (IC₅₀ > 1000 nM), however, selectivity profiles over other serine hydrolases like ABHD6 and ABHD12 are still not reported. PK studies demonstrated that high exposure level of compound **9** was observed in both plasma and brain (dose 10 mg/kg; plasma concentration 1.01 µg/mL; brain concentration 0.656 µg/g) after 1 h of oral administration to mice. PD studies showed that oral administration of compound **9** significantly reduced AA levels (25%) and increased 2-AG levels (340%) in mouse brain.

Besides, Hoffmann-La Roche recently filed several patents describing reversible MAGL inhibitors.⁵⁶⁻⁵⁸ However, limited information is available for those compounds at this moment.

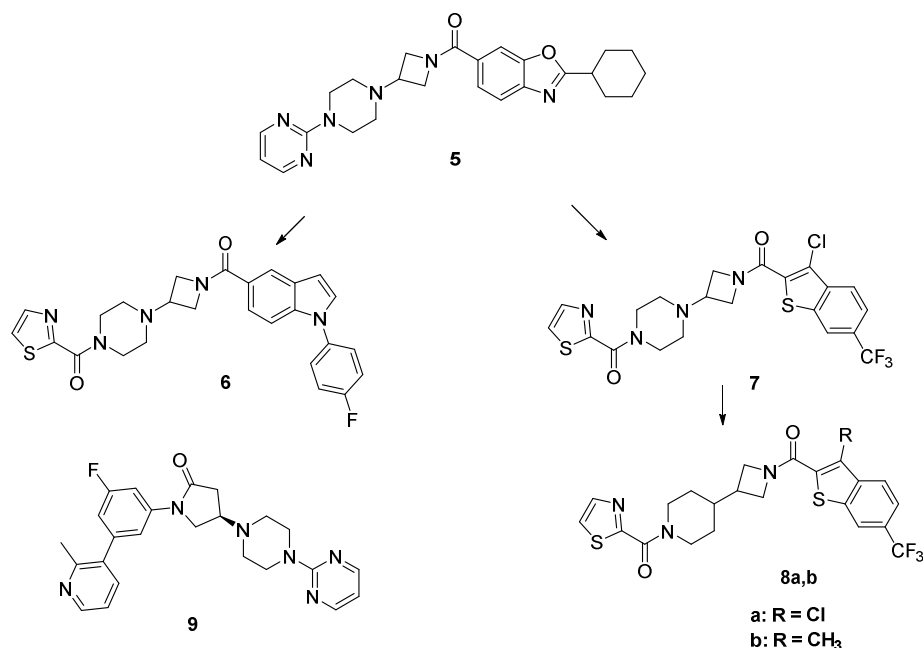


Figure 5. Chemical structures of reversible MAGL inhibitors developed by Johnson & Johnson and Takeda.

1.5 Aim and outline of this thesis

In view of the advantages of a reversible MAGL inhibitor, the aim of the research in this thesis is to develop potent, selective, reversible and *in vivo* active MAGL inhibitors. Previously, a high-throughput screening was performed in Pivot Park Screening Centre and a suitable starting point was identified.⁵⁹ In this thesis, the hit compound was further optimized which led to the discovery of novel chemotypes for MAGL inhibition. The outline of this thesis is as follows:

Chapter 2 describes the activity-driven optimization of a new hit compound of MAGL inhibitor found in a previously reported high-throughput screening campaign.⁵⁹ Ligand-based drug design approaches were carried out during the optimization progress, which led to the discovery of β -sulfinyl esters as highly potent and selective MAGL inhibitors. **Chapter 3** discusses the structure-activity relationship of α -aryl ketones as novel MAGL inhibitors which might have a covalent, reversible mode-of-action.

Chapter 4 focusses on the metabolic stability-guided optimization of β -sulfinyl esters towards drug-like MAGL inhibitors. *In vitro* metabolic stability assays using liver S9 fractions were performed to estimate the hepatic clearance rates of the new MAGL

inhibitors, which led to the discovery of LEI-515 as ultrapotent and metabolically stable MAGL inhibitor.

Chapter 5 describes the profiling of LEI-515 in biochemical, cellular and ADME-T assays as well as mouse pharmacokinetic and target engagement studies.

Chapter 6 summarizes the work presented in this thesis, and shows future directions for the disclosed research.

References

1. Adams, I. B.; Martin, B. R. Cannabis: pharmacology and toxicology in animals and humans. *Addiction (Abingdon, England)* **1996**, 91, 1585-614.
2. Di Marzo, V.; Bifulco, M.; De Petrocellis, L. The endocannabinoid system and its therapeutic exploitation. *Nat Rev Drug Discov* **2004**, 3, 771-84.
3. Kohnz, R. A.; Nomura, D. K. Chemical approaches to therapeutically target the metabolism and signaling of the endocannabinoid 2-AG and eicosanoids. *Chem Soc Rev* **2014**, 43, 6859-69.
4. Di Marzo, V.; Petrosino, S. Endocannabinoids and the regulation of their levels in health and disease. *Current opinion in lipidology* **2007**, 18, 129-140.
5. Ahn, K.; McKinney, M. K.; Cravatt, B. F. Enzymatic pathways that regulate endocannabinoid signaling in the nervous system. *Chemical reviews* **2008**, 108, 1687-1707.
6. Bisogno, T.; Howell, F.; Williams, G.; Minassi, A.; Cascio, M. G.; Ligresti, A.; Matias, I.; Schiano-Moriello, A.; Paul, P.; Williams, E.-J. Cloning of the first sn1-DAG lipases points to the spatial and temporal regulation of endocannabinoid signaling in the brain. *The Journal of cell biology* **2003**, 163, 463-468.
7. Gao, Y.; Vasilyev, D. V.; Goncalves, M. B.; Howell, F. V.; Hobbs, C.; Reisenberg, M.; Shen, R.; Zhang, M.-Y.; Strassle, B. W.; Lu, P. Loss of retrograde endocannabinoid signaling and reduced adult neurogenesis in diacylglycerol lipase knock-out mice. *Journal of Neuroscience* **2010**, 30, 2017-2024.
8. Simon, G. M.; Cravatt, B. F. Endocannabinoid biosynthesis proceeding through glycerophospho-N-acyl ethanolamine and a role for α/β -hydrolase 4 in this pathway. *Journal of Biological Chemistry* **2006**, 281, 26465-26472.
9. Blankman, J. L.; Simon, G. M.; Cravatt, B. F. A comprehensive profile of brain enzymes that hydrolyze the endocannabinoid 2-arachidonoylglycerol. *Chemistry & biology* **2007**, 14, 1347-1356.
10. Cravatt, B. F.; Giang, D. K.; Mayfield, S. P.; Boger, D. L.; Lerner, R. A.; Gilula, N. B. Molecular characterization of an enzyme that degrades neuromodulatory fatty-acid amides. *Nature* **1996**, 384, 83-7.
11. Sam, A. H.; Salem, V.; Ghatei, M. A. Rimonabant: from RIO to ban. *Journal of obesity* **2011**, 2011.
12. Huggins, J. P.; Smart, T. S.; Langman, S.; Taylor, L.; Young, T. An efficient randomised, placebo-controlled clinical trial with the irreversible fatty acid amide hydrolase-1 inhibitor PF-04457845, which modulates endocannabinoids but fails to induce effective analgesia in patients with pain due to osteoarthritis of the knee. *PAIN®* **2012**, 153, 1837-1846.
13. Cisar, J. S.; Weber, O. D.; Clapper, J. R.; Blankman, J. L.; Henry, C. L.; Simon, G. M.; Alexander, J. P.; Jones, T. K.; Ezekowitz, R. A. B.; O'Neill, G. P. Identification of ABX-1431, a selective inhibitor of monoacylglycerol lipase and clinical candidate for treatment of neurological disorders. *Journal of medicinal chemistry* **2018**, 61, 9062-9084.
14. McAllister, L. A.; Butler, C. R.; Mente, S.; O'Neil, S. V.; Fonseca, K. R.; Piro, J. R.; Cianfrogna, J. A.; Foley, T. L.; Gilbert, A. M.; Harris, A. R.; Helal, C. J.; Johnson, D. S.; Montgomery, J. I.; Nason, D. M.; Noell, S.; Pandit, J.; Rogers, B. N.; Samad, T. A.; Shaffer, C. L.; da Silva, R. G.; Uccello, D. P.; Webb, D.; Brodney, M. A. Discovery of Trifluoromethyl

Glycol Carbamates as Potent and Selective Covalent Monoacylglycerol Lipase (MAGL) Inhibitors for Treatment of Neuroinflammation. *J Med Chem* **2018**, 61, 3008-3026.

15. Kiss, L. E.; Beliaev, A.; Ferreira, H. S.; Rosa, C. P.; Bonifácio, M. J.; Loureiro, A. I.; Pires, N. M.; Palma, P. N.; Soares-da-Silva, P. Discovery of a Potent, Long-Acting, and CNS-Active Inhibitor (BIA 10-2474) of Fatty Acid Amide Hydrolase. *ChemMedChem* **2018**, 13, 2177-2188.

16. Fowler, C. J. Monoacylglycerol lipase - a target for drug development? *Br J Pharmacol* **2012**, 166, 1568-85.

17. Nomura, D. K.; Long, J. Z.; Niessen, S.; Hoover, H. S.; Ng, S. W.; Cravatt, B. F. Monoacylglycerol lipase regulates a fatty acid network that promotes cancer pathogenesis. *Cell* **2010**, 140, 49-61.

18. Senior, J. R.; Isselbacher, K. J. DEMONSTRATION OF AN INTESTINAL MONOGLYCERIDE LIPASE: AN ENZYME WITH A POSSIBLE ROLE IN THE INTRACELLULAR COMPLETION OF FAT DIGESTION. *The Journal of Clinical Investigation* **1963**, 42, 187-195.

19. Vaughan, M.; Berger, J. E.; Steinberg, D. HORMONE-SENSITIVE LIPASE AND MONOGLYCERIDE LIPASE ACTIVITIES IN ADIPOSE TISSUE. *The Journal of biological chemistry* **1964**, 239, 401-9.

20. Blankman, J. L.; Simon, G. M.; Cravatt, B. F. A comprehensive profile of brain enzymes that hydrolyze the endocannabinoid 2-arachidonoylglycerol. *Chem Biol* **2007**, 14, 1347-56.

21. Baggelaar, M. P.; Maccarrone, M.; van der Stelt, M. 2-Arachidonoylglycerol: a signaling lipid with manifold actions in the brain. *Progress in lipid research* **2018**, 71, 1-17.

22. Murataeva, N.; Straiker, A.; Mackie, K. Parsing the players: 2-arachidonoylglycerol synthesis and degradation in the CNS. *British journal of pharmacology* **2014**, 171, 1379-1391.

23. Nomura, D. K.; Morrison, B. E.; Blankman, J. L.; Long, J. Z.; Kinsey, S. G.; Marcondes, M. C. G.; Ward, A. M.; Hahn, Y. K.; Lichtman, A. H.; Conti, B. Endocannabinoid hydrolysis generates brain prostaglandins that promote neuroinflammation. *Science* **2011**, 334, 809-813.

24. Dinh, T.; Carpenter, D.; Leslie, F.; Freund, T.; Katona, I.; Sensi, S.; Kathuria, S.; Piomelli, D. Brain monoglyceride lipase participating in endocannabinoid inactivation. *Proceedings of the national Academy of sciences* **2002**, 99, 10819-10824.

25. Labar, G.; Bauvois, C.; Borel, F.; Ferrer, J. L.; Wouters, J.; Lambert, D. M. Crystal structure of the human monoacylglycerol lipase, a key actor in endocannabinoid signaling. *Chembiochem : a European journal of chemical biology* **2010**, 11, 218-27.

26. Griebel, G.; Pichat, P.; Beeske, S.; Leroy, T.; Redon, N.; Jacquet, A.; Francon, D.; Bert, L.; Even, L.; Lopez-Grancha, M.; Tolstykh, T.; Sun, F.; Yu, Q.; Brittain, S.; Arlt, H.; He, T.; Zhang, B.; Wiederschain, D.; Bertrand, T.; Houtmann, J.; Rak, A.; Vallee, F.; Michot, N.; Auge, F.; Menet, V.; Bergis, O. E.; George, P.; Avenet, P.; Mikol, V.; Didier, M.; Escoubet, J. Selective blockade of the hydrolysis of the endocannabinoid 2-arachidonoylglycerol impairs learning and memory performance while producing antinociceptive activity in rodents. *Scientific reports* **2015**, 5, 7642.

27. Aida, J.; Fushimi, M.; Kusumoto, T.; Sugiyama, H.; Arimura, N.; Ikeda, S.; Sasaki, M.; Sogabe, S.; Aoyama, K.; Koike, T. Design, Synthesis, and Evaluation of Piperazinyl Pyrrolidin-2-ones as a Novel Series of Reversible Monoacylglycerol Lipase Inhibitors. *J Med Chem* **2018**, 61, 9205-9217.

28. Bertrand, T.; Augé, F.; Houtmann, J.; Rak, A.; Vallée, F.; Mikol, V.; Berne, P.; Michot, N.;

- Cheuret, D.; Hoornaert, C. Structural basis for human monoglyceride lipase inhibition. *Journal of molecular biology* **2010**, 396, 663-673.
29. Casas-Godoy, L.; Duquesne, S.; Bordes, F.; Sandoval, G.; Marty, A. Lipases: an overview. *Methods in molecular biology (Clifton, N.J.)* **2012**, 861, 3-30.
30. Mulvihill, M. M.; Nomura, D. K. Therapeutic potential of monoacylglycerol lipase inhibitors. *Life sciences* **2013**, 92, 492-497.
31. Nomura, D. K.; Morrison, B. E.; Blankman, J. L.; Long, J. Z.; Kinsey, S. G.; Marcondes, M. C.; Ward, A. M.; Hahn, Y. K.; Lichtman, A. H.; Conti, B.; Cravatt, B. F. Endocannabinoid hydrolysis generates brain prostaglandins that promote neuroinflammation. *Science (New York, N.Y.)* **2011**, 334, 809-13.
32. Kohnz, R. A.; Nomura, D. K. Chemical approaches to therapeutically target the metabolism and signaling of the endocannabinoid 2-AG and eicosanoids. *Chemical Society Reviews* **2014**, 43, 6859-6869.
33. Piro, J. R.; Benjamin, D. I.; Duerr, J. M.; Pi, Y.; Gonzales, C.; Wood, K. M.; Schwartz, J. W.; Nomura, D. K.; Samad, T. A. A dysregulated endocannabinoid-eicosanoid network supports pathogenesis in a mouse model of Alzheimer's disease. *Cell reports* **2012**, 1, 617-623.
34. Costola-de-Souza, C.; Ribeiro, A.; Ferraz-de-Paula, V.; Calefi, A. S.; Aloia, T. P. A.; Gimenes-Júnior, J. A.; de Almeida, V. I.; Pinheiro, M. L.; Palermo-Neto, J. Monoacylglycerol lipase (MAGL) inhibition attenuates acute lung injury in mice. *PloS one* **2013**, 8, e77706.
35. Long, J. Z.; Li, W.; Booker, L.; Burston, J. J.; Kinsey, S. G.; Schlosburg, J. E.; Pavón, F. J.; Serrano, A. M.; Selley, D. E.; Parsons, L. H. Selective blockade of 2-arachidonoylglycerol hydrolysis produces cannabinoid behavioral effects. *Nature chemical biology* **2009**, 5, 37.
36. Kinsey, S. G.; Long, J. Z.; O'Neal, S. T.; Abdullah, R. A.; Poklis, J. L.; Boger, D. L.; Cravatt, B. F.; Lichtman, A. H. Blockade of endocannabinoid-degrading enzymes attenuates neuropathic pain. *Journal of Pharmacology and Experimental Therapeutics* **2009**, 330, 902-910.
37. Guindon, J.; Guijarro, A.; Piomelli, D.; Hohmann, A. G. Peripheral antinociceptive effects of inhibitors of monoacylglycerol lipase in a rat model of inflammatory pain. *British journal of pharmacology* **2011**, 163, 1464-1478.
38. Schlosburg, J. E.; Blankman, J. L.; Long, J. Z.; Nomura, D. K.; Pan, B.; Kinsey, S. G.; Nguyen, P. T.; Ramesh, D.; Booker, L.; Burston, J. J. Chronic monoacylglycerol lipase blockade causes functional antagonism of the endocannabinoid system. *Nature neuroscience* **2010**, 13, 1113-1119.
39. Ignatowska-Jankowska, B.; Ghosh, S.; Crowe, M.; Kinsey, S.; Niphakis, M.; Abdullah, R.; Tao, Q.; O'Neal, S.; Walentiny, D.; Wiley, J. In vivo characterization of the highly selective monoacylglycerol lipase inhibitor KML 29: antinociceptive activity without cannabimimetic side effects. *British journal of pharmacology* **2014**, 171, 1392-1407.
40. Crowe, M. S.; Leishman, E.; Banks, M. L.; Gujjar, R.; Mahadevan, A.; Bradshaw, H. B.; Kinsey, S. G. Combined inhibition of monoacylglycerol lipase and cyclooxygenases synergistically reduces neuropathic pain in mice. *British journal of pharmacology* **2015**, 172, 1700-1712.
41. Ransohoff, R. M. How neuroinflammation contributes to neurodegeneration. *Science (New York, N.Y.)* **2016**, 353, 777-783.
42. Long, J. Z.; Nomura, D. K.; Cravatt, B. F. Characterization of monoacylglycerol lipase inhibition reveals differences in central and peripheral endocannabinoid metabolism. *Chemistry*

& biology **2009**, 16, 744-753.

43. Chen, R.; Zhang, J.; Wu, Y.; Wang, D.; Feng, G.; Tang, Y.-P.; Teng, Z.; Chen, C. Monoacylglycerol lipase is a therapeutic target for Alzheimer's disease. *Cell reports* **2012**, 2, 1329-1339.
44. Cao, Z.; Mulvihill, M. M.; Mukhopadhyay, P.; Xu, H.; Erdélyi, K.; Hao, E.; Holovac, E.; Haskó, G.; Cravatt, B. F.; Nomura, D. K. Monoacylglycerol lipase controls endocannabinoid and eicosanoid signaling and hepatic injury in mice. *Gastroenterology* **2013**, 144, 808-817. e15.
45. Jiang, M.; van der Stelt, M. Activity-Based Protein Profiling Delivers Selective Drug Candidate ABX-1431, a Monoacylglycerol Lipase Inhibitor, To Control Lipid Metabolism in Neurological Disorders. *J Med Chem* **2018**, 61, 9059-9061.
46. Kerbrat, A.; Ferre, J. C.; Fillatre, P.; Ronziere, T.; Vannier, S.; Carsin-Nicol, B.; Lavoue, S.; Verin, M.; Gauvrit, J. Y.; Le Tulzo, Y.; Edan, G. Acute Neurologic Disorder from an Inhibitor of Fatty Acid Amide Hydrolase. *The New England journal of medicine* **2016**, 375, 1717-1725.
47. Niphakis, M. J.; Cravatt, B. F. Enzyme inhibitor discovery by activity-based protein profiling. *Annual review of biochemistry* **2014**, 83, 341-77.
48. van Esbroeck, A. C. M.; Janssen, A. P. A.; Cognetta, A. B., 3rd; Ogasawara, D.; Shpak, G.; van der Kroeg, M.; Kantae, V.; Baggelaar, M. P.; de Vrij, F. M. S.; Deng, H.; Allara, M.; Fezza, F.; Lin, Z.; van der Wel, T.; Soethoudt, M.; Mock, E. D.; den Dulk, H.; Baak, I. L.; Florea, B. I.; Hendriks, G.; De Petrocellis, L.; Overkleeft, H. S.; Hankemeier, T.; De Zeeuw, C. I.; Di Marzo, V.; Maccarrone, M.; Cravatt, B. F.; Kushner, S. A.; van der Stelt, M. Activity-based protein profiling reveals off-target proteins of the FAAH inhibitor BIA 10-2474. *Science (New York, N.Y.)* **2017**, 356, 1084-1087.
49. Aghazadeh Tabrizi, M.; Baraldi, P. G.; Baraldi, S.; Ruggiero, E.; De Stefano, L.; Rizzolio, F.; Di Cesare Mannelli, L.; Ghelardini, C.; Chicca, A.; Lapillo, M.; Gertsch, J.; Manera, C.; Macchia, M.; Martinelli, A.; Granchi, C.; Minutolo, F.; Tuccinardi, T. Discovery of 1,5-Diphenylpyrazole-3-Carboxamide Derivatives as Potent, Reversible, and Selective Monoacylglycerol Lipase (MAGL) Inhibitors. *J Med Chem* **2018**, 61, 1340-1354.
50. Granchi, C.; Caligiuri, I.; Minutolo, F.; Rizzolio, F.; Tuccinardi, T. A patent review of Monoacylglycerol Lipase (MAGL) inhibitors (2013-2017). *Expert Opin Ther Pat* **2017**, 27, 1341-1351.
51. Granchi, C.; Rizzolio, F.; Palazzolo, S.; Carmignani, S.; Macchia, M.; Saccomanni, G.; Manera, C.; Martinelli, A.; Minutolo, F.; Tuccinardi, T. Structural Optimization of 4-Chlorobenzoylpiperidine Derivatives for the Development of Potent, Reversible, and Selective Monoacylglycerol Lipase (MAGL) Inhibitors. *J Med Chem* **2016**, 59, 10299-10314.
52. Singh, J.; Petter, R. C.; Baillie, T. A.; Whitty, A. The resurgence of covalent drugs. *Nature reviews Drug discovery* **2011**, 10, 307-317.
53. King, A. R.; Dotsey, E. Y.; Lodola, A.; Jung, K. M.; Ghomian, A.; Qiu, Y.; Fu, J.; Mor, M.; Piomelli, D. Discovery of potent and reversible monoacylglycerol lipase inhibitors. *Chemistry & biology* **2009**, 16, 1045-1052.
54. JOHNSON, J. Piperidin-4-yl-azetidide diamides as monoacylglycerol lipase inhibitors. In *US20130102584*, 2013.
55. Schalk-Hihi, C.; Schubert, C.; Alexander, R.; Bayoumy, S.; Clemente, J. C.; Deckman, I.; DesJarlais, R. L.; Dzordzorme, K. C.; Flores, C. M.; Grasberger, B.; Kranz, J. K.; Lewandowski, F.; Liu, L.; Ma, H.; Maguire, D.; Macielag, M. J.; McDonnell, M. E.; Mezzasalma Haarlander,

T.; Miller, R.; Milligan, C.; Reynolds, C.; Kuo, L. C. Crystal structure of a soluble form of human monoglyceride lipase in complex with an inhibitor at 1.35 Å resolution. *Protein science : a publication of the Protein Society* **2011**, *20*, 670-83.

56. Roche. BEZOXAZINE DERIVATIVES USEFUL AS MONOACYLGLYCEROL LIPASE INHIBITORS. 2019.

57. Roche. NEW HETEROCYCLIC COMPOUNDS. 2019.

58. Roche. PIPERAZINE DERIVATIVES AS MAGL INHIBITORS. 2019.

59. van der Wel, T. Chemical genetic approaches for target validation. Leiden University, Leiden, 2020.

Chapter 2

Hit Optimization of β -Sulfinyl Esters as Highly Potent and Selective MAGL Inhibitors

M. Jiang, F. Mohr, T. van der Wel, M. C. W. Huizenga, A. Martella, C. A. A. van Boeckel, R. J. B. H. N. van den Berg, M. van der Stelt*; *manuscript in preparation.*

2.1 Introduction

2-Arachidonoylglycerol (2-AG) is an endogenous agonist of the cannabinoid CB₁ and CB₂ receptors and serves as a precursor for a pool of arachidonic acid (AA) which may form pro-inflammatory prostaglandins in the brain, lung and liver.¹ The central role of monoacylglycerol lipase (MAGL) in the metabolism of 2-AG makes it, therefore, an attractive therapeutic target for a variety of disorders, including inflammation-induced tissue injury and pain, multiple sclerosis and cancer.^{2, 3} MAGL is a membrane-associated serine hydrolase and employs a serine-histidine-aspartate catalytic triad to hydrolyze the ester moiety of monoacylglycerols.⁴ Currently, the covalent, irreversible MAGL inhibitor ABX-1431 is in clinical phase 1b studies for the treatment of post-traumatic stress disorder as well as for other indications, such as neuromyelitis optica and multiple sclerosis.⁵ Irreversible inhibitors may have several advantages to act as

therapeutics, like increased potency, long residence time and a less stringent pharmacokinetic profile.⁶ However, the irreversible mode of action may also have some drawbacks, such as reduced selectivity and the formation of covalent-protein adducts might result in idiosyncratic drug-related toxicity.⁷ In case of MAGL inhibition, chronic exposure to the covalent inhibitor JZL184 resulted in pharmacological tolerance, development of physical dependence, impaired synaptic plasticity and receptor desensitization in the nervous system.^{8, 9} Reversible inhibitors may avoid these unfavorable side-effects.¹⁰

To harness the therapeutic potential of MAGL, a high-throughput screen (HTS) was previously performed within the Cancer Drug Discovery Initiative (CDDI)¹¹ to identify novel reversible MAGL inhibitors. A natural substrate assay was employed that utilizes an enzymatic cascade to convert glycerol, a metabolite produced by MAGL, into a fluorescent signal.¹² A compound library containing 233.820 unique structures was screened. After hit triaging and hit confirmation using activity-based protein profiling (ABPP) seven hits were identified¹³, which could serve as a starting point for a drug discovery project. In this chapter the medicinal chemistry efforts to optimize hit **1** (ethyl 2-((4-(3-methyl-4-(*m*-tolyl)piperazine-1-carbonyl)-2-nitrophenyl)sulfinyl)acetate) are described (Figure 1).

Compound **1** showed a half maximal inhibitory concentration (IC₅₀) of 630 nM in the HTS and was selective over fatty acid amide hydrolase (FAAH), an enzyme that inactivates anandamide, another endocannabinoid. It has a Molecular Weight (MW) of 473.54 Da and a calculated lipophilicity (cLogP) of 3.2, which resulted in a Lipophilic Efficiency (LipE)¹⁴ of 3.0. Compound **1** has a topological polar surface area (tPSA) of 119 Å², which reduces cell penetration¹⁵. Furthermore, it contains an aromatic nitro group, which is associated with genotoxicity¹⁶ and an ester functionality that poses a metabolic liability¹⁷. The aim of the hit optimization program was, therefore a) to improve the potency, b) to reduce the polar surface area, c) to replace the aromatic nitro; and d) to improve its metabolic stability, while maintaining its selectivity.

Here, in this chapter a ligand-based drug design (LBDD) approach is used to develop a structure-activity relationship (SAR) of hit **1** and to improve its potency,

while reducing the polar surface area and genotoxicity liability by replacing the aromatic nitro group. The optimization of the metabolic stability will be described in Chapter 4.

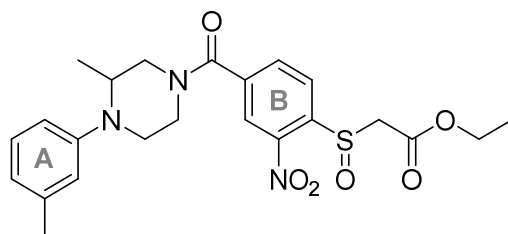
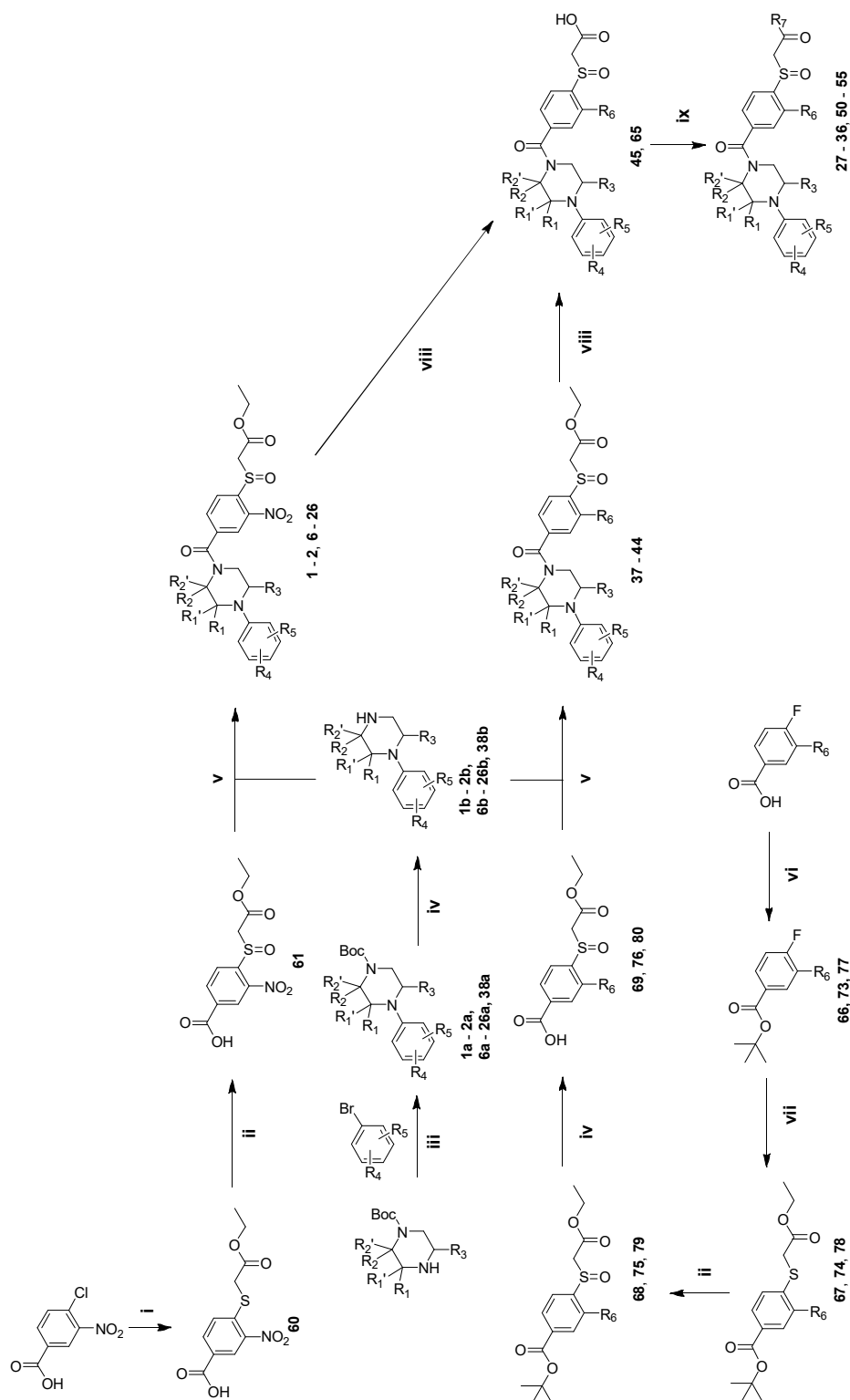


Figure 1. Chemical structure of HTS hit **1**.

2.2 Results and discussion

To study the SAR of compound **1**, various synthetic routes were employed that allowed the systematic investigation of the substitution pattern of piperazine moiety, phenyl A and B, and variations of the β -sulfinyl ester (Scheme 1 and S1). This led to the synthesis of compounds **1-55**. The synthesis started with palladium catalyzed Buchwald-Hartwig cross coupling of the appropriate Boc-piperazine and bromobenzene to obtain tertiary amine. Subsequent TFA mediated Boc-cleavage resulted in amine building block. Concurrently, nucleophilic aromatic substitution of ethyl 2-mercaptoacetate with chloro nitrobenzoic acid or appropriate *tert*-butyl 4-fluorobenzoate obtained sulfide, which was oxidized by oxone to yield sulfinylbenzoic acid building block. Peptide coupling of the amine building block with benzoic acid afforded the ethyl ester compounds. To make different ester or amide variations, the ethyl ester was hydrolyzed by using triethylamine and the obtained carboxylic acid was coupled with different alcohols or amines.

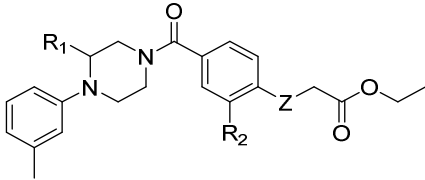
Compound **1** is a racemic mixture. To investigate which enantiomer is the most active compound, both the (*S*)-**1** and (*R*)-**1** enantiomers were synthesized and tested. Both compounds showed similar inhibitory potencies as the initial hit (Table 1), indicating that the chirality of the methyl substituent at the 3-position of piperazine did not impact the inhibition of MAGL. On the other hand, removal of the methyl group (**2**) led to a 10-fold drop in activity. The oxidation state of the sulfur atom in compound **1** was important, because reducing the sulfoxide to a sulfur (**3**) or oxidizing it to a sulfonyl



Scheme 1. General synthesis route for hit optimization of compound 1. Reagents and conditions: i) ethyl 2-mercaptoacetate, pyridine, 115 °C, 85 %. ii) Oxone, MeOH / H₂O, 70 %. iii) sodium *tert*-butoxide, BINAP, Pd(OAc)₂, 1,4-dioxane, 85 °C. iv) TFA, DCM. v) HATU, DiPEA, DCM. vi) Boc₂O, DMAP, *tert*-BuOH, 65 °C. vii) ethyl 2-mercaptoacetate, K₂CO₃, ACN. viii) TEA, MeOH, H₂O. ix) appropriate alcohol or amine, oxalyl chloride, DiPEA, DCM.

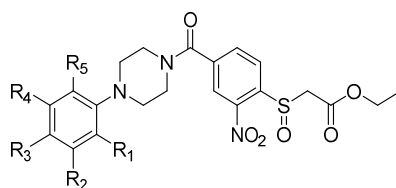
(4) abolished the activity. Removal of the nitro-group (5) also led to a significant reduction in activity.

Table 1. pIC₅₀ values of resynthesized hit **1** and designed derivatives **2 - 5**.



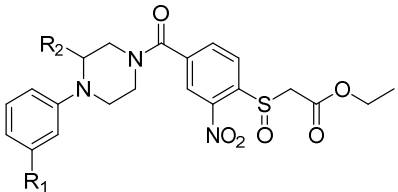
Entry	R ₁	R ₂	Z	pIC ₅₀ ± SD
(S)-1		NO ₂	SO	6.57±0.13
(R)-1		NO ₂	SO	6.71±0.05
2	H 	NO ₂	SO	5.65±0.05
3		NO ₂	S	<5
4		NO ₂	SO ₂	<5
5		H	SO	5.25±0.05

To analyze the effect of the substitution pattern on phenyl A, compounds **6-22** were evaluated (Table 2) using the scaffold of compound **2** (for the ease of synthesis). Electron donating substituents on the meta- (methyl (**2**), methoxy (**15**)) or para-position (methoxy (**16**)) reduced the potency compared to compound **6**. In contrast, electron withdrawing groups (EWG) were preferred on the meta-position (F (**7**), Cl (**8**), Br (**11**), CF₃ (**13**), but not nitro (**17**)). The electron withdrawing effect was absent or less pronounced on the para-position (Cl (**9**), Br (**12**) or CF₃ (**14**)). Of interest, a phenyl substitution (**18**) was tolerated at the meta-position, suggesting the presence of a hydrophobic pocket. Dichloro substitution did not improve the potency (**19-22**).

Table 2. pIC₅₀ values of designed analogues **6** – **22**.

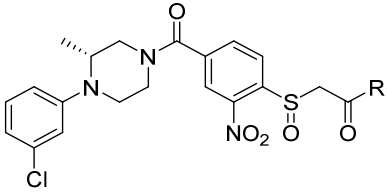
Entry	R ₁	R ₂	R ₃	R ₄	R ₅	pIC ₅₀ ± SD
2	H	CH ₃	H	H	H	5.65 ± 0.05
6	H	H	H	H	H	5.91 ± 0.11
7	H	F	H	H	H	6.20 ± 0.18
8	H	Cl	H	H	H	6.33 ± 0.08
9	H	H	Cl	H	H	6.00 ± 0.08
10	Cl	H	H	H	H	5.37 ± 0.07
11	H	Br	H	H	H	6.44 ± 0.06
12	H	H	Br	H	H	5.95 ± 0.08
13	H	CF ₃	H	H	H	6.42 ± 0.09
14	H	H	CF ₃	H	H	6.23 ± 0.13
15	H	OCH ₃	H	H	H	5.18 ± 0.07
16	H	H	OCH ₃	H	H	5.31 ± 0.04
17	H	NO ₂	H	H	H	5.59 ± 0.06
18	H	Phenyl	H	H	H	5.87±0.08
19	H	Cl	H	Cl	H	6.31 ± 0.04
20	H	Cl	Cl	H	H	5.59±0.11
21	Cl	H	Cl	H	H	5.71± 0.13
22	Cl	H	H	H	Cl	5.74 ± 0.13

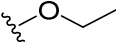
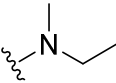
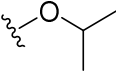
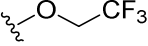
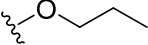
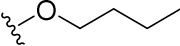
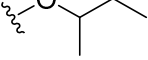
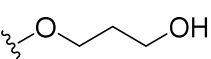
Next, an EWG at the meta-position of phenyl A was combined with the chiral substituted piperazines (**23-26**) (Table 3). Substitution of the *m*-methyl of the tolyl group with a halogen on the chiral pure scaffold of compound **1** increased the inhibitory potency on both enantiomers equally well. The *m*-chloro-substituted (*R*)-**24** and (*S*)-**24** were the most active compounds with a pIC₅₀ around 7.4.

Table 3. pIC₅₀ values of designed analogues **23** - **26**.


Entry	R ₁	R ₂	pIC ₅₀ ± SD
(<i>S</i>)-1			6.57±0.13
(<i>R</i>)-1			6.71±0.05
23			6.81±0.03
(<i>R</i>)-24			7.40±0.11
(<i>S</i>)-24			7.36±0.08
(<i>R</i>)-25			7.06±0.07
(<i>S</i>)-25			7.09±0.06
(<i>R</i>)-26			6.94±0.04
(<i>S</i>)-26			6.70±0.08

Employing the scaffold of (*R*)-**24**, which was the most active compound identified thus far, the SAR of the ester moiety was studied. To this end, compounds **27** - **35** were evaluated (Table 4). Replacement of the ethyl ester with methyl (**27**), or trifluoroethyl (**30**) esters resulted in decreased MAGL activity, while elongating the alkyl chain to a propyl (**31**) or butyl (**31**) increased the potency compared to the ethyl (**24**). Of note, branching of the alkyl chain (isopropyl (**29**), sec-butyl (**33**) and *tert*-pentyl (**34**) reduced the activity. Introduction of a polar group was tolerated, as witnessed by hydroxypropyl ester (**35**), which had a similar activity as (*R*)-**24**. However, changing the ester to a secondary amide (**28**) resulted in inactive compound.

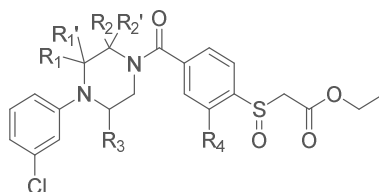
Table 4. pIC₅₀ values of different ester and amide analogues **27** - **35**.


Entry	R	pIC ₅₀ ± SD
(R)-24		7.40±0.11
27		7.11±0.10
28		<5
29		6.96±0.06
30		7.13±0.09
31		7.54±0.09
32		7.58±0.09
33		7.41±0.10
34		6.22±0.12
35		7.46±0.11

Next, the SAR of the piperazine and the 2-nitrophenyl ring was revisited. Various methyl substituted piperazines and the nitro-group bio-isosteres (compounds **36** – **44**) were analyzed. An additional methyl group at the 5-position (**36**) decreased the MAGL inhibitory activity. Replacing the nitro group with a fluorine (**37**) in the scaffold maintained the activity, and, importantly, reduced the liability for potential genotoxicity and significantly reduced the polar surface area of the compound. 2-Methyl-piperazine (**38**) had similar MAGL inhibitory activity as compound **37**. 2,2-Dimethyl (**42**) or 3,3-dimethyl (**41**) substitution resulted in decreased potency as compared to 3-methyl substituted piperazines. Interestingly, trans-2,3-dimethyl substitution (**40**) significantly elevated the potency, while cis-2,3-dimethyl substitution (**39**) slightly

decreased the MAGL activity compared to compound **37**. Furthermore, changing the fluoro to chloro (\pm **43**) and bromo (\pm **44**) further increased the potency. Compound \pm **43** was the most potent compound identified with a pIC_{50} of 8.50 ± 0.10 .

Table 5. pIC_{50} values of designed analogues **36** - **44**.



Entry	R ₁	R ₁ '	R ₂	R ₂ '	R ₃	R ₄	$\text{pIC}_{50} \pm \text{SD}$
(<i>R</i>)- 24	(<i>R</i>)CH ₃	H	H	H	H	NO ₂	7.40 \pm 0.11
36	CH ₃	H	H	H	CH ₃	NO ₂	6.68 \pm 0.07
37	(<i>R</i>)CH ₃	H	H	H	H	F	7.56 \pm 0.04
38	H	H	CH ₃	H	H	F	7.56 \pm 0.10
\pm 39	cis-CH ₃	H	cis-CH ₃	H	H	F	7.29 \pm 0.07
\pm 40	trans-CH ₃	H	trans-CH ₃	H	H	F	8.13 \pm 0.07
41	CH ₃	CH ₃	H	H	H	F	7.33 \pm 0.07
42	H	H	CH ₃	CH ₃	H	F	7.24 \pm 0.07
\pm 43	trans-CH ₃	H	trans-CH ₃	H	H	Cl	8.50 \pm 0.10
\pm 44	trans-CH ₃	H	trans-CH ₃	H	H	Br	8.24 \pm 0.17

Finally, on the basis of the potency of compound \pm **43**, several analogues (\pm **45** - \pm **55**) were evaluated (Table 6). Hydrolysis of the ethyl ester to carboxylic acid (\pm **45**) resulted in >500-fold loss of MAGL inhibitory activity, while replacing the linker amide to amine (\pm **48**) was allowed. Changing the sulfinyl group to sulfur (\pm **46**) abolished the inhibitory activity and replacing it with a sulfonyl (\pm **47**) or carbonyl (\pm **49**) resulted in a 1000-fold reduced inhibitory activity. Compounds in which the ethyl ester was replaced with an isopropyl (\pm **50**), *sec*-butyl (\pm **51**), cyclobutyl (\pm **52**), cyclopentanyl (\pm **53**) or cyclohexanyl (\pm **54**) esters displayed similar MAGL inhibitory activity, but decreased lipophilic efficiency (LipE) compared to compound \pm **43**. The polar 1-glycerol ester (\pm **55**) showed similar potency compared to the other esters. Altogether, this SAR study revealed that compounds \pm **43** and \pm **48** showed the most promising

combination of activity and physical-chemical properties (Table 6).

Table 6. pIC₅₀ values of designed analogues 45 - 55.

Entry	L	Z	R	pIC ₅₀ ± SD	cLogP	tPSA	LipE
± 43	CO	SO		8.50±0.10	4.93	67	3.57
± 45	CO	SO	H	6.18±0.06	4.22	78	1.96
± 46	CO	S		<5	6.23	50	-
± 47	CO	SO ₂		6.47±0.07	4.87	84	1.60
± 48	CH ₂	SO		8.21 ± 0.11	5.70	50	2.51
± 49	CO	CO		5.94±0.08	5.19	67	0.75
± 50	CO	SO		8.57±0.12	5.23	67	3.34
± 51	CO	SO		8.41±0.08	5.76	67	2.65
± 52	CO	SO		8.38 ± 0.09	5.31	67	3.07
± 53	CO	SO		8.41 ± 0.08	5.89	67	2.52
± 54	CO	SO		8.53 ± 0.08	6.43	67	2.10
± 55	CO	SO		8.18 ± 0.09	2.92	107	5.26

Compounds ± 43 and ± 48 were selected for further profiling. To determine the selectivity of compounds ± 43 and ± 48 over other serine hydrolases, gel-based and mass spectrometry (MS)-based activity-based protein profiling (ABPP) was employed on mouse brain proteome. ABPP is a versatile chemical proteomic method to assess target engagement and proteome-wide selectivity for small-molecule inhibitors. It

makes use of activity-based probes (ABPs) to assess the functional state of entire enzyme classes directly in native biological systems. ABPs with fluorescent reporter groups enable visualization of enzyme activities in complex proteomes by SDS-polyacrylamide gel electrophoresis (SDS-PAGE) using in-gel fluorescence scanning, while ABPs with a biotin reporter group enable affinity enrichment and identification of enzyme activities by mass spectrometry (MS)-based proteomics.¹⁸ For gel-based ABPP, two broad-spectrum probes MB064 and TAMRA-FP were used as reported before.¹⁹⁻²¹ Compound \pm **43** displayed high selectivity over the other endocannabinoid hydrolases (*e.g.* DAGL- α , FAAH, ABHD6 and ABHD12) (Figure 2A). Compound \pm **48** reduced MAGL activity with a pIC_{50} of 7.4 ± 0.1 and was able to inhibit FAAH in a dose-manner with a pIC_{50} of 6.8 ± 0.2 (Figure 2B, C). This indicates that compound \pm **43** is a selective MAGL inhibitor, while compound \pm **48** is a dual MAGL/FAAH inhibitor. It has been reported that inactivation of both MAGL and FAAH could cause catalepsy and THC-like drug discrimination responses, which limited its therapeutic applications.²² Based on these data, chemical proteomics using MB108 and FP-biotin was carried out to further investigate the selectivity of \pm **43**, but not \pm **48**, over a broader range of specified proteins. Compound \pm **43** did not reduce labeling of the detected proteins by more than 50%, except for MAGL and nitrilase family member 2 (Nit2) (Figure 2B, C). Together, these data indicate that compound \pm **43** is a highly selective MAGL inhibitor.

To study the interactions of compound \pm **43** with the amino acids in the active site of MAGL, docking studies were performed using the reported MAGL crystal structure.²³ As shown in figure 3, the carbonyl of the ester group forms two H-bonds with Ala51 and Met123, respectively, which are also frequently observed in other co-crystal structures of MAGL.²⁴⁻²⁷ The carbonyl of the ester group serves as an electrophile which could be attacked by the catalytic serine (Ser122), since the distance between them is around 3 Å. The ethyl moiety inserts into the hydrophilic cytoplasmic access (CA) channel, while the rest of the compound occupies the large hydrophobic tunnel. The chloro-group on phenyl ring B occupies a hydrophobic subpocket of MAGL, which

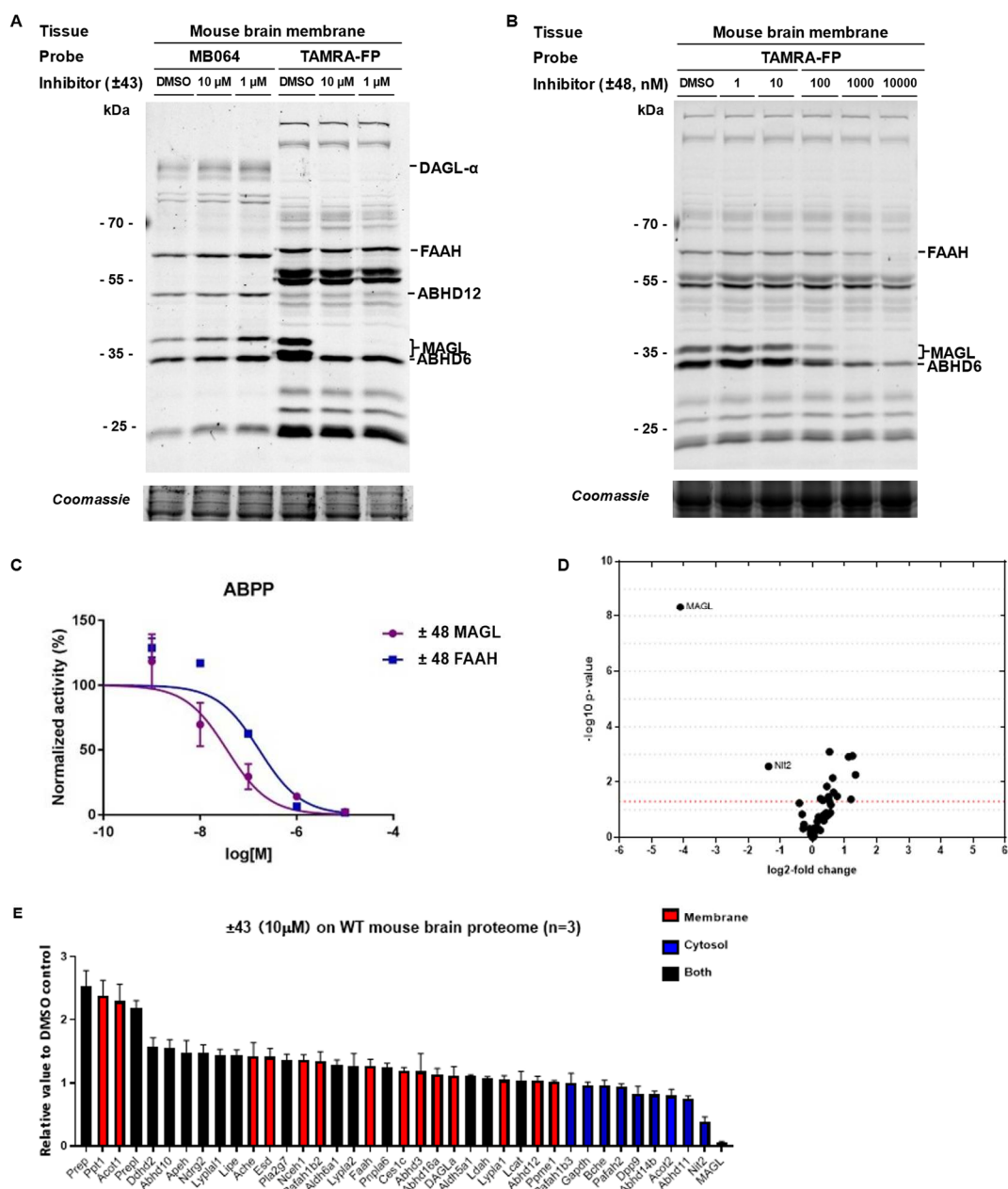


Figure 2. (A) Selectivity profiles of compound \pm 43 on mouse brain membrane proteome using broad-spectrum probe MB064 (250 nM, 10 min) or TAMRA-FP (100 nM, 10 min) for gel-based ABPP. (B, C) Selectivity profiles of compound \pm 48 on mouse brain proteome using broad-spectrum probe TAMRA-FP (100 nM, 10 min) for gel-based ABPP. (D, E) Selectivity profiles of compound \pm 43 on mouse brain proteome (MBP) using broad-spectrum probe MB108 and FP-biotin (10 μ M, 60 min) for chemical proteomics.

match the SAR data. The two methyl groups on the piperazine ring are orientated to different directions in the hydrophobic pocket, which enhance the hydrophobic interaction. No specific interaction is observed between the amide moiety of \pm 43 and MAGL, suggesting that the amide acts as a linker which is in line with compound \pm 48

being active. This proposed binding mode is thus consistent with the observed SAR reported in this chapter.

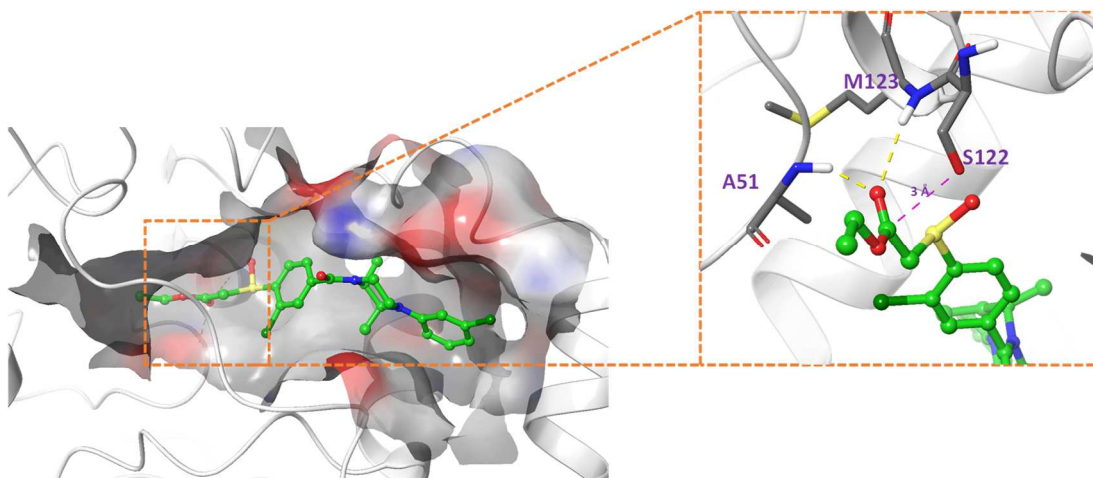


Figure 3. Docking pose of compound \pm **43** with MAGL (PDB code: 3HJU). Two H-bonds (yellow dotted line) with Ala51 and Met123 were observed in this docking model.

2.3 Conclusion

In conclusion, a ligand-based optimization of β -sulfinyl esters as MAGL inhibitors is described in this chapter, which leads to the discovery of a highly potent and selective MAGL inhibitor (compound \pm **43**). A summary of the SAR is presented in Figure 4. Compared with the original hit **1**, the MAGL inhibitory activity of \pm **43** increased around 100-fold. Importantly, by replacing the nitro group with chloro, the potential genotoxicity liability was removed. By using ABPP and chemical proteomics, the selectivity of \pm **43** was profiled and it showed high selectivity against other serine hydrolases in the ECS. Notwithstanding the important role of the ester group in the binding activity, its metabolic stability should be investigated to assess the *in vivo* stability of the compound.

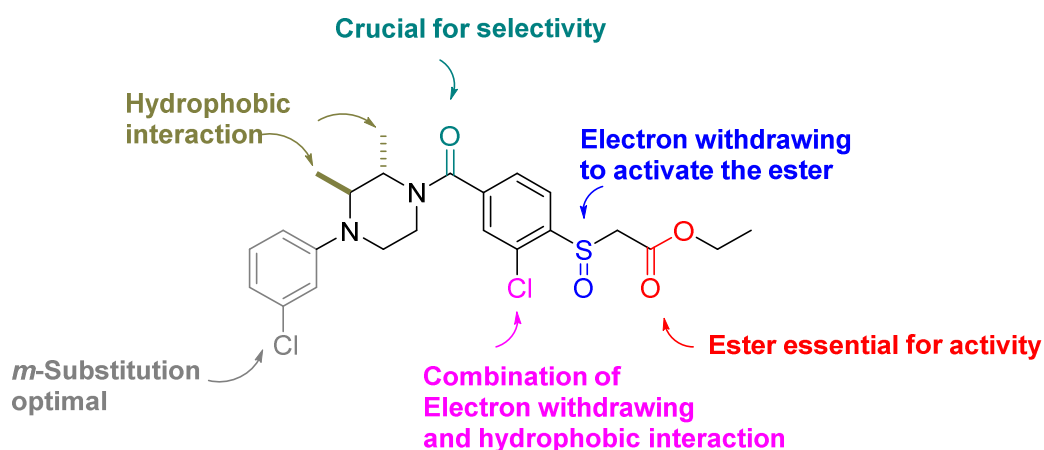


Figure 4. An overview of the structure-activity relationship for the β -sulfinyl esters MAGL inhibitor library.

2.4 Experimental procedures

Biological Procedures

MAGL natural substrate assay. The MAGL activity assay is based on the production of glycerol from 2-arachidonoylglycerol (2-AG) hydrolysis by MAGL-overexpressing membrane preparations from transiently transfected HEK293T cells, as previously reported. The produced glycerol is coupled to the oxidation of commercially available Amplifu™Red via a multi-enzyme cascade, resulting in a fluorescent signal from the dye resorufin. Standard assays were performed in HEMNB buffer (50 mM HEPES pH 7.4, 1 mM EDTA, 5 mM MgCl₂, 100 mM NaCl, 0.5% (w/v) BSA) in black, flat bottom 96-wells plates. Final protein concentration of membrane preparations from overexpressing hMAGL HEK293T cells was 1.5 μ g/mL (0.3 μ g per well). Inhibitors were added from 40x concentrated DMSO stocks. After 20 min. incubation, 100 μ L assay mix containing glycerol kinase (GK), glycerol-3-phosphate oxidase (GPO), horse radish peroxidase (HRP), adenosine triphosphate (ATP), Amplifu™Red and 2-arachidonoylglycerol (2-AG) was added and fluorescence was measured in 5 min. intervals for 60 min. on a plate reader. Final assay concentrations: 0.2 U/mL GK, GPO and HRP, 0.125 mM ATP, 10 μ M Amplifu™Red, 25 μ M 2-AG, 5% DMSO, 0.5% ACN in a total volume of 200 μ L. All measurements were performed in N = 2, n = 2 or N = 2, n = 4 for controls, with $Z' \geq 0.6$. For IC₅₀ determination, the MAGL-overexpressing membranes were incubated with different inhibitor concentrations. Slopes of corrected fluorescence in time were determined in the linear interval of t = 10 to t = 35 min and then scaled to the corrected positive control of hMAGL-overexpressing membranes treated with vehicle (DMSO) as a 100% activity reference point. The data was exported to GraphPad Prism 5.0 and analyzed in a non-linear dose-response analysis with variable slope.

Preparation of mouse brain membrane proteome. Mouse brains were isolated according to guidelines approved by the ethical committee of Leiden University (DEC#10095). Isolated brains were thawed on ice, dounce homogenized in lysis buffer A (20 mM Hepes, 2 mM DTT, 1 mM MgCl₂, 25 u/ml Benzonase, pH 7.2) and

incubated for 15 min on ice. Then debris was removed by low-speed spin (2500 g, 1 min, 4 °C) and the supernatant was subjected to ultracentrifugation (100.000 g, 45 min, 4 °C, Beckman Coulter, Type Ti70 rotor) to yielded the membrane fraction as a pellet. The pellet was resuspended in lysis buffer B (20 mM Hepes, 2 Mm DTT). The total protein concentration was determined with Quick Start Bradford assay. The obtained membranes were stored in small aliquots at -80 °C until use.

Activity based protein profiling. The competitive ABPP assay on mouse brain proteome was performed as previously reported.²⁰ In brief, to 19 µl mouse brain proteome (2mg/ml) was added 0.5 µl of the inhibitor or pure DMSO, vortexed gently and incubated for 30 min at RT. Subsequently, 0.5 µl probe was added to the proteome sample, vortexed gently and incubated for 10 min. The reaction was quenched by adding 10 µl of 4*Laemmli-buffer and 10 µl of quenched reaction mixture was resolved on 10 % acrylamide SDS-PAGE (180V, 75 min). Fluorescence was measured using a Biorad ChemiDoc MP system. Gels were then stained using Coomassie staining and imaged for protein loading control.

Chemical proteomics. Mouse brain proteome (245 µL, 2.0 mg/mL) membrane or soluble fraction was incubated with vehicle (DMSO) or inhibitor (1 µM) in DMSO for 30 minutes at 37 °C. The proteome was labeled with a probe cocktail (2.5 µM MB108 and 5 µM FP-Biotin, 30 minutes, 37 °C). Subsequently the labeling reaction was quenched and excess probe was removed by chloroform methanol precipitation. Precipitated proteome was suspended in 250 µL 6M Urea/25 mM ammonium bicarbonate and allowed to incubate overnight. 2.5 µL (1 M DTT) was added and the mixture was heated to 65 °C for 15 minutes. The sample was allowed to cool to rt before 20 µL (0.5 M) iodoacetamide was added and the sample was alkylated for 30 minutes in the dark. 70 µL 10% (wt/vol) SDS was added and the proteome was heated for 5 minutes at 65 °C. The sample was diluted with 6 mL PBS. 100 µL of 50% slurry of Avidin–Agarose from egg white (Sigma-Aldrich) was washed with PBS and added to the proteome sample. The beads were incubated with the proteome > 3h. The beads were isolated by centrifugation and washed with 0.5% (wt/vol) SDS and PBS (3x). The proteins were digested overnight with sequencing grade trypsin (Promega) in 250 µL

Hit Optimization of β -Sulfinyl Esters as Highly Potent and Selective MAGL Inhibitors

OB-Dig buffer (100 mM Tris, 100 mM NaCl, 1 mM CaCl₂, 2 % ACN and 500 ng trypsin) at 37 °C with vigorous shaking. The pH was adjusted with formic acid to pH 3 and the beads were removed from filtration. The peptides were washed and eluted with stage tips according to the procedure below.

Step	Solution	Centrifugation speed
Conditioning 1	50 μ L MeOH	2 min 300g
Conditioning 2	50 μ L Stage tip solution B	2 min 300g
Conditioning 3	50 μ L Stage tip solution A	2 min 300g
Loading		2 min 600g
Washing	100 μ L Stage tip solution A	2 min 600g
Elution	100 μ L Stage tip solution B	2 min 600g

Stage tip solution A: 0.5% (vol/vol) FA in H₂O. (Freshly prepared solution)

Stage tip solution B: 0.5% (vol/vol) FA in 80% (vol/vol) ACN/H₂O. (Freshly prepared solution).

After the final elution step, the obtained peptides were concentrated on a speedvac to remove the ACN. The residue was reconstituted in 95:3:0.1 H₂O/ACN/FA (vol/vol) before LC/MS analysis.

For LC-MS analysis, each sample in duplicate was loaded onto the ultra-performance liquid chromatography-ion mobility spectrometry-mass spectrometry system a NanoACQUITY UPLC System coupled to SYNAPT G2-Si high definition mass spectrometer²⁸. A trap-elute protocol was followed, where 1 μ L of the digest was loaded on a trap column (C18 100 Å, 5 μ M, 180 μ Mx20 mm; Waters), followed by elution and separation on an analytical column (HSS-T3 C18 1.8 μ M, 75 μ Mx250 mm; Waters). The sample was loaded onto this column at a flow rate of 10 μ L/min with 99.5% solvent A for 2 minutes before switching to the analytical column. Peptide separation was achieved by using a multistep concave gradient based on gradients previously described²⁹. The column was re-equilibrated to initial conditions after washing with 90% solvent B as previously described²⁹. The rear seals of the pump were flushed every 30 minutes with 10% (v/v) acetonitrile. [Glu1] fibrinopeptide B was used as a lock mass compound. The auxiliary pump of the LC system was used to deliver this peptide to the

reference sprayer (0.2 $\mu\text{L}/\text{min}$). An ultradefinition MSE method was set up as previously described²⁹. Briefly, the mass range was set at 50-2,000 Da, with a scan time of 0.6 seconds in positive resolution mode. The collision energy was set to 4 V in the trap cell for low-energy MS mode. For the elevated energy scan, the transfer cell collision energy was ramped using drift-time specific collision energies. The lock mass was sampled every 30 seconds.

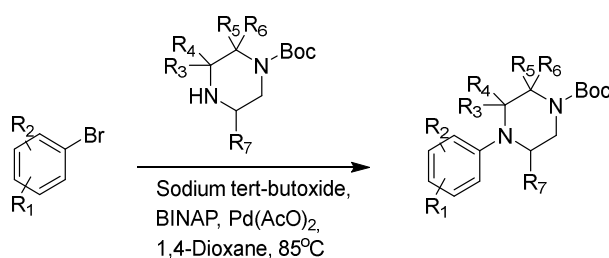
Docking studies. All docking studies were performed in the Schrödinger suite (Schrödinger Release 2017-4: Maestro, Schrödinger, LLC, New York, NY, 2017). The crystal structure of MAGL (PDB code: 3HJU) was prepared using the protein preparation wizard and ligands were prepared using LigPrep. Docking was done using induced fit docking with SP precision and poses with the best docking scores were manually examined. One pose per ligand was selected.

Chemistry procedures

General remarks. All reactions were performed using oven or flame-dried glassware and dry solvents. Reagents were purchased from Sigma Aldrich, Acros and Merck and used without further purification unless noted otherwise. All moisture sensitive reactions were performed under an argon or nitrogen atmosphere. Traces of water were removed from starting compounds by co-evaporation with toluene. Reactions were followed by thin layer chromatography and was performed using TLC Silica gel 60 F₂₄₅ on aluminum sheets. Compounds were visualized using a KMnO₄ stain (K₂CO₃ (40 g), KMnO₄ (6 g), H₂O (600 mL) and 10% NaOH (5 mL)). ¹H- and ¹³C-NMR spectra were recorded on a Bruker AV-400, 500, 600 or 850 using CDCl₃ or CD₃OD as solvent, unless stated otherwise. Chemical shift values are reported in ppm with tetramethylsilane or solvent resonance as the internal standard (CDCl₃: δ 7.26 for ¹H, δ 77.16 for ¹³C, CD₃OD: δ 3.31 for ¹H, δ 49.00 for ¹³C). Data are reported as follows: chemical shifts (δ), multiplicity (s = singlet, d = doublet, dd = double doublet, td = triple doublet, t = triplet, q = quartet, quint = quint, br = broad, m = multiplet), coupling constants *J* (Hz), and integration. LC-MS measurements were performed on a Thermo Finnigan LCQ Advantage Max ion-trap mass spectrometer (ESI⁺) coupled to a

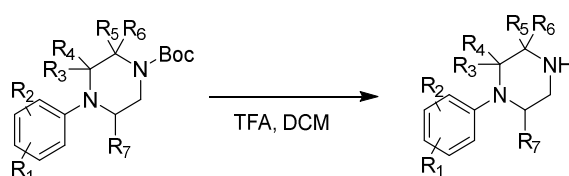
Surveyor HPLC system (Thermo Finnigan) equipped with a standard C18 (Gemini, 4.6 mmD \times 50 mmL, 5 μ m particle size, Phenomenex) analytical column and buffers A: H₂O, B: ACN, C: 0.1% aq. TFA. Preparative HPLC purification was performed on a Waters Acquity Ultra Performance LC with a C18 column (Gemini, 150 \times 21.2 mm, Phenomenex). Diode detection was done between 210 and 600 nm. Gradient: ACN in (H₂O + 0.2% TFA). High-resolution mass spectra (HRMS) were recorded on a Thermo Scientific LTQ Orbitrap XL.

General procedure A



A mixture of the appropriate bromobenzene (1 eq.), mono Boc-protected piperazine (1 eq.), palladium diacetate (0.04 eq.), BINAP (0.06 eq.) and sodium *tert*-butoxide (1.5 eq.) in degassed 1,4-dioxane was heated to 85 °C under nitrogen atmosphere overnight. The reaction progress was monitored by TLC analysis. Upon full conversion of the starting materials, the mixture was diluted with DCM, washed with water, dried (MgSO₄), filtered and concentrated under reduced pressure. The residue was purified by silica gel column chromatography (pentane/diethyl ether) to give the product.

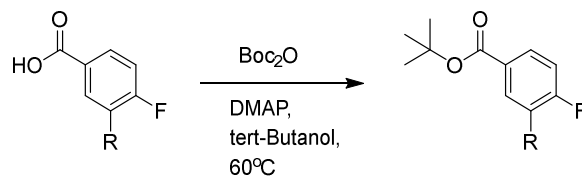
General procedure B



To a solution of the appropriate *tert*-butyl phenylpiperazine-1-carboxylate in DCM was added TFA (final TFA concentration, 20% v/v) and the mixture was stirred at room temperature for 2h. The reaction progress was monitored by TLC analysis. Upon full conversion of the starting materials, the mixture was diluted with DCM and washed with saturated aqueous NaHCO₃. The organic layer was dried (MgSO₄), filtered and

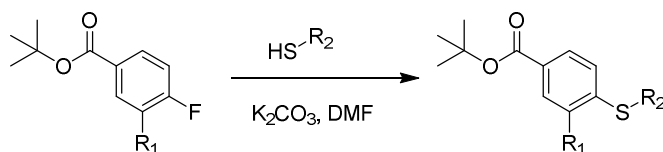
concentrated under reduced pressure. The residue was purified by silica gel column chromatography (DCM/MeOH) to give the product.

General procedure C



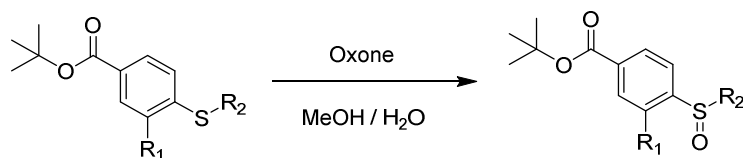
A mixture of the appropriate benzoic acid (1 eq.), di-*tert*-butyl dicarbonate (3 eq.) and DMAP (0.3 eq.) in *tert*-butanol was heated to 60 °C and stirred overnight. The reaction progress was monitored by TLC analysis. Upon full conversion of the starting materials, the solvent was evaporated and the residue was purified by silica gel column chromatography (pentane/diethyl ether) to give the product.

General procedure D



To a solution of the appropriate *tert*-butyl 4-fluorobenzoate (1.2 eq.) in ACN were added K₂CO₃ (3 eq.) and the appropriate thiol (1 eq.). The reaction mixture was stirred at RT overnight. The reaction progress was monitored by TLC analysis. Upon full conversion of the starting materials, the mixture was diluted with Et₂O and washed with water, dried (MgSO₄). After filtration, the filtrate was concentrated under reduced pressure. The residue was purified by silica gel column chromatography (pentane/diethyl ether).

General procedure E



To a cooled (0 °C) solution of the appropriate sulfure (1 eq.) in MeOH was dropwise added an oxone / water solution and the mixture was stirred at RT for 2h. The reaction progress was monitored by TLC analysis. Upon full conversion of the starting materials,

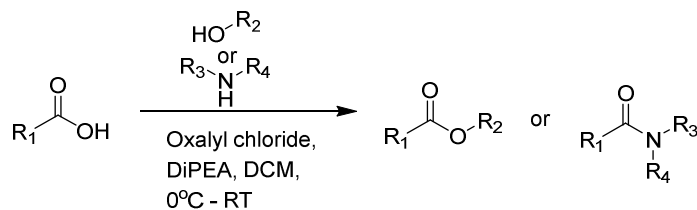
the mixture was diluted with EtOAc and washed with water. The organic layer was dried (MgSO_4), filtered and concentrated under reduced pressure. The residue was purified by silica column chromatography (pentane/EtOAc).

General procedure F



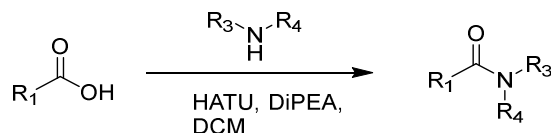
To a solution of the appropriate *tert*-butyl protected carboxylic acid in DCM was added TFA (final TFA concentration, 20% v/v) and the mixture was stirred at RT for 6 h. The reaction progress was monitored by TLC analysis. Upon full conversion of the starting materials, the solvent was removed under reduced pressure and the residue was purified silica gel column chromatography (DCM/MeOH).

General procedure G



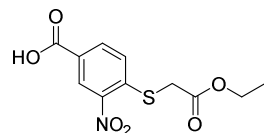
To a cooled solution of the appropriate carboxylic acid (1 eq.) in dried DCM was subsequently added 2 drops of DMF and oxalyl chloride (1.2 eq.). Then the mixture was allowed to warm to room temperature and continuously stirred for 2h. The reaction progress was monitored by TLC analysis. Upon full conversion of the starting materials, the mixture was dropwise added to a cooled (0 °C) solution of the appropriate alcohol (3eq.) or amine (3eq.) and DiPEA (3 eq.) in DCM. Then the reaction mixture was stirred at room temperature overnight. The reaction progress was monitored by TLC analysis. Upon full conversion of the starting materials, the mixture was diluted with DCM and washed with water, dried (MgSO_4), filtered and concentrated under reduced pressure. The residue was purified by HPLC-MS.

General procedure H



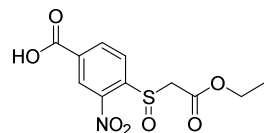
To a suspension or solution of the appropriate benzoic acid (1 eq.) in DCM was added HATU (1.5 eq.) and DiPEA (3 eq.) and then the mixture was stirred at room temperature for 1h. The appropriate phenylpiperazine (1eq.) was added and the mixture was stirred overnight. The reaction progress was monitored by TLC analysis. Upon full conversion of the starting materials, the mixture was diluted with DCM and washed with water, dried (MgSO₄), filtered and concentrated under reduce pressure. The residue was purified by silica gel column chromatography (pentane/EtOAc) or HPLC-MS.

4-((2-Ethoxy-2-oxoethyl)thio)-3-nitrobenzoic acid (60)



To a solution of 4-chloro-3-nitrobenzoic acid (1.26 mg, 6.24 mmol, 1.50 eq.) in pyridine (5 mL) was added ethyl mercaptoacetate (0.5 g, 4.16 mmol, 1.00 eq.) and the mixture was heated to 115 °C overnight in an oil bath. The reaction progress was monitored by TLC analysis. Upon full conversion of the starting materials, the mixture was allowed to cool to rt and the pH was adjusted to 1 with 1M HCl solution. The precipitate was filtered and the solid were washed with water to provide the product (1.01 g, 3.54 mmol, 85%). ¹H NMR (400 MHz, Methanol-*d*₄) δ 8.73 (d, *J* = 1.9 Hz, 1H), 8.16 (dd, *J* = 8.5, 1.9 Hz, 1H), 7.66 (d, *J* = 8.5 Hz, 1H), 4.20 (q, *J* = 7.1 Hz, 2H), 4.00 (s, 2H), 1.25 (t, *J* = 7.1 Hz, 3H). ¹³C NMR (101 MHz, Methanol-*d*₄) δ 170.38, 167.34, 143.24, 135.02, 129.44, 128.46, 128.08, 63.20, 35.65, 14.53.

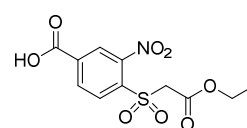
4-((2-Ethoxy-2-oxoethyl)sulfinyl)-3-nitrobenzoic acid (61)



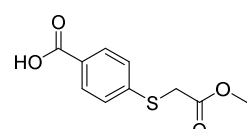
To a cooled solution of 4-((2-ethoxy-2-oxoethyl)thio)-3-nitrobenzoic acid (285 mg, 1.00 mmol, 1.00 eq.) in methanol (13mL) was dropwise added a solution of oxone (62 mg, 1.00 mmol, 1.00 eq.) in water (4 mL) and the reaction mixture was stirred at rt for 2.5 h. The reaction progress was monitored by TLC analysis. Upon full conversion of the starting materials, the mixture was diluted with water and extracted with DCM. The combined

organic layers were washed with brine, dried (MgSO_4), filtered and concentrated under reduced pressure. The residue was purified by silica gel column chromatography (MeOH/DCM, 1% \rightarrow 2%) to afford the product (210 mg, 0.70 mmol, 70%). ^1H NMR (400 MHz, Methanol- d_4) δ 8.88 (d, $J = 1.6$ Hz, 1H), 8.61 (dd, $J = 8.2, 1.6$ Hz, 1H), 8.34 (d, $J = 8.2$ Hz, 1H), 4.36 (d, $J = 14.4$ Hz, 1H), 4.29 – 4.13 (m, 2H), 3.82 (d, $J = 14.5$ Hz, 1H), 1.26 (t, $J = 7.1$ Hz, 3H). ^{13}C NMR (101 MHz, Methanol- d_4) δ 166.82, 166.60, 147.30, 136.89, 136.55, 128.43, 127.26, 63.37, 61.32, 14.54.

4-((2-Ethoxy-2-oxoethyl)sulfonyl)-3-nitrobenzoic acid (62)

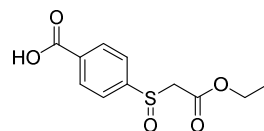
 To a solution of 4-((2-ethoxy-2-oxoethyl)thio)-3-nitrobenzoic acid (1.10 g, 3.86 mmol, 1.00 eq.) in AcOH (20mL) was added H_2O_2 (35%, 5mL), *tert*-butylammonium hydrogen sulfate (65 mg, 0.19 mmol, 0.05 eq.) and sodium tungstate dihydrate (127 mg, 0.39 mmol, 0.1 eq.) and the reaction mixture was refluxed for 3h. The reaction progress was monitored by TLC analysis. Upon full conversion of the starting materials, the mixture was cooled down to rt and diluted with water, extracted with EtOAc and dried (MgSO_4), filtered and concentrated under reduced pressure. The residue was purified by silica gel column chromatography (MeOH/DCM, 1% \rightarrow 2%) to afford the product (0.62g, 1.95 mmol, 51%). ^1H NMR (400 MHz, DMSO- d_6) δ 8.51 (d, $J = 1.6$ Hz, 1H), 8.43 (dd, $J = 8.2, 1.7$ Hz, 1H), 8.26 (d, $J = 8.2$ Hz, 1H), 4.93 (s, 2H), 4.10 (q, $J = 7.1$ Hz, 2H), 1.10 (t, $J = 7.1$ Hz, 3H). ^{13}C NMR (101 MHz, DMSO- d_6) δ 164.46, 162.06, 148.41, 137.81, 134.35, 133.34, 133.28, 125.63, 62.09, 60.66, 13.71.

4-((2-Ethoxy-2-oxoethyl)thio)benzoic acid (63)

 To a suspension of 4-mercaptobenzoic acid (0.46 g, 2.99 mmol, 1.00 eq.) in water (5mL) was added NaOH (0.18 g, 4.49 mmol, 1.50 eq.) and the resulting solution was stirred for 30min at room temperature. Then ethyl 2-bromoacetate (0.50 g, 2.99 mmol, 1.00 eq.) was slowly added to the solution and the reaction mixture was stirred for another 2h at rt. The reaction progress was monitored by TLC analysis. Upon full conversion of the starting materials, the mixture was acidified with 1M HCl and the obtained precipitate was filtered, washed with water and dried to give the product (252 mg, 1.05 mmol, 35 %). ^1H NMR

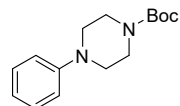
(CDCl₃, 400 MHz) δ 7.88 (d, J = 8.3 Hz, 2H), 7.40 – 7.26 (d, J = 8.3 Hz, 2H), 4.10 (q, J = 7.3 Hz, 2H), 3.79 (s, 2H), 1.15 (t, J = 7.2 Hz, 3H). ¹³C NMR (MeOD, 101 MHz) δ 170.94, 169.28, 143.74, 131.16, 129.19, 127.98, 62.72, 35.35, 14.37.

4-((2-Ethoxy-2-oxoethyl)sulfinyl)benzoic acid (64)



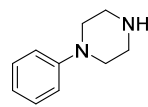
To a cooled solution of 4-((2-ethoxy-2-oxoethyl)thio)benzoic acid (100 mg, 0.42 mmol, 1.00 eq.) in methanol (5mL) was dropwise added a solution of oxone (26 mg, 1.00 mmol, 1.00 eq.) in water (5 mL) and the reaction mixture was stirred at rt for 2.5 h. The reaction progress was monitored by TLC analysis. Upon full conversion of the starting materials, the mixture was diluted with water and extracted with DCM. The combined organic layers were washed with brine, dried (MgSO₄), filtered and concentrated under reduced pressure. The residue was purified by silica gel column chromatography (MeOH/DCM, 1%→2%) to afford the product (83mg, 0.33 mmol, 78%). ¹H NMR (400 MHz, Methanol-*d*₄) δ 8.22 (d, J = 8.5 Hz, 2H), 7.84 (d, J = 8.5 Hz, 2H), 4.16 (q, J = 7.1 Hz, 2H), 4.06 (d, J = 14.4 Hz, 1H), 3.94 (d, J = 14.3 Hz, 1H), 1.20 (t, J = 7.1 Hz, 3H). ¹³C NMR (101 MHz, Methanol-*d*₄) δ 168.37, 166.14, 148.49, 135.28, 131.64, 125.61, 63.07, 61.45, 14.33.

tert-Butyl 4-phenylpiperazine-1-carboxylate (6a)



The title compound was synthesized using bromobenzene (160 mg, 1.00 mmol, 1 eq.), *tert*-butyl piperazine-1-carboxylate (190 mg, 1.00 mmol, 1 eq.), sodium *tert*-butoxide (240 mg, 2.50 mmol, 2.5 eq.), *rac*-BINAP (60 mg, 0.10 mmol, 0.10 eq.) and palladium diacetate (3 mg, 0.015 mmol, 0.015 eq.) according to general procedure A in a yield of 252mg (0.10 mmol, 97%). ¹H NMR (400 MHz, CDCl₃) δ 7.31 – 7.25 (m, 2H), 6.97 – 6.91 (m, 2H), 6.91 – 6.86 (m, 1H), 3.58 (t, J = 5.2 Hz, 4H), 3.13 (t, J = 5.2 Hz, 4H), 1.48 (s, 9H). ¹³C NMR (101 MHz, CDCl₃) δ 154.82, 151.37, 129.28, 120.37, 116.72, 79.95, 49.51, 28.53.

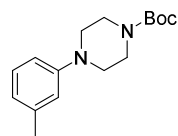
1-Phenylpiperazine (6b)



The title compound was synthesized using *tert*-butyl 4-phenylpiperazine-1-carboxylate (100 mg, 0.38 mmol, 1 eq.) according to general procedure B in a yield of 54 mg (0.34 mmol, 89%). ¹H NMR (400 MHz, CDCl₃) δ 7.31 – 7.21 (m, 2H), 6.96 – 6.88 (m, 2H), 6.90 – 6.81 (m, 1H), 3.13 (t, J = 5.2 Hz, 4H), 3.02 (t, J = 5.2 Hz,

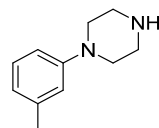
4H), 2.37 (s, 1H). ^{13}C NMR (101 MHz, CDCl_3) δ 151.57, 129.20, 120.46, 116.63, 83.53.

***tert*-Butyl 4-(*m*-tolyl)piperazine-1-carboxylate (2a)**



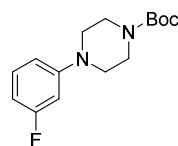
The title compound was synthesized using 1-bromo-3-methylbenzene (0.50 g, 2.92 mmol, 1 eq.), *tert*-butyl piperazine-1-carboxylate (0.82 g, 4.39 mmol, 1.5 eq.), cesium carbonate (1.43 g, 4.39 mmol, 1.5 eq.), rac-BINAP (116 mg, 0.18 mmol, 0.06 eq.) and palladium diacetate (26.3 mg, 0.12 mmol, 0.04 eq.) according to general procedure A in a yield of 0.75 g (2.70 mmol, 92%). ^1H NMR (400 MHz, CDCl_3) δ 7.13 (t, $J = 7.8$ Hz, 1H), 6.75 – 6.64 (m, 3H), 3.54 (t, $J = 5.2$ Hz, 4H), 3.06 (t, $J = 5.2$ Hz, 4H), 2.30 (s, 3H), 1.48 (s, 9H). ^{13}C NMR (101 MHz, CDCl_3) δ 154.51, 151.22, 138.59, 128.86, 121.01, 117.33, 113.63, 79.57, 49.34, 28.32, 21.63.

1-(*m*-Tolyl)piperazine (2b)



The title compound was synthesized using *tert*-butyl 4-(*m*-tolyl)piperazine-1-carboxylate (0.75 g, 2.70 mmol, 1 eq.) according to general procedure B in a yield of 450 mg (2.55 mmol, 95%). ^1H NMR (400 MHz, CDCl_3) δ 7.19 (dd, $J = 8.2, 7.2$ Hz, 1H), 6.85 – 6.68 (m, 3H), 5.93 (s, 1H), 3.37 – 3.27 (m, 4H), 3.26 – 3.19 (m, 4H), 2.35 (s, 3H). ^{13}C NMR (101 MHz, CDCl_3) δ 150.88, 138.88, 129.02, 121.48, 117.42, 113.72, 48.52, 44.66, 21.70.

***tert*-Butyl 4-(3-fluorophenyl)piperazine-1-carboxylate (7a)**



The title compound was synthesized using 1-bromo-3-fluorobenzene (100 mg, 0.57 mmol, 1 eq.), *tert*-butyl piperazine-1-carboxylate (128 mg, 0.69 mmol, 1.2 eq.), sodium *tert*-butoxide (82 mg, 0.86 mmol, 1.5 eq.), rac-BINAP (21 mg, 0.034 mmol, 0.06 eq.) and palladium diacetate (5 mg, 0.023 mmol, 0.04 eq.) according to general procedure A in a yield of 145 mg (0.52 mmol, 91%).

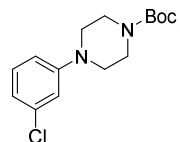
1-(3-Fluorophenyl)piperazine (7b)



The title compound was synthesized using *tert*-butyl 4-(3-fluorophenyl)piperazine-1-carboxylate (100 mg, 0.36 mmol, 1 eq.) according to general procedure B in a yield of 62 mg (0.34 mmol, 96%). ^1H NMR (400 MHz, CDCl_3) δ 7.19 (td, $J = 8.2, 7.0$ Hz, 1H), 6.67 (ddd, $J = 8.4, 2.4, 0.8$ Hz, 1H), 6.62 – 6.46 (m, 2H), 3.37 (br, 1H), 3.25 – 3.12 (m, 4H), 3.08 – 2.95 (m, 4H).

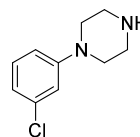
^{13}C NMR (101 MHz, CDCl_3) δ 163.89 (d, $J = 243.2$ Hz), 153.32 (d, $J = 9.7$ Hz), 130.19 (d, $J = 10.0$ Hz), 111.30, 106.05 (d, $J = 21.5$ Hz), 102.80 (d, $J = 25.0$ Hz), 49.54, 45.76.

***tert*-Butyl 4-(3-chlorophenyl)piperazine-1-carboxylate (8a)**



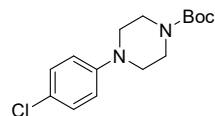
The title compound was synthesized using 1-bromo-3-chlorobenzene (191 mg, 1.00 mmol, 1 eq.), *tert*-butyl piperazine-1-carboxylate (186 mg, 1.00 mmol, 1.00 eq.), sodium *tert*-butoxide (144 mg, 1.50 mmol, 1.5 eq.), rac-BINAP (37.4 mg, 0.06 mmol, 0.06 eq.) and palladium diacetate (9 mg, 0.04 mmol, 0.04 eq.) according to general procedure A in a yield of 190 mg (0.64 mmol, 64 %). ^1H NMR (400 MHz, CDCl_3) δ 7.16 (t, $J = 8.1$ Hz, 1H), 6.87 (t, $J = 2.2$ Hz, 1H), 6.82 (ddd, $J = 7.9, 2.0, 0.9$ Hz, 1H), 6.77 (ddd, $J = 8.4, 2.4, 0.9$ Hz, 1H), 3.97 – 3.35 (m, 4H), 3.12 (t, $J = 5.2$ Hz, 4H), 1.48 (s, 9H). ^{13}C NMR (101 MHz, CDCl_3) δ 154.67, 152.31, 134.99, 130.15, 119.83, 116.30, 114.44, 80.01, 48.89, 28.45.

1-(3-Chlorophenyl)piperazine (8b)



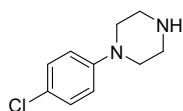
The title compound was synthesized using *tert*-butyl 4-(3-chlorophenyl)piperazine-1-carboxylate (100 mg, 0.34 mmol, 1 eq.) according to general procedure B in a yield of 62 mg (0.31 mmol, 93 %). ^1H NMR (400 MHz, CDCl_3) δ 7.18 (t, $J = 8.0$ Hz, 1H), 6.94 – 6.67 (m, 3H), 6.47 (br, 1H), 3.24 (t, $J = 5.1$ Hz, 4H), 3.14 (t, $J = 5.2$ Hz, 4H). ^{13}C NMR (101 MHz, CDCl_3) δ 152.09, 135.03, 130.23, 120.18, 116.31, 114.43, 48.41, 44.78.

***tert*-Butyl 4-(4-chlorophenyl)piperazine-1-carboxylate (9a)**



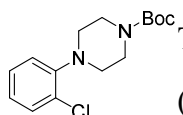
The title compound was synthesized using 1-bromo-4-chlorobenzene (191 mg, 1.00 mmol, 1 eq.), *tert*-butyl piperazine-1-carboxylate (186 mg, 1 mmol, 1.00 eq.), sodium *tert*-butoxide (144 mg, 1.50 mmol, 1.5 eq.), rac-BINAP (37.4 mg, 0.06 mmol, 0.06 eq.) and palladium diacetate (9 mg, 0.04 mmol, 0.04 eq.) according to general procedure A in a yield of 264 mg (0.89 mmol, 89 %). ^1H NMR (400 MHz, CDCl_3) δ 7.24 – 7.16 (m, 2H), 6.86 – 6.76 (m, 2H), 3.62 – 3.49 (m, 4H), 3.08 (t, $J = 5.2$ Hz, 4H), 1.48 (s, 9H). ^{13}C NMR (101 MHz, CDCl_3) δ 154.73, 149.97, 129.11, 125.18, 117.89, 80.05, 49.48, 28.50.

1-(4-Chlorophenyl)piperazine (9b)



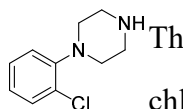
The title compound was synthesized using *tert*-butyl 4-(4-chlorophenyl)piperazine-1-carboxylate (100 mg, 0.34 mmol, 1 eq.) according to general procedure B in a yield of 66 mg (0.33 mmol, 99 %). ^1H NMR (400 MHz, CDCl_3) δ 7.23 – 7.17 (m, 2H), 6.86 – 6.79 (m, 2H), 3.12 (dt, $J = 6.1, 3.7$ Hz, 4H), 3.05 (dd, $J = 6.4, 3.3$ Hz, 4H). ^{13}C NMR (101 MHz, CDCl_3) δ 150.32, 129.06, 124.84, 117.50, 50.10, 45.81.

***tert*-Butyl 4-(2-chlorophenyl)piperazine-1-carboxylate (10a)**



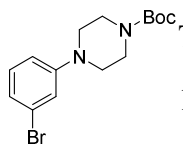
The title compound was synthesized using 1-bromo-2-chlorobenzene (191 mg, 1.00 mmol, 1 eq.), *tert*-butyl piperazine-1-carboxylate (186 mg, 1 mmol, 1.00 eq.), sodium *tert*-butoxide (144 mg, 1.50 mmol, 1.5 eq.), rac-BINAP (37.4 mg, 0.06 mmol, 0.06 eq.) and palladium diacetate (9 mg, 0.04 mmol, 0.04 eq.) according to general procedure A in a yield of 241 mg (0.81 mmol, 81 %). ^1H NMR (400 MHz, CDCl_3) δ 7.35 (dt, $J = 7.9, 1.6$ Hz, 1H), 7.28 – 7.11 (m, 1H), 7.05 – 6.89 (m, 2H), 3.68 – 3.49 (m, 4H), 3.09 – 2.83 (m, 4H), 1.49 (s, 9H). ^{13}C NMR (101 MHz, CDCl_3) δ 154.74, 149.05, 130.62, 128.87, 127.58, 123.95, 120.45, 79.66, 51.18, 44.08, 28.42.

1-(2-Chlorophenyl)piperazine (10b)



The title compound was synthesized using *tert*-butyl 4-(2-chlorophenyl)piperazine-1-carboxylate (100 mg, 0.34 mmol, 1 eq.) according to general procedure B in a yield of 63 mg (0.32 mmol, 95 %). ^1H NMR (400 MHz, CDCl_3) δ 7.35 (d, $J = 8.0$ Hz, 1H), 7.22 (t, $J = 7.7$ Hz, 1H), 7.08 – 6.90 (m, 2H), 4.27 (br, 1H), 3.21 – 2.86 (m, 8H). ^{13}C NMR (101 MHz, CDCl_3) δ 149.21, 131.61, 130.64, 127.65, 123.94, 120.50, 51.62, 45.63.

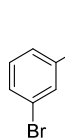
***tert*-Butyl 4-(3-bromophenyl)piperazine-1-carboxylate (11a)**



The title compound was synthesized using 1,3-dibromobenzene (236 mg, 1.00 mmol, 1 eq.), *tert*-butyl piperazine-1-carboxylate (186 mg, 1 mmol, 1.00 eq.), sodium *tert*-butoxide (144 mg, 1.50 mmol, 1.5 eq.), rac-BINAP (37.4 mg, 0.06 mmol, 0.06 eq.) and palladium diacetate (9 mg, 0.04 mmol, 0.04 eq.) according to general procedure A in a yield of 259 mg (0.76 mmol, 76 %). ^1H NMR (400 MHz, CDCl_3) δ 7.10 (t, $J = 8.1$ Hz, 1H), 7.02 (t, $J = 2.1$ Hz, 1H), 6.97 (ddd, $J = 7.9, 1.8, 0.9$ Hz, 1H), 6.81 (ddd, $J = 8.3, 2.5, 0.9$ Hz, 1H), 3.62 – 3.46 (m, 4H), 3.11 (t,

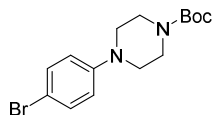
$J = 5.1$ Hz, 4H), 1.48 (s, 9H). ^{13}C NMR (101 MHz, CDCl_3) δ 154.66, 152.45, 130.44, 123.26, 122.79, 119.24, 114.94, 80.02, 48.91, 43.69, 28.46.

1-(3-Bromophenyl)piperazine (11b)



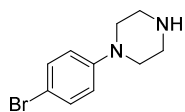
The title compound was synthesized using *tert*-butyl 4-(3-bromophenyl)piperazine-1-carboxylate (100 mg, 0.29 mmol, 1 eq.) according to general procedure B in a yield of 66 mg (0.28 mmol, 94 %). ^1H NMR (400 MHz, CDCl_3) δ 7.14 – 7.05 (m, 1H), 7.02 (t, $J = 2.1$ Hz, 1H), 6.98 – 6.89 (m, 1H), 6.82 (ddd, $J = 8.4, 2.5, 0.9$ Hz, 1H), 3.12 (m, 4H), 3.03 – 2.94 (m, 4H), 1.84 (s, 1H). ^{13}C NMR (101 MHz, CDCl_3) δ 153.02, 130.35, 123.27, 122.23, 118.71, 114.44, 49.89, 46.02.

tert-Butyl 4-(4-bromophenyl)piperazine-1-carboxylate (12a)



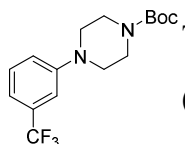
The title compound was synthesized using 1,4-dibromobenzene (236 mg, 1.00 mmol, 1 eq.), *tert*-butyl piperazine-1-carboxylate (186 mg, 1 mmol, 1.00 eq.), sodium *tert*-butoxide (144 mg, 1.50 mmol, 1.5 eq.), rac-BINAP (37.4 mg, 0.06 mmol, 0.06 eq.) and palladium diacetate (9 mg, 0.04 mmol, 0.04 eq.) according to general procedure A in a yield of 256 mg (0.75 mmol, 75 %). ^1H NMR (400 MHz, CDCl_3) δ 7.38 – 7.31 (m, 2H), 6.82 – 6.73 (m, 2H), 3.68 – 3.41 (m, 4H), 3.09 (t, $J = 5.2$ Hz, 4H), 1.48 (s, 9H). ^{13}C NMR (101 MHz, CDCl_3) δ 154.71, 150.33, 132.02, 118.25, 112.49, 80.06, 49.29, 43.74, 28.50.

1-(4-Bromophenyl)piperazine (12b)



The title compound was synthesized using *tert*-butyl 4-(4-bromophenyl)piperazine-1-carboxylate (100 mg, 0.29 mmol, 1 eq.) according to general procedure B in a yield of 66 mg (0.28 mmol, 93 %). ^1H NMR (400 MHz, CDCl_3) δ 7.37 – 7.31 (m, 2H), 6.82 – 6.75 (m, 2H), 3.16 – 3.09 (m, 4H), 3.07 – 2.97 (m, 4H). ^{13}C NMR (101 MHz, CDCl_3) δ 150.80, 131.98, 117.85, 112.07, 50.07, 45.91.

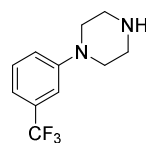
tert-Butyl 4-(3-(trifluoromethyl)phenyl)piperazine-1-carboxylate (13a)



The title compound was synthesized using 1-bromo-3-(trifluoromethyl)benzene (225 mg, 1.00 mmol, 1 eq.), *tert*-butyl piperazine-1-carboxylate (186 mg, 1 mmol, 1.00 eq.), sodium *tert*-

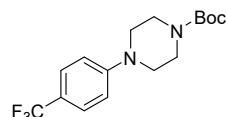
butoxide (144 mg, 1.50 mmol, 1.5 eq.), rac-BINAP (37.4 mg, 0.06 mmol, 0.06 eq.) and palladium diacetate (9 mg, 0.04 mmol, 0.04 eq.) according to general procedure A in a yield of 289 mg (0.88 mmol, 88 %). ^1H NMR (400 MHz, CDCl_3) δ 8.36 (ddt, $J = 8.2, 7.2, 0.9$ Hz, 1H), 8.14 – 8.05 (m, 3H), 4.65 – 4.55 (m, 4H), 4.19 (t, $J = 5.2$ Hz, 4H), 2.49 (s, 9H). ^{13}C NMR (101 MHz, CDCl_3) δ 154.78, 151.41, 131.65 (q, $J = 31.7$ Hz), 129.79, 124.35 (q, $J = 272.70$ Hz), 119.51, 116.65 (q, $J = 3.6$ Hz), 112.89 (q, $J = 3.8$ Hz), 80.22, 49.10, 28.54.

1-(3-(Trifluoromethyl)phenyl)piperazine (13b)



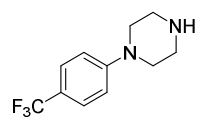
The title compound was synthesized using *tert*-butyl 4-(3-(trifluoromethyl)phenyl)piperazine-1-carboxylate (100 mg, 0.30 mmol, 1 eq.) according to general procedure B in a yield of 68 mg (0.29 mmol, 97 %). ^1H NMR (400 MHz, CDCl_3) δ 7.34 (t, $J = 7.9$ Hz, 1H), 7.17 – 6.99 (m, 3H), 3.87 (s, 1H), 3.27 – 3.19 (m, 4H), 3.14 – 3.01 (m, 4H). ^{13}C NMR (101 MHz, CDCl_3) δ 151.62, 131.43 (q, $J = 31.7$ Hz), 129.65, 124.35 (q, $J = 272.4$ Hz), 119.03, 116.19 (q, $J = 3.8$ Hz), 112.39 (q, $J = 3.9$ Hz), 49.24, 45.50.

tert-Butyl 4-(4-(trifluoromethyl)phenyl)piperazine-1-carboxylate (14a)



The title compound was synthesized using 1-bromo-4-(trifluoromethyl)benzene (225 mg, 1.00 mmol, 1 eq.), *tert*-butyl piperazine-1-carboxylate (186 mg, 1 mmol, 1.00 eq.), sodium *tert*-butoxide (144 mg, 1.50 mmol, 1.5 eq.), rac-BINAP (37.4 mg, 0.06 mmol, 0.06 eq.) and palladium diacetate (9 mg, 0.04 mmol, 0.04 eq.) according to general procedure A in a yield of 218 mg (0.66 mmol, 66 %). ^1H NMR (400 MHz, CDCl_3) δ 7.55 – 7.44 (m, 2H), 6.95 (d, $J = 8.7$ Hz, 2H), 3.65 – 3.53 (m, 4H), 3.25 (t, $J = 5.2$ Hz, 4H), 1.49 (s, 9 H).

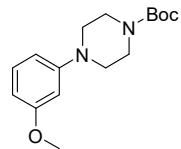
1-(4-(Trifluoromethyl)phenyl)piperazine (14b)



The title compound was synthesized using *tert*-butyl 4-(4-(trifluoromethyl)phenyl)piperazine-1-carboxylate (100 mg, 0.30 mmol, 1 eq.) according to general procedure B in a yield of 60 mg (0.26 mmol, 86 %). ^1H NMR (400 MHz, CDCl_3) δ 7.48 (d, $J = 8.7$ Hz, 2H), 6.92 (d, $J = 8.6$ Hz, 2H), 4.26 (br, 1H), 3.36 – 3.24 (m, 4H), 3.13 – 3.04 (m, 4H). ^{13}C NMR (101 MHz, CDCl_3) δ 153.48,

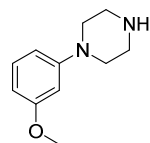
126.47 (q, $J = 3.7$ Hz), 124.75 (q, $J = 271.69$ Hz), 120.86 (q, $J = 32.6$ Hz), 114.82, 48.49, 45.36.

***tert*-Butyl 4-(3-methoxyphenyl)piperazine-1-carboxylate (15a)**



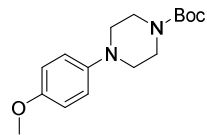
The title compound was synthesized using 1-bromo-3-methoxybenzene (374 mg, 2.00 mmol, 1 eq.), *tert*-butyl piperazine-1-carboxylate (373 mg, 2 mmol, 1.00 eq.), sodium *tert*-butoxide (288 mg, 3.00 mmol, 1.5 eq.), rac-BINAP (75 mg, 0.12 mmol, 0.06 eq.) and palladium diacetate (18 mg, 0.08 mmol, 0.04 eq.) according to general procedure A in a yield of 433 mg (1.48 mmol, 74 %). ^1H NMR (400 MHz, CDCl_3) δ 7.16 (t, $J = 8.1$ Hz, 1H), 6.52 (dd, $J = 8.3, 2.5$ Hz, 1H), 6.47 – 6.41 (m, 2H), 3.77 (s, 3H), 3.56 (t, $J = 5.0$ Hz, 4H), 3.21 – 2.99 (m, 4H), 1.48 (s, 9H). ^{13}C NMR (101 MHz, CDCl_3) δ 160.57, 154.63, 152.61, 129.81, 109.25, 104.93, 102.95, 79.77, 55.10, 49.25, 28.41.

1-(3-Methoxyphenyl)piperazine (15b)



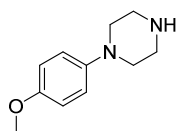
The title compound was synthesized using *tert*-butyl 4-(4-(trifluoromethyl)phenyl)piperazine-1-carboxylate (200 mg, 0.68 mmol, 1 eq.) according to general procedure B in a yield of 130 mg (0.68 mmol, 99 %). ^1H NMR (400 MHz, CDCl_3) δ 9.73 (br, 1H), 7.21 (t, $J = 8.2$ Hz, 1H), 6.55 – 6.49 (m, 2H), 6.45 (t, $J = 2.3$ Hz, 1H), 3.79 (s, 3H), 3.41 (m, 4H), 3.33 (m, 4H). ^{13}C NMR (101 MHz, CDCl_3) δ 160.81, 151.45, 130.32, 109.86, 106.53, 103.90, 55.39, 46.99, 43.47.

***tert*-Butyl 4-(4-methoxyphenyl)piperazine-1-carboxylate (16a)**



The title compound was synthesized using 1-bromo-4-methoxybenzene (500 mg, 2.67 mmol, 1 eq.), *tert*-butyl piperazine-1-carboxylate (597 mg, 3.21 mmol, 1.2 eq.), cesium carbonate (1307 mg, 4.01 mmol, 1.5 eq.), rac-BINAP (106 mg, 0.16 mmol, 0.06 eq.) and palladium diacetate (24 mg, 0.11 mmol, 0.04 eq.) according to general procedure A in a yield of 438 mg (1.50 mmol, 56 %). ^1H NMR (400 MHz, CDCl_3) δ 6.91 – 6.72 (m, 4H), 3.70 (s, 3H), 3.60 – 3.46 (m, 4H), 3.01 – 2.87 (m, 4H), 1.45 (s, 9H). ^{13}C NMR (101 MHz, CDCl_3) δ 154.52, 154.07, 145.48, 118.68, 114.30, 79.57, 55.31, 50.76, 28.32.

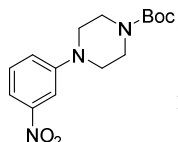
1-(4-Methoxyphenyl)piperazine (16b)



The title compound was synthesized using *tert*-butyl 4-(4-methoxyphenyl)piperazine-1-carboxylate (438 mg, 1.50 mmol, 1 eq.) according to general procedure B in a yield of 260 mg (1.35 mmol, 90%).

^1H NMR (400 MHz, CDCl_3) δ 6.89 – 6.77 (m, 4H), 3.70 (s, 3H), 2.96 (m, 8H). ^{13}C NMR (101 MHz, CDCl_3) δ 153.66, 146.20, 118.07, 114.30, 55.38, 51.76, 46.20.

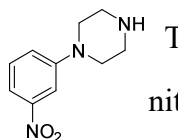
***tert*-Butyl 4-(3-nitrophenyl)piperazine-1-carboxylate (17a)**



The title compound was synthesized using 1-bromo-3-nitrobenzene (202 mg, 1.00 mmol, 1 eq.), *tert*-butyl piperazine-1-carboxylate (186 mg, 1 mmol, 1.00 eq.), sodium *tert*-butoxide (144 mg, 1.50 mmol, 1.5 eq.), rac-BINAP (37 mg, 0.06 mmol, 0.06 eq.) and palladium diacetate (9 mg, 0.04 mmol, 0.04 eq.) according to general procedure A in a yield of 150 mg (0.49 mmol, 49 %).

^1H NMR (400 MHz, CDCl_3) δ 7.80 – 7.55 (m, 2H), 7.39 (t, $J = 8.2$ Hz, 1H), 7.20 (dd, $J = 8.4, 2.5$ Hz, 1H), 4.03 – 3.44 (t, $J = 5.2$ Hz, 4H), 3.25 (t, $J = 5.2$ Hz, 4H), 1.50 (s, 9H). ^{13}C NMR (101 MHz, CDCl_3) δ 154.57, 151.71, 149.17, 129.79, 121.61, 114.61, 110.02, 80.13, 48.44, 28.38.

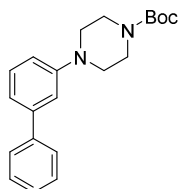
1-(3-Nitrophenyl)piperazine (17b)



The title compound was synthesized using *tert*-butyl 4-(3-nitrophenyl)piperazine-1-carboxylate (100 mg, 0.33 mmol, 1 eq.) according to general procedure B in a yield of 66 mg (0.32 mmol, 98%).

^1H NMR (400 MHz, CDCl_3) δ 7.71 (d, $J = 2.1$ Hz, 1H), 7.65 (d, $J = 8.0$ Hz, 1H), 7.38 (t, $J = 8.2$ Hz, 1H), 7.19 (d, $J = 8.3, 2.5$ Hz, 1H), 3.40 – 3.16 (m, 4H), 3.13 – 2.95 (m, 4H). ^{13}C NMR (101 MHz, CDCl_3) δ 152.31, 149.32, 129.76, 121.27, 113.80, 109.74, 49.48, 45.88.

***tert*-Butyl 4-([1,1'-biphenyl]-3-yl)piperazine-1-carboxylate (18a)**

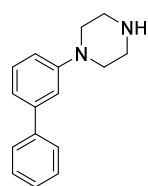


To a mixture of phenylboronic acid (107 mg, 0.88 mmol, 1.5 eq.) and *tert*-butyl 4-(3-bromophenyl)piperazine-1-carboxylate (200 mg, 0.59 mmol, 1 eq.) in 1,4-dioxane (5mL) was added cesium carbonate (573 mg, 1.76 mmol, 3 eq.) and tetrakis(triphenylphosphine)palladium (14 mg, 0.012 mmol, 0.02 eq.).

Then the reaction mixture was degassed with N_2 for 30 min. The mixture was heated to 80 °C for 5h. The reaction progress was monitored by TLC analysis. Upon full conversion of the starting materials, the mixture was diluted with

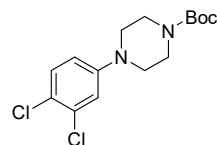
DCM and washed with water, dried (MgSO₄), filtered and concentrated under reduced pressure. The residue was purified by silica gel column chromatography (Et₂O / pentane, 0 – 10 %) to yielded the product (181 mg, 0.53 mmol, 91 %). ¹H NMR (400 MHz, CDCl₃) δ 7.55 (dt, *J* = 6.3, 1.2 Hz, 2H), 7.39 (dd, *J* = 8.4, 6.8 Hz, 2H), 7.30 (td, *J* = 7.6, 2.6 Hz, 2H), 7.14 – 7.05 (m, 2H), 6.88 (dd, *J* = 8.1, 2.5 Hz, 1H), 3.57 (t, *J* = 5.2 Hz, 4H), 3.15 (t, *J* = 5.1 Hz, 4H), 1.48 (s, 9H). ¹³C NMR (101 MHz, CDCl₃) δ 154.66, 151.64, 142.31, 141.56, 129.51, 128.67, 127.26, 127.19, 119.31, 115.59, 115.54, 79.81, 49.44, 28.42.

1-([1,1'-Biphenyl]-3-yl)piperazine (18b)



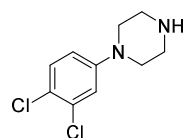
The title compound was synthesized using *tert*-butyl 4-([1,1'-biphenyl]-3-yl)piperazine-1-carboxylate (100 mg, 0.30 mmol, 1 eq.) according to general procedure B. The obtained crude product was used directly without any purification.

tert-Butyl 4-(3,4-dichlorophenyl)piperazine-1-carboxylate (20a)



The title compound was synthesized using 4-bromo-1,2-dichlorobenzene (226 mg, 1.00 mmol, 1 eq.), *tert*-butyl piperazine-1-carboxylate (186 mg, 1.00 mmol, 1 eq.), sodium *tert*-butoxide (144 mg, 1.50 mmol, 1.5 eq.), rac-BINAP (37.4 mg, 0.06 mmol, 0.06 eq.) and palladium diacetate (8.96 mg, 0.04 mmol, 0.04 eq.) according to general procedure A in a yield of 209 mg (0.63 mmol, 63%). ¹H NMR (400 MHz, CDCl₃) δ 7.37 (d, *J* = 2.4 Hz, 1H), 7.19 (dd, *J* = 8.6, 2.4 Hz, 1H), 6.93 (d, *J* = 8.6 Hz, 1H), 3.65 – 3.54 (m, 4H), 2.95 (t, *J* = 4.9 Hz, 4H), 1.49 (s, 9H). ¹³C NMR (101 MHz, CDCl₃) δ 154.86, 147.93, 130.45, 129.71, 128.67, 127.76, 121.35, 79.97, 51.29, 28.52.

1-(3,4-Dichlorophenyl)piperazine (20b)

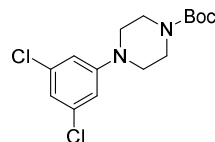


The title compound was synthesized using *tert*-butyl 4-(3,4-dichlorophenyl)piperazine-1-carboxylate (100 mg, 0.30 mmol, 1 eq.) according to general procedure B in a yield of 63 mg (0.27 mmol, 90%).

¹H NMR (400 MHz, CDCl₃) δ 7.37 (d, *J* = 2.4 Hz, 1H), 7.22 – 7.18 (m, 1H), 6.96 (d, *J*

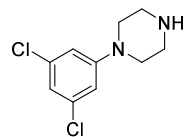
= 8.6 Hz, 1H), 3.58 (br, 1H), 3.12 (m, 4H), 3.05 (m, 4H). ^{13}C NMR (101 MHz, CDCl_3) δ 148.07, 130.45, 129.69, 128.64, 127.80, 121.39, 51.69, 45.71.

***tert*-Butyl 4-(3,5-dichlorophenyl)piperazine-1-carboxylate (19a)**



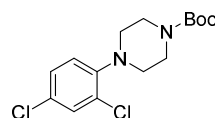
The title compound was synthesized using 1-bromo-3,5-dichlorobenzene (226 mg, 1.00 mmol, 1 eq.), *tert*-butyl piperazine-1-carboxylate (186 mg, 1.00 mmol, 1 eq.), sodium *tert*-butoxide (144 mg, 1.50 mmol, 1.5 eq.), rac-BINAP (37.4 mg, 0.06 mmol, 0.06 eq.) and palladium diacetate (8.96 mg, 0.04 mmol, 0.04 eq.) according to general procedure A in a yield of 192 mg (0.58 mmol, 58%). ^1H NMR (400 MHz, CDCl_3) δ 6.82 (t, J = 1.7 Hz, 1H), 6.74 (d, J = 1.7 Hz, 2H), 3.62 – 3.48 (m, 4H), 3.15 (t, J = 5.2 Hz, 4H), 1.48 (s, 9H). ^{13}C NMR (101 MHz, CDCl_3) δ 154.71, 152.65, 135.61, 119.44, 114.35, 80.28, 48.48, 28.52.

1-(3,5-Dichlorophenyl)piperazine (19b)



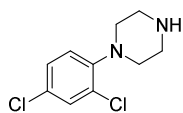
The title compound was synthesized using *tert*-butyl 4-(3,5-dichlorophenyl)piperazine-1-carboxylate (130 mg, 0.39 mmol, 1 eq.) according to general procedure B in a yield of 90 mg (0.39 mmol, 99%). ^1H NMR (400 MHz, CDCl_3) δ 6.79 (t, J = 1.7 Hz, 1H), 6.74 (d, J = 1.8 Hz, 2H), 3.17 – 3.11 (m, 4H), 3.04 – 2.96 (m, 4H), 1.42 (br, 1H). ^{13}C NMR (101 MHz, CDCl_3) δ 153.05, 135.47, 118.90, 113.87, 49.25, 45.74.

***tert*-Butyl 4-(2,4-dichlorophenyl)piperazine-1-carboxylate (21a)**



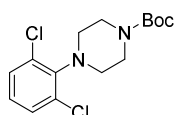
The title compound was synthesized using 1-bromo-2,4-dichlorobenzene (226 mg, 1.00 mmol, 1 eq.), *tert*-butyl piperazine-1-carboxylate (186 mg, 1.00 mmol, 1 eq.), sodium *tert*-butoxide (144 mg, 1.50 mmol, 1.5 eq.), rac-BINAP (37.4 mg, 0.06 mmol, 0.06 eq.) and palladium diacetate (8.96 mg, 0.04 mmol, 0.04 eq.) according to general procedure A in a yield of 200 mg (0.60 mmol, 60%). ^1H NMR (400 MHz, CDCl_3) δ 7.37 (d, J = 2.5 Hz, 1H), 7.19 (dd, J = 8.6, 2.4 Hz, 1H), 6.93 (d, J = 8.6 Hz, 1H), 3.59 (t, 4H), 2.95 (t, 4H), 1.49 (s, 9H). ^{13}C NMR (101 MHz, CDCl_3) δ 154.87, 147.96, 130.46, 129.72, 128.66, 127.76, 121.35, 79.97, 51.30, 28.53.

1-(2,4-Dichlorophenyl)piperazine (21b)



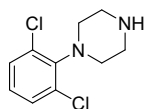
The title compound was synthesized using *tert*-Butyl 4-(2,4-dichlorophenyl)piperazine-1-carboxylate (100 mg, 0.30 mmol, 1.00 eq.) according to general procedure B in a yield of 66 mg (0.28 mmol, 96%). ¹H NMR (400 MHz, CDCl₃) δ 7.35 (s, 1H), 7.18 (d, *J* = 8.6 Hz, 1H), 6.95 (d, *J* = 8.6, 2.0 Hz, 1H), 3.06 – 3.02 (m, 4H), 3.01 – 2.90 (m, 4H), 2.14 (s, 1H). ¹³C NMR (101 MHz, CDCl₃) δ 148.48, 130.33, 129.55, 128.17, 127.66, 121.24, 52.56, 46.19.

***tert*-Butyl 4-(2,6-dichlorophenyl)piperazine-1-carboxylate (22a)**



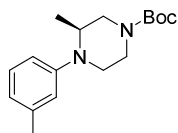
The title compound was synthesized using 2-bromo-1,3-dichlorobenzene (226 mg, 1.00 mmol, 1 eq.), *tert*-butyl piperazine-1-carboxylate (186 mg, 1.00 mmol, 1 eq.), sodium *tert*-butoxide (144 mg, 1.50 mmol, 1.5 eq.), rac-BINAP (37.4 mg, 0.06 mmol, 0.06 eq.) and palladium diacetate (8.96 mg, 0.04 mmol, 0.04 eq.) according to general procedure A in a yield of 35 mg (0.11 mmol, 11%). ¹H NMR (400 MHz, CDCl₃) δ 7.27 (d, *J* = 8.0 Hz, 2H), 6.99 (t, *J* = 8.3 Hz, 1H), 3.58 – 3.54 (m, 4H), 3.19 – 3.15 (m, 4H), 1.49 (s, 9H). ¹³C NMR (101 MHz, CDCl₃) δ 155.08, 135.18, 129.25, 126.32, 79.76, 49.56, 28.59.

1-(2,6-Dichlorophenyl)piperazine (22b)



The title compound was synthesized using *tert*-Butyl 4-(2,6-dichlorophenyl)piperazine-1-carboxylate (35 mg, 0.11 mmol, 1.00 eq.) according to general procedure B in a yield of 22 mg (0.10 mmol, 90%). ¹H NMR (400 MHz, CDCl₃) δ 7.26 (d, *J* = 8.1 Hz, 2H), 6.97 (t, 1H), 3.21 – 3.17 (m, 4H), 3.03 – 2.99 (m, 4H), 2.19 (s, 1H). ¹³C NMR (101 MHz, CDCl₃) δ 145.41, 135.29, 129.22, 126.03, 50.81, 46.81.

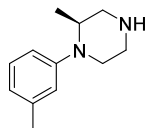
***tert*-Butyl (*S*)-3-methyl-4-(*m*-tolyl)piperazine-1-carboxylate ((*S*)-1a)**



The title compound was synthesized using 1-bromo-3-methylbenzene (100 mg, 0.59 mmol, 1 eq.), *tert*-butyl (*S*)-3-methylpiperazine-1-carboxylate (176 mg, 0.88 mmol, 1.5 eq.), Cs₂CO₃ (286 mg, 0.88 mmol, 1.5 eq.), rac-BINAP (23.25 mg, 0.04 mmol, 0.06 eq.) and palladium diacetate (5.25 mg, 0.02 mmol, 0.04 eq.) according to general procedure A in a yield of 130 mg (0.45 mmol, 77%). ¹H NMR (400 MHz, CDCl₃) δ 7.14 (t, *J* = 7.7 Hz, 1H), 6.71 – 6.67 (m, 3H), 4.04 – 3.66 (m, 3H), 3.44 – 2.99 (m, 4H), 2.30 (s, 3H), 1.48 (s, 9H), 0.98 (d, *J* = 6.5 Hz, 3H).

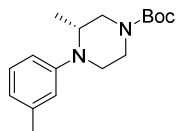
^{13}C NMR (101 MHz, CDCl_3) δ 155.13, 150.22, 138.86, 129.07, 120.93, 118.05, 114.33, 79.70, 51.65, 49.45, 48.25, 44.30, 28.50, 21.85, 12.25.

(S)-2-Methyl-1-(*m*-tolyl)piperazine ((S)-1b)



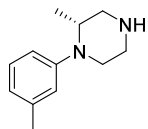
The title compound was synthesized using *tert*-butyl (*S*)-3-methyl-4-(*m*-tolyl)piperazine-1-carboxylate (150 mg, 0.52 mmol, 1.00 eq.) according to general procedure B in a yield of 90 mg (0.47 mmol, 92%). ^1H NMR (400 MHz, CDCl_3) δ 7.14 (t, $J = 7.5$ Hz, 1H), 6.78 – 6.62 (m, 3H), 3.73 (qq, $J = 6.7, 3.7, 3.3$ Hz, 1H), 3.15 – 2.78 (m, 6H), 2.31 (s, 3H), 1.03 (d, $J = 6.5$ Hz, 3H). ^{13}C NMR (101 MHz, CDCl_3) δ 150.78, 138.76, 128.94, 120.80, 118.44, 114.69, 51.85, 51.40, 46.46, 45.97, 21.83, 12.64.

***tert*-Butyl (*R*)-3-methyl-4-(*m*-tolyl)piperazine-1-carboxylate ((*R*)-1a)**



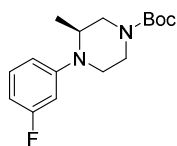
The title compound was synthesized using 1-bromo-3-methylbenzene (1 g, 5.85 mmol, 1 eq.), *tert*-butyl (*R*)-3-methylpiperazine-1-carboxylate (1.17 g, 5.85 mmol, 1 eq.), Cs_2CO_3 (2.86 g, 8.77 mmol, 1.5 eq.), rac-BINAP (233 mg, 0.35 mmol, 0.06 eq.) and palladium diacetate (52.53 mg, 0.23 mmol, 0.04 eq.) according to general procedure A in a yield of 1.05 g (3.62 mmol, 62%).

(*R*)-2-Methyl-1-(*m*-tolyl)piperazine ((*R*)-1b)



The title compound was synthesized using *tert*-butyl (*R*)-3-methyl-4-(*m*-tolyl)piperazine-1-carboxylate (0.75 g, 2.58 mmol, 1.00 eq.) according to general procedure B in a yield of 405 mg (2.13 mmol, 82%). ^1H NMR (400 MHz, CDCl_3) δ 7.20 – 7.08 (m, 1H), 6.80 – 6.68 (m, 3H), 3.72 (m, 1H), 3.67 – 3.50 (br, 1H), 3.19 – 2.82 (m, 6H), 2.31 (s, 3H), 1.03 (d, $J = 6.5$ Hz, 3H). ^{13}C NMR (101 MHz, CDCl_3) δ 150.56, 138.84, 128.98, 121.47, 119.16, 115.41, 51.38, 51.30, 46.09, 45.93, 21.78, 13.00.

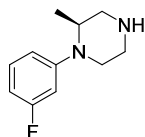
***tert*-Butyl (*S*)-4-(3-fluorophenyl)-3-methylpiperazine-1-carboxylate (23a)**



The title compound was synthesized using 1-bromo-3-fluorobenzene (175 mg, 1.00 mmol, 1 eq.), *tert*-butyl (*S*)-3-methylpiperazine-1-carboxylate (200 mg, 1.00 mmol, 1 eq.), sodium *tert*-butoxide (144 mg, 1.50 mmol, 1.5 eq.), rac-BINAP (37.4 mg, 0.06 mmol, 0.06 eq.) and palladium diacetate (8.96 mg, 0.04 mmol, 0.04 eq.) according to general procedure A in a yield of 177 mg (0.60 mmol,

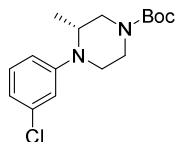
60%). ^1H NMR (400 MHz, CDCl_3) δ 7.18 (td, $J = 8.2, 7.0$ Hz, 1H), 6.62 (dd, $J = 8.3, 2.4$ Hz, 1H), 6.58 – 6.44 (m, 2H), 4.36 – 3.70 (m, 3H), 3.40 – 2.96 (m, 4H), 1.49 (s, 9H), 1.02 (d, $J = 6.5$ Hz, 3H). ^{13}C NMR (101 MHz, CDCl_3) δ 164.00 (d, $J = 243.2$ Hz), 155.09, 151.72 (d, $J = 9.8$ Hz), 130.26 (d, $J = 10.0$ Hz), 111.50, 105.71 (d, $J = 21.4$ Hz), 103.05 (d, $J = 25.3$ Hz), 79.86, 51.12, 48.96, 47.69, 42.36, 28.43, 12.05.

(S)-1-(3-Fluorophenyl)-2-methylpiperazine (23b)



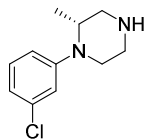
The title compound was synthesized using *tert*-butyl (*S*)-4-(3-fluorophenyl)-3-methylpiperazine-1-carboxylate (100 mg, 0.34 mmol, 1.00 eq.) according to general procedure B. The obtained crude product was used directly without any purification.

***tert*-Butyl (*R*)-4-(3-chlorophenyl)-3-methylpiperazine-1-carboxylate ((*R*)-24a)**



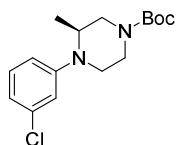
The title compound was synthesized using 1-bromo-3-chlorobenzene (191 mg, 1.00 mmol, 1 eq.), *tert*-butyl (*R*)-3-methylpiperazine-1-carboxylate (200 mg, 1.00 mmol, 1 eq.), sodium *tert*-butoxide (144 mg, 1.50 mmol, 1.5 eq.), *rac*-BINAP (37.4 mg, 0.06 mmol, 0.06 eq.) and palladium diacetate (8.96 mg, 0.04 mmol, 0.04 eq.) according to general procedure A in a yield of 233 mg (0.75 mmol, 75%). ^1H NMR (400 MHz, CDCl_3) δ 7.15 (t, $J = 8.1$ Hz, 1H), 6.95 – 6.63 (m, 3H), 4.27 – 3.70 (m, 3H), 3.40 – 2.89 (m, 4H), 1.48 (s, 9H), 1.01 (d, $J = 6.5$ Hz, 3H). ^{13}C NMR (101 MHz, CDCl_3) δ 155.07, 151.17, 135.09, 130.19, 119.25, 116.31, 114.40, 79.87, 51.22, 49.11, 47.81, 42.84, 28.46, 12.16.

(*R*)-1-(3-Chlorophenyl)-2-methylpiperazine ((*R*)-24b)



The title compound was synthesized using *tert*-butyl (*R*)-4-(3-chlorophenyl)-3-methylpiperazine-1-carboxylate (100 mg, 0.34 mmol, 1.00 eq.) according to general procedure B. The obtained crude product was used directly without any purification.

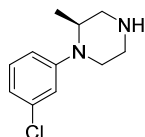
***tert*-Butyl (*S*)-4-(3-chlorophenyl)-3-methylpiperazine-1-carboxylate ((*S*)-24a)**



The title compound was synthesized using 1-bromo-3-chlorobenzene (191 mg, 1.00 mmol, 1 eq.), *tert*-butyl (*S*)-3-methylpiperazine-1-carboxylate (200 mg, 1.00 mmol, 1 eq.), sodium *tert*-butoxide (144 mg, 1.50 mmol, 1.5 eq.), *rac*-BINAP (37.4 mg, 0.06 mmol, 0.06 eq.) and palladium diacetate

(8.96 mg, 0.04 mmol, 0.04 eq.) according to general procedure A in a yield of 117 mg (0.38 mmol, 38%). ^1H NMR (400 MHz, CDCl_3) δ 7.16 (t, $J = 8.1$ Hz, 1H), 6.93 – 6.44 (m, 3H), 4.23 – 3.71 (m, 3H), 3.41 – 2.92 (m, 4H), 1.48 (s, 9H), 1.02 (d, $J = 6.5$ Hz, 3H). ^{13}C NMR (101 MHz, CDCl_3) δ 155.12, 151.18, 135.12, 130.20, 119.31, 116.38, 114.51, 79.93, 51.25, 49.15, 42.92, 28.48, 12.19.

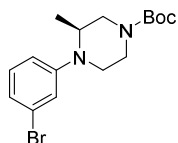
(S)-1-(3-Chlorophenyl)-2-methylpiperazine ((S)-24b)



The title compound was synthesized using *tert*-butyl (S)-4-(3-chlorophenyl)-3-methylpiperazine-1-carboxylate (100 mg, 0.34 mmol, 1.00 eq.) according to general procedure B in a yield of 56 mg (0.26 mmol, 82%).

^1H NMR (400 MHz, CDCl_3) δ 7.16 (t, $J = 8.1$ Hz, 1H), 6.92 – 6.67 (m, 3H), 3.82 (tt, $J = 6.7, 3.2$ Hz, 1H), 3.59 (br, 1H), 3.29 – 2.78 (m, 6H), 1.08 (d, $J = 6.6$ Hz, 3H). ^{13}C NMR (101 MHz, CDCl_3) δ 151.54, 135.04, 130.15, 119.50, 116.88, 114.99, 50.97, 50.72, 45.84, 44.22, 12.47.

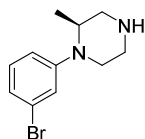
***tert*-Butyl (S)-4-(3-bromophenyl)-3-methylpiperazine-1-carboxylate ((S)-25a)**



The title compound was synthesized using 1,3-dibromobenzene (236 mg, 1.00 mmol, 1 eq.), *tert*-butyl (S)-3-methylpiperazine-1-carboxylate (200 mg, 1.00 mmol, 1 eq.), sodium *tert*-butoxide (144 mg, 1.50 mmol, 1.5 eq.),

rac-BINAP (37.4 mg, 0.06 mmol, 0.06 eq.) and palladium diacetate (8.96 mg, 0.04 mmol, 0.04 eq.) according to general procedure A in a yield of 154 mg (0.43 mmol, 43%). ^1H NMR (400 MHz, CDCl_3) δ 7.09 (t, $J = 8.1$ Hz, 1H), 7.02 – 6.89 (m, 2H), 6.78 (dd, $J = 8.3, 2.4$ Hz, 1H), 4.03 – 3.72 (m, 2H), 3.36 – 2.99 (m, 5H), 1.48 (s, 9H), 1.01 (d, $J = 6.5$ Hz, 3H). ^{13}C NMR (101 MHz, CDCl_3) δ 155.05, 151.31, 130.46, 123.37, 122.19, 119.26, 114.87, 79.87, 51.23, 49.12, 47.69, 42.78, 28.44, 12.18.

(S)-1-(3-Bromophenyl)-2-methylpiperazine ((S)-25b)

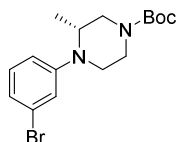


The title compound was synthesized using *tert*-Butyl (S)-4-(3-bromophenyl)-3-methylpiperazine-1-carboxylate (100 mg, 0.28 mmol, 1.00 eq.) according to general procedure B in a yield of 72 mg (0.28 mmol, 98%).

^1H NMR (400 MHz, CDCl_3) δ 7.10 (t, $J = 8.1$ Hz, 1H), 7.01 (t, $J = 2.1$ Hz, 1H), 6.95 (ddd, $J = 7.9, 1.9, 0.9$ Hz, 1H), 6.81 (ddd, $J = 8.3, 2.5, 0.9$ Hz, 1H), 3.81 (m, 1H), 3.77 (br, 1H), 3.19 – 2.86 (m, 6H), 1.07 (d, $J = 6.6$ Hz, 3H). ^{13}C NMR (101 MHz, CDCl_3) δ

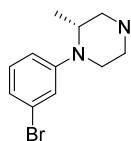
151.66, 130.41, 123.30, 122.36, 119.73, 115.42, 50.92, 50.68, 45.79, 44.17, 12.44.

***tert*-Butyl (*R*)-4-(3-bromophenyl)-3-methylpiperazine-1-carboxylate ((*R*)-25a)**



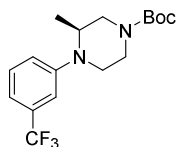
The title compound was synthesized using 1,3-dibromobenzene (236 mg, 1.00 mmol, 1 eq.), *tert*-butyl (*R*)-3-methylpiperazine-1-carboxylate (200 mg, 1.00 mmol, 1 eq.), sodium *tert*-butoxide (144 mg, 1.50 mmol, 1.5 eq.), rac-BINAP (37.4 mg, 0.06 mmol, 0.06 eq.) and palladium diacetate (8.96 mg, 0.04 mmol, 0.04 eq.) according to general procedure A in a yield of 257 mg (0.72 mmol, 72%). ¹H NMR (400 MHz, CDCl₃) δ 7.10 (t, *J* = 8.1 Hz, 1H), 7.03 – 6.90 (m, 2H), 6.78 (dd, *J* = 8.6, 2.4 Hz, 1H), 4.26 – 3.70 (m, 3H), 3.44 – 2.93 (m, 4H), 1.48 (s, 9H), 1.01 (d, *J* = 6.5 Hz, 3H). ¹³C NMR (101 MHz, CDCl₃) δ 155.10, 151.35, 130.50, 123.41, 122.25, 119.30, 114.92, 79.93, 51.28, 49.20, 47.76, 42.95, 28.48, 12.22.

(*R*)-1-(3-Bromophenyl)-2-methylpiperazine ((*R*)-25b)



The title compound was synthesized using *tert*-Butyl (*R*)-4-(3-bromophenyl)-3-methylpiperazine-1-carboxylate (100 mg, 0.28 mmol, 1.00 eq.) according to general procedure B in a yield of 68 mg (0.27 mmol, 95%). ¹H NMR (400 MHz, CDCl₃) δ 7.11 (t, *J* = 8.1 Hz, 1H), 7.06 – 6.97 (m, 2H), 6.83 (ddd, *J* = 8.3, 2.4, 0.9 Hz, 1H), 4.17 (s, 1H), 3.82 (qt, *J* = 6.7, 3.7 Hz, 1H), 3.24 – 2.90 (m, 6H), 1.09 (d, *J* = 6.6 Hz, 3H). ¹³C NMR (101 MHz, CDCl₃) δ 151.56, 130.49, 123.33, 123.00, 120.42, 116.07, 50.75, 50.61, 45.50, 44.31, 12.79.

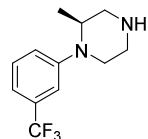
***tert*-Butyl (*S*)-3-methyl-4-(3-(trifluoromethyl)phenyl)piperazine-1-carboxylate ((*S*)-26a)**



The title compound was synthesized using 1-bromo-3-(trifluoromethyl)benzene (225 mg, 1.00 mmol, 1 eq.), *tert*-butyl (*S*)-3-methylpiperazine-1-carboxylate (200 mg, 1.00 mmol, 1 eq.), sodium *tert*-butoxide (144 mg, 1.50 mmol, 1.5 eq.), rac-BINAP (37.4 mg, 0.06 mmol, 0.06 eq.) and palladium diacetate (8.96 mg, 0.04 mmol, 0.04 eq.) according to general procedure A in a yield of 176 mg (0.51 mmol, 51%). ¹H NMR (400 MHz, CDCl₃) δ 7.34 (t, *J* = 7.8 Hz, 1H), 7.15 – 6.90 (m, 3H), 4.03 – 3.77 (m, 3H), 3.41 – 2.98 (m, 4H), 1.49 (s, 9H), 1.03 (d, *J* = 6.5 Hz, 3H). ¹³C NMR (101 MHz, CDCl₃) δ 155.06, 150.22, 131.55 (q, *J* =

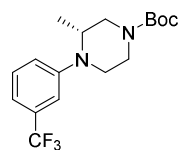
31.7 Hz), 129.70, 124.36 (q, $J = 272.4$ Hz), 119.27, 115.75, 112.67, 79.90, 51.21, 49.09, 47.81, 42.81, 28.38, 12.09.

(S)-2-Methyl-1-(3-(trifluoromethyl)phenyl)piperazine ((S)-26b)



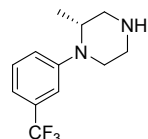
The title compound was synthesized using *tert*-butyl (S)-3-methyl-4-(3-(trifluoromethyl)phenyl)piperazine-1-carboxylate (100 mg, 0.29 mmol, 1.00 eq.) according to general procedure B in a yield of 62 mg (0.26 mmol, 95%). ^1H NMR (400 MHz, CDCl_3) δ 7.42 – 7.24 (m, 1H), 7.19 – 6.94 (m, 3H), 3.87 (qt, $J = 6.6, 3.3$ Hz, 1H), 3.32 – 2.80 (m, 6H), 2.50 (s, 1H), 1.08 (d, $J = 6.6$ Hz, 3H). ^{13}C NMR (101 MHz, CDCl_3) δ 150.63, 131.39 (q, $J = 31.5$ Hz), 129.57, 124.42 (q, $J = 272.5$ Hz), 119.28, 115.46 (q, $J = 3.8$ Hz), 112.66 (q, $J = 3.9$ Hz), 51.18, 50.60, 46.02, 44.09, 12.06.

***tert*-Butyl (R)-3-methyl-4-(3-(trifluoromethyl)phenyl)piperazine-1-carboxylate ((R)-26a)**



The title compound was synthesized using 1-bromo-3-(trifluoromethyl)benzene (225 mg, 1.00 mmol, 1 eq.), *tert*-butyl (R)-3-methylpiperazine-1-carboxylate (200 mg, 1.00 mmol, 1 eq.), sodium *tert*-butoxide (144 mg, 1.50 mmol, 1.5 eq.), rac-BINAP (37.4 mg, 0.06 mmol, 0.06 eq.) and palladium diacetate (8.96 mg, 0.04 mmol, 0.04 eq.) according to general procedure A in a yield of 176 mg (0.51 mmol, 51%). ^1H NMR (400 MHz, CDCl_3) δ 7.40 – 7.29 (m, 1H), 7.18 – 6.91 (m, 3H), 4.28 – 3.70 (m, 3H), 3.47 – 3.00 (m, 4H), 1.49 (s, 9H), 1.03 (d, $J = 6.5$ Hz, 3H). ^{13}C NMR (101 MHz, CDCl_3) δ 155.10, 150.24, 131.58 (q, $J = 31.6$ Hz), 129.73, 124.38 (q, $J = 272.4$ Hz), 119.26, 115.79, 112.70, 79.94, 51.23, 49.14, 47.83, 42.84, 28.42, 12.15.

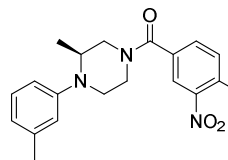
(R)-2-Methyl-1-(3-(trifluoromethyl)phenyl)piperazine ((R)-26b)



The title compound was synthesized using *tert*-Butyl (R)-3-methyl-4-(3-(trifluoromethyl)phenyl)piperazine-1-carboxylate (100 mg, 0.29 mmol, 1.00 eq.) according to general procedure B in a yield of 70 mg (0.29 mmol, 99%). ^1H NMR (400 MHz, CDCl_3) δ 7.34 (t, $J = 8.0$ Hz, 1H), 7.13 – 7.00 (m, 3H), 3.88 (qt, $J = 6.7, 3.4$ Hz, 1H), 3.25 – 2.89 (m, 6H), 1.08 (d, $J = 6.6$ Hz, 3H). ^{13}C NMR (101 MHz, CDCl_3) δ 150.64, 131.50 (q, $J = 31.6$ Hz), 129.66, 124.43 (q, $J = 272.4$ Hz),

119.68, 115.87 (q, $J = 3.8$ Hz), 113.11 (q, $J = 3.9$ Hz), 51.07, 50.70, 45.90, 44.29, 12.32.

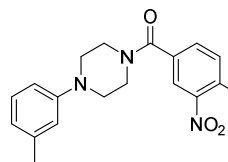
Ethyl (S)-2-((4-(3-methyl-4-(*m*-tolyl)piperazine-1-carbonyl)-2-nitrophenyl)thio)acetate (3)



The title compound was synthesized using (*R*)-2-methyl-1-

(*m*-tolyl)piperazine (60.6 mg, 0.32 mmol, 1 eq.), 4-((2-ethoxy-2-oxoethyl)thio)-3-nitrobenzoic acid (100 mg, 0.35 mmol, 1.1 eq.), HATU (147 mg, 0.48 mmol, 1.5 eq.) and DiPEA (124 mg, 0.96 mmol, 3 eq.) according to general procedure H. This yielded the product (108 mg, 0.24 mmol, 74%). ^1H NMR (400 MHz, CDCl_3) δ 8.34 (d, $J = 1.9$ Hz, 1H), 7.70 (dd, $J = 8.4, 1.9$ Hz, 1H), 7.60 (d, $J = 8.4$ Hz, 1H), 7.17 (t, $J = 7.9$ Hz, 1H), 6.75 (d, $J = 5.8$ Hz, 3H), 4.49-3.01 (m, 7H), 4.24 (q, $J = 7.1$ Hz, 2H), 3.79 (s, 2H), 2.32 (s, 3H), 1.29 (t, $J = 7.1$ Hz, 3H), 1.01 (m, 3H). ^{13}C NMR (101 MHz, CDCl_3) δ 168.26, 167.70, 149.38, 144.90, 138.78, 138.48, 132.42, 132.36, 128.85, 126.69, 124.90, 121.48, 118.91, 115.14, 61.98, 52.72, 51.87, 47.65, 45.06, 34.72, 21.49, 13.86, 12.47. HRMS: Calculated for $[\text{C}_{23}\text{H}_{27}\text{N}_3\text{O}_5\text{S} + \text{H}]^+ = 458.1744$, found = 458.1743.

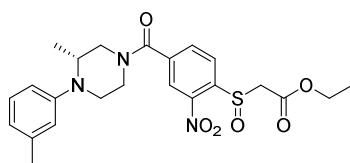
Ethyl 2-((2-nitro-4-(4-(*m*-tolyl)piperazine-1-carbonyl)phenyl)sulfinyl)acetate (2)



The title compound was synthesized using 1-(*m*-

tolyl)piperazine (29.3 mg, 0.17 mmol, 1 eq.), 4-((2-ethoxy-2-oxoethyl)sulfinyl)-3-nitrobenzoic acid (50 mg, 0.17 mmol, 1 eq.), HATU (95 mg, 0.25 mmol, 1.5 eq.) and DiPEA (64.4 mg, 0.50 mmol, 3 eq.) according to general procedure H in a yield of 53.4 mg (0.12 mmol, 70%). ^1H NMR (850 MHz, CDCl_3) δ 8.44 (d, $J = 1.7$ Hz, 1H), 8.37 (d, $J = 8.1$ Hz, 1H), 8.07 (dd, $J = 8.0, 1.6$ Hz, 1H), 7.35 (t, $J = 7.9$ Hz, 1H), 7.24 – 7.17 (m, 2H), 7.15 (dd, $J = 7.5, 1.5$ Hz, 1H), 4.32 – 4.08 (m, 5H), 3.90 (m, 2H), 3.77 (d, $J = 14.2$ Hz, 1H), 3.54 (m, 4H), 2.39 (s, 3H), 1.26 (t, $J = 7.7$ Hz, 3H). ^{13}C NMR (214 MHz, CDCl_3) δ 166.90, 164.84, 144.96, 144.18, 143.94, 140.85, 138.59, 133.88, 130.21, 128.65, 128.02, 124.49, 120.28, 116.68, 62.62, 59.96, 53.48, 53.30, 45.78, 40.63, 21.56, 14.08.

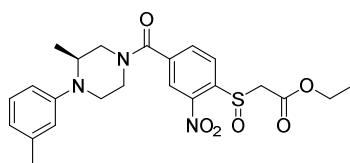
Ethyl 2-((4-((*R*)-3-methyl-4-(*m*-tolyl)piperazine-1-carbonyl)-2-nitrophenyl)sulfinyl)acetate ((*R*)-1)



The title compound was synthesized using (*R*)-2-methyl-1-*(m*-tolyl)piperazine (57.4 mg, 0.30 mmol, 1 eq.), 4-((2-ethoxy-2-oxoethyl)sulfinyl)-3-nitrobenzoic acid (100 mg,

0.33 mmol, 1.1 eq.), HATU (140 mg, 0.45 mmol, 1.5 eq.) and DiPEA (117 mg, 0.91 mmol, 3 eq.) according to general procedure H in a yield of 98 mg (0.21 mmol, 69%). ^1H NMR (850 MHz, CDCl_3) δ 8.47 – 8.34 (m, 2H), 8.07 – 7.97 (m, 1H), 7.18 (t, J = 7.8 Hz, 1H), 6.83 – 6.68 (m, 3H), 4.47 – 4.08 (m, 4H), 3.78 (d, J = 13.8 Hz, 2H), 3.72 – 3.06 (m, 5H), 2.33 (s, 3H), 1.28 (td, J = 7.1, 1.7 Hz, 3H), 1.12 – 0.92 (m, 3H). ^{13}C NMR (214 MHz, CDCl_3) δ 166.88, 164.60, 149.51, 144.89, 143.86, 139.88, 139.17, 133.69, 129.20, 127.89, 124.24, 121.93, 119.36, 115.60, 62.44, 60.04, 52.25, 47.72, 45.62, 42.59, 21.79, 14.18, 12.71.

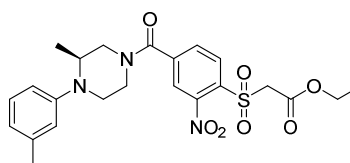
Ethyl 2-((4-((*S*)-3-methyl-4-*(m*-tolyl)piperazine-1-carbonyl)-2-nitrophenyl)sulfinyl)acetate (*(S)*-1)



The title compound was synthesized using (*S*)-2-methyl-1-*(m*-tolyl)piperazine (57.4 mg, 0.30 mmol, 1 eq.), 4-((2-ethoxy-2-oxoethyl)sulfinyl)-3-nitrobenzoic acid (100 mg,

0.33 mmol, 1.1 eq.), HATU (140 mg, 0.45 mmol, 1.5 eq.) and DiPEA (117 mg, 0.91 mmol, 3 eq.) according to general procedure H in a yield of 140 mg (0.30 mmol, 98%).

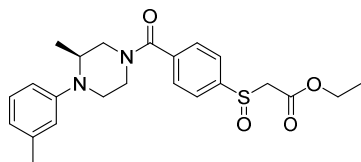
Ethyl (*S*)-2-((4-(3-methyl-4-*(m*-tolyl)piperazine-1-carbonyl)-2-nitrophenyl)sulfonyl)acetate (4)



The title compound was synthesized using (*S*)-2-methyl-1-*(m*-tolyl)piperazine (12 mg, 0.06 mmol, 1 eq.), 4-((2-ethoxy-2-oxoethyl)sulfonyl)-3-nitrobenzoic acid (20 mg,

0.06 mmol, 1 eq.), HATU (36 mg, 0.10 mmol, 1.5 eq.) and DiPEA (24 mg, 0.19 mmol, 3 eq.) according to general procedure H in a yield of 2 mg (0.004 mmol, 6%). ^1H NMR (400 MHz, CDCl_3) δ 8.30 (d, J = 8.0 Hz, 1H), 7.94 (d, J = 3.9 Hz, 1H), 7.83 (d, J = 8.0 Hz, 1H), 7.18 (t, J = 7.6 Hz, 1H), 6.76 (s, 3H), 4.68 (s, 2H), 4.45-3.05 (m, 7H), 4.22 (q, J = 7.1 Hz, 2H), 2.33 (s, 3H), 1.27 (t, J = 7.0 Hz, 4H), 1.02 (m, 3H).

Ethyl 2-((4-((*S*)-3-methyl-4-*(m*-tolyl)piperazine-1-carbonyl)phenyl)sulfinyl)acetate (5)



The title compound was synthesized using (*S*)-2-methyl-1-(*m*-tolyl)piperazine (22 mg, 0.12 mmol, 1 eq.), 4-((2-ethoxy-2-oxoethyl)sulfinyl)benzoic acid (30 mg, 0.12

mmol, 1 eq.), oxalyl chloride (16.34 mg, 0.13 mmol, 1.1 eq.) and DiPEA (45 mg, 0.35 mmol, 3 eq.) according to general procedure G in a yield of 21 mg (0.05 mmol, 42%).

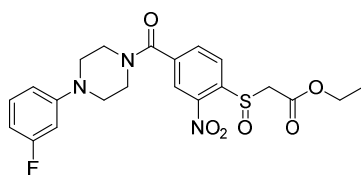
Ethyl 2-((2-nitro-4-(4-phenylpiperazine-1-carbonyl)phenyl)sulfinyl)acetate (6)



The title compound was synthesized using 1-phenylpiperazine (25 mg, 0.16 mmol, 1 eq.), 4-((2-ethoxy-2-oxoethyl)sulfinyl)benzoic acid (70 mg, 0.23 mmol, 1.5

eq.), HATU (140 mg, 0.37 mmol, 2.3 eq.) and DiPEA (65 μ l, 0.37 mmol, 2.3 eq.) according to general procedure H in a yield of 64 mg (0.14 mmol, 89%). ^1H NMR (400 MHz, CDCl_3) δ 8.43 – 8.37 (m, 2H), 8.01 (dd, J = 8.0, 1.6 Hz, 1H), 7.34 – 7.25 (m, 2H), 6.98 – 6.91 (m, 3H), 4.28 – 4.17 (m, 2H), 4.14 (d, J = 13.7 Hz, 1H), 3.98 (s, 2H), 3.77 (d, J = 13.7 Hz, 1H), 3.59 (s, 2H), 3.31 (s, 2H), 3.18 (s, 2H), 1.28 (t, J = 7.1 Hz, 3H). ^{13}C NMR (101 MHz, CDCl_3) δ 166.54, 164.58, 150.65, 144.91, 143.98, 139.79, 133.72, 129.41, 127.93, 124.22, 121.13, 117.00, 62.44, 60.08, 50.12, 49.62, 47.82, 42.51, 38.68, 14.18. HRMS: calculated for $[\text{C}_{21}\text{H}_{23}\text{N}_3\text{O}_6\text{S}+\text{H}]^+$ = 446.1380, found = 446.1379.

Ethyl 2-((4-(4-(3-fluorophenyl)piperazine-1-carbonyl)-2-nitrophenyl)sulfinyl)acetate (7)

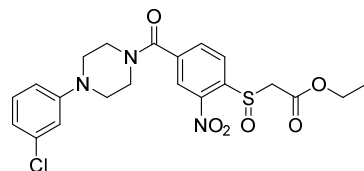


The title compound was synthesized using 1-(3-fluorophenyl)piperazine (18 mg, 0.10 mmol, 1 eq.), 4-((2-ethoxy-2-oxoethyl)sulfinyl)benzoic acid (30 mg, 0.12

mmol, 1 eq.), oxalyl chloride (13.90 mg, 0.11 mmol, 1.1 eq.) and DiPEA (39 mg, 0.30 mmol, 3 eq.) according to general procedure G in a yield of 30 mg (0.07 mmol, 42%). ^1H NMR (400 MHz, CDCl_3) δ 8.41 (dd, J = 4.8, 3.2 Hz, 2H), 8.02 (dd, J = 8.1, 1.6 Hz, 1H), 7.23 (ddd, J = 8.3, 6.6, 1.4 Hz, 1H), 6.77 – 6.66 (m, 1H), 6.65 – 6.56 (m, 2H), 4.26 – 4.18 (m, 2H), 4.14 (d, J = 13.7 Hz, 1H), 3.98 (s, 2H), 3.78 (d, J = 13.6 Hz, 1H), 3.59 (s, 2H), 3.32 – 3.20 (m, 4H), 1.29 (t, J = 7.1 Hz, 3H). ^{13}C NMR (101 MHz, CDCl_3) δ 166.63, 165.09, 163.63 (d, J = 196.4 Hz), 152.26 (d, J = 9.6 Hz), 144.98, 144.18, 139.69, 133.76, 130.58 (d, J = 9.8 Hz), 128.06, 124.28, 112.09 (d, J = 2.4 Hz), 107.46 (d, J =

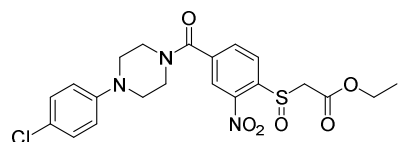
21.3 Hz), 103.81 (d, $J = 24.9$ Hz), 62.53, 60.12, 49.55, 42.32, 14.24.

Ethyl 2-((4-(4-(3-chlorophenyl)piperazine-1-carbonyl)-2-nitrophenyl)sulfinyl)acetate (8)



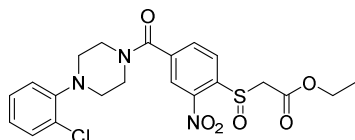
The title compound was synthesized using 1-(3-chlorophenyl)piperazine (20 mg, 0.10 mmol, 1 eq.), 4-((2-ethoxy-2-oxoethyl)sulfinyl)benzoic acid (30 mg, 0.12 mmol, 1 eq.), oxalyl chloride (13.90 mg, 0.11 mmol, 1.1 eq.) and DiPEA (39 mg, 0.30 mmol, 3 eq.) according to general procedure G in a yield of 28 mg (0.06 mmol, 57%). ^1H NMR (400 MHz, CDCl_3) δ 8.51 – 8.31 (m, 2H), 8.01 (dd, $J = 8.0, 1.6$ Hz, 1H), 7.21 (t, $J = 8.4$ Hz, 1H), 6.92 – 6.86 (m, 2H), 6.80 (ddd, $J = 8.3, 2.3, 1.0$ Hz, 1H), 4.30 – 4.16 (m, 2H), 4.13 (d, $J = 13.7$ Hz, 1H), 3.97 (s, 2H), 3.78 (d, $J = 13.7$ Hz, 1H), 3.59 (s, 2H), 3.31 – 3.19 (m, 4H), 1.33 – 1.19 (t, $J = 7.2$, 3H). ^{13}C NMR (101 MHz, CDCl_3) δ 166.62, 164.58, 151.75, 144.98, 144.18, 139.69, 135.24, 133.74, 130.40, 128.04, 124.25, 120.83, 116.86, 114.87, 62.51, 60.13, 49.58, 49.18, 47.62, 42.38, 14.24.

Ethyl 2-((4-(4-(4-chlorophenyl)piperazine-1-carbonyl)-2-nitrophenyl)sulfinyl)acetate (9)



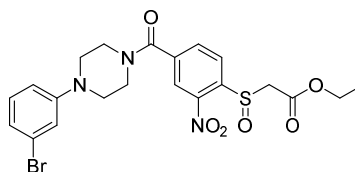
The title compound was synthesized using 1-(4-chlorophenyl)piperazine (19mg, 0.10 mmol, 1 eq.), 4-((2-ethoxy-2-oxoethyl)sulfinyl)benzoic acid (30 mg, 0.12 mmol, 1 eq.), oxalyl chloride (13.90 mg, 0.11 mmol, 1.1 eq.) and DiPEA (39 mg, 0.30 mmol, 3 eq.) according to general procedure G in a yield of 8 mg (0.02 mmol, 18%). ^1H NMR (850 MHz, CDCl_3) δ 8.47 – 8.36 (m, 2H), 8.02 (dd, $J = 8.0, 1.6$ Hz, 1H), 7.30 – 7.27 (m, 2H), 6.97 (m, 2H), 4.26 – 4.18 (m, 2H), 4.14 (d, $J = 13.8$ Hz, 1H), 4.04 (m, 2H), 3.79 (d, $J = 13.8$ Hz, 1H), 3.65 (m, 2H), 3.38 – 3.11 (m, 4H), 1.29 (t, $J = 7.2$ Hz, 3H). ^{13}C NMR (214 MHz, CDCl_3) δ 166.66, 164.61, 148.42, 145.00, 144.25, 139.55, 133.78, 129.55, 128.12, 127.21, 124.30, 118.79, 62.57, 60.09, 50.68, 50.15, 47.41, 42.17, 14.26.

Ethyl 2-((4-(4-(2-chlorophenyl)piperazine-1-carbonyl)-2-nitrophenyl)sulfinyl)acetate (10)



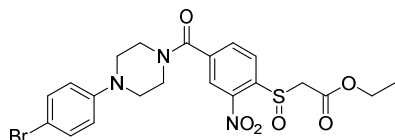
The title compound was synthesized using 1-(2-chlorophenyl)piperazine (26mg, 0.13 mmol, 1 eq.), 4-((2-ethoxy-2-oxoethyl)sulfinyl)benzoic acid (40 mg, 0.13 mmol, 1 eq.), oxalyl chloride (19 mg, 0.15 mmol, 1.1 eq.) and DiPEA (52 mg, 0.40 mmol, 3 eq.) according to general procedure G in a yield of 41 mg (0.09 mmol, 64%). ^1H NMR (400 MHz, CDCl_3) δ 8.54 – 8.26 (m, 2H), 8.03 (dd, $J = 8.0, 1.6$ Hz, 1H), 7.39 (dd, $J = 8.2, 1.5$ Hz, 1H), 7.29 – 7.22 (m, 1H), 7.11 – 6.94 (m, 2H), 4.22 (qd, $J = 7.2, 3.9$ Hz, 2H), 4.14 (d, $J = 13.7$ Hz, 1H), 4.02 (s, 2H), 3.78 (d, $J = 13.7$ Hz, 1H), 3.62 (s, 2H), 3.17 – 3.05 (m, 4H), 1.28 (t, $J = 7.1$ Hz, 3H). ^{13}C NMR (101 MHz, CDCl_3) δ 166.68, 164.61, 148.28, 144.93, 143.95, 139.99, 133.76, 130.91, 129.08, 127.97, 127.90, 124.77, 124.24, 120.73, 62.49, 60.12, 51.74, 50.99, 48.22, 42.87, 14.22. HRMS: Calculated for $[\text{C}_{21}\text{H}_{22}\text{ClN}_3\text{O}_6\text{S} + \text{H}]^+ = 480.0991$, found = 480.0991.

Ethyl 2-((4-(4-(3-bromophenyl)piperazine-1-carbonyl)-2-nitrophenyl)sulfinyl)acetate (11)



The title compound was synthesized using 1-(3-bromophenyl)piperazine (23mg, 0.10 mmol, 1 eq.), 4-((2-ethoxy-2-oxoethyl)sulfinyl)benzoic acid (30 mg, 0.10 mmol, 1 eq.), oxalyl chloride (13.90 mg, 0.11 mmol, 1.1 eq.) and DiPEA (39 mg, 0.30 mmol, 3 eq.) according to general procedure G in a yield of 26 mg (0.05 mmol, 51%). ^1H NMR (500 MHz, CDCl_3) δ 8.48 – 8.34 (m, 2H), 8.01 (dd, $J = 8.1, 1.6$ Hz, 1H), 7.15 (dd, $J = 8.6, 7.4$ Hz, 1H), 7.05 (dd, $J = 8.0, 1.2$ Hz, 2H), 6.90 – 6.78 (m, 1H), 4.28 – 4.18 (m, 2H), 4.14 (d, $J = 13.7$ Hz, 1H), 3.97 (s, 2H), 3.79 (d, $J = 13.7$ Hz, 1H), 3.70 – 3.02 (m, 6H), 1.29 (t, $J = 7.1$ Hz, 3H). ^{13}C NMR (126 MHz, CDCl_3) δ 166.66, 164.60, 151.93, 145.01, 144.21, 139.70, 133.76, 130.71, 128.09, 124.28, 123.85, 123.47, 119.85, 115.43, 62.55, 60.13, 49.65, 49.20, 47.65, 42.42, 14.27.

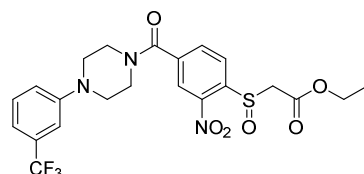
Ethyl 2-((4-(4-(4-bromophenyl)piperazine-1-carbonyl)-2-nitrophenyl)sulfinyl)acetate (12)



The title compound was synthesized using 1-(4-bromophenyl)piperazine (23mg, 0.10 mmol, 1 eq.), 4-((2-ethoxy-2-oxoethyl)sulfinyl)benzoic acid (30 mg,

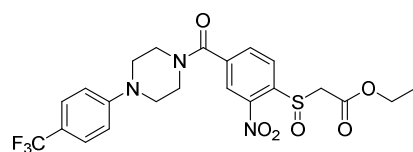
0.10 mmol, 1 eq.), oxalyl chloride (13.90 mg, 0.11 mmol, 1.1 eq.) and DiPEA (39 mg, 0.30 mmol, 3 eq.) according to general procedure G in a yield of 31 mg (0.06 mmol, 61%). ^1H NMR (850 MHz, CDCl_3) δ 8.42 (dd, $J = 4.8, 3.1$ Hz, 2H), 8.02 (dd, $J = 8.0, 1.6$ Hz, 1H), 7.41 – 7.39 (m, 2H), 6.85 (d, $J = 8.4$ Hz, 2H), 4.27 – 4.17 (m, 2H), 4.14 (d, $J = 13.7$ Hz, 1H), 4.00 (m, 2H), 3.79 (d, $J = 13.8$ Hz, 1H), 3.61 (m, 2H), 3.34 – 3.09 (m, 4H), 1.29 (t, $J = 7.2$ Hz, 3H). ^{13}C NMR (214 MHz, CDCl_3) δ 166.65, 164.61, 149.31, 145.00, 144.22, 139.63, 133.78, 132.40, 128.11, 124.30, 118.91, 62.57, 60.10, 50.31, 49.75, 47.57, 42.25, 14.26.

Ethyl 2-((2-nitro-4-(4-(3-(trifluoromethyl)phenyl)piperazine-1-carbonyl)phenyl)sulfinyl)acetate (13)



The title compound was synthesized using 1-(3-(trifluoromethyl)phenyl)piperazine (31 mg, 0.13 mmol, 1 eq.), 4-((2-ethoxy-2-oxoethyl)sulfinyl)benzoic acid (40 mg, 0.13 mmol, 1 eq.), oxalyl chloride (19 mg, 0.15 mmol, 1.1 eq.) and DiPEA (52 mg, 0.40 mmol, 3 eq.) according to general procedure G in a yield of 42 mg (0.08 mmol, 62%). ^1H NMR (400 MHz, CDCl_3) δ 8.55 – 8.29 (m, 2H), 8.02 (dd, $J = 8.1, 1.6$ Hz, 1H), 7.40 (t, $J = 8.0$ Hz, 1H), 7.21 – 7.07 (m, 3H), 4.26 – 4.18 (m, 2H), 4.14 (d, $J = 13.7$ Hz, 1H), 4.00 (br, 2H), 3.79 (d, $J = 13.7$ Hz, 1H), 3.62 (br, 2H), 3.30 (br, 4H), 1.29 (t, $J = 7.1$ Hz, 3H). ^{13}C NMR (101 MHz, CDCl_3) δ 166.67, 164.60, 150.87, 145.00, 144.23, 139.65, 133.76, 131.81 (q, $J = 32.3$ Hz), 129.99, 128.09, 124.28, 122.85 (q, $J = 273.71$ Hz), 119.87, 117.48 (q, $J = 4.04$ Hz), 113.28 (q, $J = 3.03$ Hz), 62.54, 60.11, 49.57, 47.57, 14.25. HRMS: Calculated for $[\text{C}_{22}\text{H}_{22}\text{F}_3\text{N}_3\text{O}_6\text{S} + \text{H}]^+ = 514.1254$, found = 514.1252.

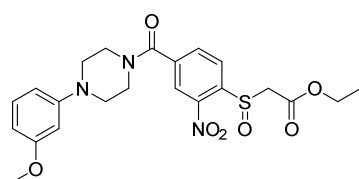
Ethyl 2-((2-nitro-4-(4-(4-(trifluoromethyl)phenyl)piperazine-1-carbonyl)phenyl)sulfinyl)acetate (14)



The title compound was synthesized using 1-(4-(trifluoromethyl)phenyl)piperazine (31 mg, 0.13 mmol, 1 eq.), 4-((2-ethoxy-2-oxoethyl)sulfinyl)benzoic acid (40 mg, 0.13 mmol, 1 eq.), oxalyl chloride (19 mg, 0.15 mmol, 1.1 eq.) and DiPEA (52 mg, 0.40 mmol, 3 eq.) according to general procedure G in a yield of 39 mg (0.08 mmol,

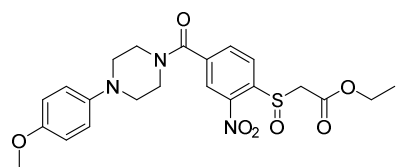
57%). ^1H NMR (400 MHz, CDCl_3) δ 8.53 – 8.29 (m, 2H), 8.02 (dd, $J = 8.1, 1.6$ Hz, 1H), 7.62 – 7.45 (m, 2H), 6.96 (d, $J = 8.5$ Hz, 2H), 4.22 (m, 2H), 4.14 (d, $J = 13.7$ Hz, 1H), 3.99 (br, 2H), 3.78 (d, $J = 13.7$ Hz, 1H), 3.62 (br, 2H), 3.35 (br, 4H), 1.28 (t, $J = 7.2$ Hz, 3H). ^{13}C NMR (101 MHz, CDCl_3) δ 166.57, 164.52, 152.66, 144.88, 144.14, 139.49, 133.67, 127.97, 126.62 (q, $J = 3.75$), 124.48 (q, $J = 271.94$ Hz), 122.32 (q, $J = 32.32$ Hz), 124.19, 115.49, 62.44, 60.01, 48.84, 48.31, 47.51, 42.15, 14.14. HRMS: Calculated for $[\text{C}_{22}\text{H}_{22}\text{F}_3\text{N}_3\text{O}_6\text{S} + \text{H}]^+ = 514.1254$, found = 514.1253.

Ethyl 2-((4-(4-(3-methoxyphenyl)piperazine-1-carbonyl)-2-nitrophenyl)sulfinyl)acetate (15)



The title compound was synthesized using 1-(3-methoxyphenyl)piperazine (19mg, 0.10 mmol, 1 eq.), 4-((2-ethoxy-2-oxoethyl)sulfinyl)benzoic acid (30 mg, 0.10 mmol, 1 eq.), oxalyl chloride (14 mg, 0.11 mmol, 1.1 eq.) and DiPEA (39 mg, 0.30 mmol, 3 eq.) according to general procedure G in a yield of 29 mg (0.06 mmol, 55%). ^1H NMR (850 MHz, CDCl_3) δ 8.43 – 8.39 (m, 2H), 8.02 (dd, $J = 8.0, 1.7$ Hz, 1H), 7.23 (t, $J = 8.2$ Hz, 1H), 6.68 – 6.45 (m, 3H), 4.26 – 4.17 (m, 2H), 4.14 (d, $J = 13.8$ Hz, 1H), 4.01 (m, 2H), 3.81 (s, 3H), 3.78 (d, $J = 13.8$ Hz, 1H), 3.60 (m, 2H), 3.39 – 3.15 (m, 4H), 1.28 (t, $J = 7.2$ Hz, 3H). ^{13}C NMR (214 MHz, CDCl_3) δ 166.51, 164.53, 160.67, 151.51, 144.87, 143.99, 139.62, 133.69, 130.19, 127.94, 124.21, 109.75, 106.14, 103.75, 62.44, 60.01, 55.32, 50.26, 49.76, 47.49, 42.20, 14.14.

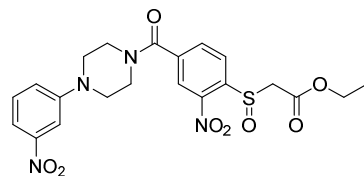
Ethyl 2-((4-(4-(4-methoxyphenyl)piperazine-1-carbonyl)-2-nitrophenyl)sulfonyl)acetate (16)



The title compound was synthesized using 1-(4-methoxyphenyl)piperazine (32 mg, 0.17 mmol, 1 eq.), 4-((2-ethoxy-2-oxoethyl)sulfonyl)-3-nitrobenzoic acid (50 mg, 0.17 mmol, 1 eq.), HATU (95 mg, 0.25 mmol, 1.5 eq.) and DiPEA (64 mg, 0.50 mmol, 3 eq.) according to general procedure H in a yield of 71 mg (0.15 mmol, 90%). ^1H NMR (850 MHz, CDCl_3) δ 8.41 (d, $J = 1.6$ Hz, 1H), 8.40 (d, $J = 8.1$ Hz, 1H), 8.02 (dd, $J = 8.0, 1.6$ Hz, 1H), 6.94 (d, $J = 8.7$ Hz, 2H), 6.89 – 6.82 (m, 2H), 4.26 – 4.16 (m, 2H), 4.14 (d, $J = 13.9$ Hz, 1H), 3.99 (m, 2H), 3.81 – 3.74 (m, 4H), 3.59 (m, 2H), 3.23 –

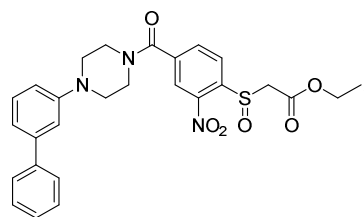
2.98 (m, 4H), 1.28 (t, $J = 7.6$ Hz, 3H). ^{13}C NMR (214 MHz, CDCl_3) δ 166.50, 164.61, 154.84, 144.87, 144.65, 143.88, 139.82, 133.73, 127.89, 124.22, 119.31, 114.63, 62.45, 60.06, 55.60, 51.59, 51.04, 47.89, 42.56, 14.17.

Ethyl 2-((2-nitro-4-(4-(3-nitrophenyl)piperazine-1-carbonyl)phenyl)sulfinyl)acetate (17)



The title compound was synthesized using 1-(3-nitrophenyl)piperazine (21 mg, 0.10 mmol, 1 eq.), 4-((2-ethoxy-2-oxoethyl)sulfinyl)benzoic acid (30 mg, 0.10 mmol, 1 eq.), oxalyl chloride (14 mg, 0.11 mmol, 1.1 eq.) and DiPEA (39 mg, 0.30 mmol, 3 eq.) according to general procedure G in a yield of 29 mg (0.05 mmol, 45%). ^1H NMR (850 MHz, CDCl_3) δ 8.44 – 8.40 (m, 2H), 8.04 (dd, $J = 8.0, 1.6$ Hz, 1H), 7.76 – 7.73 (m, 2H), 7.46 – 7.42 (m, 1H), 7.24 (ddd, $J = 8.3, 2.5, 1.0$ Hz, 1H), 4.26 – 4.18 (m, 2H), 4.15 (d, $J = 13.8$ Hz, 1H), 4.02 (m, 2H), 3.79 (d, $J = 13.8$ Hz, 1H), 3.71 – 3.60 (m, 2H), 3.50 – 3.25 (m, 4H), 1.29 (t, $J = 7.2$ Hz, 3H). ^{13}C NMR (214 MHz, CDCl_3) δ 166.69, 164.63, 151.23, 149.29, 144.95, 144.20, 139.47, 133.76, 130.15, 128.05, 124.28, 122.14, 115.19, 110.69, 62.52, 60.08, 49.17, 48.70, 47.39, 42.20, 14.21.

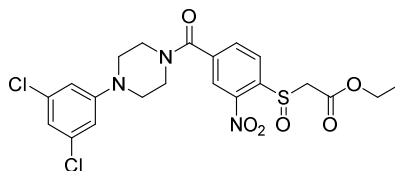
Ethyl 2-((4-(4-([1,1'-biphenyl]-3-yl)piperazine-1-carbonyl)-2-nitrophenyl)sulfinyl)acetate (18)



The title compound was synthesized using 1-([1,1'-biphenyl]-3-yl)piperazine (32 mg, 0.13 mmol, 1 eq.), 4-((2-ethoxy-2-oxoethyl)sulfinyl)benzoic acid (40 mg, 0.13 mmol, 1 eq.), oxalyl chloride (19 mg, 0.15 mmol, 1.1 eq.) and DiPEA (52 mg, 0.4 mmol, 3 eq.) according to general procedure G in a yield of 40 mg (0.08 mmol, 58%). ^1H NMR (400 MHz, CDCl_3) δ 8.56 – 8.26 (m, 2H), 8.02 (dd, $J = 8.0, 1.6$ Hz, 1H), 7.59 – 7.54 (m, 2H), 7.48 – 7.41 (m, 2H), 7.40 – 7.33 (m, 2H), 7.21 – 7.13 (m, 2H), 7.01 – 6.86 (m, 1H), 4.22 (qq, $J = 7.4, 3.6$ Hz, 2H), 4.14 (d, $J = 13.7$ Hz, 1H), 4.01 (br, 2H), 3.78 (d, $J = 13.7$ Hz, 1H), 3.62 (br, 2H), 3.31 (br, 4H), 1.28 (t, $J = 7.2$ Hz, 3H). ^{13}C NMR (101 MHz, CDCl_3) δ 166.62, 164.61, 151.12, 144.98, 144.09,

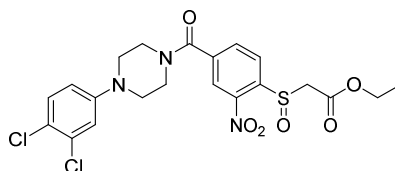
142.73, 141.42, 139.83, 133.77, 129.84, 128.88, 128.03, 127.60, 127.33, 124.29, 120.38, 116.16, 116.03, 62.52, 60.13, 50.26, 49.85, 47.82, 42.54, 14.25. HRMS: Calculated for $[C_{27}H_{27}N_3O_6S + H]^+ = 522.1693$, found = 522.1690.

Ethyl 2-((4-(4-(3,5-dichlorophenyl)piperazine-1-carbonyl)-2-nitrophenyl)sulfinyl)acetate (19)



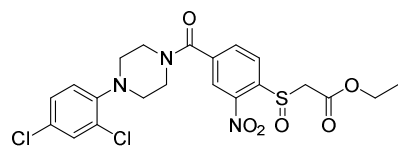
The title compound was synthesized using 1-(3,5-dichlorophenyl)piperazine (23mg, 0.10 mmol, 1 eq.), 4-((2-ethoxy-2-oxoethyl)sulfinyl)benzoic acid (30 mg, 0.10 mmol, 1 eq.), oxalyl chloride (14 mg, 0.11 mmol, 1.1 eq.) and DiPEA (39 mg, 0.3 mmol, 3 eq.) according to general procedure G in a yield of 12 mg (0.02 mmol, 23%). 1H NMR (850 MHz, $CDCl_3$) δ 8.43 – 8.40 (m, 2H), 8.02 (dd, $J = 8.0, 1.6$ Hz, 1H), 6.90 (t, $J = 1.7$ Hz, 1H), 6.79 (d, $J = 1.7$ Hz, 2H), 4.26 – 4.18 (m, 2H), 4.14 (d, $J = 13.8$ Hz, 1H), 3.97 (m, 2H), 3.79 (d, $J = 13.8$ Hz, 1H), 3.60 (m, 2H), 3.27 (m, 4H), 1.29 (t, $J = 7.2$ Hz, 3H). ^{13}C NMR (214 MHz, $CDCl_3$) δ 166.67, 164.61, 151.92, 144.97, 144.23, 139.47, 135.80, 133.75, 128.08, 124.28, 120.56, 114.91, 62.54, 60.08, 49.16, 48.70, 47.34, 42.16, 14.23.

Ethyl 2-((4-(4-(3,4-dichlorophenyl)piperazine-1-carbonyl)-2-nitrophenyl)sulfinyl)acetate (20)

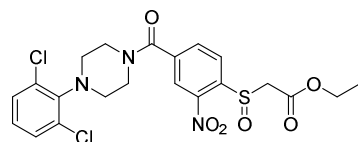


The title compound was synthesized using 1-(3,4-dichlorophenyl)piperazine (23mg, 0.10 mmol, 1 eq.), 4-((2-ethoxy-2-oxoethyl)sulfinyl)benzoic acid (30 mg, 0.10 mmol, 1 eq.), oxalyl chloride (14 mg, 0.11 mmol, 1.1 eq.) and DiPEA (39 mg, 0.3 mmol, 3 eq.) according to general procedure G in a yield of 36 mg (0.07 mmol, 72%). 1H NMR (500 MHz, $CDCl_3$) δ 8.50 – 8.33 (m, 2H), 8.02 (dd, $J = 8.1, 1.6$ Hz, 1H), 7.41 (d, $J = 2.4$ Hz, 1H), 7.23 (dd, $J = 8.6, 2.4$ Hz, 1H), 6.96 (d, $J = 8.6$ Hz, 1H), 4.28 – 4.16 (m, 2H), 4.14 (d, $J = 13.6$ Hz, 1H), 4.01 (s, 2H), 3.78 (d, $J = 13.7$ Hz, 1H), 3.61 (s, 2H), 3.08 (br, 4H), 1.28 (t, $J = 7.1$ Hz, 3H). ^{13}C NMR (126 MHz, $CDCl_3$) δ 166.70, 164.56, 147.05, 144.95, 144.06, 139.86, 133.73, 130.63, 129.85, 129.45, 128.03, 127.95, 124.21, 121.49, 62.50, 60.09, 51.70, 50.99, 48.13, 42.74, 14.21.

Ethyl 2-((4-(4-(2,4-dichlorophenyl)piperazine-1-carbonyl)-2-

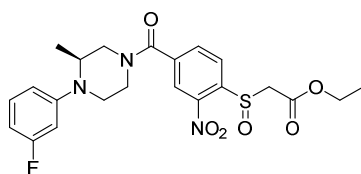
nitrophenyl)sulfinyl)acetate (21)

The title compound was synthesized using 1-(2,4-dichlorophenyl)piperazine (23 mg, 0.10 mmol, 1 eq.), 4-((2-ethoxy-2-oxoethyl)sulfonyl)-3-nitrobenzoic acid (30 mg, 0.10 mmol, 1 eq.), HATU (57 mg, 0.15 mmol, 1.5 eq.) and DiPEA (39 mg, 0.30 mmol, 3 eq.) according to general procedure H in a yield of 41 mg (0.08 mmol, 84%). ^1H NMR (400 MHz, CDCl_3) δ 8.44 – 8.37 (m, 2H), 8.02 (dd, J = 8.0, 1.6 Hz, 1H), 7.40 (d, J = 2.4 Hz, 1H), 7.23 (dd, J = 8.6, 2.4 Hz, 1H), 6.97 (d, J = 8.7 Hz, 1H), 4.28 – 4.15 (m, 2H), 4.14 (d, J = 13.7 Hz, 1H), 4.00 (s, 2H), 3.78 (d, J = 13.7 Hz, 1H), 3.61 (s, 2H), 3.15 (s, 2H), 3.01 (s, 2H), 1.28 (t, J = 7.1 Hz, 3H). ^{13}C NMR (101 MHz, CDCl_3) δ 166.66, 164.58, 147.05, 144.91, 143.99, 139.83, 133.72, 130.57, 129.79, 129.35, 127.96, 127.92, 124.20, 121.50, 62.45, 60.08, 50.93, 48.10, 14.19. HRMS: Calculated for $[\text{C}_{21}\text{H}_{21}\text{Cl}_2\text{N}_3\text{O}_6\text{S} + \text{H}]^+$ = 514.0601, found = 514.0602.

Ethyl 2-((4-(4-(2,6-dichlorophenyl)piperazine-1-carbonyl)-2-nitrophenyl)sulfinyl)acetate (22)

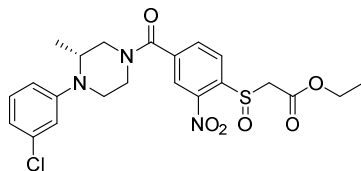
The title compound was synthesized using 1-(2,6-dichlorophenyl)piperazine (20 mg, 0.09 mmol, 1 eq.), 4-((2-ethoxy-2-oxoethyl)sulfonyl)-3-nitrobenzoic acid (39 mg, 0.14 mmol, 1.5 eq.), HATU (53 mg, 0.14 mmol, 1.5 eq.) and DiPEA (38 mg, 0.30 mmol, 3 eq.) according to general procedure H in a yield of 63 mg (0.08 mmol, 89%). ^1H NMR (400 MHz, CDCl_3) δ 8.43 – 8.37 (m, 2H), 8.01 (dd, J = 8.0, 1.6 Hz, 1H), 6.98 – 6.91 (m, 3H), 4.28 – 4.17 (m, 2H), 4.14 (d, J = 13.7 Hz, 1H), 3.98 (s, 2H), 3.77 (d, J = 13.7 Hz, 1H), 3.59 (s, 2H), 3.31 (s, 2H), 3.18 (s, 2H), 1.28 (t, J = 7.1 Hz, 3H). ^{13}C NMR (101 MHz, CDCl_3) δ 166.54, 164.58, 150.65, 144.91, 143.98, 139.79, 133.72, 129.41, 127.93, 124.22, 121.13, 117.00, 62.44, 60.08, 50.12, 49.62, 47.82, 42.51, 38.68, 14.18. HRMS: Calculated for $[\text{C}_{21}\text{H}_{21}\text{Cl}_2\text{N}_3\text{O}_6\text{S} + \text{H}]^+$ = 514.0601, found = 514.0600.

Ethyl 2-((4-((S)-4-(3-fluorophenyl)-3-methylpiperazine-1-carbonyl)-2-nitrophenyl)sulfinyl)acetate (23)

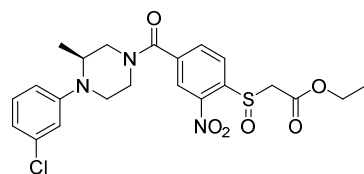


The title compound was synthesized using (*S*)-1-(3-fluorophenyl)-2-methylpiperazine (26mg, 0.13 mmol, 1 eq.), 4-((2-ethoxy-2-oxoethyl)sulfinyl)benzoic acid (40 mg, 0.13 mmol, 1 eq.), oxalyl chloride (19 mg, 0.15 mmol, 1.1 eq.) and DiPEA (52 mg, 0.40 mmol, 3 eq.) according to general procedure G in a yield of 38 mg (0.08 mmol, 60%). ¹H NMR (400 MHz, CDCl₃) δ 8.60 – 8.27 (m, 2H), 8.06 – 7.91 (m, 1H), 7.22 (td, *J* = 8.4, 6.8 Hz, 1H), 6.76 – 6.46 (m, 3H), 4.47 (m, 1H), 4.21 (m, 2H), 4.14 (d, *J* = 13.7 Hz, 1H), 3.94 (m, 1H), 3.78 (d, *J* = 13.7 Hz, 1H), 3.74 – 2.99 (m, 5H), 1.29 (t, *J* = 7.1 Hz, 3H), 1.08 (m, 3H). ¹³C NMR (101 MHz, CDCl₃) δ 167.37, 163.97 (d, *J* = 244.1 Hz), 164.59, 151.16 (d, *J* = 9.5 Hz), 144.96, 144.05, 139.73, 133.74, 130.55 (d, *J* = 9.9 Hz), 128.02, 124.22, 112.38 (d, *J* = 2.4 Hz), 106.99(d, *J* = 21.3 Hz), 104.00(d, *J* = 24.9 Hz), 62.50, 60.09, 52.53, 51.68, 47.39, 42.43, 14.23, 12.52. HRMS: Calculated for [C₂₂H₂₄FN₃O₆S + H]⁺ = 478.1443, found = 478.1440.

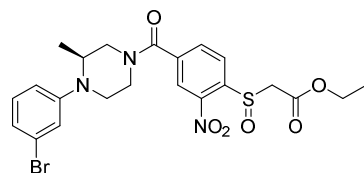
Ethyl 2-(((*R*)-4-(3-chlorophenyl)-3-methylpiperazine-1-carbonyl)-2-nitrophenyl)sulfinyl)acetate ((*R*)-24)



The title compound was synthesized using (*R*)-1-(3-chlorophenyl)-2-methylpiperazine (28mg, 0.13 mmol, 1 eq.), 4-((2-ethoxy-2-oxoethyl)sulfinyl)benzoic acid (40 mg, 0.13 mmol, 1 eq.), oxalyl chloride (19 mg, 0.15 mmol, 1.1 eq.) and DiPEA (52 mg, 0.40 mmol, 3 eq.) according to general procedure G in a yield of 22 mg (0.05 mmol, 34%). ¹H NMR (400 MHz, CDCl₃) δ 8.43 – 8.38 (m, 2H), 8.11 – 7.94 (m, 1H), 7.20 (t, *J* = 8.3 Hz, 1H), 6.90 – 6.74 (m, 3H), 4.63 – 4.27 (m, 1H), 4.22 (m, 2H), 4.14 (d, *J* = 13.7 Hz, 1H), 3.92 (m, 1H), 3.78 (d, *J* = 13.7 Hz, 1H), 3.74 – 3.00 (m, 5H), 1.28 (t, *J* = 7.1 Hz, 3H), 1.06 (m, 3H). ¹³C NMR (101 MHz, CDCl₃) δ 167.35, 164.59, 150.62, 144.95, 144.04, 139.71, 135.24, 133.73, 130.40, 128.01, 124.23, 120.43, 117.19, 115.18, 62.50, 60.10, 52.61, 51.81, 47.61, 42.41, 14.23, 12.63. HRMS: Calculated for [C₂₂H₂₄ClN₃O₆S + H]⁺ = 494.1147, found = 494.1142.

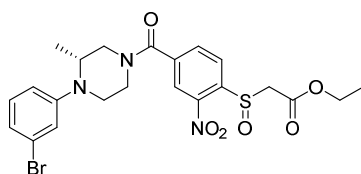
Ethyl 2-((4-((*S*)-4-(3-chlorophenyl)-3-methylpiperazine-1-carbonyl)-2-nitrophenyl)sulfinyl)acetate ((*S*)-24)

The title compound was synthesized using (*S*)-1-(3-fluorophenyl)-2-methylpiperazine (28mg, 0.13 mmol, 1 eq.), 4-((2-ethoxy-2-oxoethyl)sulfinyl)benzoic acid (40 mg, 0.13 mmol, 1 eq.), oxalyl chloride (19 mg, 0.15 mmol, 1.1 eq.) and DiPEA (52 mg, 0.40 mmol, 3 eq.) according to general procedure G in a yield of 50 mg (0.10 mmol, 76%). ¹H NMR (600 MHz, CDCl₃) δ 8.51 – 8.33 (m, 2H), 8.04 (dd, *J* = 8.0, 1.6 Hz, 1H), 7.24 (d, *J* = 8.2 Hz, 1H), 6.95 (m, 3H), 4.57 – 4.09 (m, 4H), 4.05 – 3.08 (m, 7H), 1.28 (d, *J* = 7.2Hz, 3H), 1.09 (m, 3H). ¹³C NMR (151 MHz, CDCl₃) δ 167.39, 164.59, 149.17, 144.98, 143.92, 139.42, 135.45, 133.77, 130.63, 128.09, 124.29, 121.66, 117.78, 115.87, 62.56, 60.02, 52.87, 52.41, 47.21, 42.19, 14.19, 12.81. HRMS: Calculated for [C₂₂H₂₄ClN₃O₆S + H]⁺ = 494.1147, found = 494.1143.

Ethyl 2-((4-((*R*)-4-(3-bromophenyl)-3-methylpiperazine-1-carbonyl)-2-nitrophenyl)sulfinyl)acetate ((*S*)-25)

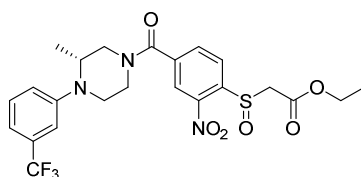
The title compound was synthesized using (*S*)-1-(3-bromophenyl)-2-methylpiperazine (34mg, 0.13 mmol, 1 eq.), 4-((2-ethoxy-2-oxoethyl)sulfinyl)benzoic acid (40 mg, 0.13 mmol, 1 eq.), oxalyl chloride (19 mg, 0.15 mmol, 1.1 eq.) and DiPEA (52 mg, 0.40 mmol, 3 eq.) according to general procedure G in a yield of 40mg (0.07 mmol, 56%). ¹H NMR (400 MHz, CDCl₃) δ 8.47 – 8.34 (m, 2H), 8.14 – 7.89 (m, 1H), 7.14 (m, 1H), 7.02 (m, 2H), 6.83 (d, *J* = 8.3 Hz, 1H), 4.42 (m, 1H), 4.22 (m, 2H), 4.14 (d, *J* = 13.7 Hz, 1H), 4.01 (m, 1H), 3.78 (d, *J* = 13.6 Hz, 1H), 3.72 – 3.02 (m, 5H), 1.28 (d, *J* = 7.1 Hz, 3H), 1.07 (m, 3H). ¹³C NMR (101 MHz, CDCl₃) δ 167.36, 164.58, 150.78, 144.94, 144.06, 139.70, 133.73, 130.69, 128.00, 124.23, 123.47, 123.40, 120.06, 115.66, 62.49, 60.08, 52.62, 51.84, 47.38, 42.40, 14.23, 12.66. HRMS: Calculated for [C₂₂H₂₄BrN₃O₆S + H]⁺ = 538.0642, found = 538.0638.

Ethyl 2-((4-((*R*)-4-(3-bromophenyl)-3-methylpiperazine-1-carbonyl)-2-nitrophenyl)sulfinyl)acetate ((*R*)-25)



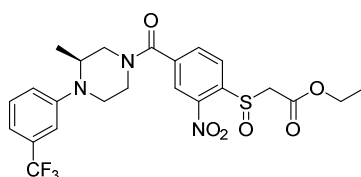
The title compound was synthesized using (*R*)-1-(3-bromophenyl)-2-methylpiperazine (34mg, 0.13 mmol, 1 eq.), 4-((2-ethoxy-2-oxoethyl)sulfinyl)benzoic acid (40 mg, 0.13 mmol, 1 eq.), oxalyl chloride (19 mg, 0.15 mmol, 1.1 eq.) and DiPEA (52 mg, 0.40 mmol, 3 eq.) according to general procedure G in a yield of 50mg (0.09 mmol, 70%). ¹H NMR (600 MHz, CDCl₃) δ 8.51 – 8.35 (m, 2H), 8.03 (dd, *J* = 8.0, 1.6 Hz, 1H), 7.23 – 7.09 (m, 3H), 6.96 (m, 1H), 4.50 – 4.04 (m, 4H), 3.99 – 3.13 (m, 7H), 1.27 (t, *J* = 7.1Hz, 3H), 1.16 – 0.92 (m, 3H). ¹³C NMR (151 MHz, CDCl₃) δ 167.42, 164.59, 149.38, 144.99, 143.89, 139.36, 133.78, 130.94, 128.10, 124.86, 124.31, 121.41, 117.19, 62.58, 60.01, 53.10, 52.37, 47.17, 42.14, 14.19, 12.89. HRMS: Calculated for [C₂₂H₂₄BrN₃O₆S + H]⁺ = 538.0642, found = 538.0639.

Ethyl 2-((4-((*R*)-3-methyl-4-(3-(trifluoromethyl)phenyl)piperazine-1-carbonyl)-2-nitrophenyl)sulfinyl)acetate ((*R*)-26)



The title compound was synthesized using (*R*)-1-(3-(trifluoromethyl)phenyl)-2-methylpiperazine (32mg, 0.13 mmol, 1 eq.), 4-((2-ethoxy-2-oxoethyl)sulfinyl)benzoic acid (40 mg, 0.13 mmol, 1 eq.), oxalyl chloride (19 mg, 0.15 mmol, 1.1 eq.) and DiPEA (52 mg, 0.40 mmol, 3 eq.) according to general procedure G in a yield of 60mg (0.11 mmol, 86%). ¹H NMR (600 MHz, CDCl₃) δ 8.51 – 8.33 (m, 2H), 8.05 (dd, *J* = 8.0, 1.6 Hz, 1H), 7.44 (m, 1H), 7.20 (m, 3H), 4.61 – 4.13 (m, 4H), 4.11 – 3.16 (m, 7H), 1.28 (t, *J* = 7.2Hz, 3H), 1.19 – 1.01 (m, 3H). ¹³C NMR (151 MHz, CDCl₃) δ 167.47, 164.60, 148.82, 145.00, 143.79, 139.39, 133.78, 131.97 (q, *J* = 32.0 Hz), 130.18, 128.10, 124.09 (q, *J* = 271.8Hz), 124.31, 120.76, 118.53, 114.60, 62.59, 59.99, 52.98, 52.47, 47.33, 42.28, 14.17, 12.81. HRMS: Calculated for [C₂₃H₂₄F₃N₃O₆S + H]⁺ = 528.1411, found = 528.1409.

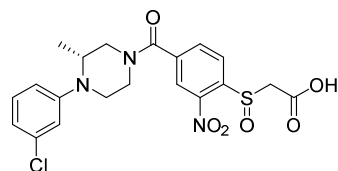
Ethyl 2-((4-((*S*)-3-methyl-4-(3-(trifluoromethyl)phenyl)piperazine-1-carbonyl)-2-nitrophenyl)sulfinyl)acetate ((*S*)-26)



The title compound was synthesized using (*S*)-1-(3-(trifluoromethyl)phenyl)-2-methylpiperazine (32mg, 0.13 mmol, 1 eq.), 4-((2-ethoxy-2-oxoethyl)sulfinyl)benzoic acid (40

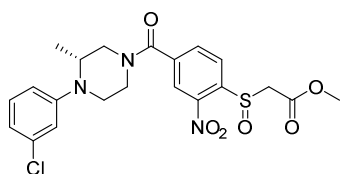
mg, 0.13 mmol, 1 eq.), oxalyl chloride (19 mg, 0.15 mmol, 1.1 eq.) and DiPEA (52 mg, 0.40 mmol, 3 eq.) according to general procedure G in a yield of 57mg (0.11 mmol, 82%). ^1H NMR (400 MHz, CDCl_3) δ 8.46 – 8.36 (m, 2H), 8.03 (dt, $J = 8.0, 1.9$ Hz, 1H), 7.40 (t, $J = 7.9$ Hz, 1H), 7.20 – 6.98 (m, 3H), 4.62 – 4.29 (m, 1H), 4.26 – 4.18 (m, 2H), 4.14 (d, $J = 13.7$ Hz, 1H), 4.11 – 3.83 (m, 1H), 3.79 (d, $J = 13.7$ Hz, 1H), 3.74 – 3.06 (m, 5H), 1.29 (t, $J = 7.2$ Hz, 3H), 1.20 – 0.93 (m, 3H). ^{13}C NMR (101 MHz, CDCl_3) δ 167.43, 164.61, 149.71, 144.96, 144.08, 139.68, 133.74, 131.78 (q, $J = 31.8$ Hz), 129.98, 128.02, 124.24, 124.22 (q, $J = 273.71$ Hz), 120.16, 117.04, 113.59, 62.49, 60.08, 52.61, 51.80, 47.38, 42.38, 14.21, 12.66. HRMS: Calculated for $[\text{C}_{23}\text{H}_{24}\text{F}_3\text{N}_3\text{O}_6\text{S} + \text{H}]^+ = 528.1411$, found = 528.1411.

2-((4-((*R*)-3-Methyl-4-(*m*-tolyl)piperazine-1-carbonyl)-2-nitrophenyl)sulfinyl)acetic acid (65)



To a solution of ethyl 2-((4-((*R*)-4-(3-chlorophenyl)-3-methylpiperazine-1-carbonyl)-2-nitrophenyl)sulfinyl)acetate (38 mg, 0.08 mmol, 1 eq.) in MeOH (2mL) were added TEA (2mL) and water (1mL). Then the reaction mixture was stirred overnight at room temperature. The reaction progress was monitored by TLC analysis. Upon full conversion of the starting materials, the pH of resulted mixture was adjusted to 1 with 1M HCl solution. Then the mixture was diluted with EtOAc and the organic layer was washed with water, dried (MgSO_4), filtered and concentrated under reduced pressure. The residue was purified by silica gel column chromatography (MeOH/DCM, 1% \rightarrow 2%) to afford the product (31 mg, 0.07 mmol, 86 %). ^1H NMR (500 MHz, CDCl_3) δ 11.31 (s, 1H), 8.51 – 8.30 (m, 2H), 8.07 – 7.96 (m, 1H), 7.20 (t, $J = 8.3$ Hz, 1H), 6.84 (m, 3H), 4.59 – 3.19 (m, 9H), 1.18 – 0.95 (m, 3H). ^{13}C NMR (126 MHz, CDCl_3) δ 167.39, 166.68, 150.52, 145.00, 143.44, 139.44, 135.30, 133.92, 130.46, 128.16, 124.32, 120.58, 117.27, 115.26, 59.62, 52.63, 51.95, 47.52, 42.50, 12.83.

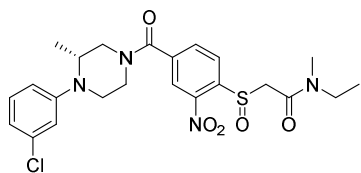
Methyl 2-((4-((*R*)-4-(3-chlorophenyl)-3-methylpiperazine-1-carbonyl)-2-nitrophenyl)sulfinyl)acetate (27)



The title compound was synthesized using 2-((4-((*R*)-4-(3-chlorophenyl)-3-methylpiperazine-1-carbonyl)-2-nitrophenyl)sulfinyl)acetic acid (40 mg, 0.09 mmol, 1 eq.),

MeOH (55 mg, 1.72 mmol, 20 eq.), oxalyl chloride (12 mg, 0.94 mmol, 1.1 eq.) and DiPEA (33 mg, 0.26 mmol, 3 eq.) according to general procedure G in a yield of 28mg (0.061 mmol, 68%). ^1H NMR (600 MHz, CDCl_3) δ 8.50 – 8.30 (m, 2H), 8.04 (dd, J = 8.0, 1.6 Hz, 1H), 7.24 (t, J = 8.2 Hz, 1H), 7.05 – 6.79 (m, 3H), 4.57 – 3.61 (m, 8H), 3.60 – 3.12 (m, 4H), 1.09 (d, J = 78.9 Hz, 3H). ^{13}C NMR (151 MHz, CDCl_3) δ 167.42, 165.03, 149.47, 145.03, 143.88, 139.53, 135.46, 133.81, 130.62, 128.05, 124.33, 122.12, 118.30, 116.40, 59.90, 53.18, 52.71, 52.44, 46.22, 42.24, 12.80. HRMS: Calculated for $[\text{C}_{21}\text{H}_{22}\text{ClN}_3\text{O}_6\text{S} + \text{H}]^+$ = 480.0991, found = 480.0989.

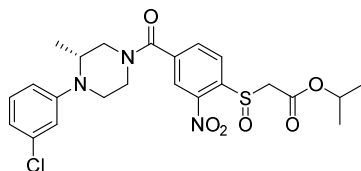
2-((4-((*R*)-4-(3-Chlorophenyl)-3-methylpiperazine-1-carbonyl)-2-nitrophenyl)sulfinyl)-*N*-ethyl-*N*-methylacetamide (28)



The title compound was synthesized using 2-((4-((*R*)-4-(3-chlorophenyl)-3-methylpiperazine-1-carbonyl)-2-nitrophenyl)sulfinyl)acetic acid (40 mg, 0.09 mmol, 1 eq.),

N-methylethanamine (102 mg, 1.72 mmol, 20 eq.), oxalyl chloride (12 mg, 0.94 mmol, 1.1 eq.) and DiPEA (33 mg, 0.26 mmol, 3 eq.) according to general procedure G in a yield of 18mg (0.036 mmol, 41%). ^1H NMR (600 MHz, CDCl_3) δ 8.39 (m, 2H), 8.01 (d, J = 7.8 Hz, 1H), 7.22 (t, J = 8.0 Hz, 1H), 6.88 (m, 3H), 4.36 – 3.91 (m, 2H), 3.76 (m, 3H), 3.58 – 3.32 (m, 4H), 3.32 – 3.12 (m, 2H), 3.09 – 2.95 (m, 3H), 1.27 – 0.91 (m, 6H). ^{13}C NMR (151 MHz, CDCl_3) δ 167.22, 163.56, 150.06, 145.10, 144.32, 139.36, 135.37, 133.70, 130.52, 128.10, 124.16, 121.00, 117.45, 115.51, 59.51, 52.40, 47.45, 45.51, 43.43, 42.30, 33.36, 13.72, 12.88. HRMS: Calculated for $[\text{C}_{23}\text{H}_{27}\text{ClN}_4\text{O}_5\text{S} + \text{H}]^+$ = 507.1463, found = 507.1463.

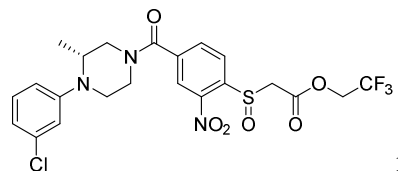
Isopropyl 2-((4-((*R*)-4-(3-chlorophenyl)-3-methylpiperazine-1-carbonyl)-2-nitrophenyl)sulfinyl)acetate (29)



The title compound was synthesized using 2-((4-((*R*)-4-(3-chlorophenyl)-3-methylpiperazine-1-carbonyl)-2-nitrophenyl)sulfinyl)acetic acid (40 mg, 0.09 mmol, 1 eq.),

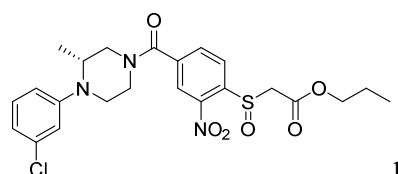
propan-2-ol (103 mg, 1.72 mmol, 20 eq.), oxalyl chloride (12 mg, 0.94 mmol, 1.1 eq.) and DiPEA (33 mg, 0.26 mmol, 3 eq.) according to general procedure G in a yield of 16mg (0.03 mmol, 37%). ^1H NMR (600 MHz, CDCl_3) δ 8.50 – 8.33 (m, 2H), 8.03 (dd, $J = 8.0, 1.6$ Hz, 1H), 7.22 (t, $J = 8.1$ Hz, 1H), 6.88 (m, 3H), 5.07 (m, 1H), 4.52 – 4.38 (m, 1H), 4.13 (d, $J = 13.8$ Hz, 1H), 3.90 (m, 1H), 3.76 (d, $J = 13.8$ Hz, 1H), 3.74 – 3.10 (m, 5H), 1.31 – 1.22 (m, 6H), 1.14 – 1.02 (m, 3H). ^{13}C NMR (151 MHz, CDCl_3) δ 167.13, 164.17, 150.12, 145.00, 144.12, 139.55, 135.39, 133.76, 130.54, 128.19, 124.28, 121.53, 117.52, 115.53, 70.72, 60.24, 52.36, 47.38, 45.08, 42.35, 21.83, 12.75. HRMS: Calculated for $[\text{C}_{23}\text{H}_{26}\text{ClN}_3\text{O}_6\text{S} + \text{H}]^+ = 508.1304$, found = 508.1305.

2,2,2-Trifluoroethyl 2-((4-((R)-4-(3-chlorophenyl)-3-methylpiperazine-1-carbonyl)-2-nitrophenyl)sulfinyl)acetate (30)



The title compound was synthesized using 2-((4-((R)-4-(3-chlorophenyl)-3-methylpiperazine-1-carbonyl)-2-nitrophenyl)sulfinyl)acetic acid (40 mg, 0.09 mmol, 1 eq.), 2,2,2-trifluoroethan-1-ol (172 mg, 1.72 mmol, 20 eq.), oxalyl chloride (12 mg, 0.94 mmol, 1.1 eq.) and DiPEA (33 mg, 0.26 mmol, 3 eq.) according to general procedure G in a yield of 8mg (0.015 mmol, 17%). ^1H NMR (600 MHz, CDCl_3) δ 8.50 – 8.33 (m, 2H), 8.10 – 7.95 (m, 1H), 7.22 (t, $J = 8.0$ Hz, 1H), 6.95 – 6.75 (m, 3H), 4.52 (qd, $J = 8.2, 1.8$ Hz, 2H), 4.35 – 3.05 (m, 9H), 1.07 (m, 3H). ^{13}C NMR (151 MHz, CDCl_3) δ 167.35, 163.16, 150.41, 145.00, 143.45, 140.02, 135.38, 133.95, 130.51, 128.18, 124.42, 122.56 (q, $J = 277.4$ Hz), 120.88, 117.47, 115.46, 61.54 (q, $J = 37.3$ Hz), 59.13, 52.62, 52.19, 47.49, 42.44, 12.72. HRMS: Calculated for $[\text{C}_{22}\text{H}_{21}\text{ClF}_3\text{N}_3\text{O}_6\text{S} + \text{H}]^+ = 548.0864$, found = 548.0864.

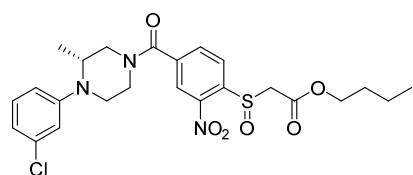
Propyl 2-((4-((R)-4-(3-chlorophenyl)-3-methylpiperazine-1-carbonyl)-2-nitrophenyl)sulfinyl)acetate (31)



The title compound was synthesized using 2-((4-((R)-4-(3-chlorophenyl)-3-methylpiperazine-1-carbonyl)-2-nitrophenyl)sulfinyl)acetic acid (40 mg, 0.09 mmol, 1 eq.), propan-1-ol (103 mg, 1.72 mmol, 20 eq.), oxalyl chloride (12 mg, 0.94 mmol, 1.1 eq.) and DiPEA (33 mg, 0.26 mmol, 3 eq.) according to general procedure G in a yield

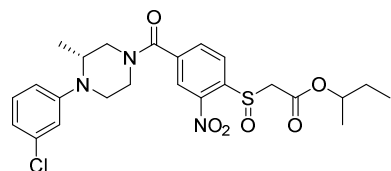
of 26mg (0.051 mmol, 60%). $^1\text{H NMR}$ (850 MHz, CDCl_3) δ 8.42 (d, $J = 7.9$ Hz, 2H), 8.04 (d, $J = 8.1$ Hz, 1H), 7.24 (s, 1H), 7.05 – 6.85 (m, 3H), 4.50 – 3.14 (m, 11H), 1.69 (p, $J = 7.0$ Hz, 2H), 1.20 – 0.98 (m, 3H), 0.96 (td, $J = 7.4, 1.1$ Hz, 3H). $^{13}\text{C NMR}$ (214 MHz, CDCl_3) δ 167.08, 164.70, 149.57, 145.00, 144.09, 139.47, 135.46, 133.78, 130.63, 128.10, 124.32, 121.58, 118.31, 116.32, 68.10, 60.15, 52.73, 52.45, 47.17, 42.22, 21.94, 12.77, 10.41. HRMS: Calculated for $[\text{C}_{23}\text{H}_{26}\text{ClN}_3\text{O}_6\text{S} + \text{H}]^+ = 508.13036$, found = 508.13022.

Butyl 2-((4-((*R*)-4-(3-chlorophenyl)-3-methylpiperazine-1-carbonyl)-2-nitrophenyl)sulfinyl)acetate (32)



The title compound was synthesized using 2-((4-((*R*)-4-(3-chlorophenyl)-3-methylpiperazine-1-carbonyl)-2-nitrophenyl)sulfinyl)acetic acid (40 mg, 0.09 mmol, 1 eq.), butan-1-ol (127 mg, 1.72 mmol, 20 eq.), oxalyl chloride (12 mg, 0.94 mmol, 1.1 eq.) and DiPEA (33 mg, 0.26 mmol, 3 eq.) according to general procedure G in a yield of 22mg (0.042 mmol, 49%). $^1\text{H NMR}$ (850 MHz, CDCl_3) δ 8.45 – 8.36 (m, 2H), 8.03 (dd, $J = 8.0, 1.6$ Hz, 1H), 7.21 (t, $J = 8.1$ Hz, 1H), 6.94 – 6.86 (m, 2H), 6.84 – 6.78 (m, 1H), 4.41 - 3.11 (m, 11H), 1.67 – 1.61 (m, 2H), 1.39 (m, 2H), 1.17 – 0.98 (m, 3H), 0.94 (td, $J = 7.4, 1.6$ Hz, 3H). $^{13}\text{C NMR}$ (214 MHz, CDCl_3) δ 167.08, 164.74, 150.24, 144.97, 143.99, 139.60, 135.34, 133.77, 130.50, 128.05, 124.29, 120.80, 117.87, 115.94, 66.42, 60.17, 52.14, 47.37, 44.79, 42.36, 30.52, 19.11, 13.77, 12.64. HRMS: Calculated for $[\text{C}_{24}\text{H}_{28}\text{ClN}_3\text{O}_6\text{S} + \text{H}]^+ = 522.14601$, found = 522.14572.

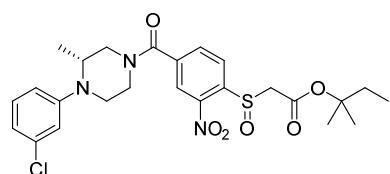
sec-Butyl 2-((4-((*R*)-4-(3-chlorophenyl)-3-methylpiperazine-1-carbonyl)-2-nitrophenyl)sulfinyl)acetate (33)



The title compound was synthesized using 2-((4-((*R*)-4-(3-chlorophenyl)-3-methylpiperazine-1-carbonyl)-2-nitrophenyl)sulfinyl)acetic acid (40 mg, 0.09 mmol, 1 eq.), butan-2-ol (127 mg, 1.72 mmol, 20 eq.), oxalyl chloride (12 mg, 0.94 mmol, 1.1 eq.) and DiPEA (33 mg, 0.26 mmol, 3 eq.) according to general procedure G in a yield of 12mg (0.023 mmol, 27%). $^1\text{H NMR}$ (850 MHz, CDCl_3) δ 8.48 – 8.35 (m, 2H), 8.08 – 8.01 (m, 1H), 7.28 (m, 1H), 7.11 – 6.91 (m, 3H), 4.93 (m, 1H), 4.47-3.20 (m, 9H),

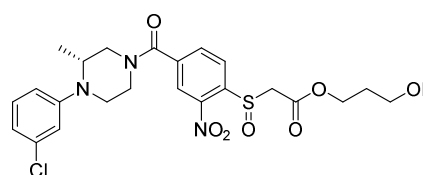
1.65 (m, 1H), 1.62 – 1.53 (m, 1H), 1.25 (m, 3H), 1.18 – 1.04 (m, 3H), 0.95 – 0.90 (m, 3H). ^{13}C NMR (214 MHz, CDCl_3) δ 167.18, 164.32, 147.91, 145.00, 144.07, 139.13, 135.67, 133.83, 130.84, 128.24, 124.38, 123.57, 118.95, 117.16, 75.40, 60.20, 54.46, 52.24, 46.99, 41.97, 28.78, 19.44, 13.27, 9.70. HRMS: Calculated for $[\text{C}_{24}\text{H}_{28}\text{ClN}_3\text{O}_6\text{S} + \text{H}]^+ = 522.14601$, found = 522.14612.

tert-Pentyl 2-((4-((R)-4-(3-chlorophenyl)-3-methylpiperazine-1-carbonyl)-2-nitrophenyl)sulfinyl)acetate (34)



The title compound was synthesized using 2-((4-((R)-4-(3-chlorophenyl)-3-methylpiperazine-1-carbonyl)-2-nitrophenyl)sulfinyl)acetic acid (40 mg, 0.09 mmol, 1 eq.), 2-methylbutan-2-ol (151 mg, 1.72 mmol, 20 eq.), oxalyl chloride (12 mg, 0.94 mmol, 1.1 eq.) and DiPEA (33 mg, 0.26 mmol, 3 eq.) according to general procedure G. This yielded the product (12 mg, 0.022 mmol, 26%). ^1H NMR (850 MHz, CDCl_3) δ 8.49 – 8.38 (m, 2H), 8.04 (d, $J = 8.0$ Hz, 1H), 7.28 (s, 1H), 7.05 (s, 3H), 4.51 – 3.19 (m, 9H), 1.80 (tt, $J = 14.1, 6.8$ Hz, 2H), 1.47 (d, $J = 13.0$ Hz, 6H), 1.19 – 1.05 (m, 3H), 0.93 (t, $J = 7.5$ Hz, 3H). ^{13}C NMR (214 MHz, CDCl_3) δ 167.13, 163.73, 145.01, 144.43, 139.13, 135.68, 133.80, 130.84, 128.26, 124.36, 86.81, 61.28, 53.78, 52.28, 46.94, 41.87, 33.64, 25.56, 13.34, 8.34. HRMS: Calculated for $[\text{C}_{25}\text{H}_{30}\text{ClN}_3\text{O}_6\text{S} + \text{H}]^+ = 536.1617$, found = 536.1617.

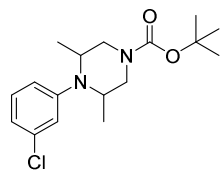
3-Hydroxypropyl 2-((4-((R)-4-(3-chlorophenyl)-3-methylpiperazine-1-carbonyl)-2-nitrophenyl)sulfinyl)acetate (35)



The title compound was synthesized using 2-((4-((R)-4-(3-chlorophenyl)-3-methylpiperazine-1-carbonyl)-2-nitrophenyl)sulfinyl)acetic acid (40 mg, 0.09 mmol, 1 eq.), propane-1,3-diol (131 mg, 1.72 mmol, 20 eq.), oxalyl chloride (12 mg, 0.94 mmol, 1.1 eq.) and DiPEA (33 mg, 0.26 mmol, 3 eq.) according to general procedure G in a yield of 12 mg (0.040 mmol, 47%). ^1H NMR (850 MHz, CDCl_3) δ 8.50 – 8.34 (m, 2H), 8.05 (s, 1H), 7.25 (s, 1H), 6.97 (m, 3H), 4.59 – 3.12 (m, 13H), 3.01 (s, 1H), 1.93 – 1.75 (m, 2H), 1.21 – 0.97 (m, 3H). ^{13}C NMR (214 MHz, CDCl_3) δ 167.21, 164.38, 149.95, 145.04, 143.65, 139.57, 135.51, 133.86, 130.67, 128.26, 124.29, 121.56, 118.46,

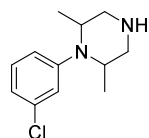
116.56, 64.61, 63.54, 59.10, 58.95, 52.47, 47.20, 42.19, 31.18, 13.06.

***tert*-Butyl 4-(3-chlorophenyl)-3,5-dimethylpiperazine-1-carboxylate (36a)**



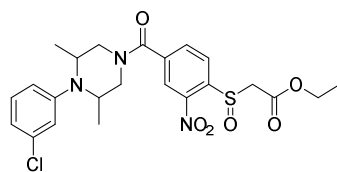
To a solution of 1-bromo-3-chlorobenzene (191 mg, 1 mmol, 1 eq.) and *tert*-butyl 3,5-dimethylpiperazine-1-carboxylate (257 mg, 1.2 mmol, 1.2 eq.) in dry 1,4-dioxane (2mL) was added KHMDS (239 mg, 1,2 mmol, 1.2 eq.) and the reaction mixture was heated to 100°C and stirred overnight. The reaction progress was monitored by TLC analysis. Upon full conversion of the starting materials, the mixture was cool to room temperature, diluted with EtOAc, washed with water, dried (MgSO₄), filtered and concentrated under reduced pressure. The residue was purified by silica gel column chromatography (diethyl ether/pentane, 5%→20%) to afford the product (70mg, 0.22 mmol, 22%). ¹H NMR (400 MHz, CDCl₃) δ 7.22 (td, *J* = 8.2, 1.4 Hz, 1H), 7.06 (dt, *J* = 8.1, 1.3 Hz, 2H), 6.94 (dq, *J* = 8.0, 1.4 Hz, 1H), 3.80 (br, 2H), 3.38 – 2.81 (m, 4H), 1.50 (s, 9H), 0.84 (dd, *J* = 6.3, 1.3 Hz, 6H). ¹³C NMR (101 MHz, CDCl₃) δ 154.75, 150.43, 134.70, 129.99, 124.18, 124.06, 122.50, 54.31, 28.54, 18.12.

1-(3-Chlorophenyl)-2,6-dimethylpiperazine (36b)



The title compound was synthesized using *tert*-butyl 4-(3-chlorophenyl)-3,5-dimethylpiperazine-1-carboxylate (70 mg, 0.22 mmol, 1 eq.) according to general procedure B in a yield of 42 mg (0.19 mmol, 86%). ¹H NMR (400 MHz, CDCl₃) δ 7.36 – 7.27 (m, 2H), 7.25 (t, *J* = 1.9 Hz, 1H), 7.16 (dt, *J* = 7.7, 1.6 Hz, 1H), 3.52 (d, *J* = 11.0 Hz, 2H), 3.44 – 3.36 (m, 2H), 2.99 (t, *J* = 11.8 Hz, 2H), 0.84 (d, *J* = 6.3 Hz, 6H). ¹³C NMR (101 MHz, CDCl₃) δ 134.97, 130.45, 127.74, 54.18, 49.39, 17.80.

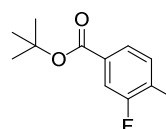
Ethyl 2-((4-(4-(3-chlorophenyl)-3,5-dimethylpiperazine-1-carbonyl)-2-nitrophenyl)sulfinyl)acetate (36)



The title compound was synthesized using 4-((2-ethoxy-2-oxoethyl)sulfinyl)-3-nitrobenzoic acid (40 mg, 0.13 mmol, 1 eq.), 1-(3-chlorophenyl)-2,6-dimethylpiperazine (30 mg, 0.13 mmol, 1 eq.), oxalyl chloride (19 mg, 0.15 mmol, 1.1 eq.) and DiPEA (52 mg, 0.40 mmol, 3 eq.) according to general procedure G in a yield of 36 mg (0.07 mmol,

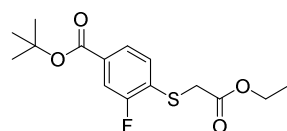
53%). ^1H NMR (850 MHz, CDCl_3) δ 8.49 (s, 1H), 8.42 (d, $J = 8.0$ Hz, 1H), 8.09 (d, $J = 8.0$ Hz, 1H), 7.55 – 7.39 (m, 4H), 4.76 (s, 1H), 4.25 – 4.12 (m, 3H), 3.92 (s, 1H), 3.80 (d, $J = 13.9$ Hz, 1H), 3.75 – 3.33 (m, 4H), 1.28 (t, $J = 7.2$ Hz, 3H), 1.06 (m, 6H). ^{13}C NMR (214 MHz, CDCl_3) δ 166.57, 164.68, 145.16, 144.39, 142.76, 138.73, 136.19, 133.88, 131.35, 129.33, 128.14, 124.78, 123.92, 123.03, 62.61, 60.63, 60.03, 51.89, 46.59, 16.21, 14.21. HRMS: Calculated for $[\text{C}_{23}\text{H}_{26}\text{ClN}_3\text{O}_6\text{S} + \text{H}]^+ = 508.1304$, found = 508.1303.

***tert*-Butyl 3,4-difluorobenzoate (66)**



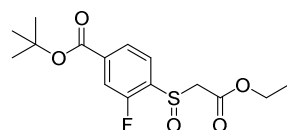
The title compound was synthesized using 3,4-difluorobenzoic acid (200 mg, 1.27 mmol, 1 eq.) according to procedure general procedure G in a yield of 198 mg (0.92 mmol, 73%). ^1H NMR (400 MHz, CDCl_3) δ 7.90 – 7.67 (m, 2H), 7.18 (q, $J = 9.5, 8.8$ Hz, 1H), 1.60 (s, 9H). ^{13}C NMR (101 MHz, CDCl_3) δ 163.74, 153.31 (dd, $J = 254.9, 12.8$ Hz), 150.00 (dd, $J = 249.3, 13.0$ Hz), 129.14 (dd, $J = 5.3, 3.6$ Hz), 126.31 (dd, $J = 7.3, 3.6$ Hz), 118.75 (d, $J = 18.6$ Hz), 117.06 (d, $J = 17.8$ Hz), 81.83, 28.07.

***tert*-Butyl 4-((2-ethoxy-2-oxoethyl)thio)-3-fluorobenzoate (67)**



The title compound was synthesized using ethyl 2-mercaptoacetate (101 mg, 0.84 mmol, 1 eq.) and *tert*-butyl 3,4-difluorobenzoate (198 mg, 0.92 mmol, 1.1eq.) according to general procedure D in a yield of 188 mg (0.60 mmol, 71%). ^1H NMR (400 MHz, CDCl_3) δ 7.73 (dd, $J = 8.1, 1.8$ Hz, 1H), 7.64 (dd, $J = 10.4, 1.7$ Hz, 1H), 7.42 (dd, $J = 8.2, 7.3$ Hz, 1H), 4.17 (q, $J = 7.1$ Hz, 2H), 3.71 (s, 2H), 1.59 (s, 9H), 1.23 (t, $J = 7.1$ Hz, 3H). ^{13}C NMR (101 MHz, CDCl_3) δ 168.86, 164.20, 160.22 (d, $J = 246.1$ Hz), 132.42 (d, $J = 7.1$ Hz), 130.11 (d, $J = 1.9$ Hz), 127.99 (d, $J = 17.4$ Hz), 125.48 (d, $J = 3.4$ Hz), 116.27 (d, $J = 23.7$ Hz), 81.72, 61.83, 34.70, 28.14, 14.10.

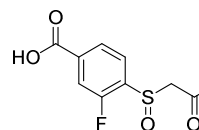
***tert*-Butyl 4-((2-ethoxy-2-oxoethyl)sulfinyl)-3-fluorobenzoate (68)**



The title compound was synthesized using *tert*-butyl 4-((2-ethoxy-2-oxoethyl)thio)-3-fluorobenzoate (40 mg, 0.13 mmol, 1.00 eq.) according to general procedure E in a yield of 38 mg (0.12 mmol, 90%). ^1H NMR (400 MHz, CDCl_3) δ 8.01 (dd, $J = 8.1, 1.4$ Hz, 1H), 7.91

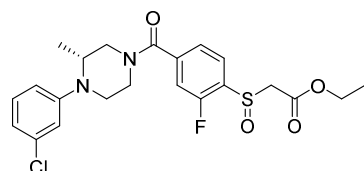
(dd, $J = 8.1, 6.6$ Hz, 1H), 7.74 (dd, $J = 10.1, 1.4$ Hz, 1H), 4.20 (qd, $J = 7.2, 1.2$ Hz, 2H), 3.97 (d, $J = 13.7$ Hz, 1H), 3.78 (d, $J = 13.7$ Hz, 1H), 1.61 (s, 9H), 1.25 (t, $J = 7.1$ Hz, 3H). ^{13}C NMR (101 MHz, CDCl_3) δ 164.23, 163.55, 157.35 (d, $J = 247.8$ Hz), 137.41 (d, $J = 6.9$ Hz), 134.60 (d, $J = 17.2$ Hz), 126.37, 126.32 (d, $J = 4.1$ Hz), 116.73 (d, $J = 22.0$ Hz), 82.65, 62.44, 58.64, 28.18, 14.17.

4-((2-Ethoxy-2-oxoethyl)sulfinyl)-3-fluorobenzoic acid (69)



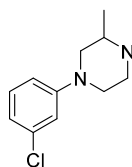
The title compound was synthesized using *tert*-butyl 4-((2-ethoxy-2-oxoethyl)sulfinyl)-3-fluorobenzoate (30mg, 0.09 mmol, 1 eq.) according to general procedure F in a yield of 18 mg (0.7 mmol, 72%). ^1H NMR (400 MHz, Methanol- d_4) δ 8.10 (dd, $J = 8.1, 1.5$ Hz, 1H), 7.95 – 7.80 (m, 2H), 4.27 – 4.05 (m, 3H), 3.95 (d, $J = 14.2$ Hz, 1H), 1.19 (t, $J = 7.1$ Hz, 3H). ^{13}C NMR (101 MHz, Methanol- d_4) δ 167.20, 165.75, 159.03 (d, $J = 247.7$ Hz), 137.86 (d, $J = 7.1$ Hz), 135.69 (d, $J = 16.9$ Hz), 127.66 (d, $J = 3.3$ Hz), 127.53 (d, $J = 2.1$ Hz), 117.91 (d, $J = 22.2$ Hz), 63.17, 59.38, 14.31.

Ethyl 2-((4-((*R*)-4-(3-chlorophenyl)-3-methylpiperazine-1-carbonyl)-2-fluorophenyl)sulfinyl)acetate (37)



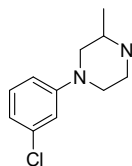
The title compound was synthesized using 4-((2-ethoxy-2-oxoethyl)sulfinyl)-3-fluorobenzoic acid (40 mg, 0.15 mmol, 1 eq.), (*R*)-1-(3-chlorophenyl)-2-methylpiperazine (31 mg, 0.15 mmol, 1 eq.), oxalyl chloride (20 mg, 0.16 mmol, 1.1 eq.) and DiPEA (57 mg, 0.44 mmol, 3 eq.) according to general procedure G in a yield of 36 mg (0.07 mmol, 53%). ^1H NMR (850 MHz, CDCl_3) δ 7.95 (t, $J = 7.2$ Hz, 1H), 7.51 (d, $J = 8.4$ Hz, 1H), 7.31 (t, $J = 11.5$ Hz, 2H), 7.24 – 6.98 (m, 3H), 4.35 – 3.17 (m, 11H), 1.25 (t, $J = 7.2$ Hz, 3H), 1.22 – 0.94 (m, 3H). ^{13}C NMR (214 MHz, CDCl_3) δ 168.20, 164.20, 157.65 (d, $J = 246.3$ Hz), 146.52, 140.01 (d, $J = 29.3$ Hz), 135.80, 132.01, 131.01, 127.15, 124.17, 124.01, 118.82, 117.08, 115.23 (d, $J = 22.0$ Hz), 62.61, 58.57, 55.09, 51.80, 46.42, 41.44, 14.10, 13.39. HRMS: Calculated for $[\text{C}_{22}\text{H}_{24}\text{ClFN}_2\text{O}_4\text{S} + \text{H}]^+$ = 467.1202, found = 467.1202.

tert-Butyl 4-(3-chlorophenyl)-2-methylpiperazine-1-carboxylate (38a)



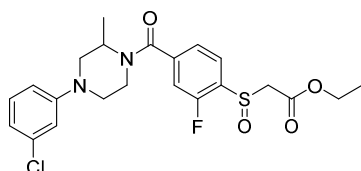
The title compound was synthesized using 1-bromo-3-chlorobenzene (96 mg, 0.50 mmol, 1 eq.), *tert*-butyl 2-methylpiperazine-1-carboxylate (100 mg, 0.50 mmol, 1 eq.), sodium *tert*-butoxide (72 mg, 0.75 mmol, 1.5 eq.), *rac*-BINAP (19 mg, 0.03 mmol, 0.06 eq.) and palladium diacetate (4.45 mg, 0.02 mmol, 0.04 eq.) according to general procedure A in a yield of 121 mg (0.39 mmol, 78%).

1-(3-Chlorophenyl)-3-methylpiperazine (38b)



The title compound was synthesized using *tert*-Butyl 4-(3-chlorophenyl)-2-methylpiperazine-1-carboxylate (104mg, 0.34 mmol, 1 eq.) according to general procedure B in a yield of 66 mg (0.31 mmol, 93%). ¹H NMR (400 MHz, CDCl₃) δ 7.15 (t, J = 8.1 Hz, 1H), 6.87 (t, J = 2.2 Hz, 1H), 6.79 (ddt, J = 9.6, 7.5, 1.2 Hz, 2H), 3.50 (dq, J = 11.5, 1.5 Hz, 2H), 3.13 (ddd, J = 12.0, 3.3, 2.3 Hz, 1H), 3.07 – 2.92 (m, 2H), 2.85 – 2.69 (m, 2H), 2.41 (dd, J = 11.9, 10.2 Hz, 1H), 1.16 (d, J = 6.4 Hz, 3H). ¹³C NMR (101 MHz, CDCl₃) δ 152.47, 134.96, 130.08, 119.33, 115.89, 114.07, 56.18, 50.59, 48.75, 45.60, 19.58.

Ethyl 2-((4-(4-(3-chlorophenyl)-2-methylpiperazine-1-carbonyl)-2-fluorophenyl)sulfinyl)acetate (38)



The title compound was synthesized using 4-((2-ethoxy-2-oxoethyl)sulfinyl)-3-fluorobenzoic acid (18 mg, 0.07 mmol, 1 eq.), 1-(3-chlorophenyl)-3-methylpiperazine (14 mg, 0.07 mmol, 1 eq.), oxalyl chloride (9 mg, 0.07 mmol, 1.1 eq.) and DiPEA (25 mg, 0.20 mmol, 3 eq.) according to general procedure G in a yield of 15 mg (0.03 mmol, 49%). ¹H NMR (850 MHz, CDCl₃) δ 8.09 – 7.88 (m, 1H), 7.56 – 7.38 (m, 1H), 7.22 (m, 2H), 7.02 – 6.75 (m, 3H), 4.79 (m, 1H), 4.36 – 4.18 (m, 2H), 3.97 (d, J = 13.8 Hz, 1H), 3.81 (d, J = 13.9 Hz, 1H), 3.51 (m, 3H), 3.13 – 2.67 (m, 3H), 1.45 (m, 3H), 1.27 (t, J = 7.0 Hz, 3H). ¹³C NMR (214 MHz, CDCl₃) δ 167.75, 164.30, 157.69 (d, J = 250.3 Hz), 152.28, 141.31, 135.19, 131.92 (d, J = 16.9 Hz), 130.38, 127.07, 123.74, 120.68, 116.95, 114.98, 114.77, 62.54, 58.99, 54.51, 49.37, 42.94, 37.36, 16.45, 14.19.

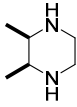
5,6-Dimethyl-2,3-dihydropyrazine (70)



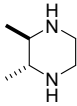
To a cooled (0°C) solution of ethylenediamine (6.6 mL, 100 mmol) in Et₂O (250 mL) was dropwise added a solution of 2,3-butanedione (8.8 mL, 100 mmol) in

Et₂O (250 mL) and the suspension was allowed to stir for 16h. The resulting clear liquid was dried using potassium hydroxide for 30 min. After filtration, the mixture was concentrated and the residue was purified by short-neck distillation which yielded the product (9.36 g; 85 mmol; 85%). ¹H NMR (400 MHz, CDCl₃) δ 3.36 (s, 4H), 2.15 (s, 6H). ¹³C NMR (101 MHz, CDCl₃) δ 159.5, 44.9, 23.4.

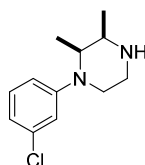
***cis*-2,3-Dimethylpiperazine (71)**

 A solution of 5,6-dimethyl-2,3-dihydropyrazine (3.49 g, 31.7 mmol, 1 eq.) in EtOH (100mL) was degassed for 30 min by bubbling argon through the solution. Palladium loaded on carbon (10%, 3.2 g, 30.1 mmol) was added under constant bubbling. The solution was flushed three times with hydrogen after which the pressure was increased to 40 bar. The reaction mixture was stirred for 72h on 40 bar. The suspension was filtered over celite and rinsed three times with EtOH (3x 50 mL). After evaporating the volatiles, the residue was purified by column chromatography (Et₂O:MeOH:NH₄OH, 10:4:1) to obtain the product (197 mg, 1.73 mmol, 5%). ¹H NMR (500 MHz, CDCl₃) δ 5.00 (s, 2H), 3.29-3.21 (m, 2H), 3.09-2.94 (m, 4H), 1.18 (d, *J* = 6.7 Hz, 6H). ¹³C NMR (126 MHz, CDCl₃) δ 51.5, 40.9, 13.7.

(±) *trans*-2,3-Dimethylpiperazine (72)

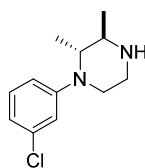
 To a solution of 5,6-dimethyl-2,3-dihydropyrazine (9.36 g, 85 mmol, 1 eq.) in absolute ethanol (300mL) was portion wise added sodium metal (23 g, 1 mol, 11.8 eq.) over six hours, after which the solution was refluxed for an additional 16h. The slurry was neutralized by addition of acetic acid (50 mL) at 0°C. The suspension was diluted with DCM, after stirring for 30 mins the precipitated sodium acetate was filtered off. The filtrate was concentrated under reduced pressure and the residue was purified by silica gel column chromatography (Et₂O : MeOH : NH₄OH, 10:4:1) to afford the product (3.71 g, 32.5 mmol, 38%). ¹H NMR (500 MHz, CDCl₃) δ 3.90 (s, 1H), 2.98 (m, 4H), 2.53 (m, 2H), 1.12-1.09 (m, 6H). ¹³C NMR (126 MHz, CDCl₃) δ 57.2, 45.8, 18.5.

(±) *cis*-1-(3-Chlorophenyl)-2,3-dimethylpiperazine (±39b)



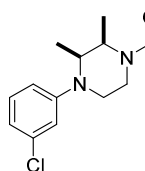
To a solution of 1-bromo-3-chlorobenzene (335 mg, 1.75 mmol, 1 eq.) in 2ml 1,4-dioxane was added cis-2,3-dimethylpiperazine (200 mg, 1.75 mmol, 1 eq.) and KHMDS (524mg, 2.63mmol, 1.5eq.). Then the reaction mixture was stirred for 2h at room temperature. The reaction progress was monitored by TLC analysis. Upon full conversion of the starting materials, the mixture was diluted with DCM, washed with water, dried (MgSO₄), filtered and concentrated under reduced pressure. The residue was purified by silica gel column chromatography (MeOH/DCM, 1%→5%) to afford the product (43 mg, 0.12 mmol, 11%). ¹H NMR (400 MHz, CDCl₃) δ 7.14 (t, J = 8.1 Hz, 1H), 6.81 (t, J = 2.2 Hz, 1H), 6.74 (tdd, J = 8.0, 2.2, 1.0 Hz, 2H), 3.76 (m, 1H), 3.26 – 2.59 (m, 5H), 1.11 (d, J = 6.7 Hz, 3H), 0.97 (d, J = 6.7 Hz, 3H). ¹³C NMR (101 MHz, CDCl₃) δ 151.40, 135.15, 130.16, 118.36, 115.43, 113.54, 54.95, 54.04, 46.07, 41.26, 19.03, 6.51.

(±) *trans*-1-(3-Chlorophenyl)-2,3-dimethylpiperazine (±40b)



To a solution of (±) *trans*-2,3-dimethylpiperazine (0.70 g, 6.1 mmol, 1 eq.) in anhydrous dioxane (17 ml) were added 1-bromo-2-chlorobenzene (0.60 ml, 6.1 mmol, 1 eq.) and KHMDS solution (1M in THF, 6.1 ml, 6.1 mmol, 1 eq.). The reaction mixture was stirred at RT for 2h. The reaction progress was monitored by TLC analysis. Upon full conversion of the starting materials, the mixture was diluted with DCM, washed with water, dried (MgSO₄), filtered and concentrated under reduced pressure. The crude product was purified using column chromatography (1% -> 10% MeOH in DCM with 1% TEA) to yielded the product (0.51 mg, 2.0 mmol, 32%). ¹H NMR (CDCl₃, 400 MHz): δ 7.20 (t, J = 8.1 Hz, 1H), 6.97 (t, J = 2.2 Hz, 1H), 6.89 (dddd, J = 18.0, 8.3, 2.1, 0.9 Hz, 2H), 3.24 – 2.82 (m, 6H), 1.31 (d, J = 6.6 Hz, 3H), 1.05 (d, J = 6.4 Hz, 3H). ¹³C NMR (400 MHz, CDCl₃) δ 153.01, 134.81, 130.07, 121.22, 120.23, 118.30, 57.84, 54.59, 48.88, 42.59, 19.04, 14.91.

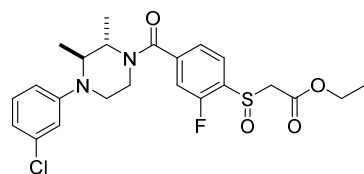
(±) Ethyl 2-((4-(4-(3-chlorophenyl)-*cis*-2,3-dimethylpiperazine-1-carbonyl)-2-fluorophenyl)sulfinyl)acetate (±39)



The title compound was synthesized using 4-((2-ethoxy-2-oxoethyl)sulfinyl)-3-fluorobenzoic acid (30 mg, 0.11 mmol, 1 eq.), *cis*-1-(3-chlorophenyl)-2,3-

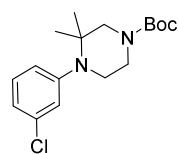
dimethylpiperazine (25 mg, 0.11 mmol, 1 eq.), oxalyl chloride (15 mg, 0.12 mmol, 1.1 eq.) and DiPEA (42 mg, 0.33 mmol, 3 eq.) according to general procedure G in a yield of 12 mg (0.03 mmol, 23%). $^1\text{H NMR}$ (400 MHz, CDCl_3) δ 7.95 (t, $J = 7.2$ Hz, 1H), 7.45 (d, $J = 7.8$ Hz, 1H), 7.32 – 7.14 (m, 4H), 7.10 (d, $J = 7.9$ Hz, 1H), 4.50 – 2.90 (m, 10H), 1.40 (dd, $J = 6.6, 1.5$ Hz, 3H), 1.26 (t, $J = 7.1$ Hz, 3H), 0.88 (d, $J = 6.3$ Hz, 3H). HRMS: Calculated for $[\text{C}_{22}\text{H}_{24}\text{ClFN}_2\text{O}_4\text{S} + \text{H}]^+ = 481.1359$, found = 481.1357.

(±)Ethyl 2-((4-(4-(3-chlorophenyl)-*trans*-2,3-dimethylpiperazine-1-carbonyl)-2-fluorophenyl)sulfinyl)acetate (±40)



The title compound was synthesized using 4-((2-ethoxy-2-oxoethyl)sulfinyl)-3-fluorobenzoic acid (30 mg, 0.11 mmol, 1 eq.), (±) *trans*-1-(3-chlorophenyl)-2,3-dimethylpiperazine (25 mg, 0.11 mmol, 1 eq.), oxalyl chloride (15 mg, 0.12 mmol, 1.1 eq.) and DiPEA (42 mg, 0.33 mmol, 3 eq.) according to general procedure G in a yield of 18 mg (0.04 mmol, 34%). $^1\text{H NMR}$ (400 MHz, CDCl_3) δ 8.00 – 7.90 (m, 1H), 7.44 (q, $J = 7.5$ Hz, 1H), 7.26 – 7.12 (m, 2H), 6.90 – 6.61 (m, 3H), 4.88 – 4.55 (m, 1H), 4.23 (q, $J = 7.1$ Hz, 2H), 3.97 (d, $J = 13.8$ Hz, 1H), 3.81 (d, $J = 13.9$ Hz, 1H), 3.71 – 3.45 (m, 2H), 3.38 – 3.05 (m, 3H), 1.56 – 1.41 (m, 3H), 1.27 (t, $J = 7.1$ Hz, 3H), 1.17 – 0.96 (m, 3H). HRMS: Calculated for $[\text{C}_{22}\text{H}_{24}\text{ClFN}_2\text{O}_4\text{S} + \text{H}]^+ = 481.1359$, found = 481.1358.

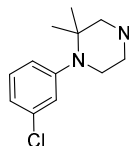
***tert*-Butyl 4-(3-chlorophenyl)-3,3-dimethylpiperazine-1-carboxylate (41a)**



To a solution of *tert*-butyl 3,3-dimethylpiperazine-1-carboxylate (0.20 g, 0.93 mmol, 1 eq.) in anhydrous dioxane (3mL) were added 1-bromo-2-chlorobenzene (179 mg, 0.93 mmol, 1 eq.) and KHMDS solution (1M in THF, 1.1 ml, 1.1 mmol, 1.2 eq.). The reaction mixture was stirred at RT for 2h. The reaction progress was monitored by TLC analysis. Upon full conversion of the starting materials, the mixture was diluted with DCM, washed with water, dried (MgSO_4), filtered and concentrated under reduced pressure. The crude product was purified using column chromatography (Diethyl ether/Pentane, 5%-15%) to yielded the product (86 mg, 0.27 mmol, 28%). $^1\text{H NMR}$ (400 MHz, CDCl_3) δ 7.18 (t, $J = 8.1$ Hz, 1H), 7.09 (d, $J = 7.5$ Hz, 2H), 6.98 (d, $J = 8.0$ Hz, 1H), 3.55 (t, $J = 7.0$ Hz, 2H), 3.32 (s, 2H), 3.05 (t, $J = 5.2$ Hz, 2H), 1.48 (s, 9H), 1.03 (s, 6H). $^{13}\text{C NMR}$ (101 MHz, CDCl_3) δ 154.88, 88

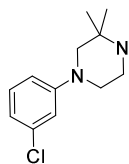
150.41, 133.71, 129.06, 127.58, 125.80, 124.78, 79.69, 56.45, 55.07, 46.91, 43.94, 28.49, 21.75.

1-(3-Chlorophenyl)-2,2-dimethylpiperazine (41b)



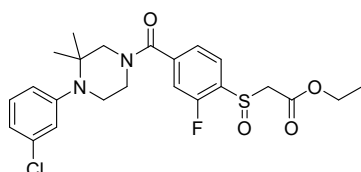
The title compound was synthesized using *tert*-butyl 4-(3-chlorophenyl)-3,3-dimethylpiperazine-1-carboxylate (86 mg, 0.27 mmol, 1 eq.) according to procedure B in a yield of 57 mg (0.25 mmol, 96 %). ¹H NMR (400 MHz, CDCl₃) δ 7.18 (ddd, J = 8.2, 7.2, 1.2 Hz, 1H), 7.09 (dd, J = 7.2, 1.3 Hz, 2H), 7.02 – 6.95 (m, 1H), 3.99 (s, 1H), 3.19 – 2.96 (m, 4H), 2.81 (s, 2H), 1.07 (s, 6H). ¹³C NMR (101 MHz, CDCl₃) δ 150.68, 133.70, 129.04, 127.54, 125.91, 124.71, 58.40, 54.59, 47.59, 46.72, 22.22.

1-(3-Chlorophenyl)-3,3-dimethylpiperazine (42b)



To a mixture of 1-bromo-3-chlorobenzene (335 mg, 1.75 mmol, 1 eq.) and 2,2-dimethylpiperazine (200 mg, 1.75 mmol, 1 eq.) in anhydrous dioxane (3mL) was added KHMDS solution (1M in THF, 2.1 ml, 2.1 mmol, 1.2 eq.). Then the reaction mixture was stirred at room temperature for 2h. The reaction progress was monitored by TLC analysis. Upon full conversion of the starting materials, the mixture was diluted with DCM, washed with water, dried (MgSO₄), filtered and concentrated under reduced pressure. The crude product was purified using column chromatography (MeOH/DCM, 1%-10%) to yielded the product (96 mg, 0.27 mmol, 28%). ¹H NMR (500 MHz, CDCl₃) δ 7.17 – 7.10 (m, 1H), 6.84 (t, J = 2.2 Hz, 1H), 6.80 – 6.74 (m, 2H), 3.11 – 2.95 (m, 4H), 2.89 (s, 2H), 1.22 (s, 6H). ¹³C NMR (126 MHz, CDCl₃) δ 153.20, 134.98, 130.09, 119.12, 116.04, 114.21, 60.82, 49.41, 48.19, 41.20, 26.29.

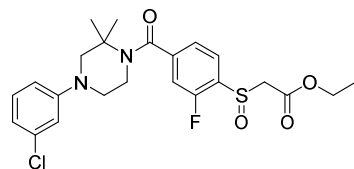
Ethyl 2-((4-(4-(3-chlorophenyl)-3,3-dimethylpiperazine-1-carbonyl)-2-fluorophenyl)sulfinyl)acetate (41)



The title compound was synthesized using 4-((2-ethoxy-2-oxoethyl)sulfinyl)-3-fluorobenzoic acid (30 mg, 0.11 mmol, 1 eq.), 1-(3-chlorophenyl)-2,2-dimethylpiperazine (25 mg, 0.11 mmol, 1 eq.), oxalyl chloride (15 mg, 0.12 mmol, 1.1 eq.) and DiPEA (42 mg, 0.33 mmol, 3 eq.) according to general procedure G in a yield of 26 mg (0.05 mmol,

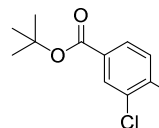
49%). ^1H NMR (400 MHz, CDCl_3) δ 7.96 (t, $J = 7.2$ Hz, 1H), 7.50 (s, 1H), 7.36 (d, $J = 6.5$ Hz, 2H), 7.29 (m, 3H), 4.27 – 3.30 (m, 10H), 1.27 (m, 6H), 1.12 (s, 3H). HRMS: Calculated for $[\text{C}_{22}\text{H}_{24}\text{ClFN}_2\text{O}_4\text{S} + \text{H}]^+ = 481.1359$, found = 481.1358.

Ethyl 2-((4-(4-(3-chlorophenyl)-2,2-dimethylpiperazine-1-carbonyl)-2-fluorophenyl)sulfinyl)acetate (42)



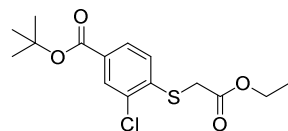
The title compound was synthesized using 4-((2-ethoxy-2-oxoethyl)sulfinyl)-3-fluorobenzoic acid (30 mg, 0.11 mmol, 1 eq.), 1-(3-chlorophenyl)-3,3-dimethylpiperazine (25 mg, 0.11 mmol, 1 eq.), oxalyl chloride (15 mg, 0.12 mmol, 1.1 eq.) and DiPEA (42 mg, 0.33 mmol, 3 eq.) according to general procedure G in a yield of 28 mg (0.06 mmol, 53%). ^1H NMR (400 MHz, CDCl_3) δ 7.95 (t, $J = 7.0$ Hz, 1H), 7.47 (s, 1H), 7.32 – 7.05 (m, 5H), 4.22 (q, $J = 7.1$ Hz, 2H), 4.07 – 3.15 (m, 8H), 1.26 (t, $J = 7.1$ Hz, 3H), 1.21 (s, 3H), 1.03 (s, 3H). HRMS: Calculated for $[\text{C}_{22}\text{H}_{24}\text{ClFN}_2\text{O}_4\text{S} + \text{H}]^+ = 481.1359$, found = 481.1358.

***tert*-Butyl 3-chloro-4-fluorobenzoate (73)**



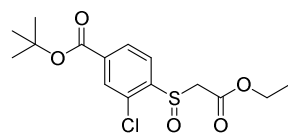
The title compound was synthesized using 4-fluoro-3-chlorobenzoic acid (1 g, 5.73 mmol, 1 eq.), Boc_2O (3.13 g, 14.3 mmol, 2.5 eq.) and DMAP (210 mg, 1.72 mmol, 0.30 eq.) according to general procedure C in a yield of 1.16 g (5.04 mmol, 88%). ^1H NMR (500 MHz, CDCl_3) δ 8.03 (dd, $J = 7.2, 2.2$ Hz, 1H), 7.88 (ddd, $J = 8.6, 4.7, 2.2$ Hz, 1H), 7.17 (t, $J = 8.6$ Hz, 1H), 1.59 (s, 9H). ^{13}C NMR (126 MHz, CDCl_3) δ 163.9, 160.9 (d, $J = 255.2$ Hz), 132.3, 129.9 (d, $J = 8.4$ Hz), 129.3 (d, $J = 3.6$ Hz), 121.3 (d, $J = 18.2$ Hz), 116.5 (d, $J = 21.6$ Hz), 82.1, 28.3.

***tert*-Butyl 3-chloro-4-((2-ethoxy-2-oxoethyl)thio)benzoate (74)**



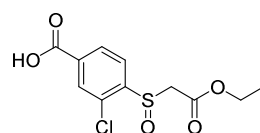
The title compound was synthesized using ethyl 2-mercaptoacetate (1.21 g, 10.1 mmol, 2 eq.) and *tert*-butyl 3-chloro-4-fluorobenzoate (1.16 g, 5.04 mmol, 1 eq.) according to general procedure D in a yield of 1.62 g (4.60 mmol, 91%). ^1H NMR (400 MHz, CDCl_3) δ 7.94 (d, $J = 1.8$ Hz, 1H), 7.83 (dd, $J = 8.3, 1.8$ Hz, 1H), 7.32 (d, $J = 8.3$ Hz, 1H), 4.20 (q, $J = 7.1$ Hz, 2H), 3.74 (s, 2H), 1.58 (s, 9H), 1.26 (t, $J = 7.1$ Hz, 3H). ^{13}C NMR (101 MHz, CDCl_3) δ 168.8, 164.4, 140.6, 132.2, 130.6, 130.5, 128.2, 126.6, 81.8, 62.2, 34.5, 90

28.3, 14.2.

***tert*-Butyl 3-chloro-4-((2-ethoxy-2-oxoethyl)sulfinyl)benzoate (75)**

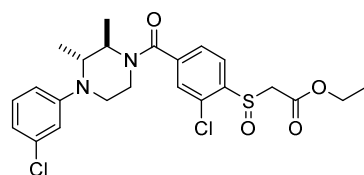
The title compound was synthesized using *tert*-butyl 3-chloro-4-((2-ethoxy-2-oxoethyl)thio)benzoate (140 mg, 0.42 mmol, 1.00 eq.) according to general procedure E in a yield of 147 mg (0.42

mmol, quant.). ^1H NMR (400 MHz, CDCl_3) δ 8.12 (d, $J = 8.1$ Hz, 1H), 8.06 – 7.92 (m, 2H), 4.29 – 4.18 (m, 2H), 4.03 (d, $J = 13.1$ Hz, 1H), 3.69 (d, $J = 13.8$ Hz, 1H), 1.61 (s, 9H), 1.26 (t, $J = 7.0$ Hz, 3H). ^{13}C NMR (126 MHz, CDCl_3) $\delta = 164.5, 163.6, 145.2, 136.5, 130.8, 130.1, 128.8, 126.5, 82.7, 62.4, 58.1, 28.2, 14.2$.

3-Chloro-4-((2-ethoxy-2-oxoethyl)sulfinyl)benzoic acid (76)

The title compound was synthesized using *tert*-butyl 3-chloro-4-((2-ethoxy-2-oxoethyl)sulfinyl)benzoate (1.39 g, 4.00 mmol, 1 eq.) according to general procedure F in a yield of 1.04 g (3.59 mmol,

90%). ^1H NMR (500 MHz, CDCl_3) δ 8.17 (dd, $J = 8.1, 1.5$ Hz, 1H), 8.07 (d, $J = 1.5, 1\text{H}$), 7.99 (d, $J = 8.1, 1\text{H}$), 4.26 – 4.14 (m, 2H), 4.04 (d, $J = 14.0$ Hz, 1H), 3.72 (d, $J = 14.0$ Hz, 1H), 1.23 (t, $J = 7.1$ Hz, 3H). ^{13}C NMR (126 MHz, CDCl_3) $\delta 166.5, 164.5, 145.4, 135.0, 131.2, 130.2, 129.3, 126.7, 62.5, 58.0, 14.1$.

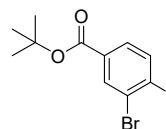
(\pm) Ethyl 2-((2-chloro-4-(4-(3-chlorophenyl)-*trans*-2,3-dimethylpiperazine-1-carbonyl)phenyl)sulfinyl)acetate (\pm 43)

The title compound was synthesized using (\pm) *trans*-1-(3-chlorophenyl)-2,3-dimethylpiperazine (23.2 mg, 0.10 μmol ,

1 eq.), 3-chloro-4-((2-ethoxy-2-oxoethyl)sulfinyl)benzoic acid (30 mg, 0.10 mmol, 1 eq.), HATU (39.2 mg, 0.10 mmol, 1.00 eq.) and DiPEA (31 mg, 0.30 mmol, 3 eq.) according to general procedure H in a yield of 38.3 mg (77.3 μmol , 75 %). ^1H NMR (500 MHz, CDCl_3) δ 8.01 (d, $J = 8.0$ Hz, 1H), 7.54 (dd, $J = 8.0, 1.6$ Hz, 1H), 7.51 – 7.42 (m, 1H), 7.16 (t, $J = 8.0$ Hz, 1H), 6.83 – 6.78 (m, 2H), 6.70 (d, $J = 8.4$ Hz, 1H), 4.80 (t, $J = 6.7$ Hz, 1H), 4.62 (s, 1H), 4.29 – 4.17 (m, 2H), 4.04 (dd, $J = 14.1, 1.7$ Hz, 1H), 3.87 (d, $J = 7.0$ Hz, 1H), 3.69 (dd, $J = 14.0, 1.2$ Hz, 1H), 3.67 – 3.60 (m, 1H), 3.57 – 3.49 (m, 1H), 3.37 – 3.06 (m, 3H), 1.52 – 1.44 (m, 3H), 1.27 (t, $J = 7.1$ Hz, 3H), 1.16 – 0.97 (m, 3H). ^{13}C NMR (126 MHz,

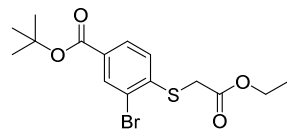
CDCl₃) δ 168.8, 168.3, 164.5, 151.3, 142.4, 140.5, 135.3, 130.8, 130.4, 128.4, 127.7, 127.1, 126.3, 125.8, 119.5, 116.3, 114.3, 62.5, 58.4, 56.2, 55.6, 49.8, 42.4, 41.3, 40.5, 36.6, 17.8, 16.8, 14.2, 12.8, 12.6. HRMS: Calculated for [C₂₃H₂₇Cl₂N₂O₄S + H]⁺ = 497.1063, found = 497.1065.

***tert*-Butyl 3-bromo-4-fluorobenzoate (77)**



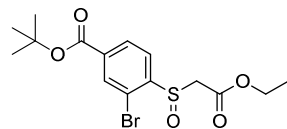
The title compound was synthesized using 3-bromo-4-fluorobenzoic acid (212 mg, 1 mmol, 1 eq.) according to general procedure C in a yield of 228 mg (0.83 mmol, 83%). ¹H NMR (300 MHz, CDCl₃) δ 8.17 (dd, *J* = 6.7, 2.0 Hz, 1H), 8.04 – 7.81 (m, 1H), 7.13 (t, *J* = 8.4 Hz, 1H), 1.58 (s, 9H). ¹³C NMR (75 MHz, CDCl₃) δ 163.10, 161.38 (d, *J* = 247.8 Hz), 134.84, 130.37 (d, *J* = 8.4 Hz), 129.38 (d, *J* = 3.4 Hz), 115.93 (d, *J* = 22.8 Hz), 108.70 (d, *J* = 21.6 Hz), 81.43, 27.86.

***tert*-Butyl 3-bromo-4-((2-ethoxy-2-oxoethyl)thio)benzoate (78)**



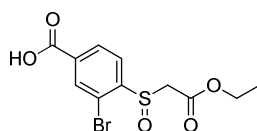
The title compound was synthesized using ethyl 2-mercaptoacetate (36 mg, 0.30 mmol, 1.1 eq.) and *tert*-butyl 3-bromo-4-fluorobenzoate (100 mg, 0.27 mmol, 1 eq.) according to procedure D in a yield of 34 mg (0.09 mmol, 34%). ¹H NMR (300 MHz, CDCl₃) δ 8.13 (d, *J* = 1.8 Hz, 1H), 7.90 (dt, *J* = 8.3, 4.3 Hz, 1H), 7.37 – 7.20 (m, 1H), 4.31 – 4.10 (m, 2H), 3.76 (s, 2H), 1.61 (s, 9H), 1.28 (t, *J* = 7.1 Hz, 3H). ¹³C NMR (75 MHz, CDCl₃) δ 168.58, 164.09, 142.52, 133.63, 130.40, 128.67, 126.12, 121.48, 81.58, 62.02, 34.90, 28.14, 13.99.

***tert*-Butyl 3-bromo-4-((2-ethoxy-2-oxoethyl)sulfinyl)benzoate (79)**



The title compound was synthesized *tert*-butyl 3-bromo-4-((2-ethoxy-2-oxoethyl)thio)benzoate (110 mg, 0.29 mmol, 1.00 eq.) according to general procedure E in a yield of 92 mg (0.23 mmol, 81%). ¹H NMR (300 MHz, CDCl₃) δ 8.16 (dd, *J* = 7.4, 1.2 Hz, 2H), 7.98 (d, *J* = 8.6 Hz, 1H), 4.22 (m, 2H), 4.07 (d, *J* = 13.8 Hz, 1H), 3.69 (d, *J* = 13.8 Hz, 1H), 1.61 (s, 9H), 1.27 (t, *J* = 7.1 Hz, 3H). ¹³C NMR (75 MHz, CDCl₃) δ 164.45, 163.31, 146.81, 136.39, 133.80, 129.24, 126.75, 118.32, 82.58, 62.32, 58.24, 28.07, 14.11.

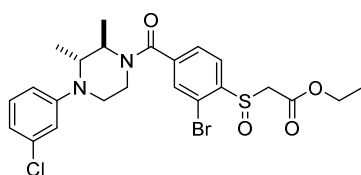
3-Bromo-4-((2-ethoxy-2-oxoethyl)sulfinyl)benzoic acid (80)



The title compound was synthesized using *tert*-butyl 3-bromo-4-

((2-ethoxy-2-oxoethyl)sulfinyl)benzoate (167 mg, 0.43 mmol, 1 eq.) according to general procedure F in a yield of 60 mg (0.18 mmol, 43 %). ^1H NMR (300 MHz, Methanol-*d*₄) δ 8.32 – 8.12 (m, 2H), 7.96 (d, J = 8.5 Hz, 1H), 4.22 – 4.18(m, 3H), 3.86 (d, J = 14.3 Hz, 1H), 1.31 – 1.10 (m, 3H). ^{13}C NMR (75 MHz, Methanol-*d*₄) δ 165.64, 164.61, 146.54, 135.50, 133.81, 129.35, 126.54, 118.38, 61.85, 57.72, 12.98.

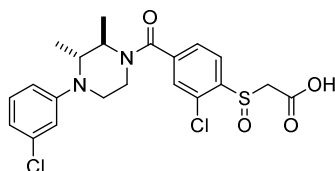
(\pm) Ethyl 2-((2-bromo-4-(4-(3-chlorophenyl)-*trans*-2,3-dimethylpiperazine-1-carbonyl)phenyl)sulfinyl)acetate (\pm 44)



The title compound was synthesized using 3-bromo-4-((2-

ethoxy-2-oxoethyl)sulfinyl)benzoic acid (50.0 mg, 0.150 mmol, 1 eq.), (\pm)-1-(3-chlorophenyl)-*trans*-2,3-dimethylpiperazine (33.6 mg, 0.150 mmol, 1 eq.), HATU (85.0 mg, 0.23 mmol, 1.5 eq.) and DiPEA (58.0 mg, 0.450 mmol) according to general procedure H in a yield of 68.4 mg (0.126 mmol, 85%). ^1H NMR (400 MHz, CDCl_3) δ 8.02 (d, J = 8.0 Hz, 1H), 7.67 (d, J = 1.2 Hz, 1H), 7.62 (dd, J = 8.0, 1.4 Hz, 1H), 7.19 (t, J = 8.2 Hz, 1H), 6.83 (dd, J = 8.1, 1.2 Hz, 2H), 6.73 (d, J = 9.0 Hz, 1H), 4.93 – 4.53 (m, 1H), 4.26 (qd, J = 7.1, 1.4 Hz, 2H), 4.10 (dd, J = 14.1, 0.8 Hz, 1H), 3.97 – 3.02 (m, 6H), 1.51 (s, 3H), 1.30 (t, J = 7.1 Hz, 3H), 1.18 – 0.99 (m, 3H). ^{13}C NMR (101 MHz, CDCl_3) δ 164.43, 158.30, 151.18, 143.91, 140.39, 135.19, 131.26, 130.29, 127.30, 126.73, 119.48, 119.26, 116.19, 114.20, 62.50, 58.46, 56.08, 49.83, 40.37, 36.62, 17.73, 14.10, 12.47.

(\pm) 2-((2-Chloro-4-(4-(3-chlorophenyl)-*trans*-2,3-dimethylpiperazine-1-carbonyl)phenyl)sulfinyl)acetic acid (\pm 45)

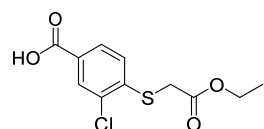


To a solution of (\pm) ethyl 2-((2-chloro-4-(4-(3-

chlorophenyl)-*trans*-2,3-dimethylpiperazine-1-carbonyl)phenyl)sulfinyl)acetate (180 mg, 0.36 mmol, 1 eq.) in MeOH (2mL) were added TEA (2mL) and water (2mL). The reaction mixture was stirred at room temperature overnight. The reaction progress was monitored by TLC analysis. Upon full conversion of the starting materials, the mixture was acidified with 3M HCl solution to pH 2, extracted with EtOAc, dried (MgSO_4), filtered and

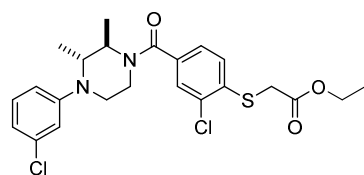
concentrated under reduced pressure. The residue was purified by silica gel column chromatography (MeOH/DCM, 1-5%) to afford the product (0.16 g, 0.35 mmol, 97%). ^1H NMR (500 MHz, CDCl_3) δ 8.03 (d, $J = 8.1$ Hz, 1H), 7.63 – 7.43 (m, 2H), 7.17 (t, $J = 8.3$ Hz, 1H), 6.85 – 6.77 (m, 2H), 6.73 – 6.69 (m, 1H), 4.85 – 4.59 (m, 2H), 4.08 (dd, $J = 14.2, 3.0$ Hz, 1H), 3.92 – 3.49 (m, 4H), 3.36 – 3.11 (m, 2H), 1.54 – 1.44 (m, 3H), 1.15 – 0.98 (m, 3H). ^{13}C NMR (126 MHz, CDCl_3) δ 176.17, 169.06, 151.35, 141.69, 140.54, 135.28, 130.87, 130.30, 128.51, 127.15, 126.01, 119.52, 116.25, 114.25, 57.76, 56.16, 49.88, 40.47, 36.69, 17.81, 12.84. HRMS: Calculated for $[\text{C}_{21}\text{H}_{22}\text{Cl}_2\text{N}_2\text{O}_4\text{S} + \text{H}]^+ = 496.0750$, found = 496.0746.

3-Chloro-4-((2-ethoxy-2-oxoethyl)thio)benzoate (81)



The title compound was synthesized using *tert*-butyl 3-chloro-4-((2-ethoxy-2-oxoethyl)sulfinyl)benzoate (62 mg, 0.19 mmol, 1 eq.) according to general procedure F in a yield of 51 mg (0.19 mmol, 92 %). ^1H NMR (400 MHz, CDCl_3) δ 8.07 (s, 1H), 7.95 (d, $J = 8.3$ Hz, 1H), 7.37 (d, $J = 8.2$ Hz, 1H), 4.23 (q, $J = 7.2$ Hz, 2H), 3.78 (s, 2H), 1.28 (t, $J = 7.1$ Hz, 3H). ^{13}C NMR (400 MHz, CDCl_3) δ 170.34, 168.37, 142.67, 130.76, 128.58, 127.15, 125.87, 61.98, 34.03, 13.91.

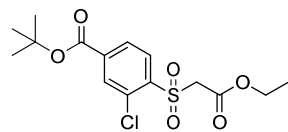
(±) Ethyl 2-((2-chloro-4-(4-(3-chlorophenyl)-*trans*-2,3-dimethylpiperazine-1-carbonyl)phenyl)thio)acetate (±46)



The title compound was synthesized using 3-chloro-4-((2-ethoxy-2-oxoethyl)thio)benzoic acid (33 mg, 0.12 mmol, 1 eq.), (±)1-(3-chlorophenyl)-*trans*-2,3-dimethylpiperazine (27 mg, 0.12 mmol, 1 eq.), HATU (68 mg, 0.18 mmol, 1.5 eq.) and DiPEA (46 mg, 0.36 mmol, 3 eq.) according to general procedure H in a yield of 11 mg (0.02 mmol, 19 %). ^1H NMR (400 MHz, CDCl_3) δ 7.48 – 7.36 (m, 2H), 7.34 – 7.27 (m, 1H), 7.17 (t, $J = 8.3$ Hz, 1H), 6.80 (d, $J = 6.1$ Hz, 2H), 6.71 (d, $J = 8.4$ Hz, 1H), 4.84 – 4.53 (m, 1H), 4.21 (q, $J = 7.1$ Hz, 2H), 3.73 (s, 2H), 3.69 – 3.01 (m, 5H), 1.51 – 1.41 (m, 3H), 1.27 (t, $J = 7.2$ Hz, 3H), 1.06 (dd, $J = 46.6, 6.5$ Hz, 3H). ^{13}C NMR (101 MHz, CDCl_3) δ 169.52, 168.85, 151.39, 137.10, 135.16, 134.77, 133.25, 130.25, 128.12, 128.87, 125.47, 119.18, 116.02, 114.05, 61.99, 56.06, 49.45, 40.43, 36.42, 34.69, 17.69, 14.13, 12.49. HRMS:

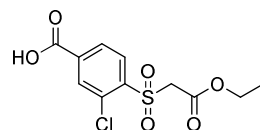
Calculated for $[\text{C}_{23}\text{H}_{26}\text{Cl}_2\text{N}_2\text{O}_3\text{S} + \text{H}]^+ = 483.1084$, found = 483.1079.

***tert*-Butyl 3-chloro-4-((2-ethoxy-2-oxoethyl)sulfonyl)benzoate (82)**



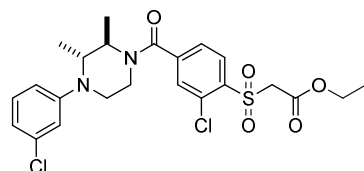
To a cooled (0°C) solution of *tert*-butyl 3-chloro-4-((2-ethoxy-2-oxoethyl)sulfonyl)benzoate (70 mg, 0.21 mmol, 1 eq.) in MeOH (7mL) was added a solution of Oxone (390 mg, 0.64 mmol, 3 eq.) in H₂O (3.5mL). The reaction mixture was stirred at RT overnight. The reaction progress was monitored by TLC analysis. Upon full conversion of the starting materials, the reaction mixture was extracted with DCM, dried (MgSO₄), filtered and concentrated under reduced pressure. The residue was purified by silica gel column chromatography (EtOAc/pentane, 0-15%) to yield the product (65 mg, 0.18 mmol, 85%). ¹H NMR (400 MHz, CDCl₃) δ 8.18 (d, $J = 8.2$ Hz, 1H), 8.14 (d, $J = 1.5$ Hz, 1H), 8.05 (dd, $J = 8.3, 1.6$ Hz, 1H), 4.47 (s, 2H), 4.12 (q, $J = 7.1$ Hz, 2H), 1.61 (s, 9H), 1.17 (t, $J = 7.2$ Hz, 3H). ¹³C NMR (400 MHz, CDCl₃) δ 162.97, 162.11, 139.35, 138.42, 132.84, 132.72, 132.25, 128.11, 83.23, 62.70, 58.74, 28.17, 13.96.

***tert*-Butyl 3-chloro-4-((2-ethoxy-2-oxoethyl)sulfonyl)benzoate (83)**



The title compound was synthesized using *tert*-butyl 3-chloro-4-((2-ethoxy-2-oxoethyl)sulfonyl)benzoate (65 mg, 0.18 mmol, 1 eq.) according to general procedure F in a yield of 50.2 mg (0.16 mmol, 91%). ¹H NMR (400 MHz, MeOD) δ 8.28 – 8.05 (m, 3H), 4.61 (s, 2H), 4.07 (q, $J = 7.1$ Hz, 2H), 1.08 (t, $J = 7.1$ Hz, 3H). ¹³C NMR (101 MHz, MeOD) δ 165.24, 162.16, 139.79, 137.42, 132.58, 132.39, 131.98, 128.13, 61.91, 58.48, 12.67.

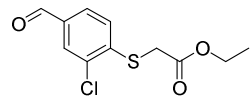
(±) Ethyl 2-((2-chloro-4-(4-(3-chlorophenyl)-*trans*-2,3-dimethylpiperazine-1-carbonyl)phenyl)sulfonyl)acetate (± 47)



The title compound was synthesized using *tert*-butyl 3-chloro-4-((2-ethoxy-2-oxoethyl)sulfonyl)benzoate (27 mg, 0.09 mmol, 1 eq.), (±)1-(3-chlorophenyl)-*trans*-2,3-dimethylpiperazine (20 mg, 0.09 mmol, 1 eq.), HATU (51 mg, 0.13 mmol, 1.5 eq.) and DiPEA (35 mg, 0.27 mmol, 3 eq.) according to general procedure H in a yield of 8 mg (0.02 mmol, 18 %). ¹H NMR (500 MHz, CDCl₃) δ 8.21 (d, $J = 8.1$ Hz, 1H), 7.67 – 7.42 (m, 2H), 7.18 (t, $J = 8.0$ Hz, 1H), 6.86 – 6.78 (m, 2H), 6.72 (d, $J = 8.5$ Hz, 1H), 4.47 (s,

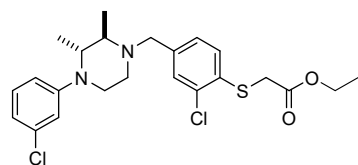
2H), 4.15 (q, $J = 7.1$ Hz, 2H), 3.95 – 3.00 (m, 6H), 1.49 (dd, $J = 16.0, 6.7$ Hz, 3H), 1.19 (td, $J = 7.2, 3.0$ Hz, 3H), 1.13 (d, $J = 6.6$ Hz, 2H), 1.02 (d, $J = 6.5$ Hz, 1H).

Ethyl 2-((2-chloro-4-formylphenyl)thio)acetate (84)



To a solution of 3-chloro-4-fluorobenzaldehyde (300 mg, 1.89 mmol, 1 eq.) in DMF (5mL) were added K_2CO_3 (523 mg, 3.78 mmol, 2 eq.) and ethyl 2-mercaptoacetate (227 mg, 1.89 mmol, 2 eq.) and stirred at rt overnight. The reaction progress was monitored by TLC analysis. Upon full conversion of the starting materials, the reaction mixture was extracted with DCM, dried ($MgSO_4$), filtered and concentrated under reduced pressure. The residue was purified by silica gel column chromatography (Et_2O /pentane, 20-35%) to yield the product (446 mg, 1.72 mmol, 91%). 1H NMR (400 MHz, $CDCl_3$) δ 9.89 (s, 1H), 7.84 (d, $J = 1.8$ Hz, 1H), 7.72 (dd, $J = 8.3, 1.8$ Hz, 1H), 7.42 (d, $J = 8.3$ Hz, 1H), 4.22 (q, $J = 7.1$ Hz, 2H), 3.78 (s, 2H), 1.27 (t, $J = 7.1$ Hz, 3H). ^{13}C NMR (126 MHz, $CDCl_3$) δ 190.1, 168.5, 143.9, 134.6, 132.6, 130.1, 128.4, 126.3, 62.3, 34.2, 14.2.

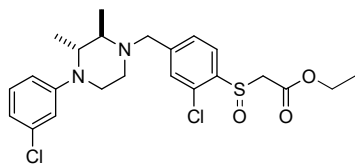
(±) Ethyl 2-((2-chloro-4-(4-(3-chlorophenyl)-trans-2,3-dimethylpiperazin-1-yl)methyl)phenyl)thio)acetate (±85)



To a solution of ethyl-2-((2-chloro-4-formylphenyl)thio)acetate (31.8 mg, 0.12 mmol, 1.2 eq.) in 1,2-dichloroethane (1.0 mL) was added (±)1-(3-chlorophenyl)-trans-2,3-dimethylpiperazine (23.0 mg, 0.10 mmol, 1 eq.) and the reaction mixture was stirred at rt for 30min. Then sodium triacetoxyborohydride (65.1 mg, 0.31 mmol, 3 eq.) was added and the reaction mixture was stirred at rt overnight. The reaction progress was monitored by TLC analysis. Upon full conversion of the starting materials, the reaction mixture was extracted with DCM, dried ($MgSO_4$), filtered and concentrated under reduced pressure. The residue was purified by silica gel column chromatography ($EtOAc$ /pentane, 20%) to yield the product (19 mg, 0.04 mmol, 40%). 1H NMR (400 MHz, $CDCl_3$) δ 7.46 (s, 1H), 7.39 (d, $J = 8.0$ Hz, 1H), 7.30 – 7.27 (m, 1H), 7.15 (t, $J = 8.0$ Hz, 1H), 6.84 – 6.79 (m, 1H), 6.73 (t, $J = 8.0$ Hz, 2H), 4.20 (q, $J = 7.2$ Hz, 2H), 3.75 – 3.67 (m, 3H), 3.57 (q, $J = 13.9$ Hz, 2H), 3.27 – 3.09 (m, 2H), 2.91 – 2.81 (m, 1H), 2.75 (td, $J = 11.4$ Hz, 1H), 2.52 (d, $J = 11.5$ Hz, 1H), 1.27 (d, $J =$

7.2 Hz, 3H), 1.24 – 1.19 (m, 3H), 1.15 (d, $J = 6.3$ Hz, 3H). ^{13}C NMR (101 MHz, CDCl_3) δ 169.4, 152.1, 140.2, 135.1, 134.6, 132.3, 130.5, 130.1, 129.9, 127.6, 118.0, 115.5, 113.6, 61.8, 58.0, 56.7, 56.6, 44.9, 42.0, 35.6, 14.2, 13.0, 9.5.

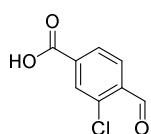
(\pm) Ethyl 2-((2-chloro-4-((4-(3-chlorophenyl)-*trans*-2,3-dimethylpiperazin-1-yl)methyl)phenyl)sulfinyl)acetate (\pm 48)



The title compound was synthesized using (\pm) ethyl 2-((2-chloro-4-((4-(3-chlorophenyl)-*trans*-2,3-dimethylpiperazin-1-yl)methyl)phenyl)thio)acetate (19 mg,

0.04 mmol, 1 eq.) according to general procedure E in a yield of 6.3 mg (0.01 mmol, 32 %). ^1H NMR (500 MHz, CDCl_3) δ 7.89 (d, $J = 8.0$ Hz, 1H), 7.55 (ddd, $J = 8.0, 3.0, 1.5$ Hz, 1H), 7.49 (dd, $J = 3.9, 1.5$ Hz, 1H), 7.14 (t, $J = 8.0$ Hz, 1H), 6.80 (t, $J = 2.2$ Hz, 1H), 6.76 – 6.68 m, 2H), 4.26 – 4.18 (m, 2H), 4.02 (dd, $J = 13.7, 2.8$ Hz, 1H), 3.75 – 3.66 (m, 2H), 3.61 (d, $J = 14.3$ Hz, 1H), 3.24 – 3.19 (m, 1H), 3.15 (dd, $J = 4.0, 1.5$ Hz, 1H), 2.85 (q, $J = 6.4$ Hz, 1H), 2.78 (td, $J = 11.5, 4.2$ Hz, 1H), 2.51 (dt, $J = 11.5, 1.8$ Hz, 1H), 1.27 (td, $J = 7.2, 1.0$ Hz, 3H), 1.22 (dd, $J = 6.6, 1.4$ Hz, 3H), 1.17 (d, $J = 6.5$ Hz, 3H). ^{13}C NMR (126 MHz, CDCl_3) δ 169.4, 152.1, 145.6, 139.3, 135.2, 130.2, 130.2, 129.8, 128.2, 126.4, 118.2, 115.6, 113.7, 62.3, 58.7, 58.2, 57.0, 56.8, 45.0, 42.0, 14.3, 13.0, 9.6. HRMS: Calculated for $[\text{C}_{23}\text{H}_{28}\text{Cl}_2\text{N}_2\text{O}_3\text{S} + \text{H}]^+ = 483.1270$, found = 483.1273.

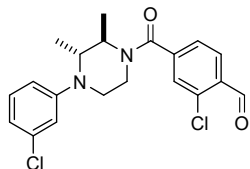
3-Chloro-4-formylbenzoic acid (86)



To a cooled (-78 °C) solution of 4-bromo-3-chlorobenzoic acid (300 mg, 1.27 mmol, 1.00 eq.) in abs. THF (5.0 mL) was added Turbo-GRIGNARD (1.3 M in THF, 2.94 ml, 3.82 mmol, 3.00 eq.). The temperature was raised to 0 °C after 10 min and the reaction mixture was stirred at 0 °C for 1 h. Subsequently DMF (6.37 ml, 0.49 mmol, 5.00 eq.) was added, the reaction mixture warmed up to room temperature and stirred further for 1.5 h. The reaction was quenched by addition of sat. aq. NH_4Cl , followed by washing with EtOAc. Then the pH of the aqueous layer was adjusted with aq. 1 N HCl and extracted with EtOAc. The combined organic layers were neutralized with sat. aq. NaHCO_3 , washed with brine, dried (Na_2SO_4) and concentrated under reduced pressure. The title compound was obtained without any further purification (165 mg, 0.89 mmol, 70%). ^1H NMR (500 MHz, $\text{DMSO}-d_6$) δ

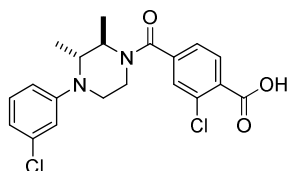
10.38 (s, 1H), 8.07 – 8.00 (m, 2H), 8.01 – 7.95 (m, 1H). ¹³C NMR (126 MHz, DMSO-*d*₆) δ 189.6, 165.4, 136.8, 136.1, 134.8, 131.1, 130.1, 128.3.

(±) **2-Chloro-4-(4-(3-chlorophenyl)-*trans*-2,3-dimethylpiperazine-1-carbonyl)benzaldehyde (±87)**



The title compound was synthesized using 3-chloro-4-formylbenzoic acid (65.0 mg, 35.0 mmol, 1.00 eq.), (±) 1-(3-chlorophenyl)-*trans*-2,3-dimethylpiperazine (79.0 mg, 0.35 mmol, 1.00 eq.), DiPEA (137 mg, 1.06 mmol, 3.00 eq.) and HATU (161 mg, 0.42 mmol, 1.20 eq.) according to procedure H in a yield of 69.0 mg (0.18 mmol, 50%). ¹H NMR (400 MHz, CDCl₃) δ 10.49 – 10.45 (m, 1H), 7.97 (d, *J* = 7.9 Hz, 1H), 7.49 (dd, *J* = 11.0, 1.5 Hz, 1H), 7.41 – 7.35 (m, 1H), 7.18 – 7.12 (m, 1H), 6.82 – 6.76 (m, 3H), 4.48 – 4.78 (m, 1H), 4.04 – 3.74 (m, 1H), 3.72 – 3.01 (m, 4H), 1.48 (d, *J* = 6.8 Hz, 1H), 1.45 (d, *J* = 6.8 Hz, 2H), 1.11 (d, *J* = 6.6 Hz, 1H), 1.00 (d, *J* = 6.6 Hz, 2H). ¹³C NMR (101 MHz, CDCl₃) δ 188.9, 168.6, 168.2, 151.3, 142.7, 142.6, 138.4, 135.2, 132.9, 130.3, 129.9, 129.8, 129.1, 128.7, 125.6, 125.2, 119.4, 116.2, 114.2, 114.1, 60.4, 56.1, 55.4, 49.5, 42.2, 41.2, 40.4, 36.4, 17.7, 16.7, 14.2, 12.8, 12.5.

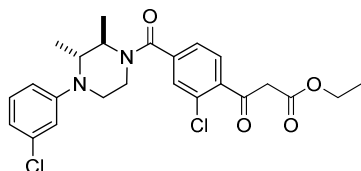
(±) **2-Chloro-4-(4-(3-chlorophenyl)-*trans*-2,3-dimethylpiperazine-1-carbonyl)benzoic acid (±88)**



To a solution of (±) 2-chloro-4-(4-(3-chlorophenyl)-*trans*-2,3-dimethylpiperazine-1-carbonyl)benzaldehyde (69.0 mg, 176 μmol, 1.00 eq.) in DMF (1.0 ml) was added oxone (108 mg, 176 μmol, 1.00 eq.) and the mixture was stirred at rt overnight. The reaction progress was monitored by TLC analysis. Upon full conversion of the starting materials, the reaction mixture was extracted with DCM, dried (MgSO₄), filtered and concentrated under reduced pressure. The residue was purified by silica gel column chromatography (MeOH/DCM, 2% - 5%) to yield the product (68.0 mg, 0.15 mmol, 50%). ¹H NMR (500 MHz, CDCl₃) δ 8.03 (s, 1H, OH), 7.74 (dd, *J* = 8.0, 3.4 Hz, 1H), 7.39 (dd, *J* = 10.4, 1.5 Hz, 1H), 7.28 – 7.22 (m, 1H), 7.17 – 7.10 (m, 1H), 6.80 – 6.74 (m, 2H), 6.71 – 6.65 (m, 1H), 4.75 (q, *J* = 6.9 Hz, 1H), 4.61 – 4.53 (m, 1H), 3.87 – 3.79 (m, 1H), 3.55 – 2.99 (m, 3H), 1.44 (d, *J* = 6.8 Hz, 1H), 1.44 (m, 2H), 1.08 (d, *J* = 6.7 Hz, 1H), 0.95 (d, *J* =

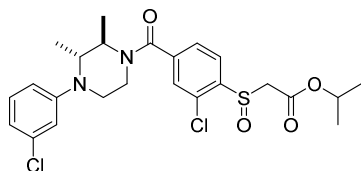
6.7 Hz, 2H). ^{13}C NMR (126 MHz, CDCl_3) δ 171.2, 169.6, 169.1, 151.4, 138.6, 135.7, 132.7, 130.9, 130.3, 128.8, 128.4, 125.2, 124.5, 119.3, 116.1, 114.2, 69.7, 56.1, 55.4, 49.6, 42.3, 41.3, 40.5, 36.5, 17.7, 16.7, 14.2, 12.8, 12.5.

(\pm) Ethyl 3-(2-chloro-4-(4-(3-chlorophenyl)-trans-2,3-dimethylpiperazine-1-carbonyl)phenyl)-3-oxopropanoate (\pm 49)



To a solution of (\pm) 2-chloro-4-(4-(3-chlorophenyl)-trans-2,3-dimethylpiperazine-1-carbonyl)benzoic acid (12.0 mg, 29.0 μmol , 1.00 eq.) in dry THF (250 μL), carbonyldiimidazole (5.30 mg, 32.0 mmol, 1.10 eq.) was added and the reaction mixture was stirred at rt for 2 h. Then a mixture of ethyl potassium malonate (5.00 mg, 29.0 μmol , 1.00 eq.) [which had been prepared from ethyl hydrogen malonate (1 g) and KOH (0.4 g) in abs. ethyl alcohol 4 ml], anhydr. MgCl_2 (5.61 mg, 59.0 μmol , 2.00 eq.) and TEA (9.86 μl , 7.16 mg, 71.0 μmol , 2.40 eq.) were added. The reaction mixture was stirred further at rt for 24 h. After concentration under reduced pressure the obtained residue was resuspended in 2 M aq. HCl and extracted with DCM. The combined organic layers were washed with sat. aq. NaHCO_3 and brine, dried (Na_2SO_4) and concentrated under reduced pressure. Purification by flash column chromatography (pentane/EtOAc, 3:1) resulted in the title compound as a colorless oil (0.82 mg, 1.72 μmol , 6%). ^1H NMR (500 MHz, CDCl_3) δ 7.66 (dd, $J = 10.0, 7.9$ Hz, 1H), 7.48 (d, $J = 4.5$ Hz, 1H), 7.35 (dd, $J = 13.4, 7.9$ Hz, 1H), 7.20 – 7.14 (m, 1H), 6.84 – 6.79 (m, 2H), 6.71 (dd, $J = 9.1, 2.1$ Hz, 1H), 5.59 – 4.71 (m, 1H), 4.29 (q, $J = 7.1$ Hz, 1H), 4.21 (q, $J = 7.1$ Hz, 1H), 4.04 (s, 2H), 3.92 – 3.09 (m, 5H), 1.47 (s, 3H), 1.35 (t, $J = 7.1$ Hz, 1H), 1.26 (t, $J = 7.1$ Hz, 2H), 1.07 (s, 3H). ^{13}C NMR (126 MHz, CDCl_3) δ 172.7, 169.4, 166.8, 151.4, 139.0, 138.8, 135.4, 132.9, 132.2, 130.5, 130.4, 119.6, 119.5, 116.3, 114.3, 94.0, 61.8, 60.9, 56.3, 49.2, 14.4, 14.2. HRMS: Calculated for $[\text{C}_{24}\text{H}_{28}\text{Cl}_2\text{N}_2\text{O}_4\text{S} + \text{H}]^+$ = 477.1342, found = 477.1346.

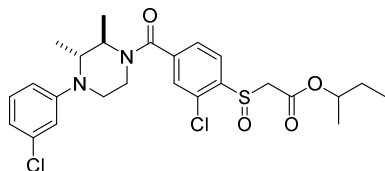
(\pm) Isopropyl 2-((2-chloro-4-(4-(3-chlorophenyl)-trans-2,3-dimethylpiperazine-1-carbonyl)phenyl)sulfinyl)acetate (\pm 50)



The title compound was synthesized using (±) 2-chloro-4-(4-(3-chlorophenyl)-trans-2,3-dimethylpiperazine-1-carbonyl)benzoic acid (30.0 mg, 64.0 μmol, 1.00 eq.),

oxalyl chloride (2 M in DCM, 35.0 μl, 70.0 μmol, 1.10 eq.), 2-propanol (19.2 mg, 320 μmol, 5.00 eq.) and DiPEA (9.09 mg, 70.0 μmol, 1.10 eq.) according to general procedure G in a yield of 14.0 mg (27.5 μmol, 43 %). ¹H NMR (500 MHz, CDCl₃) δ 8.02 (d, *J* = 7.9 Hz, 1H), 7.58 – 7.51 (m, 1H), 7.51 – 7.43 (m, 1H), 7.17 (t, *J* = 8.0 Hz, 1H), 6.84 – 6.79 (m, 2H), 6.71 (d, *J* = 8.4 Hz, 1H), 5.08 – 5.14 (m, 1H), 4.86 – 4.58 (m, 1H), 4.04 (d, *J* = 14.1 Hz, 1H), 3.92 – 3.07 (m, 6H), 1.53 – 1.44 (m, 3H), 1.32 – 1.24 (m, 6H), 1.16 – 0.99 (m, 3H). ¹³C NMR (126 MHz, CDCl₃) δ 168.8, 164.2, 151.4, 142.7, 140.6, 135.4, 130.4, 126.2, 119.6, 116.3, 114.3, 70.6, 58.8, 56.3, 55.5, 49.7, 42.4, 41.4, 40.6, 36.6, 21.9, 17.9, 16.8, 12.9, 12.6. HRMS: Calculated for [C₂₄H₂₈Cl₂N₂O₄S + H]⁺ = 511.1220, found = 511.1227.

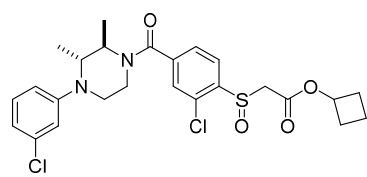
(±) *sec*-Butyl 2-((2-chloro-4-(4-(3-chlorophenyl)-trans-2,3-dimethylpiperazine-1-carbonyl)phenyl)sulfinyl)acetate (±51)



The title compound was synthesized using (±) 2-chloro-4-(4-(3-chlorophenyl)-trans-2,3-dimethylpiperazine-1-carbonyl)benzoic acid (50.0 mg, 107 μmol, 1.00 eq.),

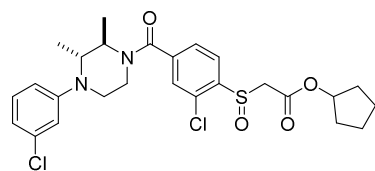
oxalyl chloride (2 M in DCM, 80.0 μl, 160 μmol, 1.50 eq.), butan-2-ol (49.0 μl, 39.5 mg, 533 μmol, 5.00 eq.) and DiPEA (28.0 μl, 20.7 mg, 160 μmol, 1.50 eq.) according to general procedure G in a yield of 14.1 mg (26.8 μmol, 25 %). ¹H NMR (400 MHz, CDCl₃) δ 8.02 (dd, *J* = 7.9, 2.0 Hz, 1H), 7.59 – 7.51 (m, 1H), 7.50 – 7.42 (m, 1H), 7.17 (t, *J* = 8.0 Hz, 1H), 6.85 – 6.77 (m, 2H), 6.70 (dd, *J* = 7.9, 3.2 Hz, 1H), 5.00 – 4.90 (m, 1H), 4.85 – 4.57 (m, 1H), 4.04 (d, *J* = 14.0 Hz, 1H), 3.92 – 3.07 (m, 5H), 1.70 – 1.53 (m, 3H), 1.53 – 1.43 (m, 3H), 1.30 – 1.21 (m, 3H), 1.16 – 0.99 (m, 2H), 0.97 – 0.88 (m, 3H). ¹³C NMR (126 MHz, CDCl₃) δ 164.4, 164.3, 151.4, 142.8, 140.7, 135.3, 130.8, 130.4, 128.6, 127.9, 127.0, 126.4, 126.2, 125.9, 119.6, 116.3, 114.3, 75.2, 59.0, 58.8, 56.2, 55.5, 49.7, 42.4, 41.4, 40.5, 36.6, 28.8, 19.5, 17.9, 16.8, 12.9, 12.6, 9.7. HRMS: Calculated for [C₂₅H₃₀Cl₂N₂O₄S + H]⁺ = 525.1376, found = 525.1385.

(±) Cyclobutyl 2-((2-chloro-4-(4-(3-chlorophenyl)-trans-2,3-dimethylpiperazine-1-

carbonyl)phenyl)sulfinyl)acetate (\pm 52)

The title compound was synthesized using (\pm) 2-chloro-4-(4-(3-chlorophenyl)-trans-2,3-dimethylpiperazine-1-carbonyl)benzoic acid (50.0 mg, 107 μ mol, 1.00 eq.),

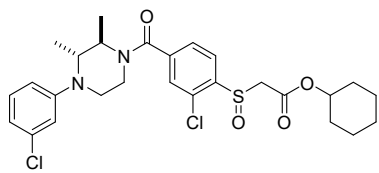
oxalyl chloride (2 M in DCM, 80.0 μ l, 160 μ mol, 1.50 eq.), cyclobutanol (77 mg, 1.07 mmol, 10 eq.) and DiPEA (28.0 μ l, 20.7 mg, 160 μ mol, 1.50 eq.) according to general procedure G in a yield of 8mg (0.015 mmol, 14%). ^1H NMR (500 MHz, CDCl_3) δ 8.03 (d, J = 8.0 Hz, 1H), 7.66 – 7.40 (m, 2H), 7.18 (t, J = 8.1 Hz, 1H), 6.89 – 6.76 (m, 2H), 6.72 (d, J = 8.4 Hz, 1H), 5.06 (tt, J = 7.9, 7.1 Hz, 1H), 4.88 – 3.00 (m, 8H), 2.45 – 2.27 (m, 2H), 2.19 – 2.00 (m, 2H), 1.89 – 1.57 (m, 2H), 1.49 (d, J = 10.0 Hz, 3H), 1.20 – 0.86 (m, 3H). ^{13}C NMR (126 MHz, CDCl_3) δ 169.03, 163.85, 151.33, 142.36, 140.47, 135.36, 130.95, 130.43, 128.36, 127.16, 125.85, 119.66, 116.37, 114.34, 70.27, 58.23, 56.27, 49.92, 40.54, 36.71, 30.37, 30.32, 18.42, 14.12, 12.61. HRMS: Calculated for $[\text{C}_{25}\text{H}_{28}\text{Cl}_2\text{N}_2\text{O}_4\text{S} + \text{H}]^+ = 523.1220$, found = 523.1218.

(\pm) Cyclopentyl 2-((2-chloro-4-(4-(3-chlorophenyl)-trans-2,3-dimethylpiperazine-1-carbonyl)phenyl)sulfinyl)acetate (\pm 53)

The title compound was synthesized using (\pm) 2-Chloro-4-(4-(3-chlorophenyl)-trans-2,3-dimethylpiperazine-1-carbonyl)benzoic acid (50.0 mg, 107 μ mol, 1.00 eq.),

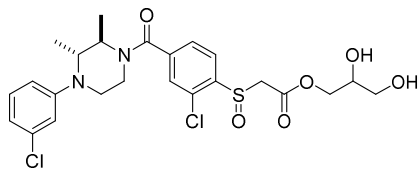
oxalyl chloride (2 M in DCM, 80.0 μ l, 160 μ mol, 1.50 eq.), cyclopentanol (92 mg, 1.07 mmol, 10 eq.) and DiPEA (28.0 μ l, 20.7 mg, 160 μ mol, 1.50 eq.) according to general procedure G in a yield of 12 mg (0.022 mmol, 21%). ^1H NMR (500 MHz, CDCl_3) δ 8.03 (d, J = 8.0 Hz, 1H), 7.63 – 7.41 (m, 2H), 7.18 (t, J = 8.1 Hz, 1H), 6.87 – 6.76 (m, 2H), 6.72 (d, J = 8.7 Hz, 1H), 5.29 – 5.19 (m, 1H), 5.12 – 3.05 (m, 8H), 1.87 (q, J = 6.9 Hz, 2H), 1.79 – 1.40 (m, 9H), 1.22 – 0.88 (m, 3H). ^{13}C NMR (126 MHz, CDCl_3) δ 169.01, 164.34, 151.32, 140.35, 135.36, 130.95, 130.43, 128.58, 127.17, 126.39, 119.68, 116.38, 114.35, 79.90, 58.42, 56.28, 49.97, 40.53, 36.75, 32.84, 32.72, 23.81, 23.78, 17.89, 12.60. HRMS: Calculated for $[\text{C}_{26}\text{H}_{30}\text{Cl}_2\text{N}_2\text{O}_4\text{S} + \text{H}]^+ = 537.1376$, found = 537.1376.

(\pm) Cyclohexyl 2-((2-chloro-4-(4-(3-chlorophenyl)-trans-2,3-dimethylpiperazine-

1-carbonyl)phenyl)sulfinyl)acetate (\pm 54)

The title compound was synthesized using (\pm) 2-chloro-4-(4-(3-chlorophenyl)-trans-2,3-dimethylpiperazine-1-carbonyl)benzoic acid (50.0 mg, 107 μ mol, 1.00 eq.),

oxalyl chloride (2 M in DCM, 80.0 μ l, 160 μ mol, 1.50 eq.), cyclohexanol (107 mg, 1.07 mmol, 10 eq.) and DiPEA (28.0 μ l, 20.7 mg, 160 μ mol, 1.50 eq.) according to general procedure G in a yield of 3 mg (0.005mmol, 5%). ^1H NMR (500 MHz, CDCl_3) δ 8.03 (d, $J = 8.0$ Hz, 1H), 7.62 – 7.43 (m, 2H), 7.18 (t, $J = 8.1$ Hz, 1H), 6.87 – 6.77 (m, 2H), 6.71 (d, $J = 8.3$ Hz, 1H), 4.88 (tt, $J = 8.9, 3.9$ Hz, 1H), 4.84 – 2.94 (m, 8H), 1.70 – 1.20 (m, 13H), 1.20 – 0.96 (m, 3H). ^{13}C NMR (126 MHz, CDCl_3) δ 168.06, 163.57, 151.37, 142.76, 140.55, 134.94, 130.90, 130.40, 128.34, 127.08, 126.37, 119.62, 116.35, 114.32, 75.45, 58.72, 56.27, 49.78, 40.54, 36.65, 31.58, 25.34, 23.73, 17.89, 12.62. HRMS: Calculated for $[\text{C}_{27}\text{H}_{32}\text{Cl}_2\text{N}_2\text{O}_4\text{S} + \text{H}]^+ = 551.1533$, found = 551.1533.

(\pm) 2,3-Dihydroxypropyl 2-((2-chloro-4-(4-(3-chlorophenyl)-trans-2,3-dimethylpiperazine-1-carbonyl)phenyl)sulfinyl)acetate (\pm 55)

The title compound was synthesized using (\pm) 2-Chloro-4-(4-(3-chlorophenyl)-trans-2,3-dimethylpiperazine-1-carbonyl)benzoic acid (50.0 mg,

107 μ mol, 1.00 eq.), oxalyl chloride (2 M in DCM, 80.0 μ l, 160 μ mol, 1.50 eq.), glycerol (98 mg, 1.07 mmol, 10 eq.) and DiPEA (28.0 μ l, 20.7 mg, 160 μ mol, 1.50 eq.) according to general procedure G. This yielded the product(3mg, 0.006mmol, 5%). ^1H NMR (500 MHz, CDCl_3) δ 7.98 – 7.87 (m, 1H), 7.60 – 7.42 (m, 2H), 7.18 (t, $J = 8.1$ Hz, 1H), 6.85 – 6.77 (m, 2H), 6.71 (d, $J = 7.5$ Hz, 1H), 4.87 – 3.05 (m, 13H), 1.95 (br, 2H), 1.50 (dd, $J = 15.0, 6.7$ Hz, 3H), 1.08 (m, 3H). HRMS: Calculated for $[\text{C}_{24}\text{H}_{28}\text{Cl}_2\text{N}_2\text{O}_6\text{S} + \text{H}]^+ = 543.1118$, found = 543.1117.

References

1. Nomura, D. K.; Morrison, B. E.; Blankman, J. L.; Long, J. Z.; Kinsey, S. G.; Marcondes, M. C. G.; Ward, A. M.; Hahn, Y. K.; Lichtman, A. H.; Conti, B. Endocannabinoid hydrolysis generates brain prostaglandins that promote neuroinflammation. *Science* **2011**, 334, 809-813.
2. Fowler, C. J. Monoacylglycerol lipase - a target for drug development? *Br J Pharmacol* **2012**, 166, 1568-85.
3. Deng, H.; Li, W. Monoacylglycerol lipase inhibitors: modulators for lipid metabolism in cancer malignancy, neurological and metabolic disorders. *Acta Pharmaceutica Sinica B* **2020**, 10, 582-602.
4. Blankman, J. L.; Simon, G. M.; Cravatt, B. F. A comprehensive profile of brain enzymes that hydrolyze the endocannabinoid 2-arachidonoylglycerol. *Chemistry & biology* **2007**, 14, 1347-1356.
5. Jiang, M.; van der Stelt, M. Activity-Based Protein Profiling Delivers Selective Drug Candidate ABX-1431, a Monoacylglycerol Lipase Inhibitor, To Control Lipid Metabolism in Neurological Disorders. *J Med Chem* **2018**, 61, 9059-9061.
6. Barf, T.; Kaptein, A. Irreversible protein kinase inhibitors: balancing the benefits and risks. *Journal of medicinal chemistry* **2012**, 55, 6243-6262.
7. Singh, J.; Petter, R. C.; Baillie, T. A.; Whitty, A. The resurgence of covalent drugs. *Nature reviews Drug discovery* **2011**, 10, 307-317.
8. Schlosburg, J. E.; Blankman, J. L.; Long, J. Z.; Nomura, D. K.; Pan, B.; Kinsey, S. G.; Nguyen, P. T.; Ramesh, D.; Booker, L.; Burston, J. J. Chronic monoacylglycerol lipase blockade causes functional antagonism of the endocannabinoid system. *Nature neuroscience* **2010**, 13, 1113-1119.
9. Chanda, P. K.; Gao, Y.; Mark, L.; Btsh, J.; Strassle, B. W.; Lu, P.; Piesla, M. J.; Zhang, M.-Y.; Bingham, B.; Uveges, A. Monoacylglycerol lipase activity is a critical modulator of the tone and integrity of the endocannabinoid system. *Molecular pharmacology* **2010**, 78, 996-1003.
10. Hernández-Torres, G.; Cipriano, M.; Hedén, E.; Björklund, E.; Canales, Á.; Zian, D.; Feliú, A.; Mecha, M.; Guaza, C.; Fowler, C. J. A reversible and selective inhibitor of monoacylglycerol lipase ameliorates multiple sclerosis. *Angewandte Chemie* **2014**, 126, 13985-13990.
11. cddi.nl.
12. van der Wel, T.; Janssen, F. J.; Baggelaar, M. P.; Deng, H.; den Dulk, H.; Overkleeft, H. S.; van der Stelt, M. A natural substrate-based fluorescence assay for inhibitor screening on diacylglycerol lipase α . *Journal of lipid research* **2015**, 56, 927-935.
13. van der Wel, T. Chemical genetic approaches for target validation. Leiden University, Leiden, 2020.
14. Tarcsay, A. k.; Nyíri, K.; Keserű, G. r. M. Impact of lipophilic efficiency on compound quality. *Journal of medicinal chemistry* **2012**, 55, 1252-1260.
15. Blake, J. F. Chemoinformatics—predicting the physicochemical properties of ‘drug-like’ molecules. *Current Opinion in Biotechnology* **2000**, 11, 104-107.
16. Tocher, J. H. Reductive activation of nitroheterocyclic compounds. *General pharmacology* **1997**, 28, 485-487.
17. Casey Laizure, S.; Herring, V.; Hu, Z.; Witbrodt, K.; Parker, R. B. The role of human

carboxylesterases in drug metabolism: have we overlooked their importance? *Pharmacotherapy: The Journal of Human Pharmacology and Drug Therapy* **2013**, 33, 210-222.

18. Van Esbroeck, A. C.; Janssen, A. P.; Cognetta, A. B.; Ogasawara, D.; Shpak, G.; Van Der Kroeg, M.; Kantae, V.; Baggelaar, M. P.; De Vrij, F. M.; Deng, H. Activity-based protein profiling reveals off-target proteins of the FAAH inhibitor BIA 10-2474. *Science* **2017**, 356, 1084-1087.

19. Baggelaar, M. P.; Janssen, F. J.; van Esbroeck, A. C.; den Dulk, H.; Allara, M.; Hoogendoorn, S.; McGuire, R.; Florea, B. I.; Meeuwenoord, N.; van den Elst, H.; van der Marel, G. A.; Brouwer, J.; Di Marzo, V.; Overkleeft, H. S.; van der Stelt, M. Development of an activity-based probe and in silico design reveal highly selective inhibitors for diacylglycerol lipase-alpha in brain. *Angew Chem Int Ed Engl* **2013**, 52, 12081-5.

20. Baggelaar, M. P.; Chameau, P. J.; Kantae, V.; Hummel, J.; Hsu, K. L.; Janssen, F.; van der Wel, T.; Soethoudt, M.; Deng, H.; den Dulk, H.; Allarà, M.; Florea, B. I.; Di Marzo, V.; Wadman, W. J.; Kruse, C. G.; Overkleeft, H. S.; Hankemeier, T.; Werkman, T. R.; Cravatt, B. F.; van der Stelt, M. Highly Selective, Reversible Inhibitor Identified by Comparative Chemoproteomics Modulates Diacylglycerol Lipase Activity in Neurons. *J Am Chem Soc* **2015**, 137, 8851-7.

21. Janssen, F. J.; Deng, H.; Baggelaar, M. P.; Allara, M.; van der Wel, T.; den Dulk, H.; Ligresti, A.; van Esbroeck, A. C.; McGuire, R.; Di Marzo, V.; Overkleeft, H. S.; van der Stelt, M. Discovery of glycine sulfonamides as dual inhibitors of sn-1-diacylglycerol lipase alpha and alpha/beta-hydrolase domain 6. *J Med Chem* **2014**, 57, 6610-22.

22. Long, J. Z.; Nomura, D. K.; Vann, R. E.; Walentiny, D. M.; Booker, L.; Jin, X.; Burston, J. J.; Sim-Selley, L. J.; Lichtman, A. H.; Wiley, J. L. Dual blockade of FAAH and MAGL identifies behavioral processes regulated by endocannabinoid crosstalk in vivo. *Proceedings of the National Academy of Sciences* **2009**, 106, 20270-20275.

23. Labar, G.; Bauvois, C.; Borel, F.; Ferrer, J. L.; Wouters, J.; Lambert, D. M. Crystal structure of the human monoacylglycerol lipase, a key actor in endocannabinoid signaling. *Chembiochem* **2010**, 11, 218-27.

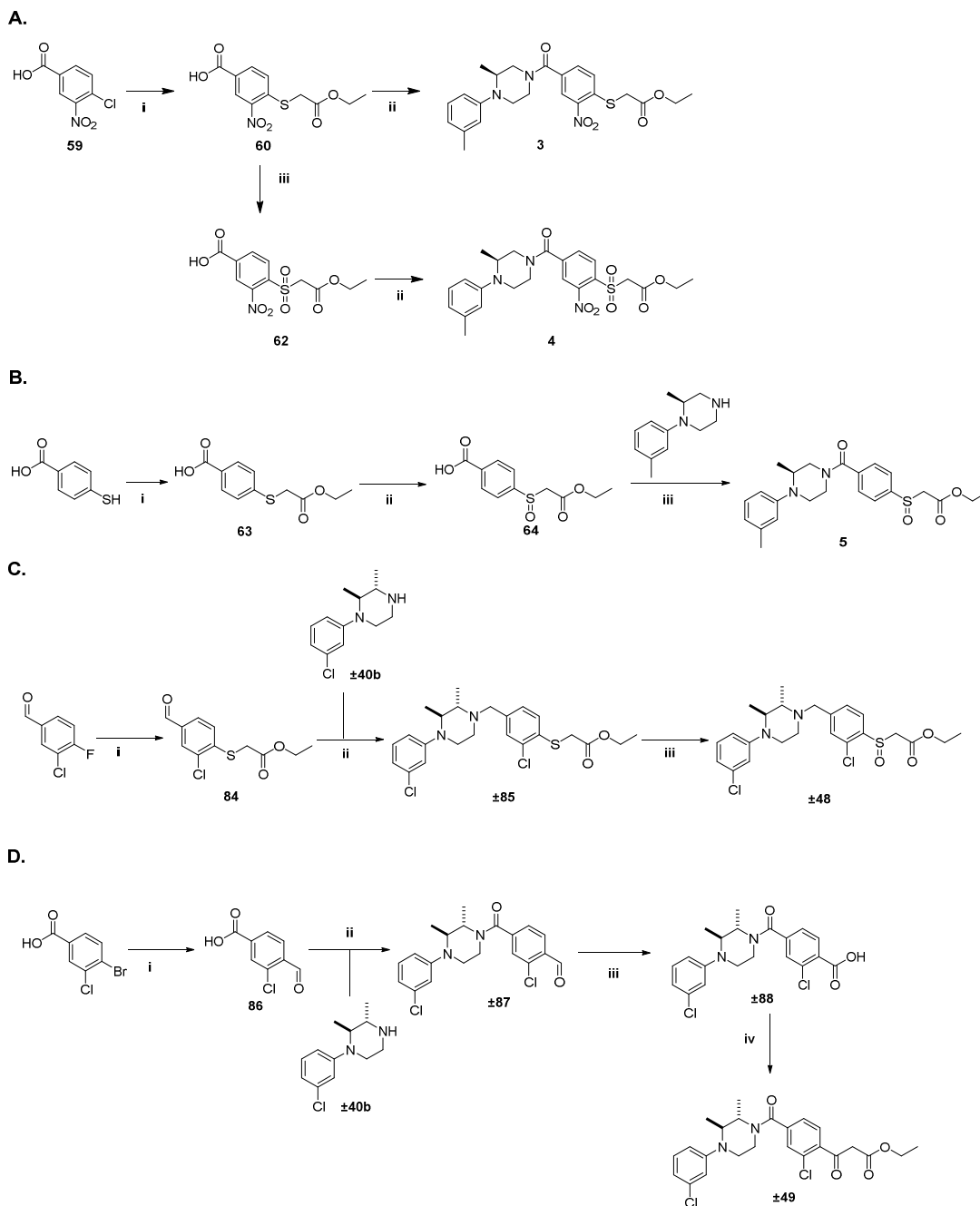
24. Griebel, G.; Pichat, P.; Beeske, S.; Leroy, T.; Redon, N.; Jacquet, A.; Francon, D.; Bert, L.; Even, L.; Lopez-Grancha, M.; Tolstykh, T.; Sun, F.; Yu, Q.; Brittain, S.; Arlt, H.; He, T.; Zhang, B.; Wiederschain, D.; Bertrand, T.; Houtmann, J.; Rak, A.; Vallee, F.; Michot, N.; Auge, F.; Menet, V.; Bergis, O. E.; George, P.; Avenet, P.; Mikol, V.; Didier, M.; Escoubet, J. Selective blockade of the hydrolysis of the endocannabinoid 2-arachidonoylglycerol impairs learning and memory performance while producing antinociceptive activity in rodents. *Scientific reports* **2015**, 5, 7642.

25. Aida, J.; Fushimi, M.; Kusumoto, T.; Sugiyama, H.; Arimura, N.; Ikeda, S.; Sasaki, M.; Sogabe, S.; Aoyama, K.; Koike, T. Design, Synthesis, and Evaluation of Piperazinyl Pyrrolidin-2-ones as a Novel Series of Reversible Monoacylglycerol Lipase Inhibitors. *J Med Chem* **2018**, 61, 9205-9217.

26. Butler, C. R.; Beck, E. M.; Harris, A.; Huang, Z.; McAllister, L. A.; Am Ende, C. W.; Fennell, K.; Foley, T. L.; Fonseca, K.; Hawrylik, S. J.; Johnson, D. S.; Knafels, J. D.; Mente, S.; Noell, G. S.; Pandit, J.; Phillips, T. B.; Piro, J. R.; Rogers, B. N.; Samad, T. A.; Wang, J.; Wan, S.; Brodney, M. A. Azetidine and Piperidine Carbamates as Efficient, Covalent Inhibitors of Monoacylglycerol Lipase. *J Med Chem* **2017**, 60, 9860-9873.

27. Schalk-Hihi, C.; Schubert, C.; Alexander, R.; Bayoumy, S.; Clemente, J. C.; Deckman, I.; DesJarlais, R. L.; Dzordzorme, K. C.; Flores, C. M.; Grasberger, B.; Kranz, J. K.; Lewandowski, F.; Liu, L.; Ma, H.; Maguire, D.; Macielag, M. J.; McDonnell, M. E.; Mezzasalma Haarlander, T.; Miller, R.; Milligan, C.; Reynolds, C.; Kuo, L. C. Crystal structure of a soluble form of human monoglyceride lipase in complex with an inhibitor at 1.35 Å resolution. *Protein science : a publication of the Protein Society* **2011**, 20, 670-83.
28. van Rooden, E. J.; Florea, B. I.; Deng, H.; Baggelaar, M. P.; van Esbroeck, A. C.; Zhou, J.; Overkleeft, H. S.; van der Stelt, M. Mapping in vivo target interaction profiles of covalent inhibitors using chemical proteomics with label-free quantification. *Nature protocols* **2018**, 13, 752.
29. Distler, U.; Kuharev, J.; Navarro, P.; Tenzer, S. Label-free quantification in ion mobility-enhanced data-independent acquisition proteomics. *Nature protocols* **2016**, 11, 795-812.

Supplementary Information



Scheme S1. (A) Synthesis route for compounds **3** and **4**. Reagents and conditions: i) 1-chloro-3-methylbenzene, sodium *tert*-butoxide, BINAP, Pd(OAc)₂, 1,4-dioxane, 85 °C. ii) TFA, DCM, iii) ethyl 2-mercaptoacetate, pyridine, 115 °C. iv) Oxone (1 eq), MeOH / H₂O. v) HATU, DiPEA, DCM. vi) Oxone (10 eq), MeOH / H₂O. (B) Synthesis route for compound **5**. Reagents and conditions: i) ethyl 2-bromoacetate, NaOH, H₂O. ii) Oxone (1 eq), MeOH / H₂O. iii) HATU, DiPEA, DCM. (C) Synthesis routes for compound **±48**. Reagents and conditions: i) ethyl 2-mercaptoacetate, K₂CO₃, ACN. ii) HATU, DiPEA, DCM. iii) oxone, MeOH / H₂O. (D) Synthesis routes for compound **±49**. iv) Turbo-Grignard, DMF, THF, -78 °C - RT. v) oxone, DMF. vi) carbonyldiimidazole, ethyl potassium malonate, MgCl₂, TEA, THF.

Chapter 3

Development of α -aryl ketones as monoacylglycerol lipase inhibitors

M. Jiang, A. Amedi, M. C. W. Huizenga, C. A. A. van Boeckel, R. J. B. H. N. van den Berg, M. van der Stelt*; *manuscript in preparation.*

3.1 Introduction

Monoacylglycerol lipase (MAGL) is a serine hydrolase and plays an important role in regulating endocannabinoid signaling and lipid metabolism.^{1, 2} MAGL inhibitors are thought to be useful for the treatment of various diseases, including (neuro)inflammation, cancer, pain and anxiety.³⁻¹³ In the past two decades a number of drug discovery programs have, therefore, been initiated to discover potent and selective MAGL inhibitors. Several chemotypes have been reported as MAGL inhibitors, such as carbamates^{5, 9, 11}, ureas¹⁴, amides⁴ and esters¹⁵. The first-in-class MAGL inhibitor ABX-1431, which has an activated carbamate warhead, is now in clinical phase 1b for the treatment of post-traumatic stress disorder.

During the Structure-Activity Relationship (SAR) study of β -sulfinyl esters in chapter 2, compound **1** (Figure 1A) was discovered as a highly potent and selective MAGL inhibitor. This compound contains an ester functionality, which is a metabolic

liability and may act as an electrophile for the incoming catalytic serine (See Chapter 2, Figure 3). To test this latter hypothesis, we envisioned that replacing the ester group with bioisosteres that covalently, albeit reversibly, bind to the nucleophilic serine may yield novel, potent MAGL inhibitors.

Previously, α -ketoheterocycle derivatives, such as OL-135 (**2**, Figure 1B) and LEI-105 (**3**, Figure 1B), have been reported as inhibitors of the serine hydrolases fatty acid amide hydrolase (FAAH) and diacylglycerol lipase (DAGL), which catalyze the hydrolysis of an amide and ester bond in anandamide and diacylglycerol, respectively.¹⁶⁻²⁰ Crystallography studies revealed the mechanism of action of α -ketoheterocycle inhibitors. For example, OL-135 interacted with FAAH through hemiketal formation with the catalytic serine (Figure 1C). Inspired by those studies, it is envisioned that replacement of the ester of compound **1** with activated ketones may also yield potent MAGL inhibitors (Figure 1A). In this chapter, a novel series of α -aryl ketones as MAGL inhibitors with the compound **1**-scaffold was generated and evaluated. Optimization of the α -aryl ketones as novel “warhead” of MAGL lead to the discovery of compound **24** as a covalent, reversible MAGL inhibitor with nanomolar potency.

3.2 Results and discussion

To test the feasibility of α -aryl ketones as MAGL inhibitors, compounds **4** to **24** were synthesized according to general synthesis scheme 1. First, an aromatic nucleophilic substitution was performed with commercially available building block **25** with sodium methylsulfide to obtain the sulfide **26**, which was oxidized by oxone to sulfoxide compound **27**. The *tert*-butyl protecting group was removed with TFA and benzoic acid was coupled with amine **29** through an EDCI/HOBt-mediated peptide coupling which furnished compound **30**. Finally, commercially available esters were reacted with compound **30** to yield the final compounds (**4** - **24**). MAGL inhibitory activities of synthesized compounds were determined using the natural substrate assay reported in Chapter 2.

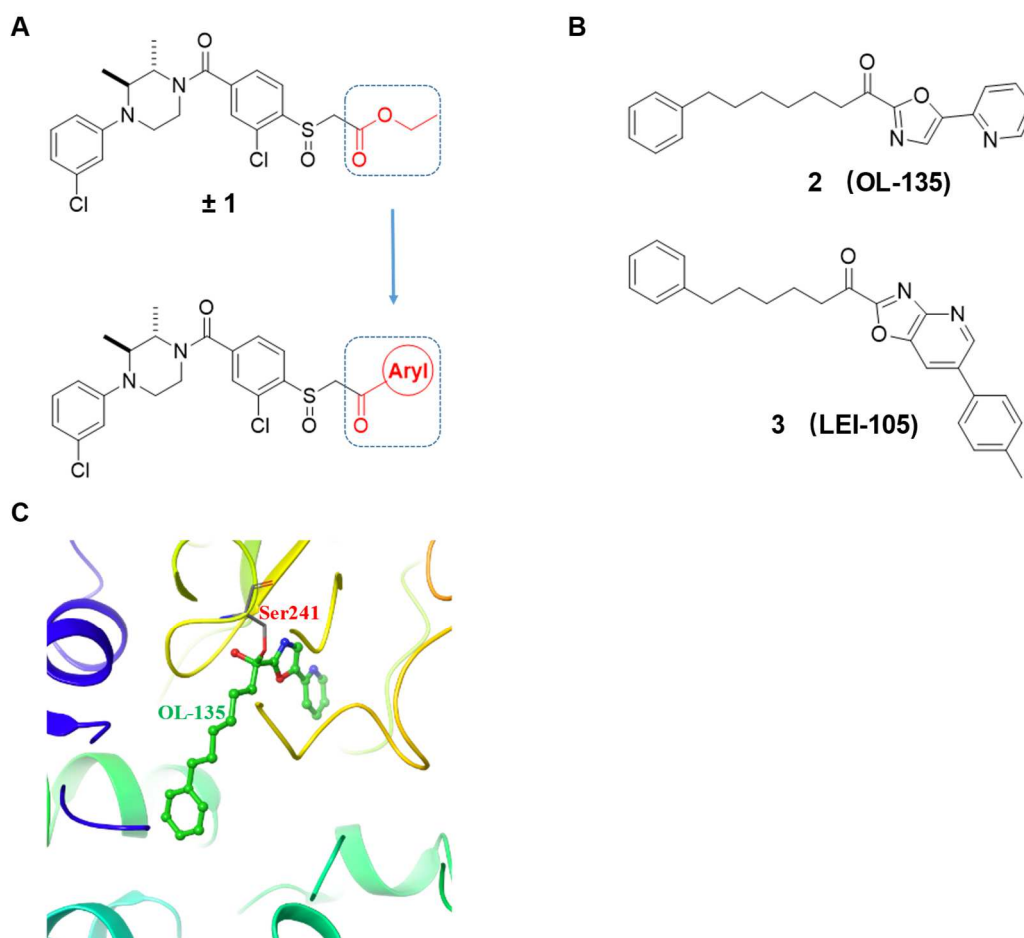
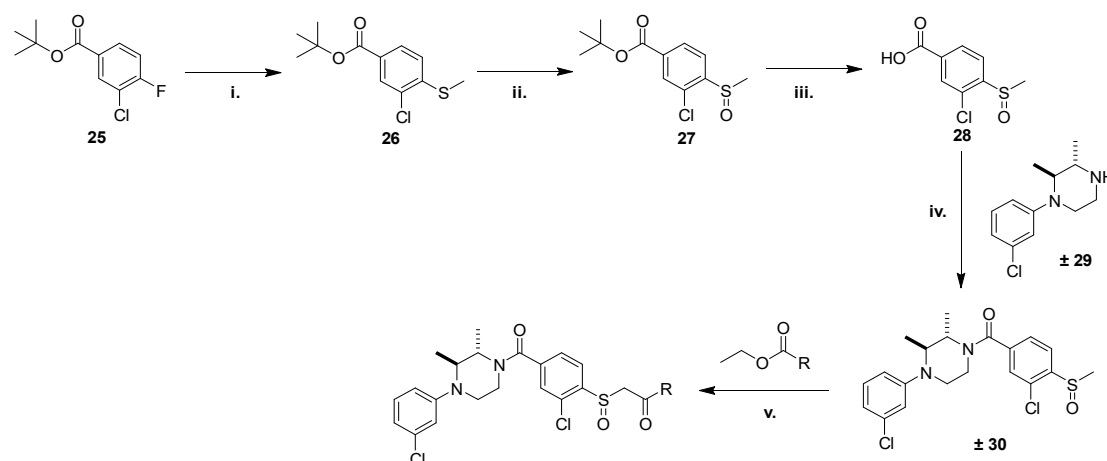
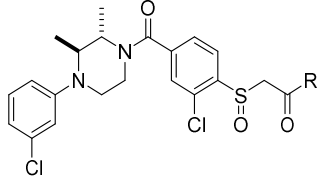


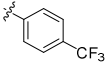
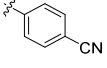
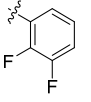
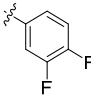
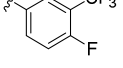
Figure 1. A) Design strategy of aryl ketones as MAGL inhibitors. B) Chemical structures of OL-135 and LEI-105. C) View of OL-135 in the binding pocket of FAAH (PDB ID: 3PR0). OL-135 binds to the catalytic Ser241 covalently and the deprotonated hemiketal mimics the enzymatic tetrahedral intermediate.

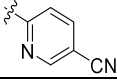


Replacing the ester moiety with phenyl ketone (**± 4**) resulted in an active MAGL inhibitor, which was therefore used as the starting point for further optimization. To analyze the effect of the substitution pattern on the phenyl ring, compounds **± 5** – **± 15** were examined. Fluorine as an electron withdrawing substituent on the *ortho*- (**± 5**) or *para*-position (**± 9**), but not *meta*-position (**± 8**), was allowed, albeit that there is hardly an increase in potency. Interestingly, the polar electron withdrawing para nitril substituent (**± 7**) significantly increased the potency. Difluoro substitution (**± 11** - **± 14**) improved the potency, but trifluoromethyl substitution on *meta*-position (**± 15**) abolished the MAGL inhibitory activity. Replacement of the phenyl ring to 3-pyridinyl ring (**± 10**) decreased the potency. The Hammett constants (σ) of the substituents was plotted against the activity of the compounds, but no correlation ($r^2 = 0.16$, Figure S1) was found, suggesting that the electron-withdrawing effect is not the main contributor to the potency.

Since polar substitution is favored and reduces the lipophilicity, the phenyl ring was replaced with five or six-membered heterocycles (**± 16** - **± 24**). These compounds displayed an increased MAGL inhibitory activity and lipophilic efficiency (LipE). Compounds with oxazol-2-yl (**± 16**), 5-methyloxazol-2-yl (**± 17**) and thiazol-2-yl (**± 18**) groups showed around 10-fold increase in potency and 100-fold increase in LipE. For compounds with a six-membered heterocycle, hetero atoms at the 2- and/or 4-positions (**± 21** - **± 22**) were more favored than at the 3-position (**± 19**, **± 20** and **± 23**). Of these, compound **± 22** showed a higher LipE than compound **± 1**. Finally, 5-cyanopyridin-2-yl ketone (**± 24**) was designed and evaluated. Compound **± 24** showed a pIC₅₀ of 8.00 ± 0.10, which is 250-fold higher than the starting compound **± 4** and similar in magnitude as compound **± 1** (pIC₅₀ = 8.50 ± 0.10).

Table 1. pIC₅₀ values of α -aryl ketones (± 2 - ± 24).


Entry	R	pIC ₅₀ \pm SD	MW	cLogP	tPSA	LipE
± 1		8.50 \pm 0.10	497.63	4.93	67	3.57
± 4		5.64 \pm 0.14	529.48	5.68	58	-0.04
± 5		5.72 \pm 0.04	547.47	5.90	58	-0.18
± 6		5.53 \pm 0.10	597.47	6.70	58	-1.17
± 7		7.04 \pm 0.06	554.49	5.29	81	1.75
± 8		<5	547.47	5.90	58	N.A.
± 9		5.79 \pm 0.22	547.47	5.45	58	-0.11
± 10		5.01 \pm 0.05	530.46	4.58	70	0.43
± 11		5.68 \pm 0.23	565.46	6.07	58	-0.39
± 12		6.24 \pm 0.20	565.46	5.55	58	0.17
± 13		6.12 \pm 0.21	565.46	6.00	58	0.05
± 14		6.63 \pm 0.07	565.46	6.07	58	0.56
± 15		<5	615.46	6.87	58	N.A.
± 16		6.69 \pm 0.15	520.43	4.16	79	2.53
± 17		6.42 \pm 0.07	534.45	4.42	79	2.00
± 18		6.63 \pm 0.10	536.49	4.81	70	1.82
± 19		6.60 \pm 0.07	531.45	3.59	82	3.01

Entry	R	pIC ₅₀ ± SD	MW	cLogP	tPSA	LipE
± 20		6.15 ± 0.05	531.45	3.59	82	2.56
± 21		7.06 ± 0.16	531.45	4.02	82	3.47
± 22		7.55 ± 0.14	531.45	4.02	82	3.96
± 23		5.96 ± 0.12	531.45	4.02	82	2.37
± 24		8.00 ± 0.10	555.47	4.53	94	3.47

3.3 Conclusion

In conclusion, a series of α -aryl ketones as MAGL inhibitors is reported in this chapter. SAR investigation supported the original hypothesis that the ester group of compound ± 1 may serve as an electrophilic site for a nucleophilic attack by the catalytic serine of MAGL. Replacing the ester with aryl ketones resulted in the discovery of ± 22 and ± 24 as potent MAGL inhibitors. Since these compounds contain a similar “warhead” as the FAAH inhibitor OL-135, they are expected to inhibit MAGL in a similar fashion through a covalent, reversible mechanism. To our knowledge, these α -aryl ketones are the first MAGL inhibitors with an activated ketone reported so far. The metabolic stability of this chemical series will be examined in Chapter 4.

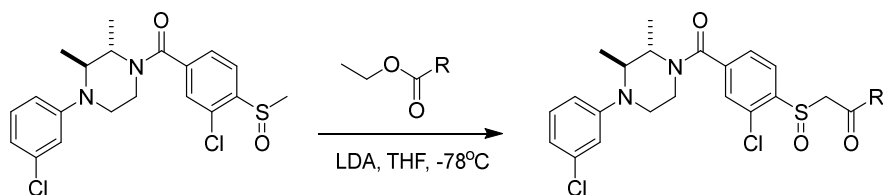
3.4 Experimental procedures

MAGL natural substrate assay

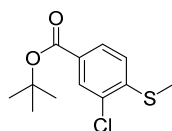
The natural substrate assay for MAGL was performed as previously reported in Chapter 2.²¹

Chemistry procedures

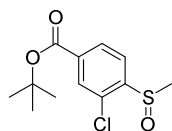
General remarks. All reactions were performed using oven or flame-dried glassware and dry solvents. Reagents were purchased from Sigma Aldrich, Acros and Merck and used without further purification unless noted otherwise. All moisture sensitive reactions were performed under an argon or nitrogen atmosphere. Traces of water were removed from starting compounds by co-evaporation with toluene. Reactions were followed by thin layer chromatography and was performed using TLC Silica gel 60 F₂₄₅ on aluminum sheets. Compounds were visualized using a KMnO₄ stain (K₂CO₃ (40 g), KMnO₄ (6 g), H₂O (600 mL) and 10% NaOH (5 mL)). ¹H- and ¹³C-NMR spectra were recorded on a Bruker AV-400, 500, 600 or 850 using CDCl₃ or CD₃OD as solvent, unless stated otherwise. Chemical shift values are reported in ppm with tetramethylsilane or solvent resonance as the internal standard (CDCl₃: δ 7.26 for ¹H, δ 77.16 for ¹³C, CD₃OD: δ 3.31 for ¹H, δ 49.00 for ¹³C). Data are reported as follows: chemical shifts (δ), multiplicity (s = singlet, d = doublet, dd = double doublet, td = triple doublet, t = triplet, q = quartet, quintet = quint, br = broad, m = multiplet), coupling constants *J* (Hz), and integration. LC-MS measurements were performed on a Thermo Finnigan LCQ Advantage Max ion-trap mass spectrometer (ESI⁺) coupled to a Surveyor HPLC system (Thermo Finnigan) equipped with a standard C18 (Gemini, 4.6 mmD \times 50 mmL, 5 μ m particle size, Phenomenex) analytical column and buffers A: H₂O, B: ACN, C: 0.1% aq. TFA. Preparative HPLC purification was performed on a Waters Acquity Ultra Performance LC with a C18 column (Gemini, 150 \times 21.2 mm, Phenomenex). Diode detection was done between 210 and 600 nm. Gradient: ACN in (H₂O + 0.2% TFA). High-resolution mass spectra (HRMS) were recorded on a Thermo Scientific LTQ Orbitrap XL.

General procedure I

To a solution of (\pm) (3-chloro-4-(methylsulfinyl)phenyl)(4-(3-chlorophenyl)-trans-2,3-dimethylpiperazin-1-yl)methanone (1 eq.) in anhydrous THF was added LDA (2 eq.) at $-78\text{ }^{\circ}\text{C}$ and the reaction mixture was stirred for 30 min before the appropriate ester (10 eq.) was added. The reaction progress was monitored by TLC. Once completed, the mixture was quenched with NH_4Cl solution, extracted with DCM and dried over anhydrous MgSO_4 . After filtration, the filtrate was concentrated under reduced pressure. The residue was purified by silica gel column chromatography.

***tert*-Butyl 3-chloro-4-(methylthio)benzoate (26)**

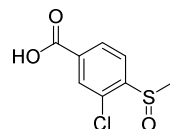
To a solution of *tert*-butyl 3-chloro-4-(methylthio)benzoate (**25**) (0.510 g, 2.22 mmol, 1 eq.) in degassed DMF was added sodium methanethiolate (0.230 g, 3.32 mmol, 1.5 eq.) at $-10\text{ }^{\circ}\text{C}$ and the mixture was stirred at RT overnight. The reaction progress was monitored by TLC. Once completed, the mixture was diluted with Et_2O , washed with water, dried over anhydrous MgSO_4 and concentrated under reduced pressure. The residue was purified using column chromatography (Et_2O / pentane, 0-10%) to yield the product (0.24 g, 0.91 mmol, 41%). ^1H NMR (400 MHz, CDCl_3) δ 7.91 (d, $J = 1.8$ Hz, 1H), 7.85 (dd, $J = 8.3, 1.8$ Hz, 1H), 7.13 (d, $J = 8.4$ Hz, 1H), 2.49 (s, 3H), 1.59 (s, 9H). ^{13}C NMR (400 MHz, CDCl_3) δ 164.54, 143.80, 130.83, 129.94, 129.04, 128.05, 123.94, 81.49, 28.22, 14.92.

***tert*-Butyl 3-chloro-4-(methylsulfinyl)benzoate (27)**

To a solution of *tert*-butyl 3-chloro-4-(methylthio)benzoate (**26**) (0.24 g, 0.91 mmol, 1 eq.) in 10 mL MeOH was added Oxone (0.56 g, 0.91 mmol, 1 eq.) / H_2O (5 mL) solution at $0\text{ }^{\circ}\text{C}$ and the mixture was stirred at RT for 1 h. The reaction progress was monitored by TLC. Once completed, the mixture was diluted with DCM, washed with water, dried over anhydrous MgSO_4 and concentrated under reduced pressure. The residue was purified using column chromatography (Et_2O

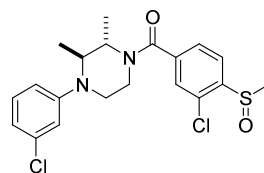
/ pentane, 25-40%) to yield the product (0.290 g, 1.17 mmol, quant.). ^1H NMR (500 MHz, CDCl_3) δ 8.13 (dd, $J = 8.0, 1.6$ Hz, 1H), 8.03 – 7.98 (m, 2H), 2.86 (s, 3H), 1.62 (s, 9H). ^{13}C NMR (126 MHz, CDCl_3) δ 163.34, 147.97, 135.70, 130.48, 129.52, 128.73, 125.20, 82.24, 41.37, 27.94.

3-Chloro-4-(methylsulfinyl)benzoic acid (**28**)



To a solution of *tert*-butyl 3-chloro-4-(methylsulfinyl)benzoate (**27**) (0.26 g, 0.94 mmol) in 8 mL DCM was added 2 mL TFA and the mixture was stirred at RT for 6 h. The reaction progress was monitored by TLC. Once completed, the mixture was diluted with DCM, washed with saturated NaHCO_3 solution, dried over anhydrous MgSO_4 and concentrated under reduced pressure. The residue was purified using column chromatography (MeOH / DCM, 1-5%) to yield the product (0.19 g, 0.87 mmol, 92%). ^1H NMR (400 MHz, Methanol- d_4) δ 8.22 (dd, $J = 8.2, 1.6$ Hz, 1H), 8.08 (d, $J = 1.6$ Hz, 1H), 7.98 (d, $J = 8.1$ Hz, 1H), 2.90 (s, 3H). ^{13}C NMR (126 MHz, Methanol- d_4) δ 167.19, 148.93, 136.49, 132.03, 131.20, 130.45, 126.47, 41.68.

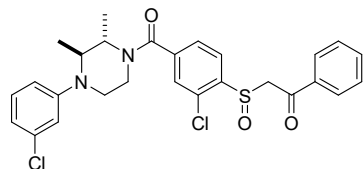
(\pm) (3-Chloro-4-(methylsulfinyl)phenyl)(4-(3-chlorophenyl)-*trans*-2,3-dimethylpiperazin-1-yl)methanone (**30**)



To a stirred suspension of 3-chloro-4-((2-ethoxy-2-oxoethyl)sulfinyl)benzoic acid (**28**) (0.19 g, 0.87 mmol, 1 eq.) in DCM (10 ml) were added (\pm) *trans*-1-(3-chlorophenyl)-2,3-dimethylpiperazine (**30**) (0.230 g, 1.04 mmol, 1.2 eq.), DiPEA (0.34 mg, 2.59 mmol, 3 eq.), HOBt (0.18 mg, 1.30 mmol, 1.5 eq.) and EDCI (0.25 mg, 1.30 mmol, 1.5 eq.). The mixture was stirred at RT overnight. The reaction progress was monitored by TLC. Once completed, the mixture was washed with water and brine, dried (MgSO_4), filtered and concentrated. The crude product was purified using column chromatography (EtOAc / pentane, 0%-60%) to yield the product (0.27 mg, 0.64 mmol, 74%). ^1H NMR (400 MHz, CDCl_3) δ 8.04 – 7.97 (m, 2H), 7.56 – 7.38 (m, 2H), 7.14 (t, $J = 8.2$ Hz, 1H), 6.60 (d, $J = 2.4$ Hz, 1H), 6.56 – 6.47 (m, 1H), 4.85 – 4.49 (m, 1H), 3.98 – 3.07 (m, 5H), 2.82 (s, 3H), 1.42 – 1.33 (m, 3H), 1.28 – 1.06 (m, 3H). ^{13}C NMR (126 MHz, CDCl_3) δ 168.83, 151.33, 145.25, 140.18, 135.19, 130.47, 130.33, 128.43, 127.77, 125.85, 119.34,

116.13, 114.19, 56.08, 49.57, 42.29, 41.64, 36.46, 17.76, 12.52.

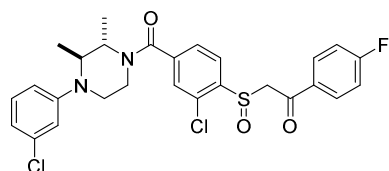
(±) **2-((2-Chloro-4-(4-(3-chlorophenyl)-trans-2,3-dimethylpiperazine-1-carbonyl)phenyl)sulfinyl)-1-phenylethan-1-one (4)**



The title compound was synthesized using (±) (3-chloro-4-(methylsulfinyl)phenyl)(trans-4-(3-chlorophenyl)-2,3-dimethylpiperazin-1-yl)methanone (**30**) (50 mg, 0.12

mmol, 1 eq.) and ethyl benzoate (177 mg, 1.175 mmol, 10 eq.) according to General Procedure I. This yielded the product (38.5 mg, 0.073 mmol, 62%). ¹H NMR (500 MHz, CDCl₃) δ 8.00 (d, J = 8.0 Hz, 1H), 7.93 (d, J = 7.2 Hz, 2H), 7.64 (t, J = 7.4 Hz, 1H), 7.52 (d, J = 10.6 Hz, 2H), 7.49 (d, J = 7.5 Hz, 2H), 7.19 (t, J = 8.1 Hz, 1H), 6.83 (d, J = 7.8 Hz, 1H), 6.82 (d, J = 2.1 Hz, 1H), 6.73 (d, J = 10.1 Hz, 1H), 4.66 (dd, J = 14.7, 3.6 Hz, 1H), 4.42 (dd, J = 14.7, 2.7 Hz, 1H), 3.96 – 3.07 (br, 6H), 1.51 (d, J = 6.5 Hz, 3H), 1.06 (br, 3H). HRMS: calculated for [C₂₇H₂₆Cl₂N₂O₃S+ H]⁺ = 529.1114, found: 529.1112.

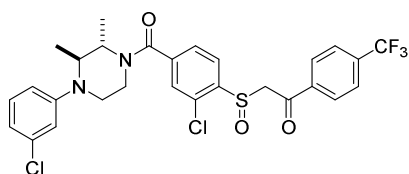
(±) **2-((2-Chloro-4-(4-(3-chlorophenyl)-trans-2,3-dimethylpiperazine-1-carbonyl)phenyl)sulfinyl)-1-(4-fluorophenyl)ethan-1-one (5)**



The title compound was synthesized using (±) (3-chloro-4-(methylsulfinyl)phenyl)(trans-4-(3-chlorophenyl)-2,3-dimethylpiperazin-1-yl)methanone

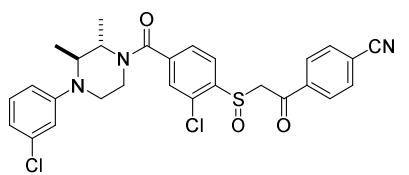
(**30**) (50 mg, 0.12 mmol, 1 eq.) and ethyl 4-fluorobenzoate (198 mg, 1.18 mmol, 10.0 eq.) according to general procedure I. This yielded the product (17 mg, 0.030? mmol, 26%). ¹H NMR (400 MHz, CDCl₃) δ 7.98 (dd, J = 5.0, 1.8 Hz, 1H), 7.97 (s, 1H), 7.95 (d, J = 3.0 Hz, 1H), 7.54 – 7.47 (m, 2H), 7.21 – 7.15 (m, 3H), 6.85 – 6.80 (m, 2H), 6.75 – 6.70 (dd, 1H), 4.64 – 4.60 (m, 1H), 4.35 (dd, J = 14.3, 1.9 Hz, 1H), 4.09 – 2.97 (m, 6H), 1.51 (d, J = 7.2 Hz, 3H), 1.07 (m, 3H). HRMS: calculated for [C₂₇H₂₅Cl₂FN₂O₃S+ H]⁺ = 547.1020, found: 547.1018.

(±) **2-((2-Chloro-4-(4-(3-chlorophenyl)-trans-2,3-dimethylpiperazine-1-carbonyl)phenyl)sulfinyl)-1-(4-(trifluoromethyl)phenyl)ethan-1-one (6)**



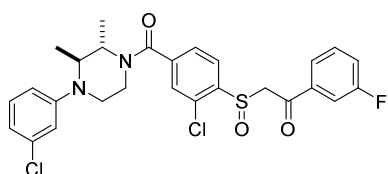
The title compound was synthesized using (±) (3-chloro-4-(methylsulfinyl)phenyl)(trans-4-(3-chlorophenyl)-2,3-dimethylpiperazin-1-yl)methanone (**30**) (50 mg, 0.12 mmol, 1 eq.) and ethyl 4-(trifluoromethyl)benzoate (256 mg, 1.178 mmol, 10.0 eq.) according to general procedure I. This yielded the product (16.2 mg, 0.027 mmol, 23%). $^1\text{H NMR}$ (500 MHz, CDCl_3) δ 8.05 (d, $J = 8.6$ Hz, 2H), 7.96 (d, $J = 8.0$ Hz, 1H), 7.77 (d, $J = 8.6$ Hz, 2H), 7.53 (dd, $J = 8.0, 1.4$ Hz, 1H), 7.51 (d, $J = 1.3$ Hz, 1H), 7.18 (t, $J = 8.1$ Hz, 1H), 6.84 (d, $J = 7.8$ Hz, 1H), 6.81 (t, $J = 2.0$ Hz, 1H), 6.73 (d, $J = 8.4$ Hz, 1H), 4.70 (dd, $J = 14.4, 3.8$ Hz, 1H), 4.40 (dd, $J = 14.4, 3.3$ Hz, 1H), 3.89 – 3.15 (br, 6H), 1.52 (d, $J = 6.6$ Hz, 3H), 1.05 (br, 3H). HRMS: calculated for $[\text{C}_{25}\text{H}_{24}\text{Cl}_2\text{N}_4\text{O}_3\text{S} + \text{H}]^+ = 597.0988$, found: 597.0984.

(±) **4-(2-((2-Chloro-4-(4-(3-chlorophenyl)-trans-2,3-dimethylpiperazine-1-carbonyl)phenyl)sulfinyl)acetyl)benzonitrile (7)**



The title compound was synthesized using (±) (3-chloro-4-(methylsulfinyl)phenyl)(trans-4-(3-chlorophenyl)-2,3-dimethylpiperazin-1-yl)methanone (**30**) (50 mg, 0.12 mmol, 1 eq.) and ethyl 4-cyanobenzoate (206 mg, 1.18 mmol, 10 eq.) according to General Procedure I. This yielded the product (12 mg, 0.022 mmol, 18%). $^1\text{H NMR}$ (500 MHz, CDCl_3) δ 8.05 (d, $J = 8.0$ Hz, 2H), 7.92 (d, $J = 8.1$ Hz, 1H), 7.82 (d, $J = 7.6$ Hz, 2H), 7.53 (d, $J = 8.8$ Hz, 2H), 7.20 (t, $J = 8.1$ Hz, 1H), 6.85 (d, $J = 8.3$ Hz, 2H), 6.76 (d, $J = 8.5$ Hz, 1H), 4.69 (dd, $J = 14.0, 3.4$ Hz, 1H), 4.36 (dd, $J = 14.1, 2.9$ Hz, 1H), 3.83 – 3.17 (br, 6H), 1.53 (d, $J = 6.7$ Hz, 3H), 1.09 (br, 3H). HRMS: calculated for $[\text{C}_{27}\text{H}_{24}\text{Cl}_2\text{F}_2\text{N}_2\text{O}_3\text{S} + \text{H}]^+ = 554.1066$, found: 554.1066.

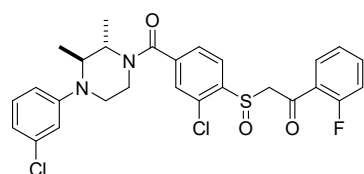
(±) **2-((2-Chloro-4-(4-(3-chlorophenyl)-trans-2,3-dimethylpiperazine-1-carbonyl)phenyl)sulfinyl)-1-(3-fluorophenyl)ethan-1-one (8)**



The title compound was synthesized using (±) (3-chloro-4-(methylsulfinyl)phenyl)(trans-4-(3-chlorophenyl)-2,3-dimethylpiperazin-1-yl)methanone (**30**) (50 mg, 0.12 mmol, 1 eq.) and ethyl 3-fluorobenzoate (198 mg, 1.18 mmol, 10.00 eq.) according to general procedure I. This yielded the product (8.0 mg, 0.002 mmol,

12%). $^1\text{H NMR}$ (400 MHz, CDCl_3) δ 7.95 (d, $J = 8.2$ Hz, 1H), 7.72 (d, $J = 7.8$ Hz, 1H), 7.62 (d, $J = 9.1$ Hz, 1H), 7.54 – 7.46 (m, 3H), 7.34 (t, $J = 8.2$ Hz, 1H), 7.19 (t, $J = 7.8$ Hz, 1H), 6.82 (d, $J = 7.5$ Hz, 2H), 6.72 (d, $J = 8.1$ Hz, 1H), 4.67 – 4.57 (m, 1H), 4.33 (d, $J = 14.3$ Hz, 1H), 3.92 – 3.12 (br, 6H), 1.54 – 1.45 (m, 3H), 1.16 – 1.00 (m, 3H). HRMS: calculated for $[\text{C}_{27}\text{H}_{25}\text{Cl}_2\text{FN}_2\text{O}_3\text{S} + \text{H}]^+ = 547.1020$, found: 547.1019.

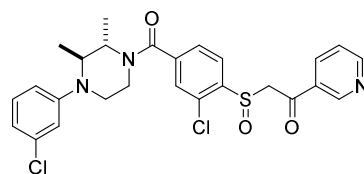
(\pm) **2-((2-Chloro-4-(4-(3-chlorophenyl)-trans-2,3-dimethylpiperazine-1-carbonyl)phenyl)sulfinyl)-1-(2-fluorophenyl)ethan-1-one (9)**



The title compound was synthesized using (\pm) (3-chloro-4-(methylsulfinyl)phenyl)(trans-4-(3-chlorophenyl)-2,3-dimethylpiperazin-1-yl)methanone (**30**) (50 mg, 0.12

mmol, 1 eq.) and ethyl 2-fluorobenzoate (198 mg, 1.178 mmol, 10.0 eq.) according to general procedure I. This yielded the product (5.5 mg, 0.001 mmol, 9%). $^1\text{H NMR}$ (600 MHz, CDCl_3) δ 8.01 (d, $J = 7.9$ Hz, 1H), 7.96 (t, $J = 8.5$ Hz, 1H), 7.61 (d, $J = 6.2$ Hz, 1H), 7.53 (d, $J = 7.9$ Hz, 1H), 7.48 (d, $J = 7.6$ Hz, 1H), 7.30 (d, $J = 7.4$ Hz, 1H), 7.21 – 7.11 (m, 2H), 6.98 (d, $J = 10.9$ Hz, 1H), 6.84 (d, $J = 7.4$ Hz, 1H), 6.75 (d, $J = 8.3$ Hz, 1H), 4.68 (d, $J = 22.3$ Hz, 1H), 4.37 (dt, $J = 14.7, 2.8$ Hz, 1H), 3.91 – 3.17 (br, 6H), 1.51 (d, $J = 6.8$ Hz, 3H), 1.08 (br, 3H). HRMS: calculated for $[\text{C}_{27}\text{H}_{25}\text{Cl}_2\text{FN}_2\text{O}_3\text{S} + \text{H}]^+ = 547.1020$, found: 547.1024.

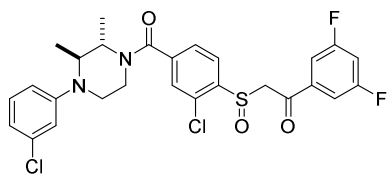
(\pm) **2-((2-Chloro-4-(4-(3-chlorophenyl)-trans-2,3-dimethylpiperazine-1-carbonyl)phenyl)sulfinyl)-1-(pyridin-3-yl)ethan-1-one (10)**



The title compound was synthesized using (\pm) (3-chloro-4-(methylsulfinyl)phenyl)(trans-4-(3-chlorophenyl)-2,3-dimethylpiperazin-1-yl)methanone (**30**) (50 mg, 0.12

mmol, 1 eq.) and ethyl nicotinate (178 mg, 1.18 mmol, 10 eq.) according to general procedure I. This yielded the product (5 mg, 0.01 mmol, 8%). $^1\text{H NMR}$ (400 MHz, CDCl_3) δ 9.41 (s, 1H), 8.99 (d, $J = 5.0$ Hz, 1H), 8.80 (m, 1H), 7.98 (s, 1H), 7.79 (d, $J = 7.6$ Hz, 1H), 7.53 (d, $J = 8.8$ Hz, 2H), 7.19 (t, $J = 8.3$ Hz, 1H), 6.85 (d, $J = 6.5$ Hz, 2H), 6.76 (d, $J = 8.4$ Hz, 1H), 4.92 (d, $J = 13.0$ Hz, 1H), 4.47 (d, $J = 13.2$ Hz, 1H), 3.88 – 3.13 (br, 6H), 1.52 (d, $J = 6.5$ Hz, 3H), 1.09 (br, 3H). HRMS: calculated for $[\text{C}_{26}\text{H}_{25}\text{Cl}_2\text{N}_3\text{O}_3\text{S} + \text{H}]^+ = 530.1066$, found: 530.1069.

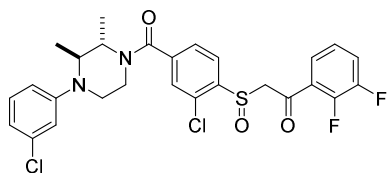
(±) **2-((2-Chloro-4-(4-(3-chlorophenyl)-trans-2,3-dimethylpiperazine-1-carbonyl)phenyl)sulfinyl)-1-(3,5-difluorophenyl)ethan-1-one (11)**



The title compound was synthesized using (±) (3-chloro-4-(methylsulfinyl)phenyl)(trans-4-(3-chlorophenyl)-2,3-dimethylpiperazin-1-yl)methanone

(**30**) (50 mg, 0.12 mmol, 1 eq.) and ethyl 3,5-difluorobenzoate (219 mg, 1.175 mmol, 10 eq.) according to general procedure I. This yielded the product (21 mg, 0.037 mmol, 32%). $^1\text{H NMR}$ (400 MHz, CDCl_3) δ 7.94 (dd, $J = 8.0, 1.2$ Hz, 1H), 7.46 (dd, $J = 7.5, 2.1$ Hz, 2H), 7.18 (t, $J = 8.2$ Hz, 1H), 7.12 (dt, $J = 8.3, 2.3$ Hz, 2H), 7.09 (t, $J = 2.3$ Hz, 1H), 6.85 – 6.79 (m, 2H), 6.73 (d, $J = 9.2$ Hz, 1H), 4.60 (dd, $J = 14.1, 2.8$ Hz, 1H), 4.30 (dd, $J = 14.1, 2.8$ Hz, 1H), 3.82 – 2.53 (br, 6H), 1.50 (d, $J = 6.5$ Hz, 3H), 1.09 (d, $J = 34.8$ Hz, 3H). HRMS: calculated for $[\text{C}_{27}\text{H}_{24}\text{Cl}_2\text{F}_2\text{N}_2\text{O}_3\text{S}+\text{H}]^+ = 565.0926$, found: 565.0926.

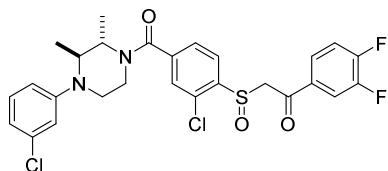
(±) **2-((2-Chloro-4-(4-(3-chlorophenyl)-trans-2,3-dimethylpiperazine-1-carbonyl)phenyl)sulfinyl)-1-(2,3-difluorophenyl)ethan-1-one (12)**



The title compound was synthesized using (±) (3-chloro-4-(methylsulfinyl)phenyl)(trans-4-(3-chlorophenyl)-2,3-dimethylpiperazin-1-yl)methanone

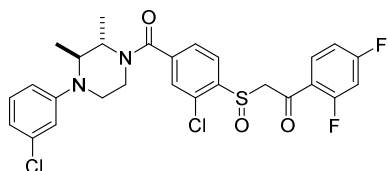
(**30**) (50 mg, 0.12 mmol, 1 eq.) and ethyl 2,3-difluorobenzoate (278 mg, 1.18 mmol, 10 eq.) according to general procedure I. This yielded the product (26 mg, 0.046 mmol, 39%). $^1\text{H NMR}$ (400 MHz, CDCl_3) δ 7.99 (dd, $J = 8.0, 2.2$ Hz, 1H), 7.72 – 7.66 (t, 1H), 7.54 (dd, $J = 8.0, 1.4$ Hz, 1H), 7.50 (s, 1H), 7.44 (d, $J = 8.0$ Hz, 1H), 7.26 – 7.22 (dd, 1H), 7.19 (t, $J = 8.3$ Hz, 1H), 6.84 (d, $J = 6.6$ Hz, 2H), 6.74 (d, $J = 9.2$ Hz, 1H), 4.70 (dt, $J = 15.3, 2.7$ Hz, 1H), 4.39 (dt, $J = 15.3, 2.7$ Hz, 1H), 4.06 – 2.73 (br, 6H), 1.51 (d, $J = 6.7$ Hz, 3H), 1.08 (br, 3H). HRMS: calculated for $[\text{C}_{27}\text{H}_{24}\text{Cl}_2\text{F}_2\text{N}_2\text{O}_3\text{S}+\text{H}]^+ = 565.0926$, found: 565.0926.

(±) **2-((2-Chloro-4-(4-(3-chlorophenyl)-trans-2,3-dimethylpiperazine-1-carbonyl)phenyl)sulfinyl)-1-(3,4-difluorophenyl)ethan-1-one (13)**



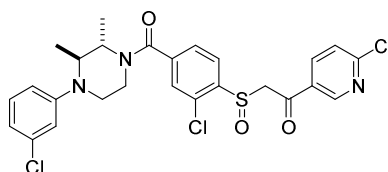
The title compound was synthesized using (\pm) (3-chloro-4-(methylsulfinyl)phenyl)(trans-4-(3-chlorophenyl)-2,3-dimethylpiperazin-1-yl)methanone (**30**) (50 mg, 0.12 mmol, 1 eq.) and ethyl 3,4-difluorobenzoate (278 mg, 1.18 mmol, 10 eq.) according to general procedure I. This yielded the product (18.0 mg, 0.032 mmol, 27%). $^1\text{H NMR}$ (400 MHz, CDCl_3) δ 7.95 (d, $J = 7.9$ Hz, 1H), 7.81 (t, $J = 8.0$ Hz, 1H), 7.76 (d, $J = 6.3$ Hz, 1H), 7.54 (d, $J = 11.3$ Hz, 2H), 7.36 – 7.30 (br, 1H), 7.21 (t, $J = 8.1$ Hz, 1H), 6.86 (d, $J = 8.7$ Hz, 2H), 6.76 (d, $J = 8.8$ Hz, 1H), 4.63 (dd, $J = 14.2, 2.5$ Hz, 1H), 4.34 (dd, $J = 14.2, 2.2$ Hz, 1H), 4.00 – 2.99 (br, 6H), 1.54 (d, $J = 6.7$ Hz, 3H), 1.10 (br, 3H). HRMS: calculated for $[\text{C}_{27}\text{H}_{24}\text{Cl}_2\text{F}_2\text{N}_2\text{O}_3\text{S} + \text{H}]^+ = 565.0926$, found: 565.0925.

(\pm) **2-((2-Chloro-4-(4-(3-chlorophenyl)-trans-2,3-dimethylpiperazine-1-carbonyl)phenyl)sulfinyl)-1-(2,4-difluorophenyl)ethan-1-one (14)**



The title compound was synthesized using (\pm) (3-chloro-4-(methylsulfinyl)phenyl)(trans-4-(3-chlorophenyl)-2,3-dimethylpiperazin-1-yl)methanone (**30**) (50 mg, 0.12 mmol, 1 eq.) and ethyl 2,4-difluorobenzoate (218 mg, 1.17 mmol, 10 eq.) according to general procedure I. This yielded the product (29.7 mg, 0.053 mmol, 45%). $^1\text{H NMR}$ (400 MHz, CDCl_3) δ 8.07 – 8.03 (m, 1H), 8.04 – 8.00 (m, 1H), 7.57 (dd, $J = 8.0, 1.5$ Hz, 1H), 7.52 (d, $J = 1.4$ Hz, 1H), 7.21 (t, $J = 8.1$ Hz, 1H), 7.08 – 7.02 (ddd, 1H), 6.92 (ddd, $J = 11.1, 8.5, 2.3$ Hz, 1H), 6.86 (d, $J = 8.0$ Hz, 2H), 6.76 (d, $J = 9.1$ Hz, 1H), 4.69 (dt, $J = 15.5, 2.7$ Hz, 1H), 4.38 (dt, $J = 15.5, 2.5$ Hz, 1H), 4.17 – 2.55 (br, 6H), 1.54 (d, $J = 6.7$ Hz, 3H), 1.11 (br, 3H). HRMS: calculated for $[\text{C}_{27}\text{H}_{24}\text{Cl}_2\text{F}_2\text{N}_2\text{O}_3\text{S} + \text{H}]^+ = 565.0926$, found: 565.0923.

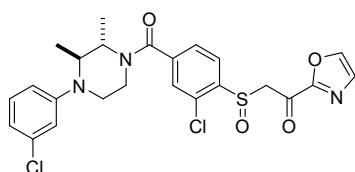
(\pm) **2-((2-Chloro-4-(4-(3-chlorophenyl)-trans-2,3-dimethylpiperazine-1-carbonyl)phenyl)sulfinyl)-1-(6-(trifluoromethyl)pyridin-3-yl)ethan-1-one (15)**



The title compound was synthesized using (\pm) (3-chloro-4-(methylsulfinyl)phenyl)(trans-4-(3-chlorophenyl)-2,3-dimethylpiperazin-1-yl)methanone (**30**) (50 mg, 0.12 mmol, 1 eq.) and ethyl 6-(trifluoromethyl)nicotinate (258 mg, 1.18 mmol, 10 eq.) according to general procedure I. This yielded the product (4.7 mg, 120

0.0078 mmol, 7%). ^1H NMR (600 MHz, CDCl_3) δ 9.20 (s, 1H), 8.45 (d, $J = 8.1$ Hz, 1H), 7.86 (t, $J = 8.3$ Hz, 2H), 7.53 (d, $J = 7.6$ Hz, 2H), 7.20 (t, $J = 8.3$ Hz, 1H), 6.85 (s, 2H), 6.77 (d, $J = 8.2$ Hz, 1H), 4.74 (dd, $J = 13.7, 4.0$ Hz, 1H), 4.36 (dd, $J = 13.7, 4.6$ Hz, 1H), 3.83 – 3.16 (br, 6H), 1.52 (d, $J = 6.7$ Hz, 3H), 1.09 (br, 3H). HRMS: calculated for $[\text{C}_{27}\text{H}_{24}\text{Cl}_2\text{F}_3\text{N}_3\text{O}_3\text{S} + \text{H}]^+ = 598.0940$, found: 598.0942.

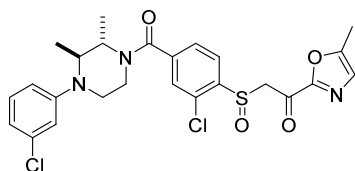
(\pm) **2-((2-Chloro-4-(4-(3-chlorophenyl)-trans-2,3-dimethylpiperazine-1-carbonyl)phenyl)sulfinyl)-1-(oxazol-2-yl)ethan-1-one (16)**



The title compound was synthesized using (\pm) (3-chloro-4-(methylsulfinyl)phenyl)(trans-4-(3-chlorophenyl)-2,3-dimethylpiperazin-1-yl)methanone (**30**) (65 mg, 0.15 mmol,

1 eq.) and ethyl oxazole-2-carboxylate (216 mg, 1.53 mmol, 10 eq.) according to procedure I. This yielded the product (3.2 mg, 0.15 mmol, 3%). ^{13}C NMR (126 MHz, CDCl_3) δ 178.05, 168.68, 168.22, 151.35, 142.95, 142.25, 140.76, 135.28, 131.01, 130.37, 129.97, 128.58, 126.92, 126.05, 119.49, 116.25, 114.25, 61.04, 60.50, 49.66, 42.35, 36.53, 14.29, 12.58. HRMS: Calculated for $[\text{C}_{24}\text{H}_{23}\text{Cl}_2\text{N}_3\text{O}_4\text{S} + \text{H}]^+ = 520.0859$, found = 520.0857.

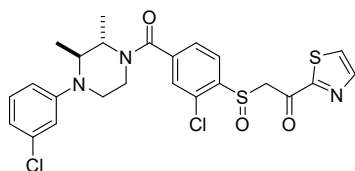
(\pm) **2-((2-Chloro-4-(4-(3-chlorophenyl)-trans-2,3-dimethylpiperazine-1-carbonyl)phenyl)sulfinyl)-1-(5-methyloxazol-2-yl)ethan-1-one (17)**



The title compound was synthesized using (\pm) (3-chloro-4-(methylsulfinyl)phenyl)(trans-4-(3-chlorophenyl)-2,3-dimethylpiperazin-1-yl)methanone (**30**) (60 mg, 0.14 mmol,

1 eq.) and ethyl 5-methyloxazole-2-carboxylate (44 mg, 0.28 mmol, 2.00 eq.) according to general procedure I. This yielded the product (15 mg, 0.03 mmol, 20%). ^1H NMR (400 MHz, CDCl_3) δ 7.98 (d, $J = 8.0$ Hz, 1H), 7.54 – 7.44 (m, 2H), 7.18 (t, $J = 7.7$ Hz, 1H), 7.01 – 6.98 (m, 1H), 6.84 – 6.80 (m, 2H), 6.72 (d, $J = 8.4$ Hz, 1H), 4.87 – 3.05 (m, 8H), 2.44 (s, 3H), 1.53 – 1.46 (m, 3H), 1.08 (dd, $J = 44.8, 6.6$ Hz, 3H). HRMS: calculated for $[\text{C}_{25}\text{H}_{25}\text{Cl}_2\text{N}_3\text{O}_4\text{S} + \text{H}]^+ = 534.1016$, found: 534.1017.

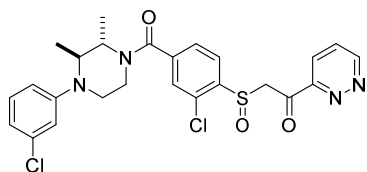
(\pm) **2-((2-Chloro-4-(4-(3-chlorophenyl)-trans-2,3-dimethylpiperazine-1-carbonyl)phenyl)sulfinyl)-1-(thiazol-2-yl)ethan-1-one (18)**



The title compound was synthesized using (\pm) (3-chloro-4-(methylsulfinyl)phenyl)(trans-4-(3-chlorophenyl)-2,3-dimethylpiperazin-1-yl)methanone (**30**) (40 mg, 0.09 mmol,

1 eq.) and ethyl thiazole-2-carboxylate (148 mg, 0.94 mmol, 10 eq.) according to procedure I. This yielded the product (32 mg, 0.06 mmol, 63%). ^1H NMR (600 MHz, CDCl_3) δ 8.02 – 7.95 (m, 2H), 7.76 (dd, $J = 3.0, 1.4$ Hz, 1H), 7.53 – 7.44 (m, 2H), 7.18 (t, $J = 8.1$ Hz, 1H), 6.84 – 6.79 (m, 2H), 6.73 (d, 1H), 4.83 – 4.68 (m, 2H), 3.95 – 3.11 (m, 6H), 1.50 (d, $J = 6.8$ Hz, 3H), 1.16 – 0.97 (m, 3H). ^{13}C NMR (151 MHz, CDCl_3) δ 184.64, 166.56, 152.19, 146.31, 143.48, 141.28, 136.27, 132.04, 132.00, 131.32, 128.93, 127.99, 127.03, 125.25, 120.60, 117.30, 115.26, 61.84, 61.79, 57.22, 56.24, 30.72, 13.80, 1.02. HRMS: Calculated for $[\text{C}_{24}\text{H}_{23}\text{Cl}_2\text{N}_3\text{O}_3\text{S}_2 + \text{H}]^+ = 538.0600$, found = 538.0600.

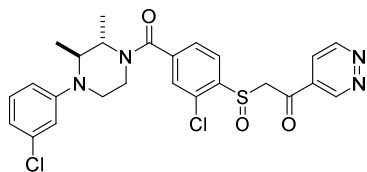
(\pm) **2-((2-Chloro-4-(4-(3-chlorophenyl)-trans-2,3-dimethylpiperazine-1-carbonyl)phenyl)sulfinyl)-1-(pyridazin-3-yl)ethan-1-one (19)**



The title compound was synthesized using (\pm) (3-chloro-4-(methylsulfinyl)phenyl)(trans-4-(3-chlorophenyl)-2,3-dimethylpiperazin-1-yl)methanone (**30**) (50 mg, 0.12

mmol, 1 eq.) and ethyl pyridazine-3-carboxylate (179 mg, 1.18 mmol, 10 eq.) according to general procedure I. This yielded the product (13 mg, 0.024 mmol, 20%). ^1H NMR (400 MHz, CDCl_3) δ 9.37 (d, $J = 4.9$ Hz, 1H), 8.21 (d, $J = 8.5$ Hz, 1H), 7.97 (d, $J = 8.0$ Hz, 1H), 7.75 (dd, $J = 8.5, 5.0$ Hz, 1H), 7.50 (d, $J = 7.9$ Hz, 1H), 7.46 (s, 1H), 7.21 (d, $J = 8.3$ Hz, 1H), 6.86 (d, $J = 6.2$ Hz, 2H), 6.77 (d, $J = 6.3$ Hz, 1H), 5.07 – 4.96 (m, 2H), 3.83 – 3.15 (br, 6H), 1.52 (d, $J = 6.8$ Hz, 3H), 1.09 (d, $J = 6.2$ Hz, 3H). HRMS: calculated for $[\text{C}_{25}\text{H}_{24}\text{Cl}_2\text{N}_4\text{O}_3\text{S} + \text{H}]^+ = 531.1019$, found: 531.1020.

(\pm) **2-((2-Chloro-4-(4-(3-chlorophenyl)-trans-2,3-dimethylpiperazine-1-carbonyl)phenyl)sulfinyl)-1-(pyridazin-4-yl)ethan-1-one (20)**

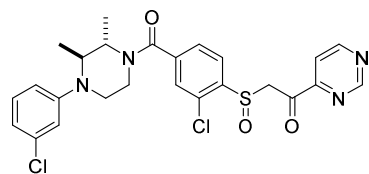


The title compound was synthesized using (\pm) (3-chloro-4-(methylsulfinyl)phenyl)(trans-4-(3-chlorophenyl)-2,3-dimethylpiperazin-1-yl)methanone (**30**) (50 mg, 0.12

mmol, 1 eq.) and methyl pyridazine-4-carboxylate (162 mg, 1.175 mmol, 10 eq.)

according to general procedure I. This yielded the product (42 mg, 0.079 mmol, 67%). ^1H NMR (400 MHz, CDCl_3) δ 9.53 (d, $J = 4.2$ Hz, 2H), 7.97 (dt, $J = 5.2, 2.3$ Hz, 1H), 7.78 (d, $J = 7.9$ Hz, 1H), 7.54 – 7.47 (m, 2H), 7.19 (t, $J = 8.3$ Hz, 1H), 6.84 (d, $J = 7.4$ Hz, 2H), 6.75 (d, $J = 9.2$ Hz, 1H), 4.74 (dd, $J = 13.5, 2.3$ Hz, 1H), 4.42 (dd, $J = 13.5, 3.4$ Hz, 1H), 3.97 – 3.00 (br, 6H), 1.51 (d, $J = 6.7$ Hz, 3H), 1.08 (br, 3H). HRMS: calculated for $[\text{C}_{25}\text{H}_{24}\text{Cl}_2\text{N}_4\text{O}_3\text{S} + \text{H}]^+ = 531.1019$, found: 531.1019.

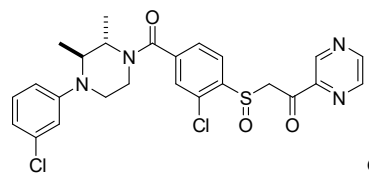
(\pm) **2-((2-Chloro-4-(4-(3-chlorophenyl)-trans-2,3-dimethylpiperazine-1-carbonyl)phenyl)sulfinyl)-1-(pyrimidin-4-yl)ethan-1-one (21)**



The title compound was synthesized using (\pm) (3-chloro-4-(methylsulfinyl)phenyl)(trans-4-(3-chlorophenyl)-2,3-dimethylpiperazin-1-yl)methanone (**30**) (50 mg, 0.12

mmol, 1 eq.) and ethyl pyrimidine-4-carboxylate (179 mg, 1.175 mmol, 10 eq.) according to general procedure I. This yielded the product (3 mg, 0.0056 mmol, 5%). ^1H NMR (500 MHz, CDCl_3) δ 9.36 (s, 1H), 9.04 (d, $J = 6.8$ Hz, 1H), 7.99 – 7.93 (m, 2H), 7.54 – 7.48 (m, 2H), 7.22 (t, $J = 8.4$ Hz, 1H), 6.88 (d, $J = 7.0$ Hz, 2H), 6.80 (d, $J = 7.9$ Hz, 1H), 4.91 (dd, $J = 13.8, 3.5$ Hz, 1H), 4.77 (d, $J = 13.8$ Hz, 1H), 3.85 – 3.15 (br, 6H), 1.53 (dd, $J = 6.8, 3.3$ Hz, 3H), 1.10 (br, 3H). HRMS: calculated for $[\text{C}_{25}\text{H}_{24}\text{Cl}_2\text{N}_4\text{O}_3\text{S} + \text{H}]^+ = 531.1019$, found: 531.1018.

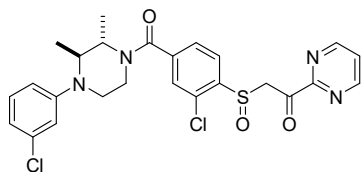
(\pm) **2-((2-Chloro-4-(4-(3-chlorophenyl)-trans-2,3-dimethylpiperazine-1-carbonyl)phenyl)sulfinyl)-1-(pyrazin-2-yl)ethan-1-one (22)**



The title compound was synthesized using (\pm) (3-chloro-4-(methylsulfinyl)phenyl)(trans-4-(3-chlorophenyl)-2,3-dimethylpiperazin-1-yl)methanone (**30**) (50 mg, 0.12

mmol, 1 eq.) and ethyl pyrazine-2-carboxylate (179 mg, 1.18 mmol, 10.0 eq.) according to general procedure I. This yielded the product (27 mg, 0.051 mmol, 43%). ^1H NMR (500 MHz, CDCl_3) δ 9.25 (s, 1H), 8.81 (s, 1H), 8.66 (s, 1H), 7.96 (d, $J = 7.5$ Hz, 1H), 7.50 (d, $J = 9.7$ Hz, 2H), 7.19 (t, $J = 8.1$ Hz, 1H), 6.87 – 6.81 (m, 2H), 6.74 (d, $J = 8.2$ Hz, 1H), 4.92 (d, $J = 14.0$ Hz, 1H), 4.77 (d, $J = 14.0$ Hz, 1H), 3.94 – 3.05 (br, 6H), 1.52 (d, $J = 6.7$ Hz, 3H), 1.08 (br, 3H). HRMS: calculated for $[\text{C}_{25}\text{H}_{24}\text{Cl}_2\text{N}_4\text{O}_3\text{S} + \text{H}]^+ = 531.1019$, found: 531.1019.

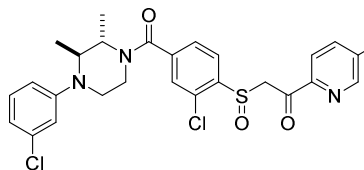
(±) **2-((2-Chloro-4-(4-(3-chlorophenyl)-trans-2,3-dimethylpiperazine-1-carbonyl)phenyl)sulfinyl)-1-(pyrimidin-2-yl)ethan-1-one (23)**



The title compound was synthesized using (±) (3-chloro-4-(methylsulfinyl)phenyl)(trans-4-(3-chlorophenyl)-2,3-dimethylpiperazin-1-yl)methanone (**30**) (50 mg, 0.12

mmol, 1 eq.) and ethyl pyrimidine-2-carboxylate (179 mg, 1.18 mmol, 10 eq.) according to general procedure I. This yielded the product (30 mg, 0.056 mmol, 47 %). ¹H NMR (500 MHz, CDCl₃) δ 8.97 (d, J = 4.9 Hz, 2H), 7.96 (d, J = 7.9 Hz, 1H), 7.55 (t, J = 4.9 Hz, 1H), 7.52 – 7.45 (t, 2H), 7.18 (t, J = 8.1 Hz, 1H), 6.83 (d, J = 12.3 Hz, 2H), 6.73 (d, J = 10.1 Hz, 1H), 5.01 (d, J = 13.9 Hz, 1H), 4.79 (d, J = 13.9 Hz, 1H), 4.03 – 3.07 (br, 6H), 1.51 (d, J = 6.6 Hz, 3H), 1.06 (br, 3H). HRMS: calculated for [C₂₅H₂₄Cl₂N₄O₃S+ H]⁺ = 531.1019, found: 531.1017.

(±) **6-(2-((2-Chloro-4-(4-(3-chlorophenyl)-trans-2,3-dimethylpiperazine-1-carbonyl)phenyl)sulfinyl)acetyl)nicotinonitrile (24)**



The title compound was synthesized using (±) (3-chloro-4-(methylsulfinyl)phenyl)(trans-4-(3-chlorophenyl)-2,3-dimethylpiperazin-1-yl)methanone

(**30**) (50 mg, 0.12 mmol, 1 eq.) and methyl 5-cyanopicolinate (191 mg, 1.18 mmol, 10 eq.) according to general procedure I. This yielded the product (31 mg, 0.057 mmol, 48%). ¹H NMR (600 MHz, CDCl₃) δ 8.91 (s, 1H), 8.17 (s, 2H), 7.96 (d, J = 8.0 Hz, 1H), 7.51 (d, J = 7.2 Hz, 1H), 7.46 (d, J = 21.8 Hz, 1H), 7.18 (t, J = 8.0 Hz, 1H), 6.82 (d, J = 8.2 Hz, 2H), 6.72 (s, 1H), 4.93 (s, 1H), 4.73 (s, 1H), 3.92 – 3.08 (br, 6H), 1.50 (d, J = 11.6 Hz, 3H), 1.08 (br, 3H). HRMS: calculated for [C₂₇H₂₄Cl₂N₄O₃S+ H]⁺ = 555.1019, found: 555.1022.

References

1. Nomura, D. K.; Lombardi, D. P.; Chang, J. W.; Niessen, S.; Ward, A. M.; Long, J. Z.; Hoover, H. H.; Cravatt, B. F. Monoacylglycerol lipase exerts dual control over endocannabinoid and fatty acid pathways to support prostate cancer. *Chemistry & biology* **2011**, *18*, 846-56.
2. Nomura, D. K.; Long, J. Z.; Niessen, S.; Hoover, H. S.; Ng, S. W.; Cravatt, B. F. Monoacylglycerol lipase regulates a fatty acid network that promotes cancer pathogenesis. *Cell* **2010**, *140*, 49-61.
3. Aghazadeh Tabrizi, M.; Baraldi, P. G.; Baraldi, S.; Ruggiero, E.; De Stefano, L.; Rizzolio, F.; Di Cesare Mannelli, L.; Ghelardini, C.; Chicca, A.; Lapillo, M.; Gertsch, J.; Manera, C.; Macchia, M.; Martinelli, A.; Granchi, C.; Minutolo, F.; Tuccinardi, T. Discovery of 1,5-Diphenylpyrazole-3-Carboxamide Derivatives as Potent, Reversible, and Selective Monoacylglycerol Lipase (MAGL) Inhibitors. *J Med Chem* **2018**, *61*, 1340-1354.
4. Aida, J.; Fushimi, M.; Kusumoto, T.; Sugiyama, H.; Arimura, N.; Ikeda, S.; Sasaki, M.; Sogabe, S.; Aoyama, K.; Koike, T. Design, Synthesis, and Evaluation of Piperazinyl Pyrrolidin-2-ones as a Novel Series of Reversible Monoacylglycerol Lipase Inhibitors. *J Med Chem* **2018**, *61*, 9205-9217.
5. Cisar, J. S.; Weber, O. D.; Clapper, J. R.; Blankman, J. L.; Henry, C. L.; Simon, G. M.; Alexander, J. P.; Jones, T. K.; Ezekowitz, R. A. B.; O'Neill, G. P.; Grice, C. A. Identification of ABX-1431, a Selective Inhibitor of Monoacylglycerol Lipase and Clinical Candidate for Treatment of Neurological Disorders. *J Med Chem* **2018**, *61*, 9062-9084.
6. Cisneros, J. A.; Bjorklund, E.; Gonzalez-Gil, I.; Hu, Y.; Canales, A.; Medrano, F. J.; Romero, A.; Ortega-Gutierrez, S.; Fowler, C. J.; Lopez-Rodriguez, M. L. Structure-activity relationship of a new series of reversible dual monoacylglycerol lipase/fatty acid amide hydrolase inhibitors. *J Med Chem* **2012**, *55*, 824-36.
7. Granchi, C.; Rizzolio, F.; Palazzolo, S.; Carmignani, S.; Macchia, M.; Saccomanni, G.; Manera, C.; Martinelli, A.; Minutolo, F.; Tuccinardi, T. Structural Optimization of 4-Chlorobenzoylpiperidine Derivatives for the Development of Potent, Reversible, and Selective Monoacylglycerol Lipase (MAGL) Inhibitors. *Journal of medicinal chemistry* **2016**, *59*, 10299-10314.
8. Kapanda, C. N.; Masquelier, J.; Labar, G.; Muccioli, G. G.; Poupaert, J. H.; Lambert, D. M. Synthesis and pharmacological evaluation of 2,4-dinitroaryldithiocarbamate derivatives as novel monoacylglycerol lipase inhibitors. *Journal of medicinal chemistry* **2012**, *55*, 5774-83.
9. Long, J. Z.; Li, W.; Booker, L.; Burston, J. J.; Kinsey, S. G.; Schlosburg, J. E.; Pavon, F. J.; Serrano, A. M.; Selley, D. E.; Parsons, L. H.; Lichtman, A. H.; Cravatt, B. F. Selective blockade of 2-arachidonoylglycerol hydrolysis produces cannabinoid behavioral effects. *Nature chemical biology* **2009**, *5*, 37-44.
10. Matuszak, N.; Muccioli, G. G.; Labar, G.; Lambert, D. M. Synthesis and in vitro evaluation of N-substituted maleimide derivatives as selective monoglyceride lipase inhibitors. *Journal of medicinal chemistry* **2009**, *52*, 7410-20.
11. McAllister, L. A.; Butler, C. R.; Mente, S.; O'Neil, S. V.; Fonseca, K. R.; Piro, J. R.; Cianfrogna, J. A.; Foley, T. L.; Gilbert, A. M.; Harris, A. R.; Helal, C. J.; Johnson, D. S.; Montgomery, J. I.; Nason, D. M.; Noell, S.; Pandit, J.; Rogers, B. N.; Samad, T. A.; Shaffer, C. L.; da Silva, R. G.; Uccello, D. P.; Webb, D.; Brodney, M. A. Discovery of Trifluoromethyl

Glycol Carbamates as Potent and Selective Covalent Monoacylglycerol Lipase (MAGL) Inhibitors for Treatment of Neuroinflammation. *J Med Chem* **2018**, 61, 3008-3026.

12. Muccioli, G. G.; Labar, G.; Lambert, D. M. CAY10499, a novel monoglyceride lipase inhibitor evidenced by an expeditious MGL assay. *ChemBioChem* **2008**, 9, 2704-2710.

13. Zvonok, N.; Pandarinathan, L.; Williams, J.; Johnston, M.; Karageorgos, I.; Janero, D. R.; Krishnan, S. C.; Makriyannis, A. Covalent inhibitors of human monoacylglycerol lipase: ligand-assisted characterization of the catalytic site by mass spectrometry and mutational analysis. *Chemistry & biology* **2008**, 15, 854-62.

14. Aaltonen, N.; Savinainen, J. R.; Ribas, C. R.; Rönkkö, J.; Kuusisto, A.; Korhonen, J.; Navia-Paldanius, D.; Häyrynen, J.; Takabe, P.; Käsnänen, H. Piperazine and piperidine triazole ureas as ultrapotent and highly selective inhibitors of monoacylglycerol lipase. *Chemistry & biology* **2013**, 20, 379-390.

15. Hernandez-Torres, G.; Cipriano, M.; Heden, E.; Bjorklund, E.; Canales, A.; Zian, D.; Feliu, A.; Mecha, M.; Guaza, C.; Fowler, C. J.; Ortega-Gutierrez, S.; Lopez-Rodriguez, M. L. A reversible and selective inhibitor of monoacylglycerol lipase ameliorates multiple sclerosis. *Angew Chem Int Ed Engl* **2014**, 53, 13765-70.

16. Ezzili, C.; Mileni, M.; McGlinchey, N.; Long, J. Z.; Kinsey, S. G.; Hochstatter, D. G.; Stevens, R. C.; Lichtman, A. H.; Cravatt, B. F.; Bilsky, E. J.; Boger, D. L. Reversible competitive α -ketoheterocycle inhibitors of fatty acid amide hydrolase containing additional conformational constraints in the acyl side chain: orally active, long-acting analgesics. *J Med Chem* **2011**, 54, 2805-22.

17. Mileni, M.; Garfinkle, J.; Ezzili, C.; Cravatt, B. F.; Stevens, R. C.; Boger, D. L. Fluoride-mediated capture of a noncovalent bound state of a reversible covalent enzyme inhibitor: X-ray crystallographic analysis of an exceptionally potent α -ketoheterocycle inhibitor of fatty acid amide hydrolase. *J Am Chem Soc* **2011**, 133, 4092-100.

18. Janssen, F. J.; Baggelaar, M. P.; Hummel, J. J.; Overkleeft, H. S.; Cravatt, B. F.; Boger, D. L.; van der Stelt, M. Comprehensive Analysis of Structure-Activity Relationships of α -Ketoheterocycles as sn-1-Diacylglycerol Lipase α Inhibitors. *J Med Chem* **2015**, 58, 9742-53.

19. Baggelaar, M. P.; Chameau, P. J.; Kantae, V.; Hummel, J.; Hsu, K. L.; Janssen, F.; van der Wel, T.; Soethoudt, M.; Deng, H.; den Dulk, H.; Allarà, M.; Florea, B. I.; Di Marzo, V.; Wadman, W. J.; Kruse, C. G.; Overkleeft, H. S.; Hankemeier, T.; Werkman, T. R.; Cravatt, B. F.; van der Stelt, M. Highly Selective, Reversible Inhibitor Identified by Comparative Chemoproteomics Modulates Diacylglycerol Lipase Activity in Neurons. *J Am Chem Soc* **2015**, 137, 8851-7.

20. Baggelaar, M. P.; Janssen, F. J.; van Esbroeck, A. C.; den Dulk, H.; Allarà, M.; Hoogendoorn, S.; McGuire, R.; Florea, B. I.; Meeuwenoord, N.; van den Elst, H.; van der Marel, G. A.; Brouwer, J.; Di Marzo, V.; Overkleeft, H. S.; van der Stelt, M. Development of an activity-based probe and in silico design reveal highly selective inhibitors for diacylglycerol lipase- α in brain. *Angew Chem Int Ed Engl* **2013**, 52, 12081-5.

21. van der Wel, T.; Janssen, F. J.; Baggelaar, M. P.; Deng, H.; den Dulk, H.; Overkleeft, H. S.; van der Stelt, M. A natural substrate-based fluorescence assay for inhibitor screening on diacylglycerol lipase α . *Journal of Lipid Research* **2015**, 56, 927-935.

Supplementary Information

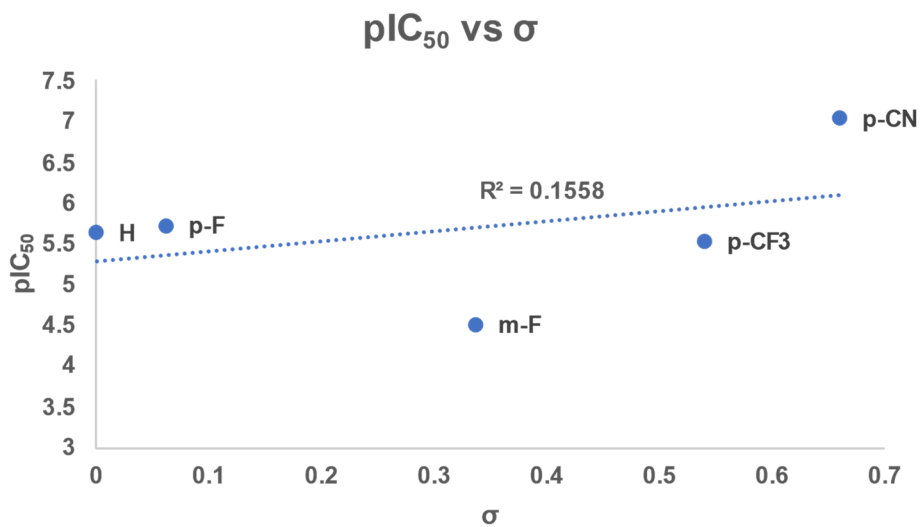


Figure S1. Plot of pIC₅₀-values of the aryl ketone series versus the corresponding substituent σ -values.

Chapter 4

Discovery of LEI-515 as a novel ultrapotent, reversible MAGL inhibitor with improved metabolic stability

M. Jiang, M. C. W. Huizenga, R. Bakker, R. J. B. H. N. van den Berg, C. A. A. van Boeckel, M. van der Stelt*; *manuscript in preparation.*

4.1 Introduction

A primary concern for medicinal chemists is to design molecules that not only show desired activity and selectivity, but also display suitable pharmacokinetic (PK) properties to have an appropriate duration of action. The primary PK properties are Volume of distribution (V_d (L/kg)) and Clearance (Cl (mL/min/kg)), which determine the *in vivo* half-life ($t_{1/2} = 0.7 \times V_d / Cl$ (h)) of a compound.¹ The V_d is not a real volume, but is a theoretical amount of fluid required to dissolve the compound to obtain the measured plasma concentration at the time of administration. It is an assessment of the compound's ability to distribute through the body. The V_d is an intrinsic property of the compound and determined to a large extent by the lipophilicity and acidity of a compound. Basic compounds have a high V_d , whereas acidic compounds have a low

V_d . Increasing the V_d will increase the half life of a compound. Clearance indicates the volume of blood that is cleared from the compound per unit of time. It is a first order process and not dependent on plasma concentration of the compound. It is an intrinsic property of the drug. Clearance is defined as the extraction ratio times the blood flow. Hepatic clearance is performed by metabolic enzymes in the liver and its maximum equals the liver blood flow. Increasing the metabolic stability of a compound reduces the hepatic clearance and increases its half life.

In the early phases of drug discovery, it is impossible for new chemical entities to be administered to humans, therefore, human PK predictions are made from *in vivo* and *in vitro* systems.² Since hepatic clearance is considered a major determinant for overall clearance for many compounds, metabolic stability studies using *in vitro* test systems are employed to assess and optimize the clearance of compounds. Metabolic stability is defined as the percentage of parent compound lost over time in the presence of a metabolically active test system.³ Several types of systems are currently available, including recombinant enzymes, liver microsomes, liver S9 fractions and hepatocytes, to test the metabolic stability. A liver S9 fraction is usually the preferred test system. It consists of the 9000g supernatant of a liver homogenate preparation (Figure 1) and contains both Phase I and Phase II metabolic enzymes^{4,5}. Compared to hepatocytes the S9 fraction does not have an extra layer of complexity (*i.e.*, permeability across the hepatocyte cell membrane to gain access to the metabolizing enzymes). A metabolic stability assay using the S9 fraction provides the same quality of data in a more efficient, high throughput and cost-effective manner compared to intact hepatocytes assays.⁶ The liver S9 system is therefore widely used as a primary *in vitro* screen to guide the optimization of the metabolic stability of compounds.⁷ In Chapter 2, compound **± 1** has been described as highly potent and selective MAGL inhibitor. Here, the metabolic stability of compound **± 1** was evaluated and optimized.

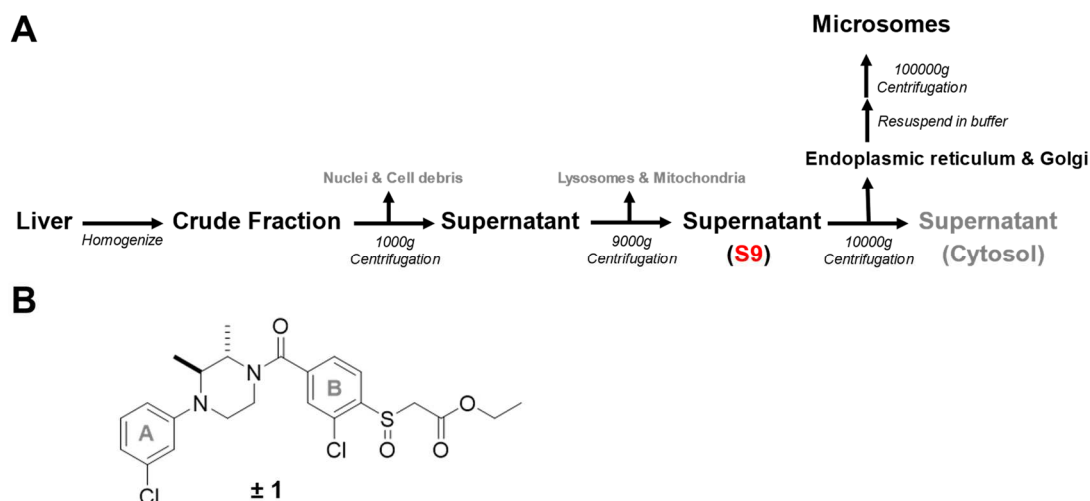


Figure 1. (A) Preparation of liver subcellular fractions. (B) Chemical structure of compound ± 1 .

4.2 Results and Discussion

The metabolic stability of compound ± 1 was evaluated by using a liver S9 stability assay. The compound was incubated with liver S9 fraction and the amount of remaining compound was determined with liquid chromatography–mass spectrometry/mass spectrometry (LC-MS/MS) in time-dependent manner. The results are presented as intrinsic clearance (Cl_{int}), which is calculated as $V \times 0.693 / t_{1/2}$ ($\mu\text{L}/\text{min}/\text{mg}$) in which V is the volume of incubation in μL per mg protein and $t_{1/2}$ is the measured half life in min. Compound ± 1 showed a high Cl_{int} ($> 346 \mu\text{L}/\text{min}/\text{mg}$, Table 1), revealing that compound ± 1 is rapidly metabolized by the enzymes from the liver. This is not surprising, because compound has a high lipophilicity (calculated octanol-water partition coefficient (cLogP) of 4.9) and contains a potential metabolically labile ester functionality. Since it is well known that reducing lipophilicity may increase metabolic stability, several analogues (compound ± 2 - ± 6) were synthesized in which phenyl ring A was replaced with different pyridyls (compound ± 2 - ± 5) or in which the ethyl ester was substituted with a more polar group (compound ± 6) (Synthetic scheme in SI). Of note, compounds (± 2 - ± 6) showed high MAGL inhibitory activities (Table 1), while the cLogP was ten-fold lower compared to compound ± 1 . The metabolic stability of these compounds was, however, not improved (Table 1). This indicated that Cl_{int} of

compound ± 1 cannot be improved by only reducing the lipophilicity and suggested that the ester was the main metabolic hot spot. To test this hypothesis, compound ± 7 was synthesized in which the ester moiety was replaced by a metabolically stable ether. Indeed, the intrinsic clearance dropped significantly from > 346 ($\mu\text{L}/\text{min}/\text{mg}$) to < 4 ($\mu\text{L}/\text{min}/\text{mg}$), indicating that the ester group was the primary site of metabolism. Of note, as expected compound ± 7 displayed no MAGL inhibitory activity anymore.

Table 1. pIC_{50} values, intrinsic clearance rate and physical-chemical parameters of compound ± 1 derivatives.

Entry	X ₁	X ₂	X ₃	X ₄	R ₁	R ₂	$\text{pIC}_{50} \pm \text{SD}$	Cl_{int} ($\mu\text{L}/\text{min}/\text{mg}$)	cLogP	LipE
± 1	CH	CH	CH	CH		Cl	8.50 ± 0.10	> 346	4.93	3.57
± 2	CH	CH	N	CH		Cl	7.68 ± 0.14	-	3.89	3.79
± 3	CH	N	CH	CH		Cl	7.06 ± 0.13	-	3.89	3.17
± 4	N	CH	CH	CH		Cl	8.04 ± 0.11	> 346	3.89	4.15
± 5	CH	CH	CH	N		Cl	8.06 ± 0.12	-	3.89	4.17
± 6	CH	CH	CH	CH		Cl	8.04 ± 0.10	> 346	4.34	3.70
± 7	CH	CH	CH	CH		F	< 5	3.6	4.40	-

Introducing steric hindrance has been previously successfully applied as a strategy to stabilize ester functionalities by preventing the attack of a catalytic serine of carboxylesterases on the carbonyl⁸. Here, this strategy was employed by introducing a methyl group on the alpha-carbon (compounds ± 8 and ± 9) or next to the oxygen (compound ± 10) (Table 2). While compounds (± 8 and ± 10) showed slightly decreased MAGL inhibitory activity, they were still rapidly metabolized with a $\text{Cl}_{\text{int}} > 346$ ($\mu\text{L}/\text{min}/\text{mg}$). Introducing more bulky group, such as 3,4-methylenedioxybenzyl group in compound (± 11), which was previously used in an in vivo active MAGL inhibitor⁹,

Discovery of LEI-515 as a Novel Ultrapotent, Reversible MAGL Inhibitor with Improved Metabolic Stability

also did not improve the metabolic stability (Table 2).

Table 2. pIC₅₀ values, intrinsic clearance rate and physical-chemical parameters of compound ± 1 derivatives.

Entry	R ₁	R ₂	pIC ₅₀ ± SD	Cl _{int} (μL/min/mg)	cLogP	LipE
± 8	CH ₃		7.86 ± 0.12	> 346	5.23	2.63
± 9	CH ₃		8.35 ± 0.08	-	6.07	2.28
± 10	H		7.95 ± 0.13	> 346	4.87	3.08
± 11	H		8.21 ± 0.11	> 346	5.71	2.50

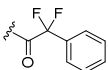
Since introducing steric hinderance did not improve metabolic stability, it was decided to replace the ester group with a bioisostere, such as an amide (± 12), an oxadiazole (± 13) or an alpha-ketoheterocycle (see Chapter 3). See SI for their synthesis. Unfortunately, compounds ± 12 and ± 13 are not MAGL inhibitors and therefore not tested in the metabolic stability assay (Table 3). Previously, compound ± 14 was found to be a potent MAGL inhibitor. Gratifyingly, it showed an improved stability with a Cl_{int} of 169 (μL/min/mg). Thus, compound ± 14 provided the first indication that it was possible to increase the metabolic stability, while maintaining MAGL inhibitory activity at the same time. Encouraged by this result, other activated ketones were explored, such as trifluoromethyl (±15 and ±16), difluoromethyl (± 18) and difluoro alkyl groups (± 19 - ± 21) (See SI for synthesis). Compound ± 16 with a trifluoromethylketone showed high MAGL inhibitory activity (pIC₅₀ = 8.2) (Table 4) and was the most stable compound with a Cl_{int} of 19 μL/min/mg. Of note, if the carbonyl was reduced to the corresponding hydroxyl (± 17), the compound was inactive (pIC₅₀ < 5). This is in line with the hypothesis that the carbonyl acts as an electrophilic warhead for the nucleophilic serine of MAGL. Moreover, the sulfinyl group was not essential for the MAGL inhibitory activity, as compound ± 15 still showed reasonable inhibitory activity

with a $pIC_{50} = 7.8$. Replacing the trifluoromethyl group to difluoromethyl (\pm **18**) increased the MAGL inhibitory activity by 3-fold, but slightly decreased the metabolic stability ($Cl_{int} = 35 \mu\text{L}/\text{min}/\text{mg}$). Substituting a fluorine with a phenyl group resulted in compound \pm **21**, which decreased the potency 50-fold. Changing the trifluoromethyl group to difluoroethyl (\pm **19**) or difluoropropyl (\pm **20**), however, significantly improved the potency. Compound \pm **20 (LEI-515)** is the most potent compound identified in this study with subnanomolar potency ($pIC_{50} = 9.3$). Importantly, both compounds displayed good metabolic stability ($Cl_{int} = 27$ and $30 \mu\text{L}/\text{min}/\text{mg}$, respectively). Finally, compounds \pm **22** to \pm **25**, in which phenyl ring A was replaced with a pyridyl to reduce the lipophilicity, were synthesized. All four compounds showed high MAGL inhibitory activity and enhanced lipophilic efficiency, however, their metabolic stability was significantly decreased. This might be possibly attributed to the potential reactivity of the chloropyridine moieties.^{10, 11}

Table 3. pIC_{50} values, intrinsic clearance rate and physical-chemical parameters of compound \pm **1** derivatives.

Entry	X ₁	X ₂	L	R	$pIC_{50} \pm SD$	Cl_{int} ($\mu\text{L}/\text{min}/\text{mg}$)	cLogP	LipE	tPSA
\pm 12	CH	CH	SO		<5	-	4.07	-	70
\pm 13	CH	CH	SO		<5	-	3.68	-	75
\pm 14	CH	CH	SO		8.00 ± 0.10	169	4.53	3.47	94
\pm 15	CH	CH	S		7.68 ± 0.13	33	5.87	1.81	41
\pm 16	CH	CH	SO		8.13 ± 0.08	19	4.69	3.44	58
\pm 17	CH	CH	SO		<5	-	4.74	-	61
\pm 18	CH	CH	SO		8.63 ± 0.06	35	4.43	4.20	58

Discovery of LEI-515 as a Novel Ultrapotent, Reversible MAGL Inhibitor with Improved Metabolic Stability

± 19	CH	CH	SO		8.83 ± 0.05	27	4.96	3.87	58
± 20 (LEI-515)	CH	CH	SO		9.30 ± 0.04	30	5.49	3.81	58
± 21	CH	CH	SO		7.06 ± 0.21	-	6.44	0.62	58
± 22	CH	N	SO		9.07 ± 0.07	108	3.92	5.63	70
± 23	CH	N	SO		9.19 ± 0.06	126	4.45	4.74	70
± 24	N	CH	SO		8.47 ± 0.10	100	3.92	4.55	70
± 25	N	CH	SO		8.55 ± 0.09	95	4.45	4.10	70

4.3 Conclusion

In this chapter the optimization of the metabolic stability of β -sulfinyl esters as MAGL inhibitors is described. Three different strategies were employed to improve the metabolic stability. 1) reducing the lipophilicity; 2) applying steric hindrance and 3) replacing the ester group with bioisosteres. This led to the discovery of compound ± 20 (named LEI-515), in which the ethyl ester group of compound ± 1 was replaced by a difluoropropyl. LEI-515 is the most active, reversible MAGL inhibitor reported to date, showing subnanomolar potency ($pIC_{50} = 9.3$). Importantly, LEI-515 has improved metabolic stability ($Cl_{int} = 30 \mu\text{L}/\text{min}/\text{mg}$) compared to compound ± 1 ($Cl_{int} > 346 \mu\text{L}/\text{min}/\text{mg}$). Further biological and ADME profiling of LEI-515 will be described in Chapter 5.

4.4 Experimental procedures

MAGL natural substrate assay. The MAGL activity assay is based on the production of glycerol from 2-arachidonoylglycerol (2-AG) hydrolysis by MAGL-overexpressing membrane preparations from transiently transfected HEK293T cells, as previously reported. The produced glycerol is coupled to the oxidation of commercially available Amplifu™Red via a multi-enzyme cascade, resulting in a fluorescent signal from the dye resorufin. Standard assays were performed in HEMNB buffer (50 mM HEPES pH 7.4, 1 mM EDTA, 5 mM MgCl₂, 100 mM NaCl, 0.5% (w/v) BSA) in black, flat bottom 96-wells plates. Final protein concentration of membrane preparations from overexpressing hMAGL HEK293T cells was 1.5 µg/mL (0.3 µg per well). Inhibitors were added from 40x concentrated DMSO stocks. After 20 min. incubation, 100 µL assay mix containing glycerol kinase (GK), glycerol-3-phosphate oxidase (GPO), horse radish peroxidase (HRP), adenosine triphosphate (ATP), Amplifu™Red and 2-arachidonoylglycerol (2-AG) was added and fluorescence was measured in 5 min. intervals for 60 min. on a plate reader. Final assay concentrations: 0.2 U/mL GK, GPO and HRP, 0.125 mM ATP, 10 µM Amplifu™Red, 25 µM 2-AG, 5% DMSO, 0.5% ACN in a total volume of 200 µL. All measurements were performed in N = 2, n = 2 or N = 2, n = 4 for controls, with $Z' \geq 0.6$. For IC₅₀ determination, the MAGL-overexpressing membranes were incubated with different inhibitor concentrations. Slopes of corrected fluorescence in time were determined in the linear interval of t = 10 to t = 35 min and then scaled to the corrected positive control of hMAGL-overexpressing membranes treated with vehicle (DMSO) as a 100% activity reference point. The data was exported to GraphPad Prism 5.0 and analysed in a non-linear dose-response analysis with variable slope.

Liver S9 stability assay. The rate of metabolism was assessed by incubation at 37 °C, pH 7.4 with mouse liver S9 fraction (1 mg protein/ mL) supplemented with 5 mM NADP, 25 mM G6P and 25 U/ml G6PD. The concentration of the initial substrate is 1 µM. Substrate depletion over a time course was measured by LC-MS/MS following protein precipitation. Amitryptilin (2.5 µM in ACN) was used as internal standard. The

ln peak area ratio (compound peak area/internal standard peak area) is plotted against time and the gradient of the line determined.

Elimination rate constant (k) = (- gradient)

Half life ($t_{1/2}$, min) = $0.693 / k$

V ($\mu\text{L} / \text{mg}$) = volume of incubation (μL) / protein in the incubation (mg)

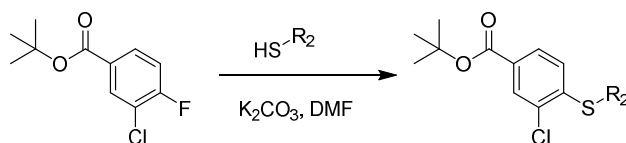
Intrinsic Clearance (CL_{int} , $\mu\text{L}/\text{min}/\text{mg}$) = $V \times 0.693 / t_{1/2}$

Chemistry procedures

General remarks. All reactions were performed using oven or flame-dried glassware and dry solvents. Reagents were purchased from Sigma Aldrich, Acros and Merck and used without further purification unless noted otherwise. All moisture sensitive reactions were performed under an argon or nitrogen atmosphere. Traces of water were removed from starting compounds by co-evaporation with toluene. Reactions were followed by thin layer chromatography and was performed using TLC Silica gel 60 F₂₄₅ on aluminum sheets. Compounds were visualized using a KMnO₄ stain (K₂CO₃ (40 g), KMnO₄ (6 g), H₂O (600 mL) and 10% NaOH (5 mL)). ¹H- and ¹³C-NMR spectra were recorded on a Bruker AV-400, 500, 600 or 850 using CDCl₃ or CD₃OD as solvent, unless stated otherwise. Chemical shift values are reported in ppm with tetramethylsilane or solvent resonance as the internal standard (CDCl₃: δ 7.26 for ¹H, δ 77.16 for ¹³C, CD₃OD: δ 3.31 for ¹H, δ 49.00 for ¹³C). Data are reported as follows: chemical shifts (δ), multiplicity (s = singlet, d = doublet, dd = double doublet, td = triple doublet, t = triplet, q = quartet, quint = quint, br = broad, m = multiplet), coupling constants J (Hz), and integration. LC-MS measurements were performed on a Thermo Finnigan LCQ Advantage Max ion-trap mass spectrometer (ESI⁺) coupled to a Surveyor HPLC system (Thermo Finnigan) equipped with a standard C18 (Gemini, 4.6 mmD \times 50 mmL, 5 μm particle size, Phenomenex) analytical column and buffers A: H₂O, B: ACN, C: 0.1% aq. TFA. Preparative HPLC purification was performed on a Waters Acquity Ultra Performance LC with a C18 column (Gemini, 150 \times 21.2 mm, Phenomenex). Diode detection was done between 210 and 600 nm. Gradient: ACN in (H₂O + 0.2% TFA). High-resolution mass spectra (HRMS) were recorded on a Thermo

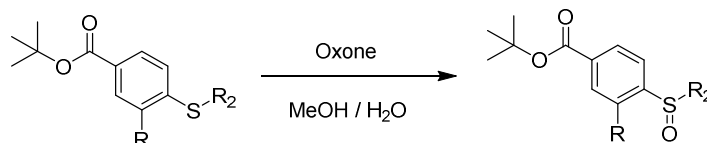
Scientific LTQ Orbitrap XL.

General procedure A



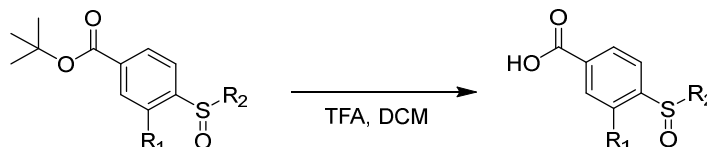
To a solution of appropriate *tert*-butyl 4-fluorobenzoate (1.2 eq.) in ACN were added K₂CO₃ (3 eq.) and appropriate thiol (1eq.). The reaction mixture was stirred at RT overnight. The reaction progress was monitored by TLC analysis. Once completed, the mixture was diluted with Et₂O, washed with water, dried over anhydrous MgSO₄. After filtration, the filtrate was concentrated under reduced pressure. The residue was purified by silica gel column chromatography.

General procedure B



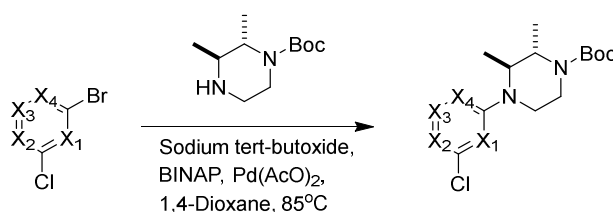
To a solution of appropriate sulfur (1 eq.) in MeOH was added oxone / water solution dropwise at 0 °C and the mixture was stirred at RT for 2h. The reaction progress was monitored by TLC analysis. Once completed, the mixture was diluted with EtOAc and washed with water. The organic layer was dried over anhydrous MgSO₄ and after filtration, the filtrate was concentrated under reduced pressure. The residue was purified by silica column chromatography.

General procedure C



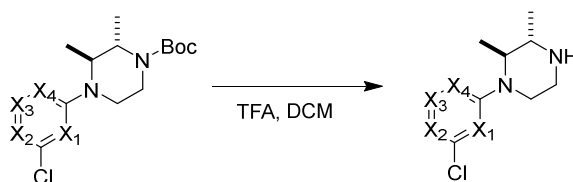
To a solution of appropriate *tert* butyl protected carboxylic acid in DCM was added TFA (20%) and the mixture was stirred at RT for 6 h. The reaction progress was monitored by TLC analysis. Once completed, the solvent was removed under reduced pressure and the residue was purified silica gel column chromatography.

General procedure D



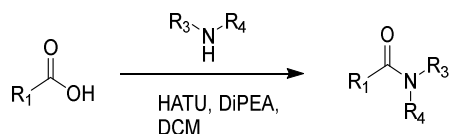
A mixture of appropriate bromobenzene (1eq.) and appropriate mono boc-protected piperazine (1eq.) in the presence of palladium diacetate (0.04eq.), BINAP (0.06eq.) and sodium tert-butoxide (1.5eq.) in degassed 1,4-dioxane was heated to 85 °C under nitrogen atmosphere overnight. The reaction progress was monitored by TLC analysis. Once completed, the reaction mixture was diluted with DCM, washed with water, dried over anhydrous MgSO₄, filtrated and concentrated under reduced pressure. The residue was purified by silica gel column chromatography to give the product.

General procedure E



To a solution of appropriate tert-butyl phenylpiperazine-1-carboxylate in DCM was added TFA (20%, v/v) and the mixture was stirred at RT for 2h. The reaction progress was monitored by TLC. Once completed, then the mixture was diluted with DCM and washed with saturated aqueous NaHCO₃. The organic layers were collected and dried over anhydrous MgSO₄, filtrated and concentrated under reduced pressure. The residue was purified silica gel column chromatography to give the product.

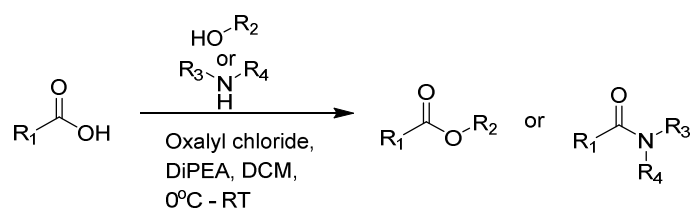
General procedure F



To a suspension or solution of appropriate benzoic acid (1eq.) in DCM was added HATU (1.5eq.) and DiPEA (3eq.) and the mixture was stirred for 1h. The appropriate phenylpiperazine(1eq.) was added and the mixture was stirred overnight. The reaction

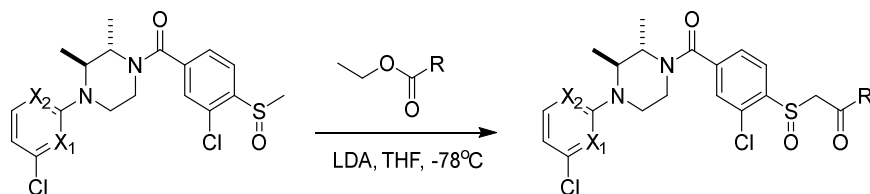
progress was monitored by TLC analysis. Once completed, the mixture was diluted with DCM, washed with water (1x), dried over anhydrous MgSO₄, filtered and concentrated under reduce pressure. The residue was purified by silica gel column chromatography or prep-HPLC to give the product.

General procedure G



To a solution of appropriate carboxylic acid (1eq.) in anhydrous DCM was cooled down to 0 °C with an ice bath. Then, two drops of DMF and oxalyl chloride (1.2 eq.) were added and the mixture was allowed to warm to room temperature and continuously stirred for 2h. The reaction progress was monitored by TLC analysis. Once completed, the mixture was added to a solution of appropriate alcohol or amine (3eq.) and DiPEA (3eq.) in a dropwise manner at 0 °C. Then, the reaction mixture was stirred at room temperature overnight and diluted with DCM, washed with water (1x), dried over anhydrous MgSO₄ and concentrated under reduced pressure. The residue was purified by HPLC-MS to give the product.

General procedure H

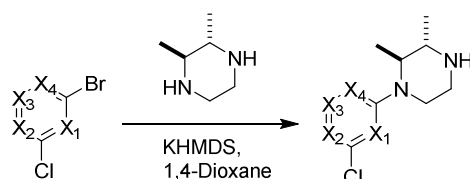


To a solution of appropriate methyl sulfoxide (1 eq.) in anhydrous THF was added LDA (2 eq.) at -78 °C and the reaction mixture was stirred for 30 min before the appropriate ester (10 eq.) was added. The reaction progress was monitored by TLC analysis. Once completed, the mixture was quenched with NH₄Cl solution, extracted with DCM and dried over anhydrous MgSO₄. After filtration, the filtrate was concentrated under

Discovery of LEI-515 as a Novel Ultrapotent, Reversible MAGL Inhibitor with Improved Metabolic Stability

reduced pressure. The residue was purified by silica gel column chromatography or prep-HPLC.

General procedure I



To a solution of appropriate piperazine (1 eq.) and bromochloropyridine (1 eq.) in anhydrous 1,4-dioxane was added KHMDS (1.5 eq.) and the mixture was stirred overnight at 100 °C or RT. The reaction progress was monitored by TLC analysis. Once completed, the reaction mixture was diluted with DCM, washed with water and dried over anhydrous MgSO₄. After filtration, the filtrate was concentrated under reduced pressure. The residue was purified by silica gel column chromatography.

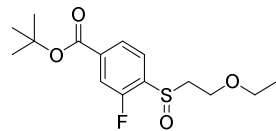
tert-Butyl 4-((2-ethoxyethyl)thio)-3-fluorobenzoate (7a)

The chemical structure of *tert*-butyl 4-((2-ethoxyethyl)thio)-3-fluorobenzoate (7a) is shown. It consists of a benzene ring with a *tert*-butyl ester group at the 1-position, a fluorine atom at the 3-position, and a (2-ethoxyethyl)thio group at the 4-position.

To a solution of *tert*-butyl 3,4-difluorobenzoate (191mg, 0.89mmol, 1eq.) in 5ml DMF was added NaHS (50mg, 0.89mmol, 1eq.), K₂CO₃ (370mg, 0.89mmol, 1eq.) and 1-chloro-2-ethoxyethane(97mg, 0.89mmol, 1eq.) and the mixture was stirred at 65 °C overnight under nitrogen. The reaction progress was monitored with TLC analysis. Once completed, the reaction mixture was diluted with diethyl ether, washed with water and dried over anhydrous MgSO₄. After filtration, the filtrate was concentrated under reduced pressure. The residue was purified by silica gel column chromatography (Diethyl ether/pentane, 5-25%) to give the product (130mg, 0.43mmol, 49%). ¹H NMR (400 MHz, CDCl₃) δ 7.72 (dd, *J* = 8.1, 1.8 Hz, 1H), 7.61 (dd, *J* = 10.5, 1.7 Hz, 1H), 7.39 – 7.34 (m, 1H), 3.65 (t, *J* = 6.7 Hz, 2H), 3.51 (q, *J* = 7.0 Hz, 2H), 3.17 (t, *J* = 6.7 Hz, 2H), 1.59 (s, 9H), 1.19 (t, *J* = 7.0 Hz, 3H). ¹³C NMR (101 MHz, CDCl₃) δ164.33,

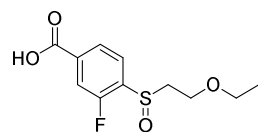
159.91 (d, $J = 245.1$ Hz), 131.22 (d, $J = 7.0$ Hz), 129.76 (d, $J = 17.4$ Hz), 128.75, 125.37 (d, $J = 3.3$ Hz), 116.05 (d, $J = 23.7$ Hz), 81.52, 68.78, 66.55, 31.76, 28.13, 15.12.

***tert*-Butyl 4-((2-ethoxyethyl)sulfinyl)-3-fluorobenzoate (7b)**



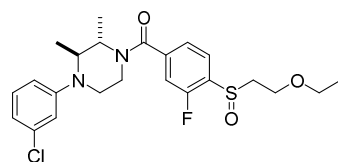
The title compound was synthesized using *tert*-butyl 4-((2-ethoxyethyl)thio)-3-fluorobenzoate (130mg, 0.43mmol, 1eq.) according to procedure B. This yielded the product (7a) (97mg, 0.31mmol, 71%). ^1H NMR (400 MHz, CDCl_3) δ 7.99 (dd, $J = 8.1, 1.5$ Hz, 1H), 7.90 (dd, $J = 8.1, 6.6$ Hz, 1H), 7.71 (dd, $J = 10.1, 1.4$ Hz, 1H), 3.92 (dddd, $J = 10.7, 8.6, 4.2, 0.8$ Hz, 1H), 3.79 (dt, $J = 10.4, 5.0$ Hz, 1H), 3.50 (qq, $J = 9.3, 7.0$ Hz, 2H), 3.35 – 3.23 (m, 1H), 3.03 (dt, $J = 13.5, 4.6$ Hz, 1H), 1.61 (s, 9H), 1.15 (t, $J = 7.0$ Hz, 3H). ^{13}C NMR (101 MHz, CDCl_3) δ 163.61, 158.42, 155.96, 136.55, 135.96, 125.83, 116.57, 82.31, 66.66, 62.18, 55.10, 28.07, 14.93.

4-((2-Ethoxyethyl)sulfinyl)-3-fluorobenzoic acid (7c)



The title compound was synthesized using *tert*-butyl 4-((2-ethoxyethyl)sulfinyl)-3-fluorobenzoate (7b) (97mg, 0.31mmol, 1eq.) according to procedure C. This yielded the product (74mg, 0.28mmol, 93%). ^1H NMR (400 MHz, CDCl_3) δ 10.96 (br, 1H), 8.12 (dd, $J = 8.1, 1.4$ Hz, 1H), 7.99 (dd, $J = 8.1, 6.6$ Hz, 1H), 7.83 (dd, $J = 9.8, 1.5$ Hz, 1H), 4.15 – 3.74 (m, 2H), 3.66 – 3.33 (m, 3H), 3.19 (ddd, $J = 13.5, 4.9, 3.8$ Hz, 1H), 1.13 (t, $J = 7.0$ Hz, 3H). ^{13}C NMR (101 MHz, CDCl_3) δ 168.19, 157.39 (d, $J = 248.4$ Hz), 136.16, 134.75, 126.86 (d, $J = 3.2$ Hz), 126.40 (d, $J = 2.2$ Hz), 117.18 (d, $J = 22.2$ Hz), 66.83, 62.12, 54.80, 14.92.

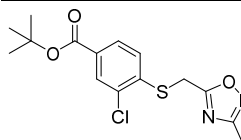
(±) (4-(3-Chlorophenyl)-*trans*-2,3-dimethylpiperazin-1-yl)(4-((2-ethoxyethyl)sulfinyl)-3-fluorophenyl)methanone (7)



The title compound was synthesized using 4-((2-ethoxyethyl)sulfinyl)-3-fluorobenzoic acid (7c) (30mg, 0.115mmol, 1eq.) according to procedure F. This yielded the product (10mg, 0.021mmol, 19%).

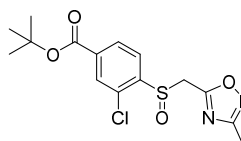
***tert*-Butyl 3-chloro-4-(((3-methyl-1,2,4-oxadiazol-5-yl)methyl)sulfinyl)benzoate (13a)**

Discovery of LEI-515 as a Novel Ultrapotent, Reversible MAGL Inhibitor with Improved Metabolic Stability



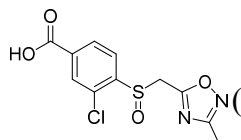
To a solution of *tert*-butyl 3-chloro-4-fluorobenzoate (200 mg, 0.867 mmol, 1eq.), NaHS (97 mg, 1.73 mmol, 2eq.) and 5-(chloromethyl)-3-methyl-1,2,4-oxadiazole (115 mg, 0.867 mmol, 1eq.) were dissolved in DMF (2 ml). The mixture was allowed to stir for 17 h. Then reaction was monitored by TLC analysis. Once complete, the mixture was diluted with DCM and washed with water and brine. The organic layer was dried over MgSO₄, filtered and concentrated. The residue was further purified by column chromatography (0-50% Et₂O in pentane). This yielded the product (65.5 mg, 0.192 mmol, 22%). ¹H NMR (400 MHz, CDCl₃) δ 7.98 (d, *J* = 1.8 Hz, 1H), 7.86 (dd, *J* = 8.3, 1.8 Hz, 1H), 7.45 (d, *J* = 8.3 Hz, 1H), 4.34 (s, 2H), 2.39 (s, 3H), 1.60 (s, 9H). ¹³C NMR (101 MHz, CDCl₃) δ 175.18, 167.59, 164.03, 138.61, 133.12, 131.46, 130.56, 128.27 (d, *J* = 9.3 Hz), 127.88, 81.87, 28.13, 26.82, 11.59.

***tert*-Butyl 3-chloro-4-(((3-methyl-1,2,4-oxadiazol-5-yl)methyl)sulfinyl)benzoate (13b)**



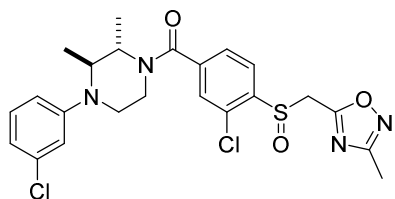
The title compound was synthesized using *tert*-butyl 3-chloro-4-(((3-methyl-1,2,4-oxadiazol-5-yl)methyl)sulfinyl) benzoate (**13a**) (65.0 mg, 0.191 mmol, 1eq.) according to procedure B. This yielded the product (71.1 mg, 0.199 mmol, quantitative). ¹H NMR (400 MHz, CDCl₃) δ 8.04 (dd, *J* = 8.1, 1.5 Hz, 1H), 8.01 (d, *J* = 1.3 Hz, 1H), 7.75 (d, *J* = 8.1 Hz, 1H), 4.47 (dd, *J* = 66.0, 13.8 Hz, 2H), 2.34 (s, 3H), 1.59 (s, 9H). ¹³C NMR (101 MHz, CDCl₃) δ 169.65, 167.81, 163.34, 144.02, 136.82, 130.89, 130.19, 128.82, 126.40, 82.78, 49.80, 28.15, 11.61.

3-Chloro-4-(((3-methyl-1,2,4-oxadiazol-5-yl)methyl)sulfinyl)benzoic acid (13c)



The title compound was synthesized using *tert*-butyl 3-chloro-4-(((3-methyl-1,2,4-oxadiazol-5-yl)methyl)sulfinyl) benzoate (**13b**) (68 mg, 0.191 mmol, 1eq.) according to procedure C. This yielded the product (47 mg, 0.156 mmol, 82%). ¹H NMR (400 MHz, Methanol-*d*₄) δ 8.16 – 8.04 (dd, *J* = 10.2, 2.1 Hz, 2H), 7.69 (d, *J* = 8.1 Hz, 1H), 4.73 (dd, *J* = 69.2, 14.2 Hz, 2H), 2.28 (s, 3H). ¹³C NMR (101 MHz, Methanol-*d*₄) δ 171.62, 168.89, 167.08, 145.37, 137.13, 132.00, 131.67, 130.03, 127.52, 50.26, 11.19.

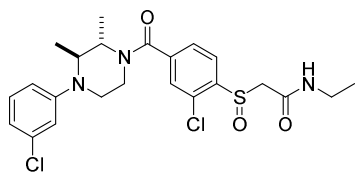
(±)- **(3-Chloro-4-(((3-methyl-1,2,4-oxadiazol-5-yl)methyl)sulfinyl)phenyl)-(4-(3-chlorophenyl)-trans-2,3-dimethylpiperazin-1-yl)methanone (13)**



The title compound was synthesized using 3-chloro-4-(((3-methyl-1,2,4-oxadiazol-5-yl)methyl)sulfinyl)benzoic acid (**13c**) (45.0 mg, 0.150 mmol, 1 eq.) according to procedure F. This yielded the

product (61.8 mg, 0.122 mmol, 81%). ¹H NMR (400 MHz, CDCl₃) δ 7.78 (d, *J* = 6.8 Hz, 1H), 7.48 (d, *J* = 12.7 Hz, 2H), 7.17 (t, *J* = 8.1 Hz, 1H), 6.81 (d, *J* = 7.0 Hz, 2H), 6.71 (d, *J* = 9.2 Hz, 1H), 4.85 – 4.38 (m, 3H), 3.92 – 3.02 (m, 5H), 2.37 (d, *J* = 3.4 Hz, 3H), 1.48 (d, *J* = 4.7 Hz, 3H), 1.06 (d, *J* = 43.9 Hz, 3H). ¹³C NMR (101 MHz, CDCl₃) δ 169.68, 168.76, 167.82, 151.28, 141.28, 140.85, 135.29, 131.02, 130.38, 128.31, 126.81, 125.87, 119.60, 116.31, 114.28, 56.19, 55.67, 49.72, 40.48, 36.66, 17.80, 12.47, 11.55. LC-MS, *m/z*: calculated for C₂₃H₂₄Cl₂N₄O₃S, 506.09; found 507.29 ([*M* + H⁺])

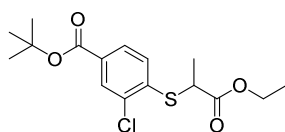
(±) **2-((2-Chloro-4-(trans-4-(3-chlorophenyl)-2,3-dimethylpiperazine-1-carbonyl)phenyl)sulfinyl)-N-ethylacetamide (12)**



The title compound was synthesized using (±) 2-((2-chloro-4-(trans-4-(3-chlorophenyl)-2,3-dimethylpiperazine-1-carbonyl)phenyl)sulfinyl)propanoic acid (0.16 g, 0.34

mmol, 1 eq.) according to procedure G. This yielded the product (1.5 mg, 3.0 μmol, 2%). HRMS: Calculated for [C₂₃H₂₇Cl₂N₃O₃S + H]⁺ = 496.1223, found = 496.1220.

***tert*-Butyl 3-chloro-4-((1-ethoxy-1-oxopropan-2-yl)thio)benzoate (8a)**

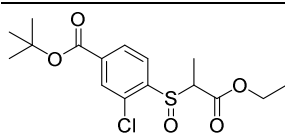


The title compound was synthesized using *tert*-butyl 3-chloro-4-fluorobenzoate (0.270 g, 1.18 mmol, 1.2 eq.) and ethyl 2-mercaptopropanoate (0.13 ml, 0.98 mmol, 1 eq.) according to

procedure A. This yielded the product (0.27 g, 0.78 mmol, 79 %). ¹H NMR (400 MHz, CDCl₃) δ 7.96 (s, 1H), 7.82 (d, *J* = 8.5 Hz, 1H), 7.47 (d, *J* = 8.3 Hz, 1H), 4.22 – 4.10 (m, 2H), 4.07 – 3.97 (m, 1H), 1.59 (m, 12H), 1.21 (t, *J* = 7.1 Hz, 3H). ¹³C NMR (101 MHz, CDCl₃) δ 171.99, 164.21, 139.65, 133.70, 131.23, 130.49, 129.45, 127.94, 81.76, 61.69, 43.25, 28.17, 17.18, 14.11.

***tert*-Butyl 3-chloro-4-((1-ethoxy-1-oxopropan-2-yl)sulfinyl)benzoate (8b)**

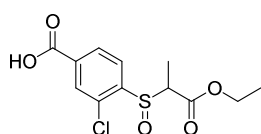
Discovery of LEI-515 as a Novel Ultrapotent, Reversible MAGL Inhibitor with Improved Metabolic Stability



The title compound was synthesized using *tert*-butyl 3-chloro-4-((1-ethoxy-1-oxopropan-2-yl)thio)benzoate (**8a**) (0.13 g, 0.38 mmol, 1 eq.) according to procedure B. This yielded the product

(0.13 g, 0.35 mmol, 92%). ¹H NMR (400 MHz, CDCl₃) δ 8.11 (dd, *J* = 8.2, 1.5 Hz, 1H), 8.00 (d, *J* = 1.6 Hz, 1H), 7.90 (d, *J* = 8.1 Hz, 1H), 4.31 (q, *J* = 8 Hz, 2H), 3.91 (q, *J* = 8 Hz, 1H), 1.61 (s, 9H), 1.35 (t, *J* = 7.1 Hz, 3H), 1.25 (d, *J* = 7.2 Hz, 3H). ¹³C NMR (101 MHz, CDCl₃) δ 168.58, 163.61, 144.19, 136.33, 130.88, 130.32, 128.49, 127.58, 82.73, 77.48, 77.16, 76.85, 62.57, 60.49, 28.21, 14.26, 6.62.

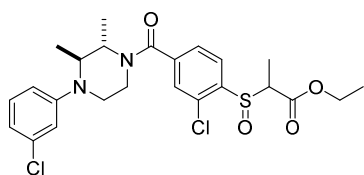
3-Chloro-4-((1-ethoxy-1-oxopropan-2-yl)sulfinyl)benzoic acid (8c)



The title compound was synthesized using *tert*-butyl 3-chloro-4-((2-ethoxy-2-oxoethyl)sulfinyl)benzoate (**8b**) (0.14 g, 0.40 mmol, 1 eq.) according to procedure C. This yielded the product (0.12 g,

0.40 mmol, 100%). ¹H NMR (400 MHz, Methanol-*d*₄): δ 8.22 (dd, *J* = 8.1, 1.5 Hz, 1H), 8.11 (d, *J* = 1.5 Hz, 1H), 7.89 (d, *J* = 8.1 Hz, 1H), 4.30 (qd, *J* = 7.1, 2.3 Hz, 2H), 4.13 (q, *J* = 7.1 Hz, 1H), 1.32 (t, *J* = 7.1 Hz, 3H), 1.21 (d, *J* = 7.1 Hz, 3H). ¹³C NMR (101 MHz, Methanol-*d*₄): δ 169.70, 144.80, 136.92, 132.16, 131.70, 129.93, 128.61, 63.50, 61.67, 48.58, 14.42, 6.78.

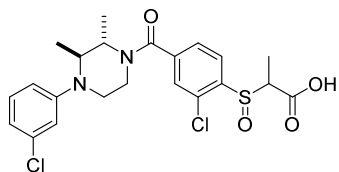
(±) Ethyl 2-((2-chloro-4-(4-(3-chlorophenyl)-*trans*-2,3-dimethylpiperazine-1-carbonyl)phenyl)sulfinyl)propanoate (8)



The title compound was synthesized using 3-chloro-4-((1-ethoxy-1-oxopropan-2-yl)sulfinyl)benzoic acid (0.10 g, 0.34 mmol, 1 eq.) according to procedure F. This yield the

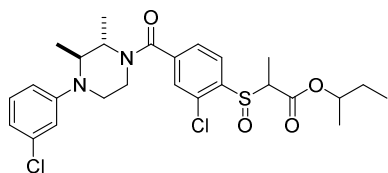
product (0.15 g, 0.29 mmol, 85%). ¹H NMR (400 MHz, CDCl₃) δ 7.95 – 7.85 (m, 1H), 7.60 – 7.39 (m, 2H), 7.17 (t, *J* = 8.3 Hz, 1H), 6.86 – 6.78 (m, 2H), 6.78 – 6.66 (m, 1H), 4.91 – 4.53 (m, 1H), 4.32 (q, *J* = 7.2 Hz, 1H), 4.10 – 3.05 (m, 7H), 1.56 – 1.43 (m, 3H), 1.40 – 1.31 (m, 3H), 1.31 – 1.24 (m, 3H), 1.17 – 0.97 (m, 3H). ¹³C NMR (126 MHz, CDCl₃) δ 168.56, 166.53, 151.31, 140.49, 135.26, 131.61, 131.03, 130.34, 128.61, 128.10, 125.35, 119.45, 116.21, 114.20, 62.50, 60.52, 56.14, 40.47, 38.68, 36.50, 17.81, 14.21, 12.57, 6.60. HRMS: Calculated for [C₂₄H₂₈Cl₂N₂O₄S + Na]⁺ = 535.1008, found = 535.1009.

(±) **2-((2-Chloro-4-(4-(3-chlorophenyl)-trans-2,3-dimethylpiperazine-1-carbonyl)phenyl)sulfinyl)propanoic acid (9a)**



To a solution of (±) ethyl 2-((2-chloro-4-(4-(3-chlorophenyl)-trans-2,3-dimethylpiperazine-1-carbonyl)phenyl)sulfinyl)propanoate (0.15 g, 0.29 mmol, 1 eq.) in 4ml MeOH was added 4ml TEA and 2ml water. Then, the mixture was stirred overnight. The reaction progress was monitored by TLC analysis. Once completed, the mixture was extracted with DCM and washed with water, dried over anhydrous Mg₂SO₄. After filtration, the filtrate was concentrated under reduced pressure. The residue was purified by silica gel column chromatography (MeOH/DCM, 0-5%). This yielded the product (0.13 g, 0.28 mmol, quant.). ¹H NMR (500 MHz, CDCl₃) δ 8.28 (s, 1H), 7.96 (dd, *J* = 23.2, 7.9 Hz, 1H), 7.58 – 7.42 (m, 2H), 7.18 (t, *J* = 8.1 Hz, 1H), 6.85 – 6.79 (m, 2H), 6.71 (d, *J* = 8.3 Hz, 1H), 4.95 – 4.58 (m, 1H), 3.96 (q, *J* = 7.1 Hz, 1H), 3.92 – 3.02 (m, 5H), 1.74 (d, *J* = 7.0 Hz, 1H), 1.54 – 1.45 (m, 3H), 1.30 (d, *J* = 7.2 Hz, 3H), 1.17 – 0.96 (m, 3H). ¹³C NMR (126 MHz, CDCl₃) δ 170.41, 169.00, 151.30, 140.59, 140.22, 135.34, 131.47, 130.42, 128.78, 128.21, 126.10, 119.64, 116.36, 114.33, 60.57, 56.25, 39.89, 36.77, 17.88, 16.84, 12.56, 7.02.

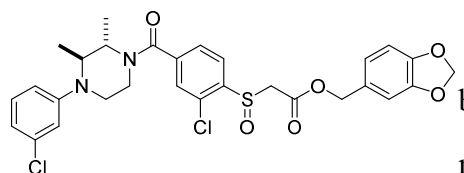
(±) **sec-Butyl 2-((2-chloro-4-(4-(3-chlorophenyl)-trans-2,3-dimethylpiperazine-1-carbonyl)phenyl)sulfinyl)propanoate (9)**



The title compound was synthesized using (±) 2-((2-chloro-4-(trans-4-(3-chlorophenyl)-2,3-dimethylpiperazine-1-carbonyl)phenyl)sulfinyl)propanoic acid (**9a**) (60 mg, 0.12 mmol, 1 eq.), butan-2-ol (1 ml, 10.87 mmol, 88 eq.), 2M oxalyl chloride solution (0.07 ml, 0.14 mmol, 1.1 eq.) and DIPEA (0.1 ml, 0.57 mmol, 4.6 eq.) according to the G. This yielded the product (8.1 mg, 0.02 mmol, 12%). ¹H NMR (500 MHz, CDCl₃) δ 7.93 (d, 1H), 7.57 – 7.46 (m, 2H), 7.19 (t, *J* = 8.0 Hz, 1H), 6.86 – 6.81 (m, 2H), 6.74 (d, *J* = 8.4 Hz, 1H), 5.06 – 4.99 (m, 1H), 3.90 (qd, *J* = 7.2, 5.0 Hz, 1H), 3.84 – 3.11 (m, 6H), 1.77 – 1.60 (m, 2H), 1.51 (d, *J* = 6.7 Hz, 3H), 1.31 (dd, *J* = 6.3, 0.9 Hz, 3H), 1.27 (ddd, *J* = 7.3, 6.0, 1.5 Hz, 3H), 1.14 – 1.04 (m, 3H), 0.97 (dt, *J* = 11.0, 7.4 Hz, 3H). ¹³C NMR (126 MHz, CDCl₃) δ

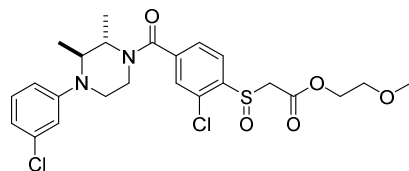
166.53, 165.29, 151.34, 141.97, 140.49, 135.38, 131.84, 130.42, 128.30, 127.91, 125.92, 119.66, 116.37, 114.35, 74.55, 74.38, 62.00, 61.35, 56.31, 28.74, 19.34, 12.46, 12.24, 9.61. HRMS: Calculated for $[C_{26}H_{32}Cl_2N_2O_4S + H]^+ = 541.1503$, found = 541.1501.

(±) **Benzo[d][1,3]dioxol-5-ylmethyl 2-((2-chloro-4-(4-(3-chlorophenyl)-trans-2,3-dimethylpiperazine-1-carbonyl)phenyl)sulfinyl)acetate (11)**



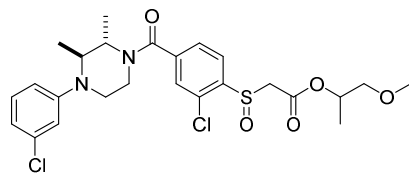
The title compound was synthesized using benzo[d][1,3]dioxol-5-ylmethanol (20 mg, 0.13 mmol, 3 eq.) according to general procedure G. This yielded the product (8 mg, 0.01 mmol, 31%). 1H NMR (500 MHz, $CDCl_3$) δ 7.98 (d, $J = 8.0$ Hz, 1H), 7.57 – 7.39 (m, 2H), 7.18 (t, $J = 8.0$ Hz, 1H), 6.88 – 6.76 (m, 5H), 6.71 (d, $J = 8.4$ Hz, 1H), 5.98 (s, 2H), 5.18 – 5.04 (m, 2H), 4.16 – 3.08 (m, 8H), 1.55 – 1.43 (m, 3H), 1.30 – 1.22 (m, 3H). HRMS: Calculated for $[C_{29}H_{28}Cl_2N_2O_6S + H]^+ = 603.1118$, found = 603.1116.

(±) **2-Methoxyethyl 2-((2-chloro-4-(4-(3-chlorophenyl)-trans-2,3-dimethylpiperazine-1-carbonyl)phenyl)sulfinyl)acetate (6)**



The title compound was synthesized using 2-methoxyethan-1-ol (1 ml, 12.68 mmol, 238 eq.) according to procedure G. This yielded the product (8 mg, 0.02 mmol, 29%). 1H NMR (500 MHz, $CDCl_3$) δ 8.03 (d, $J = 8.0$ Hz, 1H), 7.56 (d, $J = 9.5$ Hz, 1H), 7.49 (d, $J = 1.5$ Hz, 1H), 7.18 (t, $J = 8.0$ Hz, 1H), 6.83 (d, $J = 9.3$ Hz, 2H), 6.72 (d, $J = 8.4$ Hz, 1H), 4.72 (d, $J = 75.1$ Hz, 1H), 4.40 – 4.27 (m, 2H), 4.11 (dd, $J = 14.0, 1.1$ Hz, 1H), 3.87 (s, 1H), 3.75 (d, $J = 14.0$ Hz, 1H), 3.61 (ddd, $J = 5.8, 3.8, 2.2$ Hz, 4H), 3.39 (s, 3H), 3.34 – 3.08 (m, 2H), 1.50 (d, $J = 6.6$ Hz, 3H), 1.31 – 0.94 (m, 3H). HRMS: Calculated for $[C_{24}H_{28}Cl_2N_2O_5S + H]^+ = 527.1169$, found = 527.1163.

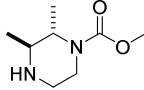
(±) **1-Methoxypropan-2-yl 2-((2-chloro-4-(4-(3-chlorophenyl)-trans-2,3-dimethylpiperazine-1-carbonyl)phenyl)sulfinyl)acetate (10)**



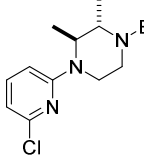
The title compound was synthesized using 1-methoxypropan-2-ol (1 ml, 10.21 mmol, 192 eq.) according to procedure G. This yielded the product (5.3 mg, 9.8 μ mol, 18%). 1H NMR (500 MHz, $CDCl_3$) δ 8.03 (d, $J = 7.9$ Hz, 1H), 7.64 –

7.39 (m, 2H), 7.18 (t, $J = 8.1$ Hz, 1H), 6.87 – 6.77 (m, 2H), 6.72 (d, $J = 8.5$ Hz, 1H), 5.24 – 5.11 (m, 1H), 5.04 – 4.54 (m, 1H), 4.08 (d, $J = 10.6$ Hz, 1H), 3.87 (s, 1H), 3.70 (dd, $J = 14.0, 3.7, 0.8$ Hz, 1H), 3.52 – 3.40 (m, 3H), 3.38 (s, 3H), 3.19 (s, 3H), 1.49 (d, $J = 6.7$ Hz, 3H), 1.28 (dd, $J = 19.0, 6.5$ Hz, 3H), 1.18 – 0.96 (m, 3H). HRMS: Calculated for $[\text{C}_{25}\text{H}_{30}\text{Cl}_2\text{N}_2\text{O}_5\text{S} + \text{H}]^+ = 541.1325$, found = 541.1323.

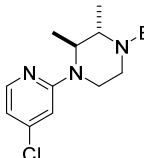
(±) *tert* Butyl trans-2,3-dimethylpiperazine-1-carboxylate (4a)

 (±) *trans*-2,3-Dimethylpiperazine (262 mg, 2.29 mmol, 1 eq.) was dissolved in DCM (100 ml). Boc_2O (500 mg, 2.29 mmol, 1 eq.) dissolved in DCM (10 ml) was added slowly via a syringe pump over 45 h at rt. After adding, the reaction mixture was concentrated and the residue was purified by column chromatography (0-10% MeOH in DCM). This yielded the product as a yellow oil (282 mg, 1.31 mmol, 57%). ^1H NMR (400 MHz, CDCl_3) δ 5.19 (br, 1H), 3.92 (dd, $J = 5.5, 1.6$ Hz, 1H), 3.80 (d, $J = 10.5$ Hz, 1H), 3.12 – 2.71 (m, 4H), 1.38 (s, 9H), 1.24 (d, $J = 5.2$ Hz, 3H), 1.23 (d, $J = 5.1$ Hz, 3H). ^{13}C NMR (101 MHz, CDCl_3) δ 155.12, 79.87, 51.40, 50.70, 38.46, 37.41, 28.39, 17.21, 16.19.

(±) *tert*-Butyl 4-(6-chloropyridin-2-yl)-*trans*-2,3-dimethylpiperazine-1-carboxylate (4b)

 The title compound was synthesized using 2-bromo-6-chloropyridine (45 mg, 0.23 mmol, 1 eq.) and (±) *tert*-butyl *trans*-2,3-dimethylpiperazine-1-carboxylate (50 mg, 0.23 mmol, 1 eq.) according to procedure D. This yielded the product (35 mg, 0.11 mmol, 46%). ^1H NMR (400 MHz, CDCl_3) δ 7.37 (t, $J = 7.9$ Hz, 1H), 6.56 (d, $J = 7.4$ Hz, 1H), 6.42 (dd, $J = 8.4, 2.8$ Hz, 1H), 4.25 – 3.81 (m, 4H), 3.25 – 3.05 (m, 2H), 1.47 (s, 9H), 1.21 (d, $J = 6.8$ Hz, 3H), 1.17 (d, $J = 6.7$ Hz, 3H). ^{13}C NMR (101 MHz, CDCl_3) δ 159.04, 155.48, 149.65, 139.84, 111.85, 104.33, 79.95, 51.9, 50.54, 38.69, 37.37, 28.55, 17.20, 15.08.

(±) *tert*-Butyl 4-(4-chloropyridin-2-yl)-*trans*-2,3-dimethylpiperazine-1-carboxylate (5b)

 The title compound was synthesized using 2-bromo-4-chloropyridine (45 mg, 0.23 mmol, 1 eq.), (±) *tert*-butyl *trans*-2,3-dimethylpiperazine-1-carboxylate (50 mg, 0.23 mmol, 1 eq.) according to procedure D. This

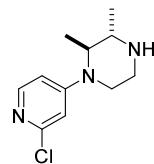
yielded the product (14.5 mg, 0.045 mmol, 19%). ^1H NMR (400 MHz, CDCl_3) δ 8.05 (d, $J = 5.3$ Hz, 1H), 6.59 (dd, $J = 5.4, 1.6$ Hz, 1H), 6.55 (s, 1H), 4.65 – 3.63 (m, 4H), 3.31 – 2.88 (m, 2H), 1.48 (s, 9H), 1.23 (d, $J = 6.8$ Hz, 3H), 1.17 (d, $J = 6.7$ Hz, 3H). ^{13}C NMR (101 MHz, CDCl_3) δ 160.09, 149.01, 145.17, 128.48, 113.23, 106.50, 80.00, 52.03, 50.61, 38.93, 37.43, 28.59, 17.27, 15.20.

(±) 1-(5-Chloropyridin-3-yl)-trans-2,3-dimethylpiperazine (2c)



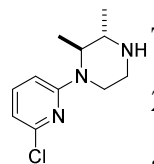
The title compound was synthesized using 3-bromo-5-chloropyridine (385 mg, 2 mmol, 2 eq.) and (±) trans-2,3-dimethylpiperazine (114 mg, 1 mmol, 1 eq.) according to procedure I. This yielded the product (9.3 mg, 0.041 mmol, 4%). ^1H NMR (400 MHz, CDCl_3) δ 8.17 (d, $J = 2.5$ Hz, 1H), 8.09 (d, $J = 2.0$ Hz, 1H), 7.19 (t, $J = 2.3$ Hz, 1H), 3.36 – 3.29 (m, 1H), 3.22 – 3.09 (m, 3H), 3.04 – 2.90 (m, 2H), 2.29 (br, 1H), 1.34 (d, $J = 6.7$ Hz, 3H), 1.11 (d, $J = 6.5$ Hz, 3H). ^{13}C NMR (101 MHz, CDCl_3) δ 147.95, 140.23, 139.53, 132.17, 125.13, 56.92, 53.98, 46.70, 41.54, 18.74, 14.70.

(±) 1-(2-Chloropyridin-4-yl)-trans-2,3-dimethylpiperazine (3c)



The title compound was synthesized using 4-bromo-2-chloropyridine (385 mg, 2 mmol, 2 eq.) and (±) trans-2,3-dimethylpiperazine (114 mg, 1 mmol, 1 eq.) according to procedure I. This yielded the product (11 mg, 0.049 mmol, 5%). ^1H NMR (400 MHz, CDCl_3) δ 7.99 (d, $J = 6.1$ Hz, 1H), 6.59 (d, $J = 2.4$ Hz, 1H), 6.52 (dd, $J = 6.1, 2.4$ Hz, 1H), 3.76 – 3.58 (m, 1H), 3.51 – 3.36 (m, 1H), 3.24 – 2.83 (m, 4H), 2.48 (br, 1H), 1.30 (d, $J = 6.7$ Hz, 3H), 1.25 (d, $J = 6.7$ Hz, 3H). ^{13}C NMR (101 MHz, CDCl_3) δ 156.95, 152.91, 149.67, 107.19, 107.07, 54.06, 51.98, 40.48, 39.12, 18.70, 14.37.

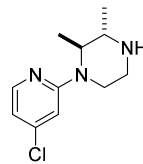
(±) 1-(6-Chloropyridin-2-yl)-trans-2,3-dimethylpiperazine (4c)



The title compound was synthesized using (±) *tert*-butyl-4-(6-chloropyridin-2-yl)-trans-2,3-dimethylpiperazine-1-carboxylate (35 mg, 0.11 mmol) according to procedure E. This yielded the product (19 mg, 0.083 mmol, 77%). ^1H NMR (400 MHz, CDCl_3) δ 7.39 (dd, $J = 8.3, 7.6$ Hz, 1H), 6.58 (d, $J = 7.5$ Hz, 1H), 6.43 (d, $J = 8.4$ Hz, 1H), 4.34 (br, 1H), 3.54 (dq, $J = 14.5, 7.3$ Hz, 1H), 3.28 – 3.02 (m, 5H), 1.39 (d, $J = 6.8$ Hz, 3H), 1.33 (d, $J = 6.9$ Hz, 3H). ^{13}C NMR (101 MHz,

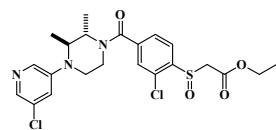
CDCl₃) δ 158.78, 149.66, 139.96, 112.23, 104.46, 52.06, 51.73, 38.68, 37.85, 17.39, 14.57.

(\pm) 1-(4-Chloropyridin-2-yl)-trans-2,3-dimethylpiperazine (5c)



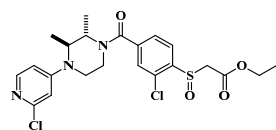
The title compound was synthesized using (\pm) *tert*-butyl-4-(4-chloropyridin-2-yl)-trans-2,3-dimethylpiperazine-1-carboxylate (14.5 mg, 0.045 mmol) according to procedure E. This yielded the product (7.2 mg, 0.032 mmol, 72%). ¹H NMR (400 MHz, CDCl₃) δ 8.06 (d, *J* = 5.3 Hz, 1H), 6.66 (dd, *J* = 5.4, 1.6 Hz, 1H), 6.58 (d, *J* = 1.6 Hz, 1H), 4.38 (q, *J* = 6.4 Hz, 1H), 4.27 – 4.17 (m, 1H), 3.56 (qd, *J* = 7.0, 1.7 Hz, 1H), 3.47 – 3.23 (m, 3H), 1.54 (d, *J* = 6.8 Hz, 3H), 1.45 (d, *J* = 6.8 Hz, 3H). ¹³C NMR (101 MHz, CDCl₃) δ 159.21, 149.07, 145.56, 114.45, 106.82, 52.27, 51.02, 37.92, 36.48, 15.88, 14.68.

(\pm) Ethyl 2-((2-chloro-4-(4-(5-chloropyridin-3-yl)-trans-2,3-dimethylpiperazine-1-carbonyl) phenyl)sulfinyl)acetate (2)



The title compound was synthesized using 3-chloro-4-((2-ethoxy-2-oxoethyl)sulfinyl)benzoic acid (11.6 mg, 0.04 mmol, 1 eq.) and (\pm) 1-(5-chloropyridin-3-yl)-trans-2,3-dimethylpiperazine (9 mg, 0.04 mmol, 1 eq.) according to the procedure F. This yielded the product (12.4 mg, 0.025 mmol, 62%). ¹H NMR (400 MHz, CDCl₃) δ 8.40 (s, 1H), 8.08 (s, 1H), 8.04 (d, *J* = 7.9 Hz, 1H), 7.62 – 7.54 (m, 1H), 7.47 (d, *J* = 13.7 Hz, 2H), 4.98 – 4.65 (m, 1H), 4.33 – 4.17 (m, 2H), 4.06 (dd, *J* = 14.0, 1.9 Hz, 1H), 4.00 – 3.19 (m, 6H), 1.52 – 1.17 (m, 9H). ¹³C NMR (101 MHz, CDCl₃) δ 168.99, 164.36, 148.19, 142.53, 139.55, 135.34, 131.00, 130.26, 128.53, 128.24, 127.90, 127.09, 126.08, 62.57, 58.06, 54.94, 49.27, 40.23, 35.82, 17.67, 14.07, 13.76.

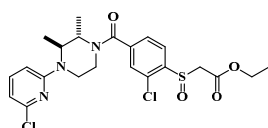
(\pm) Ethyl 2-((2-chloro-4-(4-(2-chloropyridin-4-yl)-trans-2,3-dimethylpiperazine-1-carbonyl) phenyl)sulfinyl) acetate (3)



The title compound was synthesized using 3-chloro-4-((2-ethoxy-2-oxoethyl)sulfinyl)benzoic acid (14.5 mg, 0.05 mmol) and (\pm) 1-(2-chloropyridin-4-yl)-trans-2,3-dimethylpiperazine (11 mg, 0.05 mmol, 1eq.) according to the procedure F. This yielded the product (7.5 mg, 0.015 mmol, 30%). ¹H NMR (400 MHz, CDCl₃) δ 8.29 (d, *J* = 6.4 Hz, 1H), 8.04

(d, $J = 7.9$ Hz, 1H), 7.60 – 7.42 (m, 2H), 6.77 (d, $J = 7.5$ Hz, 2H), 4.96 – 4.62 (m, 1H), 4.24 (qd, $J = 7.1, 1.5$ Hz, 2H), 4.10 – 3.27 (m, 7H), 1.47 – 1.20 (m, 9H). ^{13}C NMR (101 MHz, CDCl_3) δ 168.88, 164.42, 158.23, 146.19, 143.54, 142.89, 139.39, 131.04, 128.60, 127.27, 126.28, 107.48, 106.82, 62.53, 58.17, 54.62, 49.33, 40.32, 35.84, 17.78, 15.38, 14.09.

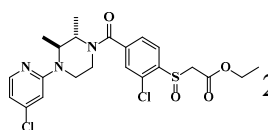
(±) Ethyl 2-((2-chloro-4-(4-(6-chloropyridin-2-yl)-trans-2,3-dimethylpiperazine-1-carbonyl) phenyl)sulfinyl)acetate (4)



The title compound was synthesized using 3-chloro-4-((2-ethoxy-2-oxoethyl)sulfinyl)benzoic acid (24 mg, 0.082 mmol, 1 eq.) and (±) 1-(6-chloropyridin-2-yl)-trans-2,3-dimethylpiperazine (18.6

mg, 0.082 mmol) according to the procedure F. This yielded the product (32.6 mg, 0.065 mmol, 79%). ^1H NMR (400 MHz, CDCl_3) δ 8.05 (dd, $J = 8.0, 2.8$ Hz, 1H), 7.61 – 7.41 (m, 3H), 6.66 (dd, $J = 7.5, 2.9$ Hz, 1H), 6.49 (dd, $J = 12.1, 8.4$ Hz, 1H), 4.91 – 4.56 (m, 1H), 4.38 – 4.05 (m, 5H), 3.77 – 3.06 (m, 4H), 1.45 – 1.14 (m, 9H). ^{13}C NMR (101 MHz, CDCl_3) δ 168.96, 164.51, 158.63, 149.76, 142.42, 140.45, 140.15, 130.89, 128.59, 127.19, 126.41, 112.80, 104.55, 62.59, 58.36, 51.75, 49.08, 38.85, 36.52, 17.81, 16.81, 14.21.

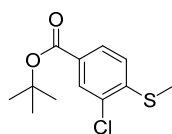
(±) Ethyl 2-((2-chloro-4-(4-(4-chloropyridin-2-yl)-trans-2,3-dimethylpiperazine-1-carbonyl) phenyl)sulfinyl)acetate (5)



The title compound was synthesized using 3-chloro-4-((2-ethoxy-2-oxoethyl)sulfinyl)benzoic acid (9.3 mg, 0.032 mmol, 1 eq.) and (±) 1-(4-chloropyridin-2-yl)-trans-2,3-dimethylpiperazine (7.2 mg,

0.032 mmol, 1 eq.) according to the procedure F. This yielded the product (15.6 mg, 0.031 mmol, 98%). ^1H NMR (400 MHz, CDCl_3) δ 8.21 (t, $J = 3.8$ Hz, 1H), 8.06 (d, $J = 6.1$ Hz, 1H), 7.63 – 7.46 (m, 2H), 6.93 – 6.87 (m, 2H), 4.96 – 4.63 (m, 1H), 4.41 – 3.96 (m, 5H), 3.83 – 3.28 (m, 4H), 1.48 – 1.24 (m, 9H). ^{13}C NMR (101 MHz, CDCl_3) δ 168.89, 164.49, 155.08, 150.38, 143.34, 142.86, 139.46, 130.96, 128.56, 127.02, 126.32, 114.69, 109.82, 62.47, 58.29, 54.03, 49.17, 40.73, 35.82, 17.50, 15.63, 14.10.

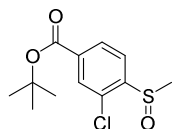
***tert*-Butyl 3-chloro-4-(methylthio)benzoate (26)**



To a solution of *tert*-butyl 3-chloro-4-fluorobenzoate (0.510 g, 2.22 mmol, 1 eq.) in degassed DMF was added sodium methanethiolate (0.230 g, 3.32 mmol, 1.5 eq.) at -10 °C and the mixture was stirred at RT overnight. The

reaction progress was monitored by TLC. Once completed, the mixture was diluted with Et₂O, washed with water, dried over anhydrous MgSO₄ and concentrated under reduced pressure. The residue was purified using column chromatography (Et₂O / pentane, 0-10%) to yield the product (0.24 g, 0.91 mmol, 41%). ¹H NMR (400 MHz, CDCl₃) δ 7.91 (d, *J* = 1.8 Hz, 1H), 7.85 (dd, *J* = 8.3, 1.8 Hz, 1H), 7.13 (d, *J* = 8.4 Hz, 1H), 2.49 (s, 3H), 1.59 (s, 9H). ¹³C NMR (400 MHz, CDCl₃) δ 164.54, 143.80, 130.83, 129.94, 129.04, 128.05, 123.94, 81.49, 28.22, 14.92.

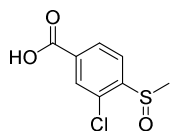
***tert*-Butyl 3-chloro-4-(methylsulfinyl)benzoate (27)**



The title compound was synthesized using *tert*-butyl 3-chloro-4-(methylthio)benzoate (0.24 g, 0.91 mmol, 1 eq.) according to procedure B. This yielded the product (0.290 g, 1.17 mmol, quant.). ¹H NMR (500

MHz, CDCl₃) δ 8.13 (dd, *J* = 8.0, 1.6 Hz, 1H), 8.03 – 7.98 (m, 2H), 2.86 (s, 3H), 1.62 (s, 9H). ¹³C NMR (500 MHz, CDCl₃) δ 163.34, 147.97, 135.70, 130.48, 129.52, 128.73, 125.20, 82.24, 41.37, 27.94.

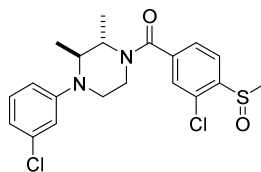
3-Chloro-4-(methylsulfinyl)benzoic acid (28)



The title compound was synthesized using *tert*-butyl 3-chloro-4-(methylsulfinyl)benzoate (0.26 g, 0.94 mmol) according to procedure C.

This yielded the product (0.19 g, 0.87 mmol, 92%). ¹H NMR (400 MHz, Methanol-*d*₄) δ 8.22 (dd, *J* = 8.2, 1.6 Hz, 1H), 8.08 (d, *J* = 1.6 Hz, 1H), 7.98 (d, *J* = 8.1 Hz, 1H), 2.90 (s, 3H). ¹³C NMR (400 MHz, Methanol-*d*₄) δ 167.19, 148.93, 136.49, 132.03, 131.20, 130.45, 126.47, 41.68.

(±) (3-Chloro-4-(methylsulfinyl)phenyl)(4-(3-chlorophenyl)-*trans*-2,3-dimethylpiperazin-1-yl)methanone (29)

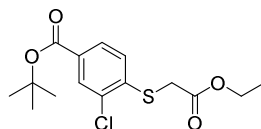


To a stirred suspension of 3-chloro-4-((2-ethoxy-2-oxoethyl)sulfinyl)benzoic acid (0.19 g, 0.87 mmol, 1 eq.) in DCM (10 ml) were added (±) *trans*-1-(3-chlorophenyl)-2,3-

dimethylpiperazine (32, 0.230 g, 1.04 mmol, 1.2 eq.), DIPEA (0.34 mg, 2.59 mmol, 3

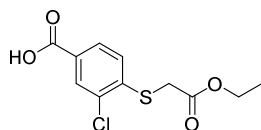
eq.), HOBt (0.18 mg, 1.30 mmol, 1.5 eq.) and EDCI (0.25 mg, 1.30 mmol, 1.5 eq.). The mixture was stirred overnight. The reaction progress was monitored by TLC analysis. Once completed, the mixture was washed with water and brine, dried over anhydrous MgSO_4 , filtered and concentrated. The crude product was purified using column chromatography (EtOAc / pentane, 0%-60%) to yield the product (0.27 mg, 0.64 mmol, 74%). ^1H NMR (400 MHz, CDCl_3) δ 8.04 – 7.97 (m, 2H), 7.56 – 7.38 (m, 2H), 7.14 (t, $J = 8.2$ Hz, 1H), 6.60 (d, $J = 2.4$ Hz, 1H), 6.56 – 6.47 (m, 1H), 4.85 – 4.49 (m, 1H), 3.98 – 3.07 (m, 5H), 2.82 (s, 3H), 1.42 – 1.33 (m, 3H), 1.28 – 1.06 (m, 3H). ^{13}C NMR (126 MHz, CDCl_3) δ 168.83, 151.33, 145.25, 140.18, 135.19, 130.47, 130.33, 128.43, 127.77, 125.85, 119.34, 116.13, 114.19, 56.08, 49.57, 42.29, 41.64, 36.46, 17.76, 12.52.

***tert*-Butyl 3-chloro-4-((2-ethoxy-2-oxoethyl)thio)benzoate (30)**



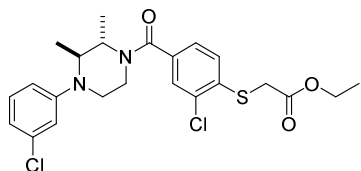
The title compound was synthesized using *tert*-butyl 3-chloro-4-fluorobenzoate (0.33 g, 1.45 mmol, 1.2 eq.) and ethyl 2-mercaptoacetate (0.13 ml, 1.21 mmol, 1 eq.) according to procedure A. This yielded the product (0.31 g, 0.95 mmol, 95%). ^1H NMR (400 MHz, CDCl_3): δ 7.94 (d, $J = 1.8$ Hz, 1H), 7.83 (dd, $J = 8.3, 1.8$ Hz, 1H), 7.33 (d, $J = 8.3$ Hz, 1H), 4.21 (q, $J = 7.1$ Hz, 2H), 3.75 (s, 2H), 1.58 (s, 9H), 1.26 (t, $J = 7.2$ Hz, 3H). ^{13}C NMR (101 MHz, CDCl_3): δ 168.75, 164.35, 140.61, 132.17, 130.61, 130.44, 128.19, 126.62, 81.79, 62.12, 34.51, 28.25, 14.21.

3-Chloro-4-((2-ethoxy-2-oxoethyl)thio)benzoate (31)



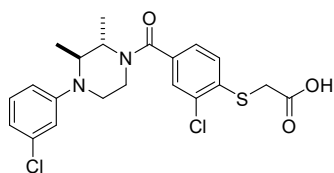
The title compound was synthesized using *tert*-butyl 3-chloro-4-((2-ethoxy-2-oxoethyl)thio)benzoate (61.5 mg, 0.19 mmol) according to procedure C. This yielded the product (51.1 mg, 0.19 mmol, 92%). ^1H NMR (400 MHz, CDCl_3) δ 8.07 (s, 1H), 7.95 (d, $J = 8.3$ Hz, 1H), 7.37 (d, $J = 8.2$ Hz, 1H), 4.23 (q, $J = 7.2$ Hz, 2H), 3.78 (s, 2H), 1.28 (t, $J = 7.1$ Hz, 3H). ^{13}C NMR (400 MHz, CDCl_3) δ 170.34, 168.37, 142.67, 130.76, 128.58, 127.15, 125.87, 61.98, 34.03, 13.91.

(±) Ethyl 2-((2-chloro-4-(4-(3-chlorophenyl)-*trans*-2,3-dimethylpiperazine-1-carbonyl)phenyl)thio)acetate (32)



The title compound was synthesized using 3-chloro-4-((2-ethoxy-2-oxoethyl)thio)benzoic acid (27, 0.15 mg, 0.54 mmol, 1 eq.) according to procedure F. This yielded the product (0.25 g, 0.46 mmol, 85%). ^1H NMR (400 MHz, CDCl_3) δ 7.48 – 7.36 (m, 2H), 7.34 – 7.27 (m, 1H), 7.17 (t, $J = 8.3$ Hz, 1H), 6.80 (d, $J = 6.1$ Hz, 2H), 6.71 (d, $J = 8.4$ Hz, 1H), 4.84 – 4.53 (m, 1H), 4.21 (q, $J = 7.1$ Hz, 2H), 3.73 (s, 2H), 3.69 – 3.01 (m, 5H), 1.51 – 1.41 (m, 3H), 1.27 (t, $J = 7.2$ Hz, 3H), 1.06 (dd, $J = 46.6, 6.5$ Hz, 3H). ^{13}C NMR (101 MHz, CDCl_3) δ 169.52, 168.85, 151.39, 137.10, 135.16, 134.77, 133.25, 130.25, 128.12, 128.87, 125.47, 119.18, 116.02, 114.05, 61.99, 56.06, 49.45, 40.43, 36.42, 34.69, 17.69, 14.13, 12.49 (carbon spectrum shows a mixture of rotamers). HRMS: Calculated for $[\text{C}_{23}\text{H}_{26}\text{Cl}_2\text{N}_2\text{O}_3\text{S} + \text{H}]^+ = 483.1084$, found = 483.1079.

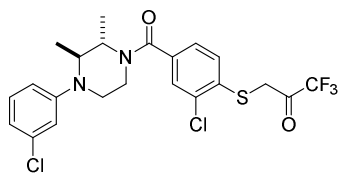
(±) **2-((2-Chloro-4-(4-(3-chlorophenyl)-trans-2,3-dimethylpiperazine-1-carbonyl)phenyl)thio)acetic acid (33)**



To a solution of (±) ethyl 2-((2-chloro-4-(4-(3-chlorophenyl)-trans-2,3-dimethylpiperazine-1-carbonyl)phenyl)thio)acetate (0.36 mg, 0.75 mmol, 1 eq.) in MeOH (10 ml) was added 2 M NaOH solution (0.75 ml, 1.25 mmol, 2 eq.) and the reaction mixture was stirred for 2h. The reaction progress was monitored by TLC analysis. Once completed, the solution was acidified to pH 3 using 3M HCl and extracted with DCM. The organic layer was dried over anhydrous MgSO_4 , filtered and concentrated under reduced pressure. The residue was purified with column chromatography (EtOAc / pentane, 0 – 100 % with 1 % acetic acid) to yield the product (0.33 mg, 0.72 mmol, 96%). ^1H NMR (400 MHz, CDCl_3) δ 7.48 – 7.36 (m, 2H), 7.29 (d, $J = 6.0$ Hz, 1H), 7.17 (t, $J = 8.3$ Hz, 1H), 6.80 (d, $J = 6.1$ Hz, 2H), 6.71 (d, $J = 8.4$ Hz, 1H), 4.80 – 4.50 (m, 1H), 4.04 – 3.95 (m, 1H), 3.90 (s, 2H), 3.86 – 3.38 (m, 2H), 3.32 – 3.06 (m, 2H), 1.52 – 1.45 (m, 3H), 1.04 (dd, $J = 55.7, 6.5$ Hz, 3H). ^{13}C NMR (101 MHz, CDCl_3) δ 172.24, 170.27, 151.35, 137.79, 135.25, 133.79, 132.72, 130.33, 129.11, 128.18, 125.37, 119.39, 116.17, 114.18, 56.16, 49.90, 40.48, 36.75, 34.50, 17.75, 12.49.

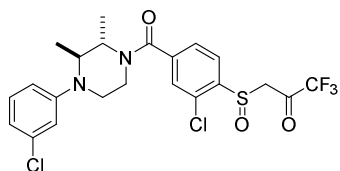
(±) **3-((2-Chloro-4-(4-(3-chlorophenyl)-trans-2,3-dimethylpiperazine-1-**

carbonyl)phenyl)thio)-1,1,1-trifluoropropan-2-one (34)



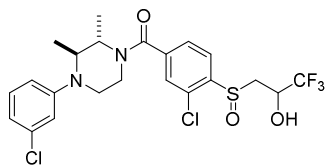
To a solution of trifluoroacetic anhydride (34 μl , 0.24 mmol, 2.2 eq.) in toluene (0.5 ml) was added (\pm) 2-((2-chloro-4-(4-(3-chlorophenyl)-trans-2,3-dimethylpiperazine-1-carbonyl)phenyl)thio)acetic acid (50 mg, 0.11 mmol, 1 eq.) and the mixture was cooled to 0 °C. Then, pyridine (22 μl , 0.28 mmol, 2.5 equiv.) in toluene (0.5 ml) was slowly added and the mixture was stirred at 65 °C overnight. Afterwards it was cooled to 0 °C and 1 ml water was added dropwise. Then the temperature was brought up to 45 °C and maintained for 2h. After cooling, the aqueous phase of the mixture was separated and washed with ethyl acetate. The combined organic layers were washed with water and brine, dried (MgSO_4), filtered and concentrated. The crude product was purified by prep HPLC to provide a white solid (9.4 mg, 0.11 mmol, 17%). ^1H NMR (400 MHz, CDCl_3) δ 7.63 – 7.27 (m, 3H), 7.17 (t, J = 8.4 Hz, 1H), 6.81 (d, J = 7.2 Hz, 2H), 6.71 (d, J = 8.5 Hz, 1H), 4.69 (dd, J = 76.4, 10.1 Hz, 1H), 4.06 (s, 1H), 3.98 – 3.02 (m, 5H), 1.47 (dd, J = 9.7, 6.7 Hz, 3H), 1.06 (dd, J = 45.1, 6.7 Hz, 3H). HRMS: Calculated for $[\text{C}_{22}\text{H}_{21}\text{Cl}_2\text{F}_3\text{N}_2\text{O}_2\text{S} + \text{H}_2\text{O} + \text{H}]^+ = 523.0831$, found = 523.0828.

(\pm) 3-((2-Chloro-4-(4-(3-chlorophenyl)-trans-2,3-dimethylpiperazine-1-carbonyl)phenyl)sulfinyl)-1,1,1-trifluoropropan-2-one (16)



The title was synthesized using (\pm) (3-chloro-4-(methylsulfinyl)phenyl)(trans-4-(3-chlorophenyl)-2,3-dimethylpiperazin-1-yl)methanone (50 mg, 0.12 mmol, 1 eq.) and ethyl 2,2,2-trifluoroacetate (167 mg, 1.18 mmol, 10 eq.) according to procedure H. This yielded the product (48 mg, 0.09 mmol, 79%). ^1H NMR (600 MHz, CDCl_3) δ 8.07 (d, J = 8.0 Hz, 1H), 7.66 – 7.47 (m, 2H), 7.19 (t, J = 8.1 Hz, 1H), 6.86 – 6.80 (m, 2H), 6.72 (dd, J = 8.4, 2.4 Hz, 1H), 3.77 – 2.99 (m, 7H), 1.52 (d, J = 6.8 Hz, 3H), 1.07 (m, 3H). ^{13}C NMR (126 MHz, CDCl_3) δ 168.76, 168.28, 151.30, 141.82, 140.78, 135.27, 130.60, 130.38, 128.68, 126.78, 121.76 (q, J = 287.3 Hz), 119.53, 116.26, 114.26, 93.88 (q, J = 33.8 Hz), 56.18, 53.97, 49.80, 40.45, 36.64, 17.81, 12.25 (carbon spectrum shows a mixture of rotamers). HRMS: Calculated for $[\text{C}_{22}\text{H}_{21}\text{Cl}_2\text{F}_3\text{N}_2\text{O}_3\text{S} + \text{H}_2\text{O} + \text{H}]^+ = 539.0780$, found = 539.0779.

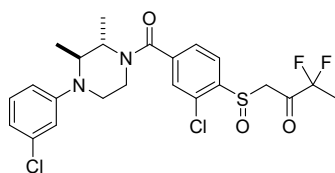
(±) **(3-chloro-4-((3,3,3-trifluoro-2-hydroxypropyl)sulfinyl)phenyl)(trans-4-(3-chlorophenyl)-2,3-dimethylpiperazin-1-yl)methanone (17)**



To a cooled (0°C) solution of (±) 3-((2-chloro-4-(trans-4-(3-chlorophenyl)-2,3-dimethylpiperazine-1-carbonyl)phenyl)sulfinyl)-1,1,1-trifluoropropan-2-one

1,1,1-trifluoropropan-2-one (25 mg, 0.05 mmol, 1 eq.) in MeOH (1.7 mL) was added NaBH₄ (1.5 mg, 0.04 mmol, 0.8 eq.). The resulting solution was stirred for 1h. The reaction was quenched with sat. aq. NH₄Cl, extracted with DCM (3x), dried (MgSO₄), filtered and concentrated. The crude product, which was purified with prep HPLC to afford compound as a white solid (9.3 mg, 0.05 mmol, 37%). HRMS: Calculated for [C₂₂H₂₃Cl₂F₃N₂O₃S + H]⁺ = 523.0829, found = 523.0831.

(±) **1-((2-Chloro-4-(4-(3-chlorophenyl)-trans-2,3-dimethylpiperazine-1-carbonyl)phenyl)sulfinyl)-3,3-difluorobutan-2-one (19)**

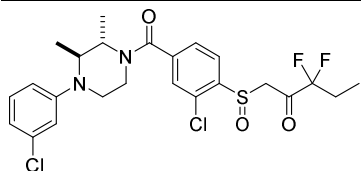


The title compound was synthesized using (±) (3-chloro-4-(methylsulfinyl)phenyl)(trans-4-(3-chlorophenyl)-2,3-dimethylpiperazin-1-yl)methanone (25 mg, 0.06 mmol, 1 eq.)

and ethyl 2,2-difluoropropanoate (81 mg, 0.59 mmol, 10 eq.) according to procedure H. This yielded the product (4.9 mg, 0.06 mmol, 16%). ¹H NMR (500 MHz, CDCl₃) δ 8.06 (dd, *J* = 18.3, 8.0 Hz, 1H), 7.63 – 7.49 (m, 2H), 7.20 (t, *J* = 8.0 Hz, 1H), 6.88 – 6.82 (m, 2H), 6.76 (d, *J* = 8.4 Hz, 1H), 4.44 (dd, *J* = 15.1, 4.4 Hz, 1H), 4.07 (dd, *J* = 15.1, 3.4 Hz, 1H), 3.85 – 3.10 (m, 6H), 1.78 (t, *J* = 19.3 Hz, 3H), 1.52 (d, *J* = 6.8 Hz, 3H), 1.10 (s, 3H). ¹³C NMR (101 MHz, CDCl₃) δ 168.67, 168.19, 151.36, 142.33, 140.83, 135.32, 130.67, 130.40, 128.68, 126.98, 126.52, 119.56, 117.31 (t, *J* = 249 Hz), 116.30, 114.28, 59.45, 56.22, 49.72, 40.52, 36.58, 18.73 (t, *J* = 24 Hz), 17.87, 12.60 (carbon spectrum shows a mixture of rotamers). HRMS: Calculated for [C₂₃H₂₄Cl₂F₂N₂O₃S + H₂O + H]⁺ = 535.1031, found = 535.1027.

(±) **1-((2-Chloro-4-(4-(3-chlorophenyl)-trans-2,3-dimethylpiperazine-1-carbonyl)phenyl)sulfinyl)-3,3-difluoropentan-2-one (20)**

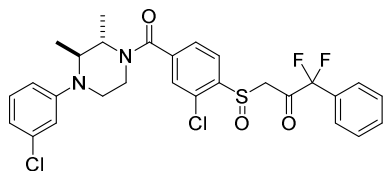
Discovery of LEI-515 as a Novel Ultrapotent, Reversible MAGL Inhibitor with Improved Metabolic Stability



The title compound was synthesized using (±) (3-chloro-4-(methylsulfinyl)phenyl)(trans-4-(3-chlorophenyl)-2,3-dimethylpiperazin-1-yl)methanone (20 mg, 0.05 mmol, 1

eq.) and ethyl 2,2-difluorobutanoate (72 mg, 0.47 mmol, 10 eq.) according to procedure H. This yielded the product (2.5 mg, 0.05 mmol, 10%). ¹H NMR (500 MHz, CDCl₃) δ 8.04 (dd, *J* = 8.1, 4.5 Hz, 1H), 7.62 – 7.49 (m, 2H), 7.22 (t, *J* = 8.3 Hz, 1H), 6.89 (d, *J* = 7.2 Hz, 2H), 6.81 (d, *J* = 8.4 Hz, 1H), 4.41 (dd, *J* = 15.1, 4.3 Hz, 1H), 4.05 (dd, *J* = 15.2, 3.4 Hz, 1H), 3.85 – 3.13 (m, 8H), 2.17 – 2.02 (m, 3H), 1.54 (d, *J* = 6.8 Hz, 3H), 1.08 (t, *J* = 7.5 Hz, 3H). ¹³C NMR (101 MHz, CDCl₃) δ 168.65, 168.17, 151.36, 142.26, 140.93, 135.33, 130.65, 130.40, 128.67, 127.08, 126.51, 119.55, 118.14 (t, *J* = 253 Hz), 116.30, 114.28, 60.15, 56.22, 49.70, 40.52, 36.57, 25.52 (t, *J* = 23 Hz), 17.86, 12.60, 5.47 (t, *J* = 5 Hz). HRMS: Calculated for [C₂₄H₂₆Cl₂F₂N₂O₃S + H₂O + H]⁺ = 549.1188, found = 549.1183.

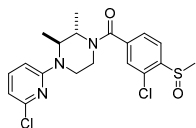
(±) **3-((2-Chloro-4-(4-(3-chlorophenyl)-trans-2,3-dimethylpiperazine-1-carbonyl)phenyl)sulfinyl)-1,1-difluoro-1-phenylpropan-2-one (21)**



The title compound was synthesized using (±) (3-chloro-4-(methylsulfinyl)phenyl)(trans-4-(3-chlorophenyl)-2,3-dimethylpiperazin-1-yl)methanone

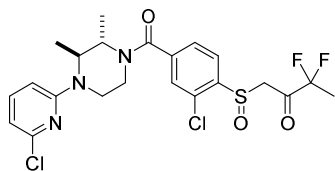
(40 mg, 0.09 mmol, 1 eq.) and ethyl 2,2-difluoro-2-phenylacetate (188 mg, 0.94 mmol, 10 eq.) according to procedure LDA. This yielded the product (13.4 mg, 0.02 mmol, 25%). ¹H NMR (600 MHz, CDCl₃) δ 7.95 (d, *J* = 7.9 Hz, 1H), 7.63 – 7.42 (m, 7H), 7.17 (t, *J* = 8.1, 2.4 Hz, 1H), 6.85 – 6.78 (m, 2H), 6.74 – 6.68 (m, 1H), 4.69 – 4.32 (m, 1H), 4.07 – 3.01 (m, 5H), 1.54 – 1.41 (m, 3H), 1.17 – 0.97 (m, 3H). ¹³C NMR (151 MHz, CDCl₃) δ 191.69, 191.44, 152.19, 143.10, 141.58, 136.27, 132.65 (t), 131.65, 131.31, 131.18, 130.07, 129.20, 128.43, 128.03, 126.86 (t), 120.59, 117.27, 116.39 (t), 115.24, 61.07, 61.04, 57.17, 56.53, 30.71, 13.74, 1.01. HRMS: Calculated for [C₂₈H₂₆Cl₂F₂N₂O₃S + H₂O + H]⁺ = 597.1188, found = 597.1189.

(±) **(3-Chloro-4-(methylsulfinyl)phenyl)(4-(6-chloropyridin-2-yl)-trans-2,3-dimethylpiperazin-1-yl)methanone (35)**



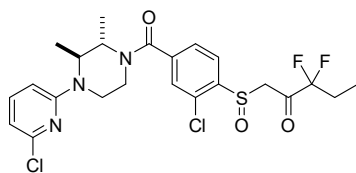
The title compound was synthesized using (±) 1-(6-chloropyridin-2-yl)-trans-2,3-dimethylpiperazine (70 mg, 0.31 mmol, 1.2 eq.) and 3-chloro-4-(methylsulfinyl)benzoic acid (57 mg, 0.26 mmol, 1 eq.) according to procedure F. This yielded the product (86 mg, 0.20 mmol, 78 %). ¹H NMR (500 MHz, CDCl₃) δ 8.04 (dd, *J* = 8.0, 3.8 Hz, 1H), 7.66 – 7.37 (m, 3H), 6.63 (dd, *J* = 7.5, 3.7 Hz, 1H), 6.48 (dd, *J* = 15.7, 8.4 Hz, 1H), 4.84 – 3.15 (m, 6H), 2.86 (d, *J* = 1.9 Hz, 3H), 1.47 – 1.04 (m, 6H). ¹³C NMR (126 MHz, CDCl₃) δ 168.83, 158.60, 149.60, 145.35, 140.04, 130.46, 128.43, 127.74, 126.38, 125.85, 112.59, 104.46, 52.20, 42.10, 41.61, 36.28, 29.72, 17.74, 14.28

(±) **1-((2-chloro-4-(4-(6-chloropyridin-2-yl)-trans-2,3-dimethylpiperazine-1-carbonyl)phenyl)sulfinyl)-3,3-difluorobutan-2-one (24)**



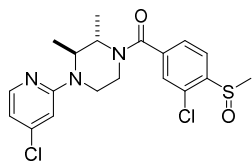
The title compound was synthesized using (±) (3-chloro-4-(methylsulfinyl)phenyl)(4-(6-chloropyridin-2-yl)-trans-2,3-dimethylpiperazin-1-yl)methanone (33 mg, 0.08 mmol, 1.0 eq.) and ethyl 2,2-difluoropropanoate (107 mg, 0.77 mmol, 10 eq.) according to general procedure I. This yielded the product (18 mg, 0.04 mmol, 45%). HRMS: Calculated for [C₂₂H₂₃Cl₂F₂N₃O₃S + H₂O + H]⁺ = 536.0984, found = 536.0984.

(±) **1-((2-Chloro-4-(4-(6-chloropyridin-2-yl)-trans-2,3-dimethylpiperazine-1-carbonyl)phenyl)sulfinyl)-3,3-difluoropentan-2-one (25)**



The title compound was synthesized using (±) (3-chloro-4-(methylsulfinyl)phenyl)(4-(6-chloropyridin-2-yl)-trans-2,3-dimethylpiperazin-1-yl)methanone (33 mg, 0.08 mmol, 1.0 eq.) and ethyl 2,2-difluorobutanoate (118 mg, 0.77 mmol, 10 eq.) according to general procedure I. This yielded the product (18 mg, 0.02 mmol, 29%). HRMS: Calculated for [C₂₃H₂₅Cl₂F₂N₃O₃S + H₂O + H]⁺ = 550.1140, found = 550.1141.

(±) **(3-chloro-4-(methylsulfinyl)phenyl)(4-(4-chloropyridin-2-yl)-trans-2,3-dimethylpiperazin-1-yl)methanone (36)**

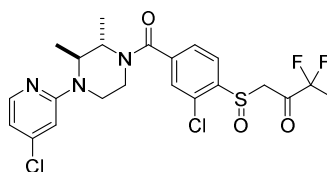


The title compound was synthesized using (±) 1-(4-chloropyridin-2-yl)-trans-2,3-dimethylpiperazine (40 mg, 0.18 mmol, 1.2 eq.) and 3-chloro-4-(methylsulfinyl)benzoic acid (32 mg, 0.15 mmol, 1 eq.)

Discovery of LEI-515 as a Novel Ultrapotent, Reversible MAGL Inhibitor with Improved Metabolic Stability

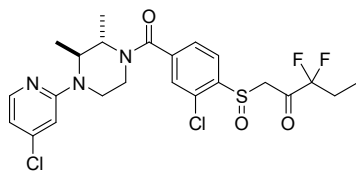
according to procedure F. This yielded the product (56 mg, 0.13 mmol, 89 %). ^1H NMR (500 MHz, CDCl_3) δ 8.40 – 7.81 (m, 2H), 7.70 – 7.33 (m, 2H), 6.94 – 6.57 (m, 2H), 5.11 – 3.06 (m, 6H), 2.89 (d, J = 4.4 Hz, 3H), 1.44 – 1.19 (m, 6H). ^{13}C NMR (126 MHz, CDCl_3) δ 169.10, 156.72, 149.65, 145.50, 144.74, 139.58, 130.74, 128.58, 126.49, 126.11, 114.61, 109.18, 53.64, 49.32, 41.53, 39.62, 36.02, 17.63, 15.48.

(\pm) **1-((2-Chloro-4-(4-(4-chloropyridin-2-yl)-trans-2,3-dimethylpiperazine-1-carbonyl)phenyl)sulfinyl)-3,3-difluorobutan-2-one (22)**



The title compound was synthesized using (\pm) (3-chloro-4-(methylsulfinyl)phenyl)(4-(4-chloropyridin-2-yl)-trans-2,3-dimethylpiperazin-1-yl)methanone (55 mg, 0.13 mmol, 1.0 eq.) and ethyl 2,2-difluoropropanoate (89 mg, 0.65 mmol, 5 eq.) according to general procedure I. This yielded the product (26 mg, 0.05 mmol, 39 %). HRMS: Calculated for $[\text{C}_{22}\text{H}_{23}\text{Cl}_2\text{F}_2\text{N}_3\text{O}_3\text{S} + \text{H}_2\text{O} + \text{H}]^+ = 536.0984$, found = 536.0983.

(\pm) **1-((2-Chloro-4-(4-(4-chloropyridin-2-yl)-trans-2,3-dimethylpiperazine-1-carbonyl)phenyl)sulfinyl)-3,3-difluoropentan-2-one (23)**

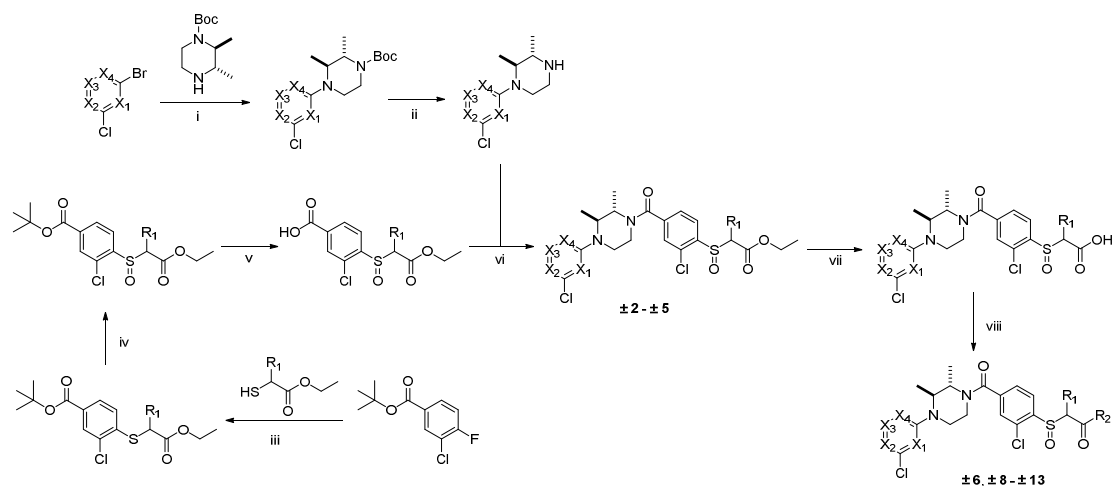


The title compound was synthesized using (\pm) (3-chloro-4-(methylsulfinyl)phenyl)(4-(4-chloropyridin-2-yl)-trans-2,3-dimethylpiperazin-1-yl)methanone (55 mg, 0.13 mmol, 1.0 eq.) and ethyl 2,2-difluorobutanoate (98 mg, 0.65 mmol, 5 eq.) according to general procedure I. This yielded the product (29 mg, 0.05 mmol, 42 %).

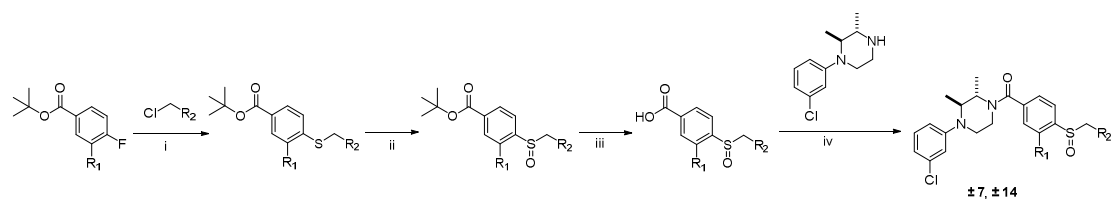
References

1. Thompson, T. N. Optimization of metabolic stability as a goal of modern drug design. *Medicinal research reviews* **2001**, 21, 412-49.
2. Masimirembwa, C. M.; Bredberg, U.; Andersson, T. B. Metabolic stability for drug discovery and development: pharmacokinetic and biochemical challenges. *Clinical pharmacokinetics* **2003**, 42, 515-28.
3. Ackley, D. C.; Rockich, K. T.; Baker, T. R. Metabolic stability assessed by liver microsomes and hepatocytes. In *Optimization in drug discovery*, Springer: 2004; pp 151-162.
4. Li, A. P. Screening for human ADME/Tox drug properties in drug discovery. *Drug discovery today* **2001**, 6, 357-366.
5. Moghaddam, M. F. Metabolite profiling and structural identification. *Pharmaceutical Sciences Encyclopedia: Drug Discovery, Development, and Manufacturing* **2010**, 1-38.
6. J Richardson, S.; Bai, A.; A Kulkarni, A.; F Moghaddam, M. Efficiency in drug discovery: liver S9 fraction assay as a screen for metabolic stability. *Drug metabolism letters* **2016**, 10, 83-90.
7. Kulkarni, A.; Riggs, J.; Phan, C.; Bai, A.; Calabrese, A.; Shi, T.; Moghaddam, M. F. Proposing advancement criteria for efficient DMPK triage of new chemical entities. *Future medicinal chemistry* **2014**, 6, 131-139.
8. Buchwald, P.; Bodor, N. Quantitative structure–metabolism relationships: Steric and nonsteric effects in the enzymatic hydrolysis of noncongener carboxylic esters. *Journal of medicinal chemistry* **1999**, 42, 5160-5168.
9. Hernández-Torres, G.; Cipriano, M.; Hedén, E.; Björklund, E.; Canales, Á.; Zian, D.; Feliú, A.; Mecha, M.; Guaza, C.; Fowler, C. J. A reversible and selective inhibitor of monoacylglycerol lipase ameliorates multiple sclerosis. *Angewandte Chemie* **2014**, 126, 13985-13990.
10. Inoue, K.; Ohe, T.; Mori, K.; Sagara, T.; Ishii, Y.; Chiba, M. Aromatic substitution reaction of 2-chloropyridines catalyzed by microsomal glutathione S-transferase 1. *Drug metabolism and disposition* **2009**, 37, 1797-1800.
11. Madhura, D. B.; Liu, J.; Meibohm, B.; Lee, R. E. Phase II metabolic pathways of spectinamide antitubercular agents: a comparative study of the reactivity of 4-substituted pyridines to glutathione conjugation. *Medchemcomm* **2016**, 7, 114-117.

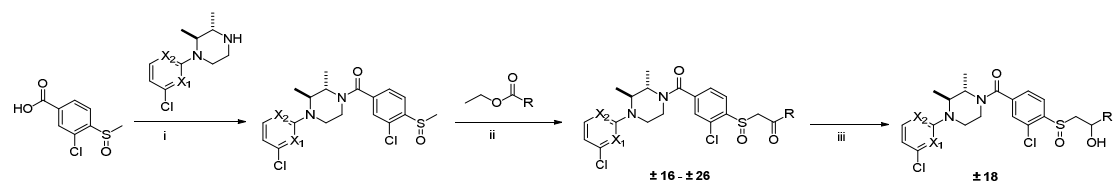
Supplementary information



Scheme S1. Synthesis route of compounds $\pm 2 - \pm 6$ and $\pm 8 - \pm 13$. Reagents and conditions: i) sodium *tert*-butoxide, BINAP, Pd(OAc)₂, 1,4-dioxane, 85 °C. ii) TFA, DCM. iii) K₂CO₃, ACN. iv) Oxone, MeOH / H₂O. v) TFA, DCM. vi) HATU, DiPEA, DCM. vii) TEA, MeOH, H₂O. viii) appropriate alcohol or amine, oxalyl chloride, DiPEA, DCM.



Scheme S2. Synthesis route of compounds ± 7 and ± 14 . Reagents and conditions: i) NaHS, K₂CO₃, DMF. ii) Oxone, MeOH / H₂O. iii) TFA, DCM. iv) HATU, DiPEA, DCM.



Scheme S3. Synthesis route of compounds $\pm 16 - \pm 26$. Reagents and conditions: i) HATU, DiPEA, DCM. ii) LDA, THF, -78 °C. iii) NaBH₄, MeOH.

Chapter 5

LEI-515 is an orally available and peripherally restricted MAGL inhibitor

M. Jiang, T. van der Wel, F. Stevens, X. Di, P. M. Gomezbarila, J. P. Medema, J. Benz, U. Grether, B.F. Florea, R. van den Berg, C. A. A. van Boeckel, M. van der Stelt*; *manuscript in preparation.*

5.1 Introduction

Monoacylglycerol lipase (MAGL) is a 33 kDa serine hydrolase that catalyzes the hydrolysis of monoacylglycerols to corresponding fatty acids and glycerol^{1,2}. Although MAGL is expressed throughout the body in various organs, such as liver, lung, testis and adipose tissue,³ most of the current interest in the target has emerged from the finding that it is responsible for the bulk (~85%) of the metabolism of the signaling lipid 2-arachidonoyl glycerol (2-AG) in the brain⁴. 2-AG is an endocannabinoid and behaves as a full agonist for the cannabinoid CB1 and CB2 receptors.⁵⁻⁷ 2-AG plays important roles in the regulation of many physiological processes, such as neuro-inflammation⁸, food intake⁹, pain and addiction¹⁰. It was also demonstrated that disrupting MAGL activity significantly reduced the levels of arachidonic acid (AA) and downstream AA-derived eicosanoids in the brain. Therefore, inhibition of MAGL could

have several therapeutic applications, like neuroprotection, anti-neuroinflammation and antinociception.¹¹ To date, most reported MAGL inhibitors have been designed to target the central nervous system (CNS) (See Chapter 1).¹²⁻¹⁵

Of note, MAGL blockade exerted also protective effects in lung and liver injury models through enhancing endocannabinoid and lowering eicosanoid levels.^{16, 17} Since MAGL only controls eicosanoid metabolism in specific tissues such as the brain, liver and lung, but not in the gut¹⁸, MAGL inhibitors might avoid some of the mechanism-based gastrointestinal and cardiovascular side effects observed with dual cyclooxygenase 1/2 (COX1/2) and selective COX2 inhibitors¹⁹. It is suggested that MAGL inhibitors may even protect against COX inhibitor-induced gastrointestinal injury via endocannabinoid-dependent mechanisms.^{18, 20} Moreover, pharmacological and genetical inhibition of MAGL reduced tumor growth in ovarian, melanoma and prostate xenograft models.^{21, 22} Therefore, development of selective peripherally restricted MAGL inhibitor may be of great value for the treatment of inflammatory and cancer.

In this chapter, **LEI-515** (Figure 1), which was identified in chapter 4 as a subnanomolar potent MAGL inhibitor with a pKi of 9.4, is further profiled in biochemical, cellular and ADME-T assays as well as mouse pharmacokinetic and target engagement studies to assess its ability to act as a reversible and in vivo active MAGL inhibitor.

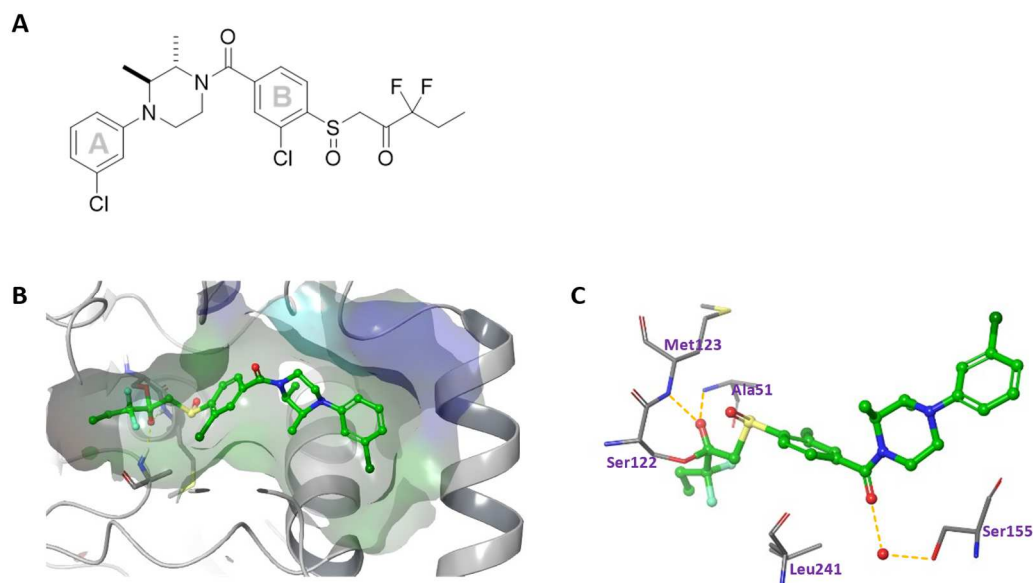


Figure 1. (A) Chemical structure of **LEI-515**. (B, C) X-ray cocrystal structure of **LEI-515** bound to hMAGL.

5.2 Results

LEI-515 is thought to inhibit MAGL via forming a covalent, though reversible, enzyme-inhibitor hemiketal adduct. To investigate this hypothesis, co-crystallization studies were performed using human recombinant MAGL²³ and racemic **LEI-515**. The X-ray structure of one isomer of **LEI-515** (1-((2-Chloro-4-((2*S*,3*S*)-4-(3-chlorophenyl)-2,3-dimethylpiperazine-1-carbonyl)phenyl)sulfinyl)-3,3-difluoropentan-2-one) bound to MAGL was obtained and solved at 1.55 Å resolution (Figure B and C). **LEI-515** was found to covalently attach to the catalytic Ser122 residue through its electrophilic carbonyl group as a deprotonated hemiketal. The negative charge was stabilized by two hydrogen bonds (yellow dotted lines, Figure 3C) with Ala51 and Met123, respectively. The terminal ethyl group inserted into the hydrophilic cytoplasmic access (CA) channel, while the rest of the compound occupies the large hydrophobic tunnel and the terminal chlorophenyl ring (ring A) orientated to the lid domain. The chloro group on ring B occupied a hydrophobic subpocket and the two methyl groups on the piperazine ring adopt a di-axial conformation, which enhance the hydrophobic interaction. The carbonyl of the amide group formed a water-mediated hydrogen bond with the side chain of Ser155.

Next, the selectivity of **LEI-515** over a panel of serine hydrolases was assessed by using activity-based protein profiling (ABPP), which has emerged as a powerful chemical biological technique to assess inhibitor activity and selectivity in complex and native proteomes.^{24, 25} It makes use of activity-based probes (ABPs) to assess the functional state of entire enzyme classes directly in biological systems. Fluorophosphonates (FPs) and β -lactones are used as ABPs targeting serine hydrolases.^{26, 27} ABPs with fluorescent reporter groups enable visualization of enzyme activities in complex proteomes by SDS–polyacrylamide gel electrophoresis (SDS-PAGE) and in-gel fluorescence scanning, while ABPs with a biotin reporter group enable affinity enrichment and identification of enzyme activities by mass spectrometry (MS)-based proteomics.²⁶ As shown in Figure 2A, **LEI-515** reduced MAGL activity in a dose-dependent manner with a half maximal inhibitory concentration (IC_{50}) of 25 nM in mouse brain proteome and displayed >500-fold selectivity over diacylglycerol lipase (DAGL- α) and α/β -hydrolase domain containing 6 and 12 (ABHD6 and 12), which are enzymes involved in 2-AG biosynthesis and degradation, respectively. Moreover, **LEI-515** did not inhibit fatty acid amide hydrolase (FAAH), which degrades the other endocannabinoid anandamide. Mass spectrometry (MS)-based chemical proteomics using MB108 and FP-biotin confirmed the gel-based ABPP findings²⁸. **LEI-515** did not reduce labeling of the detected proteins by more than 50%, except for MAGL and identified only hormone sensitive lipase (LIPE) as a potential off-target in lung, liver and brain (Figure 2B). Next, **LEI-515** was profiled for general off-target pharmacology in a binding/functional panel comprising a panel of 44 enzymes, transporters, receptors, and ion channel targets (CEREP). **LEI-515** showed >100-fold selectivity over those ion channels, receptors and enzymes, including the cannabinoid receptors (CB1R and CB2R), hERG channel and cyclooxygenases (COX1 and COX2) (Table S1).

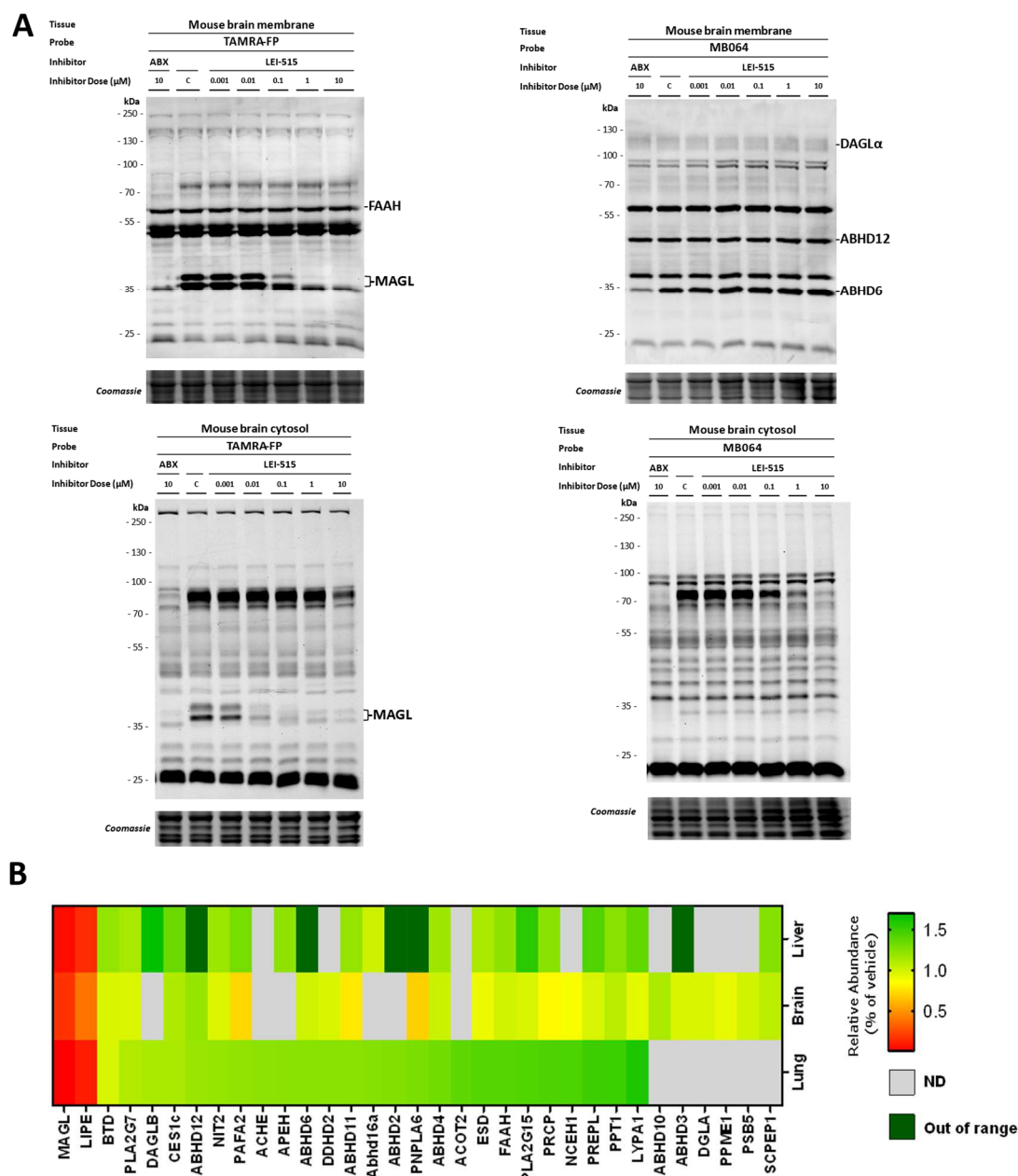


Figure 2. Selectivity profiling of **LEI-515**. (A) Competitive ABPP with **LEI-515** in mouse brain proteome using broad-spectrum probes TAMRA-FP (100 nM, 10 min) and MB064 (250 nM, 10 min). (B) Selectivity profiles of **LEI-515** on mouse brain, lung and liver proteomes using broad-spectrum probes MB108 and FP-biotin (10 μ M, 60min) for chemical proteomics (N = 4).

To determine the mode-of-action (covalent reversible versus irreversible) of **LEI-515**, mouse brain membrane proteome was pre-incubated with **LEI-515** or the irreversible MAGL inhibitor ABX-1431 at the IC₈₀ concentration and the remaining MAGL activity was visualized with an irreversible MAGL-specific probe LEI-463²⁹ in a time-dependent manner. No recovery of MAGL activity was found for ABX-1431,

whereas MAGL activity was regained after approximately 40 min with **LEI-515** (Figure 3A and B). This indicated that **LEI-515** is a reversible MAGL inhibitor.

Having established that **LEI-515** is a selective covalent, reversible MAGL inhibitor, we then investigated whether **LEI-515** inhibits endogenous MAGL in living cells. To this end, a panel of human breast cancer cell lines was screened with MAGL-specific probe for endogenous MAGL activity, in which four cell lines (UACC893, MDA-MB-415, HS578t and MDA-MB-435s) were found to express high level of MAGL protein and activity (Figure S1). HS578t was selected as a representative example for cellular target engagement studies using targeted lipidomics. The cells were incubated with **LEI-515** and the cellular 2-AG and AA levels were determined with liquid chromatography–mass spectrometry/mass spectrometry (LC-MS/MS). **LEI-515** increased 2-AG levels in a time-dependent manner and the cellular 2-AG level reached a plateau (around 2000 fmol/mg) after 1 h inhibitor incubation (Figure 3C). Treatment of intact HS578t cells with **LEI-515** following an 1 h inhibitor incubation time caused concentration dependent inhibition of MAGL activity with an IC_{50} value between 300 nM and 1 μ M (Figure 3D), which is over 600-fold less potent than that observed in the biochemical assay (Chapter 4, Table 3). One potential explanation for the gap is that the local 2-AG concentration in the intact cells is higher than in the biochemical assay. In addition, **LEI-515** also decreased the cellular level of AA and anandamide (AEA) (Figure 3E). It is normal to see a reduction of AA level as AA is the product of 2-AG hydrolysis and the decreased AA level might cause the reduction of AEA level.

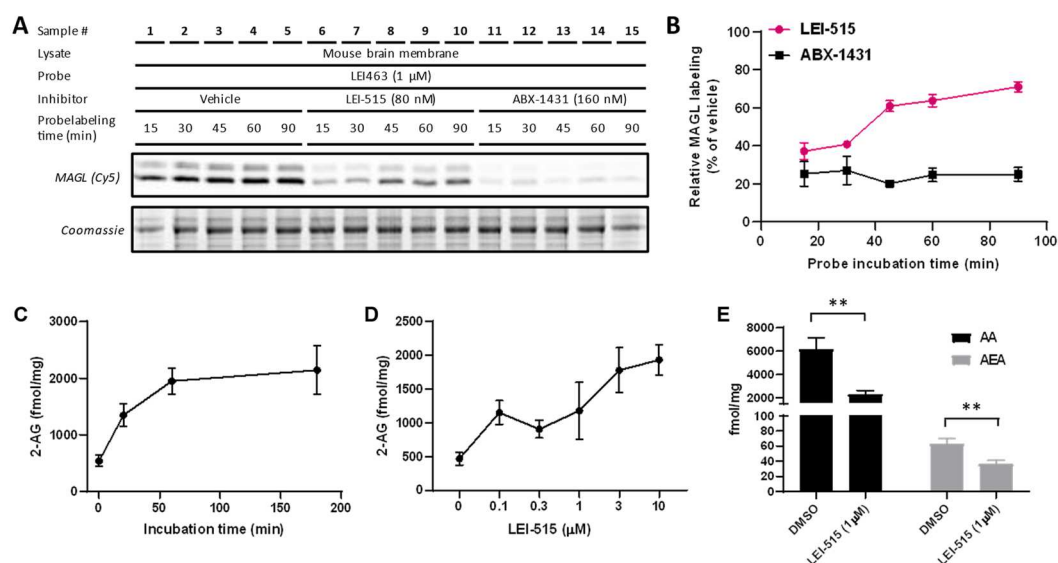


Figure 3. Reversibility profiling of **LEI-515**. (A, B) Time-dependent recovery of MAGL activity as determined by using competitive ABPP with MAGL selective probe LEI-463. Mouse brain proteome (2 mg/ml) was preincubated with **LEI-515** (10 min) or ABX-1431 (15 min). (C) *In situ* treatment of HS578t cells with **LEI-515** (1 μ M) time-dependently increased cellular 2-AG levels (N = 5). (D) *In situ* treatment of HS578t cells with **LEI-515** (1 h) dose-dependently increased cellular 2-AG levels (N = 4). (E) *In situ* treatment of HS578t cells with **LEI-515** (1 μ M, 1 h) decreased cellular AA and AEA levels. Statistical analysis: one-way ANOVA (***) = $p < 0.001$, ** = $p < 0.01$, * = $p < 0.05$ vs vehicle).

Inhibition of MAGL has been shown to suppress tumorigenesis and progression in a number of cancer cell lines, including colorectal cancer cells.^{30, 31} To investigate whether **LEI-515** inhibits cancer cell growth, a cell viability assay was performed. Eighteen colorectal cancer cell lines were incubated with **LEI-515** for 72 h in delipidated medium and the cell viability was determined. **LEI-515** impaired those colorectal cancer cells growth with concentration for 50% of maximal effect (EC_{50}) in the range from 2 to 20 μ M, except for MDST8, LS1031 and Snu-c1 cell lines (Figure 4). The EC_{50} values were plotted against MAGL mRNA levels in the colorectal cancer cell lines and no correlation was found. Actually, **LEI-515** showed higher EC_{50} on the cell lines with lower MAGL mRNA level (Figure S2). This might due to off-target effects of **LEI-515**, such as the inhibition of LipE. It would be interesting to also determine the MAGL and LipE protein levels with western blot and MAGL activity levels with ABPP in those cell lines.

Before testing whether **LEI-515** possesses *in vivo* efficacy, the absorption,

distribution, metabolism and excretion (ADME) profile of **LEI-515** was determined. **LEI-515** demonstrates acceptable physicochemical properties for oral bioavailability (MW = 531 Da, cLogP = 4.7 and topological polar surface area (tPSA) = 58 Å²). **LEI-515** shows high stability (100 % remaining after 180 min) in both human and mouse plasma. Clearance in human microsomes (30.9 µL/min/mg) is moderate and low in mouse microsomes (< 3.4 µL/min/mg). **LEI-515** exhibits high human and mouse protein binding (99.6% for both). **LEI-515** shows negligible cell permeability in Caco-2 cells ($P_{appA-B} < 0.01 \times 10^{-6}$ cm/s and $P_{appB-A} < 0.005 \times 10^{-6}$ cm/s). This might be due to the specific binding of **LEI-515** with endogenous MAGL in Caco cells or transporter proteins which efflux **LEI-515** out of the cells. Pharmacokinetic analysis (DMSO/Kolliphore/5% mannitol in water (1/1/8, v/v) was used as vehicle) (Figure 5) for **LEI-515** in male C57BL/6J mice reveals a moderate clearance (CL = 35 mL/min/kg) and volume of distribution ($V_{ss} = 2.1$ L/kg), resulting in a half-life of 4.5 h. In the same species **LEI-515** shows excellent bioavailability after oral administration ($F_{po} = 81$ %) and quick absorption ($T_{max} = 0.5$ h). These results are contradictory with the result from Caco-2 assay. A possible explanation is that the compound was directly absorbed through the stomach. Most interestingly, the brain to plasma ratio was 0.01 at maximum serum concentration (C_{max}), which demonstrates that **LEI-515** is a peripherally restricted MAGL inhibitor.

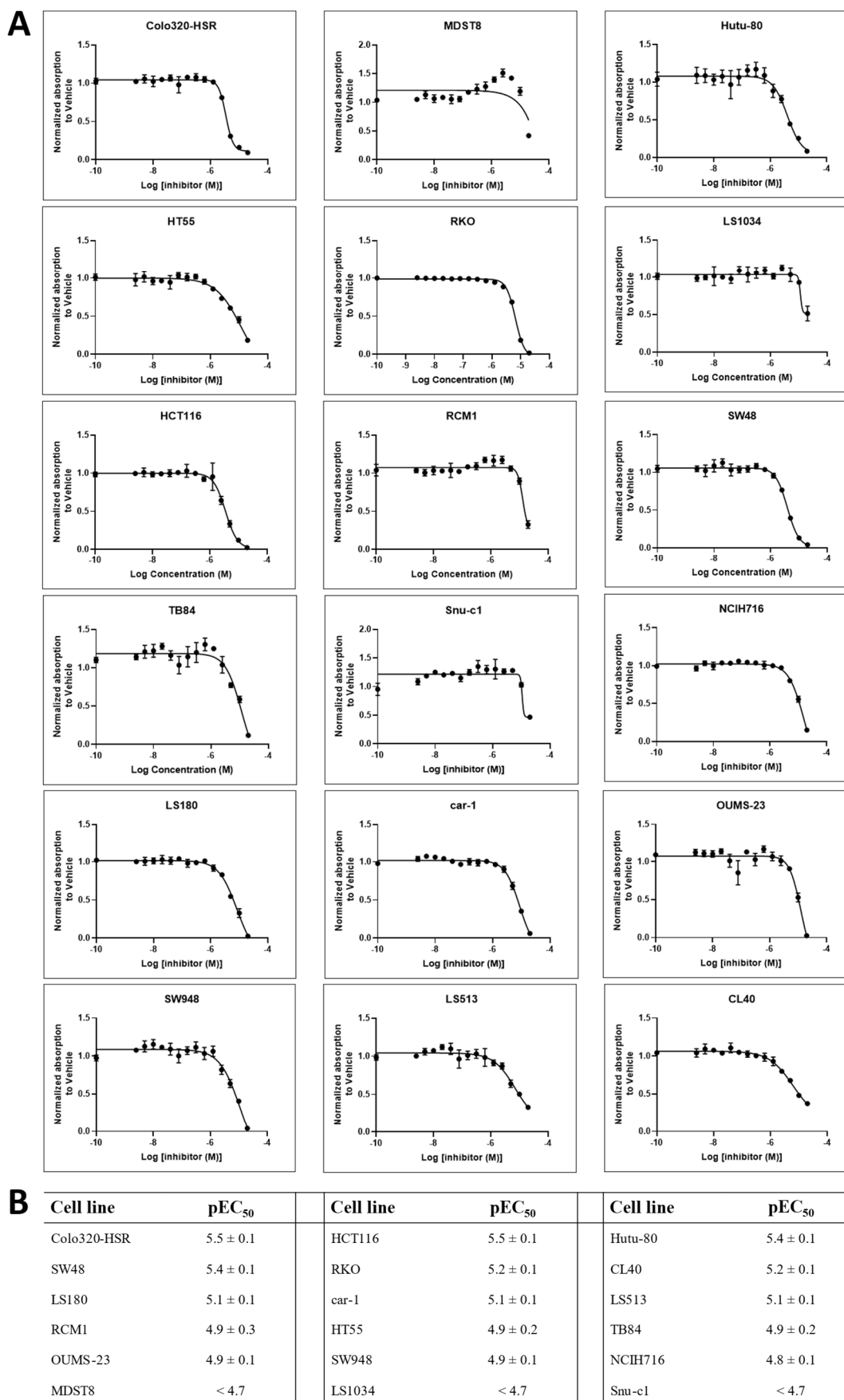


Figure 4. Anti-cancer effects of LEI-515 on 18 colorectal cancer cell lines (n = 3).

In view of the encouraging PK properties, *in vivo* target engagement experiments were performed. Male C57/6J mice were treated with LEI-515 (3 and 10 mg/kg, p.o.) or vehicle (DMSO/Kolliphore/5% mannitol in water (1/1/8, v/v)) and then sacrificed after 1h to determine whether 2-AG levels were elevated. To this end, lipid levels as well as **LEI-515** concentration in the brain and lung were analyzed by LC-MS. **LEI-515** appeared to increase 2-AG levels and decrease AA levels in the lung at 10 mg/kg. However, the difference is not statistically significant (Figure 6A). The lack of effect might be due to the high protein binding of the compound, which may have reduced the available free fraction of **LEI-515**, or insufficient exposure time. Of note, a correlation ($R^2 = 0.7$, $q < 0.001$) between LEI-515 concentration and 2-AG levels in the lung was observed (Figure S3). No significant change of the 2-AG, AA and eicosanoids levels in the brain was observed after treatment of **LEI-515** (Figure 6B and Figure S3), which is in agreement with the reduced brain penetration.

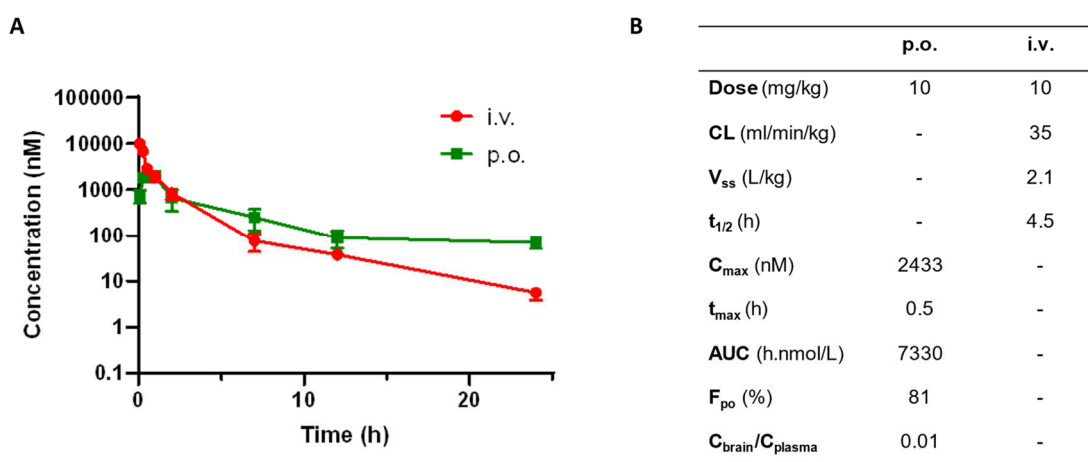


Figure 5. Pharmacokinetics (PK) profile of **LEI-515** in C57BL/6J mice. (A) *In vivo* PK of **LEI-515** in plasma of mice via intravenous (i.v., 10 mg/kg) or oral (p.o., 10 mg/kg) administration. (B) PK parameters of **LEI-515** in mice after p.o. and i.v. administration. CL = clearance. V_{ss} = volume of distribution at steady state. $t_{1/2}$ = half life. C_{max} = maximum plasma drug concentration. t_{max} = time to reach C_{max} . AUC = area under plasma concentration time curve. F_{po} = bioavailability.

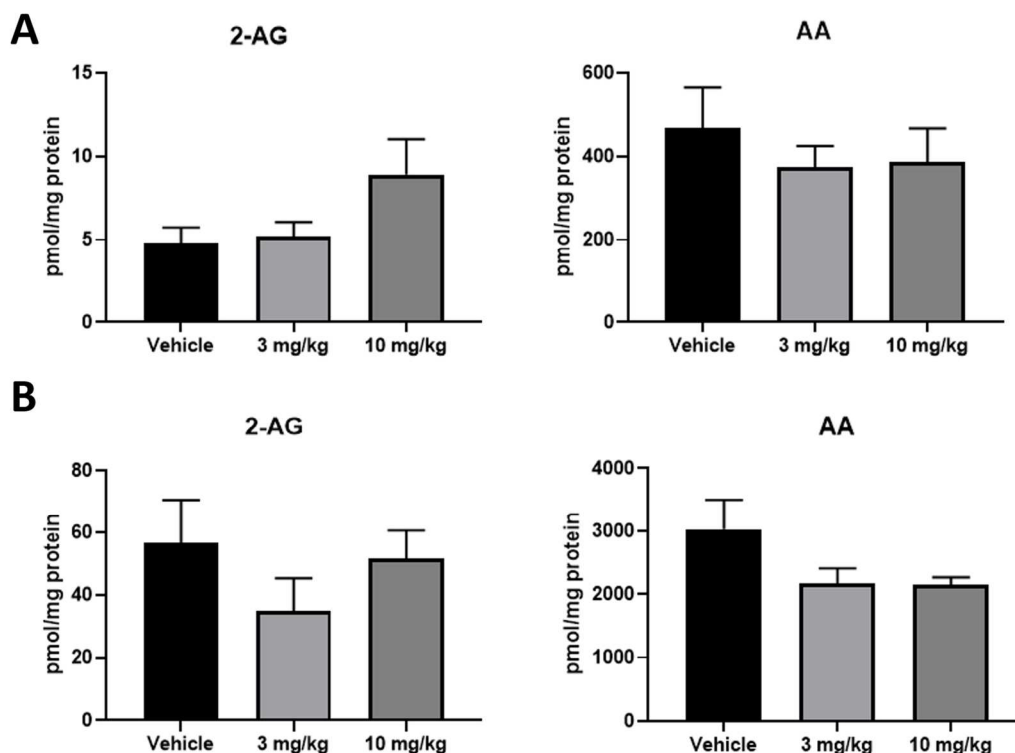


Figure 6. *In vivo* target engagement of **LEI-515** in C57BL/6J mice. (A) Absolute lipid levels of 2-AG and AA in the lung (n = 5). (B) Absolute lipid levels of 2-AG and AA in the brain (n = 5).

5.3 Conclusion

In conclusion, crystallography studies showed that **LEI-515** bound to MAGL covalently and only one isomer of **LEI-515** (1-((2-Chloro-4-((2*S*,3*S*)-4-(3-chlorophenyl)-2,3-dimethylpiperazine-1-carbonyl)phenyl)sulfinyl)-3,3-difluoropentan-2-one) was observed in the binding pocket. Comparative and competitive chemical proteomics using broad-spectrum probes (MB-064 and TAMRA-FP) in combination with MAGL-specific probe **LEI-463** was applied to characterize the MAGL inhibitor **LEI-515**. This inhibitor was found to be a reversible MAGL inhibitor with high selectivity against a panel of serine hydrolases, enzymes, receptors and ion channels. Targeted lipidomics revealed that **LEI-515** is able to increase 2-AG levels in a time- and concentration-dependent manner in human breast cancer cells and could inhibit cell proliferation in an array of colon cancer cell lines. Pharmacokinetics studies demonstrated that **LEI-515** is an orally available and peripherally restricted MAGL inhibitor. According to our

knowledge, **LEI-515** is the first and most selective peripherally restricted MAGL inhibitor to date. **LEI-515** showed low *in vivo* efficacy, which might be due to the high protein binding or insufficient exposure time. For future investigation, the *in vivo* target engagement experiment should be repeated with higher dosing (such as 30 mg/kg) or longer exposure time (such as 2 h.). It would also be interesting to study **LEI-515** in various animal models of human diseases, such as hepatic ischemia/reperfusion (I/R), lung I/R and cancer. Taken together, **LEI-515** could be a useful compound to study MAGL function in peripheral tissues without disturbing the MAGL activity in the CNS or further developed as drug candidate with limited central side effects.

5.4 Experimental procedures

Crystallization studies. Human MAGL protein with mutations introduced at positions Lys36Ala, Leu169Ser and Leu176Ser²³ was concentrated to 10.8 mg/ml. Crystallization trials were performed in sitting drop vapor diffusion setups at 21 °C. Crystals appeared within 2 days out of 0.1M MES pH 6.5, 6 to 13% PEG MME5K, 12% isopropanol. Crystals were soaked in crystallization solution supplemented with 10 mM LEI-515 for 16 hours.

For data collection crystals were flash cooled at 100 K with 20 % ethylene glycol added as cryo- protectant. X-ray diffraction data were collected at a wavelength of 1.00009 Å using an Eiger2X 16M detector at the beamline X10SA of the Swiss Light Source (Villigen, Switzerland). Data have been processed with XDS³² and scaled with SADABS (BRUKER). The crystals belong to space group C222₁ with cell axes of a= 91.62 Å, b= 127.57 Å, c= 60.36 Å with $\beta=90.57^\circ$ and diffract to a resolution of 1.55Å. The structure was determined by molecular replacement with PHASER³³ using the coordinates of PDB entry 3pe6²³ as search model. Difference electron density was used to place LEI-515. The structure was refined with programs from the CCP4 suite³⁴. Manual rebuilding was done with COOT³⁵. Data collection and refinement statistics are summarized in Table 1.

Preparation of mouse tissue proteome. Mouse tissues were isolated according to guidelines approved by the ethical committee of Leiden University. Isolated tissues were thawed on ice, dounce homogenized in lysis buffer A (20 mM HEPES, 2 mM DTT, 1 mM MgCl₂, 25 u/ml Benzonase, pH 7.2) and incubated for 15 min on ice. Then debris was removed by low-speed spin (2500 g, 1 min, 4 °C) and the supernatant was subjected to ultracentrifugation (100.000 g, 45 min, 4 °C, Beckman Coulter, Type Ti70 rotor) to yielded the membrane fraction as a pellet and the cytosolic fraction in the supernatant. The membrane fraction was resuspended in lysis buffer B (20 mM HEPES, 2 mM DTT). The total protein concentration was determined with Quick Start Bradford assay. The obtained membranes and supernatant were flash frozen in liquid nitrogen and stored in small aliquots at -80 °C until use.

Activity based protein profiling on mouse brain proteome. The competitive ABPP assay on mouse brain proteome was performed as previously reported.³⁶ In brief, to 19 μ l mouse brain proteome (2mg/ml) was added 0.5 μ l of the inhibitor or pure DMSO, vortexed gently and incubated for 30 min at RT. Subsequently, 0.5 μ l probe was added to the proteome sample, vortexed gently and incubated for 10 min. The reaction was quenched by adding 10 μ l of 4*Laemmli-buffer and 10 μ l of quenched reaction mixture was resolved on 10 % acrylamide SDS-PAGE (180V, 75 min). Fluorescence was measured using a Biorad ChemiDoc MP system. Gels were then stained using Coomassie staining and imaged for protein loading control.

Table 1: Data collection and refinement statistics for human MAGL LEI-515 complex.

hMAGL-LEI-515 complex	
Data collection	
Space group	C222 ₁
Cell dimensions	
<i>a, b, c</i> (Å)	91.62, 127.57, 60.36
α, β, γ (°)	90, 90, 90
Resolution (Å)	1.55 (1.65-1.55)
<i>R</i> _{sym} or <i>R</i> _{merge}	0.059 (0.78)
<i>I</i> / σ <i>I</i>	11.69 (1.13)
Completeness (%)	99.6 (99.4)
Redundancy	6.62 (6.16)
Refinement	
Resolution (Å)	48.3 – 1.55
No. reflections	48898
<i>R</i> _{work} / <i>R</i> _{free}	15.43/18.03
No. atoms	
Protein	2299
Water	325
Ligand	34
<i>B</i> -factors	
Protein	25.56
Water	47.53
Ligand	33.07
R.m.s. deviations	
Bond lengths (Å)	0.016
Bond angles (°)	1.999

*Values in parentheses are for highest-resolution shell.

Chemical proteomics. Activity-based proteomics was performed based on previously described procedures.³⁷ Mouse tissue proteome (245 μ L, 2.0 mg/mL) membrane or soluble fraction was incubated with vehicle (DMSO) or inhibitor (1 μ M) in DMSO for 30 minutes at 37 °C. The proteome was labeled with a probe cocktail (2.5 μ M MB108 and 5 μ M FP-Biotin, 30 minutes, 37 °C). Subsequently the labeling reaction was quenched and excess probe was removed by chloroform methanol precipitation. Precipitated proteome was suspended in 250 μ L 6M Urea/25 mM ammonium bicarbonate and allowed to incubate overnight. 2.5 μ L (1 M DTT) was added and the mixture was heated to 65 °C for 15 minutes. The sample was allowed to cool to rt before 20 μ L (0.5 M) iodoacetamide was added and the sample was alkylated for 30 minutes in the dark. 70 μ L 10% (wt/vol) SDS was added and the proteome was heated for 5 minutes at 65 °C. The sample was diluted with 6 mL PBS. 100 μ L of 50% slurry of Avidin–Agarose from egg white (Sigma-Aldrich) was washed with PBS and added to the proteome sample. The beads were incubated with the proteome > 3h. The beads were isolated by centrifugation and washed with 0.5% (wt/vol) SDS and PBS (3x). The proteins were digested overnight with sequencing grade trypsin (Promega) in 250 μ L OB-Dig buffer (100 mM Tris, 100 mM NaCl, 1 mM CaCl₂, 2 % ACN and 500 ng trypsin) at 37 °C with vigorous shaking. The pH was adjusted with formic acid to pH 3 and the beads were removed and the beads were removed from filtration. The peptides were washed and eluted with stage tips according to the procedure below.

Step	Solution	Centrifugation speed
Conditioning 1	50 μ L MeOH	2 min 300g
Conditioning 2	50 μ L Stage tip solution B	2 min 300g
Conditioning 3	50 μ L Stage tip solution A	2 min 300g
Loading		2 min 600g
Washing	100 μ L Stage tip solution A	2 min 600g
Elution	100 μ L Stage tip solution B	2 min 600g

Stage tip solution A: 0.5% (vol/vol) FA in H₂O. (Freshly prepared solution)

Stage tip solution B: 0.5% (vol/vol) FA in 80% (vol/vol) ACN/H₂O. (Freshly prepared solution).

After the final elution step, the obtained peptides were concentrated on a speedvac to remove the ACN. The residue was reconstituted in 95:3:0.1 H₂O/ACN/FA (vol/vol) before LC/MS analysis.

For LC-MS analysis, each sample in duplicate was loaded onto the ultra-performance liquid chromatography-ion mobility spectrometry-mass spectrometry system a NanoACQUITY UPLC System coupled to SYNAPT G2-Si high-definition mass spectrometer³⁷. A trap-elute protocol was followed, where 1 μ L of the digest was loaded on a trap column (C18 100 Å, 5 μ M, 180 μ Mx20 mm; Waters), followed by elution and separation on an analytical column (HSS-T3 C18 1.8 μ M, 75 μ Mx250 mm; Waters). The sample was loaded onto this column at a flow rate of 10 μ L/min with 99.5% solvent A for 2 minutes before switching to the analytical column. Peptide separation was achieved by using a multistep concave gradient based on gradients previously described³⁸. The column was re-equilibrated to initial conditions after washing with 90% solvent B as previously described³⁸. The rear seals of the pump were flushed every 30 minutes with 10% (v/v) acetonitrile. [Glu1] fibrinopeptide B was used as a lock mass compound. The auxiliary pump of the LC system was used to deliver this peptide to the reference sprayer (0.2 μ L/min). An ultradefinition MSE method was set up as previously described³⁸. Briefly, the mass range was set at 50-2,000 Da, with a scan time of 0.6 seconds in positive resolution mode. The collision energy was set to 4 V in the trap cell for low-energy MS mode. For the elevated energy scan, the transfer cell collision energy was ramped using drift-time specific collision energies. The lock mass was sampled every 30 seconds.

Targeted lipidomics

The targeted lipidomics experiments are based on previously reported methods with small alterations²⁶.

Cell culture. All cells were cultured at 37 °C and 7 % CO₂ in RPMI-1640 with GlutaMax (2 mM), penicillin (100 μ g/ml), streptomycin (100 μ g/ml) and 10 % fetal bovine serum (Biowest).

Activity based protein profiling in breast cancer cells. The cells pellets were suspended in lysis buffer (20 mM HEPES pH7.2, 2 mM DTT, 1 mM MgCl₂, 25 u/ml

Benzonase) and homogenized. The protein **ABPP in human breast cancer cells**. Cell pellets were suspended in lysis buffer (20 mM HEPES pH 7.2, 2 mM DTT, 1 mM MgCl₂, 25 u/mL Benzonase) and homogenized. The protein concentration was determined by Quick Start Bradford assay (Biorad). The breast cancer cell proteome (2 mg/ml) was incubated with ABP LEI-463 (100 nM) for 30 min. Then the reaction was quenched with standard SDS PAGE sample buffer. Gels were scanned using a ChemiDoc MP system.

Western Blot. Proteins on SDS-PAGE gels were transferred to 0.2 µm PVDF membranes using the Trans-Blot Turbo transfer system (Bio-Rad) and blocked with blocking buffer (5% (w/v) milk in 10 mL TBS-Tween) for 1 hour. Membranes were stained with primary rabbit anti-MAGL antibody (Abcam #ab24701; 0.5% (v/v) in 2 mL blocking buffer) for 16h at 4°C. After three washing steps with TBS-Tween, goat anti-rabbit IgG-HRP antibody (Santa Cruz sc-2030; 0.02% (v/v) in 2 mL blocking buffer) was added and incubated for 1 hour at rt. The blot was washed three times with TBS-Tween and once with TBS before analysis. All washing steps were performed with 5 mL for 10 min. The western blot was visualized by discarding the TBS buffer and addition of imaging solution (10 mL luminal, 100 µL ECL enhancer, 3 µL H₂O₂) in the dark. After 5 minutes, the blot was scanned for chemiluminescence. Actin was used as a loading control. After imaging, blots were blocked as previously described and stained with primary mouse anti-Actin antibody (Abcam #ab8226; 0.1 (v/v) in 2 mL blocking buffer) for 1 hour at rt. After washing, blots were stained with secondary goat anti-mouse IgG-HRP antibody (Santa Cruz sc-2031; 0.02% (v/v) in 2 mL blocking buffer) for 1 hour at rt. After washing three times with TBS-Tween and once with TBS, blots were scanned for chemiluminescence. Images were analyzed with Image Lab 4.1.

Lipidomics Sample preparation. Here, 3×10^6 HS578t cells were seeded 1 d before treatment in 10 cm dishes. Before treatment, cells were washed twice with warm PBS and then treated with vehicle or compound in 10 ml medium without serum. Washing with cold PBS (1×) followed by gathering in 1.5 ml Eppendorf tubes and centrifugation (10 min, 1,500 r.p.m.). PBS was removed and the cell pellets were flash frozen with liquid nitrogen and stored at -80 °C. Next, 10% of each cell sample (collected during

harvesting) was used to determine the protein concentration using a Bradford assay (Bio-Rad) for normalization after lipid measurements.

Lipid extraction. Lipid extraction was performed on ice. Samples were thawed on ice and spiked with 10 μ L deuterium labeled internal standard mix (Table 1), vortex and incubate for 5 minutes on ice. Subsequently 100 μ L 0.5 % sodium chloride and 100 μ L ammonium acetate buffer (0.1 M, pH 4) were added. After extraction with 1 mL methyl tert-butyl ether (MTBE), tubes were thoroughly mixed for 7 min using a bullet blender blue (Next advance Inc., Averill park, NY, USA) at speed 8, followed by a centrifugation step (16,000g, 11 min, 4 °C). Next, 925 μ L of the upper MTBE layer was transferred into a clean 1.5 mL Safe-Lock Eppendorf tube. Samples were dried in a speedvac (Eppendorf, 45 min, 30 °C) and reconstituted in acetonitrile/water (30 μ L, 90:10, v/v). The samples were thoroughly mixed for 4 min, followed by a centrifugation step (10,000g, 4 min, 4°C) and transferred to a LC-MS vial (9 mm, 1.5 mL, amber screw vial, KG 090188, Screening Devices) with insert (0.1 mL, tear drop with plastic spring, ME 060232, Screening devices). 5 μ l of each sample was injected in to the LC-MS/MS system.

LC-MS/MS Analysis. A targeted analysis of 26 compounds, including endocannabinoids, related N-acylethanolamines (NAEs) and free fatty acids (Table 2), was measured using an Acquity UPLC I class binary solvent manager pump in conjugation with a tandem quadrupole mass spectrometer as mass analyzer (Waters Corporation, Milford, USA). The separation was performed with an Acquity HSS T3 column (2.1 \times 100 mm, 1.8 μ m) maintained at 45 °C. The aqueous mobile phase A consisted of 2 mM ammonium formate and 10 mM formic acid, and the organic mobile phase B was acetonitrile. The flow rate was set to 0.55 mL/min; initial gradient conditions were 55 % B held for 0.5 min and linearly ramped to 60 % B over 1.5 min. Then the gradient was linearly ramped to 100 % over 5 min and held for 2 min; after 10 s the system returned to initial conditions and held 2 min before next injection. Electrospray ionization-MS and a selective Multiple Reaction Mode (sMRM) was used for endocannabinoid quantification. Individually optimized MRM transitions using their synthetic standards for target compounds and internal standards are described in 180

Table 2. Peak area integration was performed with MassLynx 4.1 software (Waters Corporation). The obtained peak areas of targets were corrected by appropriate internal standards peak area. Calculated response ratios, determined as the peak area ratios of the target analyte to the respective internal standard peak area, were used to obtain absolute concentrations from their respective calibration curves.

Table 2: LC-MS Standards and deuterium labeled internal standards for lipidomics analysis. Q1 and Q3 are optimized precursor ion and product ion respectively and expressed as m/z. DP and CE are declustering potential (volt) and collision energy (Volt) respectively.

Abbreviation	Name	Q1	Q3	DP, CE	Polarity
1 & 2-AG (20:4)	1-Arachidonoyl Glycerol	379.21	287.2	45, 10	+
1-LG (18:2)	1-Linoleoyl Glycerol	355.34	246	48, 10	
2-LG (18:2)	2-Linoleoyl Glycerol	357.34	247.5	48, 10	
2-OG (18:1)	2-Oleoyl Glycerol	357.34	247.5	40, 12	
1-OG (18:1)	1-Oleoyl Glycerol	357.34	247.5	40, 12	
AEA (20:4)	Arachidonoyl Ethanolamide	348.40	62.02	35, 16	
DEA (22:4)	Docosatetraenoyl Ethanolamide	376.38	61.92	55, 18	
DGLEA (18:3)	Dihomo- γ -Linolenoyl Ethanolamide	350.38	61.98	40, 14	
DHEA (22:6)	Docosahexaenoyl Ethanolamide	372.38	62.01	50, 14	
EPEA (20:5)	Eicosapentaenoyl Ethanolamide	346.34	61.98	36, 16	
LEA (18:2)	Linoleoyl Ethanolamide	324.34	61.98	35, 14	
OEA (18:1)	Oleoyl Ethanolamide	326.4	62.01	45, 16	
PDEA (15:0)	Pentadecanoyl Ethanolamide	286.34	62.01	45, 12	
PEA (16:0)	Palmitoyl Ethanolamide	300.34	61.98	42, 14	
POEA (16:1)	Palmitoleoyl Ethanolamide	298.34	62.01	45, 14	
SEA (18:0)	Stearoyl Ethanolamide	328.38	61.98	45, 16	
AA (20:4)	Arachidonic Acid	302.28	259.3	-40, -12	

Chapter 5

PA (FA 16:0)	Palmitic Acid	255.33	237.24	-50, -20
SA (FA 18:0)	Stearic Acid	283.34	265.31	-60, -22
OA (FA 18:1)	Oleic Acid	281.34	263.31	-50, -20
LA (FA 18:2)	Linoleic Acid	279.34	261.25	-64, -16
GLA (FA 18:3)	γ -Linolenic Acid	277.3	58	-60, -20
ETA (FA 20:3. (ω-3))	11(Z).14(Z).17(Z)-Eicosatrienoic Acid	305.28	306.09	-60, -18
DGLA (FA 20:3. (ω-6))	Dihomo- γ -Linolenic Acid (20:3)	305.28	306.03	-66, -18
EPA (FA 20:5.(ω-3))	Eicosapentaenoic Acid	301.34	257.3	-60, -10
DHA (FA 22:6. (ω-3))	Docosahexaenoic Acid	327.28	283.31	-60, -10
2-AG-d8 (20:4)	2-Arachidonoyl Glycerol-d8	387.38	294.2	45, 10
AEA-d8 (20:4)	Arachidonoyl Ethanolamide-d8	356.38	62.79	35, 16
DHEA-d4 (22:6)	Docosahexaenoyl Ethanolamide-d4	376.38	66.01	50, 14
LEA-d4 (18:2)	Linoleoyl Ethanolamide-d4	328.34	66.01	35, 16
OEA-d4 (18:1)	Oleoyl Ethanolamide-d4	330.38	66.01	45, 16
PEA-d5 (16:0)	Palmitoyl Ethanolamide-d5	305.34	61.98	42, 16
SEA-d3 (18:0)	Stearoyl Ethanolamide-d3	331.38	61.91	45, 16
EPEA-d4 (20:5)	Eicosapentaenoyl Ethanolamide-d4	350.34	66.08	36, 18
AA-d8 (20:4)	Arachidonic Acid-d8	311.34	267.30	-40, -12
PA (16:0)-d31	Palmitic Acid-d31	286.5	266.37	-40, -22

Statistical analysis. Absolute values of lipid levels were corrected using the measured protein concentrations. Data were tested for significance with GraphPad v.6 using one-way analysis of variance (ANOVA) with Tukey correction for multiple

comparisons. $P < 0.05$ was considered significant.

***In situ* anti-cancer profile**

Cell culture. Eighteen CRC cell lines were kindly provided by Sanger Institute (Cambridge, UK; authenticated by STR Genotyping). Cell lines RKO, SW48, HT55, SW948, SW1463, CL-40, LS-180, CaR-1, HUTU-80 and OUMS-23 were cultured in Dulbecco's modified Eagle's medium/F-12 medium with L-glutamine, 15 mM HEPES (Thermo-Fisher Scientific, Bleiswijk, The Netherlands) with added fetal bovine serum (Lonza, Breda, The Netherlands) and penicillin and streptomycin. HCT-116, KM12, RCM-1, SNUC1, LS-513, COLO-320-HSR, MDST8 and NCI-H716 were cultured in RPMI 1640 with L-glutamine, 25 mM HEPES (Thermo-Fisher Scientific, Bleiswijk, The Netherlands) added fetal bovine serum, penicillin and streptomycin, 1% D-glucose solution plus (Sigma-Aldrich, Zwijndrecht, The Netherlands) and 100 μ M sodium pyruvate (Life Technologies, Bleiswijk, The Netherlands). All cultures were maintained in humidified 37 °C 5% CO₂ incubators and cells were regularly tested for mycoplasma infection

Cell viability assay. Cell lines were seeded in 100 μ l delipidated medium in a 96 well cell tissue culture plate and treated in triplicate with DMSO or a titration of the drug printed using a HP D300e Digital Dispenser one day after plating (Hewlett-Packard, Palo Alto, CA, USA). CellTiter-Blue® Cell Viability Assay (cat. #G8082, Promega) was used as a read-out three days after exposure to treatment, measured on a Synergy™ HT multi-detection microplate reader (BioTek Instruments, Winooski, VT, USA). Blank signal of medium only control was deducted from all reads before normalizing all values to the average value of the DMSO treated control (= value treated replicate / average value DMSO triplicate).

***In vitro* ADME profile and *in vivo* pharmacokinetics**

Microsomal clearance. The microsomal clearance assay was performed as previously described³⁹. Pooled commercially available microsome preparations from male mouse microsomes. For human, ultrapooled liver microsomes were purchased to account for the biological variance *in vivo* from human liver tissues. For the microsome incubations (incubation buffer 0.1 M phosphate buffer pH 7.4), 96-deep well plates were applied,

which were incubated at 37 °C on a TECAN equipped with Te-Shake shakers and a warming device. The reduced nicotinamide adenine dinucleotide phosphate regenerating system consisted of 30 mM glucose-6-phosphate disodium salt hydrate; 10 mM NADP; 30 mM MgCl₂ × 6H₂O and 5 µg/µl glucose-6-phosphate dehydrogenase in 0.1 M potassium phosphate buffer pH 7.4. Incubations of LEI-401 at 1 µM in microsome incubations of 0.5 µg/µl plus cofactor reduced nicotinamide adenine dinucleotide phosphate were performed in 96-well plates at 37 °C. After 1, 3, 6, 9, 15, 25, 35 and 45 min 40 µl incubation solutions were transferred and quenched with 3:1 (v/v) acetonitrile containing internal standards. Samples were then cooled and centrifuged before analysis by LC–MS/MS. The log peak area ratios (test compound peak area/internal standard peak area) were plotted against incubation time using a linear fit. The calculated slope was used to determine the intrinsic clearance: CL_{int} (µL /min/ mg protein) = $-\text{slope} (\text{min}^{-1}) \times 1,000 / (\text{protein concentration} (\mu\text{g}/\mu\text{L}))$.

Plasma protein binding. The plasma protein binding assay was performed as previously described³⁹. Pooled and frozen plasma from human and mouse were obtained from BioreclamationIVT. The Teflon equilibrium dialysis plate (96-well, 150 µl, half-cell capacity) and cellulose membranes (12–14 kDa molecular weight cut-off) were purchased from HT-Dialysis (Gales Ferry). Both biological matrix and phosphate buffer pH were adjusted to 7.4 on the day of the experiment. The determination of unbound compound was performed using a 96-well format equilibrium dialysis device with a molecular weight cut-off membrane of 12 – 14 kDa. The equilibrium dialysis device itself was made of Teflon to minimize nonspecific binding of the test substance. Compound were tested with an initial total concentration of 1,000 nM, one of the cassette compounds being the positive control diazepam. Equal volumes of matrix samples containing substances and blank dialysis buffer (Soerensen buffer at pH 7.4) were loaded into the opposite compartments of each well. The dialysis block was sealed and kept for 5 h at a temperature of 37 °C and 5% CO₂ environment in an incubator. After this time, equilibrium has been reached for most small molecule compounds with a molecular weight of <600. The seal was then removed and matrix and buffer from each dialysis was prepared for analysis by LC–MS/MS. All protein

binding determinations were performed in triplicate. The integrity of membranes was tested in the HT-Dialysis device by determining the unbound fraction values for the positive control diazepam in each well. At equilibrium, the unbound drug concentration in the biological matrix compartment of the equilibrium dialysis apparatus was the same as the concentration of the compound in the buffer compartment. Thus, the percentage unbound fraction (f_u) was calculated by determining the compound concentrations in the buffer and matrix compartments after dialysis as follows: $\%f_u = 100 \times \text{buffer concentration after dialysis} / \text{matrix concentration after dialysis}$. The device recovery was checked by measuring the compound concentrations in the matrix before dialysis and calculating the percent recovery (mass balance). The recovery must be within 80 – 120% for data acceptance.

Pharmacokinetic analysis of LEI-515. Test compounds were formulated according to respective protocols either by dissolution (intravenous, i.v.) or in a glass potter until homogeneity was achieved (oral, p.o.). Formulations were injected i.v. using a 30 G needle in the lateral tail vein mice yielding a 10 mg/kg dose. For p.o. applications, animals were gavaged (yielding a 10 mg/kg dose). At the following time points blood was drawn into EDTA: 0.083, 0.25, 0.5, 1, 2, 4, 7 and 24 h. Three animals each were used for the i.v. and p.o. arm. Animals were distributed randomly over the time course and at each time point, a volume of 100 μ l of blood was taken. Quantitative plasma measurement of the compound was performed by LC–MS/MS analysis. Pharmacokinetic analysis was conducted using Phoenix WinNonlin v.6.4 software using a noncompartmental approach consistent with the route of administration. For assessment of the exposure C_{max} , T_{max} , area under curve and bioavailability were determined from the plasma concentration profiles. Parameters (CL, V_{ss} , $t_{1/2}$) were estimated using nominal sampling times relative to the start of each administration.

***In vivo* targets engagement studies of LEI-515 in mice.** Male C57BL/6J mice 8-10 weeks old at the time of dosing were maintained under a 12 h light/dark cycle and allowed free access to food and water. **LEI-515** was prepared fresh on the day of dosing in a DMSO/Kolliphore/5% mannitol in water (1/1/8, v/v) vehicle. Compounds were administered in a volume of 0.1 mL. Animals were administered single oral doses of

LEI-515 (5, 10 and 30 mg/kg) or vehicle. One hour after **LEI-515** administration, animals were killed by decapitation. The brains and lungs were collected and frozen in liquid nitrogen.

Lipid measurements in mouse brain and lung. Levels of 2-AG, AEA, AA and eicosanoids were measured by stable isotope dilution liquid chromatography/tandem mass spectrometry (LC-MS/MS) as described previously⁴⁰.

References

1. Senior, J. R.; Isselbacher, K. J. Demonstration of an intestinal monoglyceride lipase: an enzyme with a possible role in the intracellular completion of fat digestion. *The Journal of Clinical Investigation* **1963**, 42, 187-195.
2. Vaughan, M.; Berger, J. E.; Steinberg, D. Hormone-sensitive lipase and monoglyceride lipase activities in adipose tissue. *Journal of Biological Chemistry* **1964**, 239, 401-409.
3. Karlsson, M.; Contreras, J. A.; Hellman, U.; Tornqvist, H.; Holm, C. cDNA cloning, tissue distribution, and identification of the catalytic triad of monoglyceride lipase Evolutionary relationship to esterases, lysophospholipases, and haloperoxidases. *Journal of Biological Chemistry* **1997**, 272, 27218-27223.
4. Blankman, J. L.; Simon, G. M.; Cravatt, B. F. A comprehensive profile of brain enzymes that hydrolyze the endocannabinoid 2-arachidonoylglycerol. *Chemistry & biology* **2007**, 14, 1347-1356.
5. Baggelaar, M. P.; Maccarrone, M.; van der Stelt, M. 2-Arachidonoylglycerol: a signaling lipid with manifold actions in the brain. *Progress in lipid research* **2018**, 71, 1-17.
6. Sugiura, T.; Kodaka, T.; Nakane, S.; Miyashita, T.; Kondo, S.; Suhara, Y.; Takayama, H.; Waku, K.; Seki, C.; Baba, N. Evidence That the Cannabinoid CB1 Receptor Is a 2-Arachidonoylglycerol Receptor Structure-Activity Relationship of 2-Arachidonoylglycerol, Ether-linked Analogues, and Related Compounds. *Journal of Biological Chemistry* **1999**, 274, 2794-2801.
7. Sugiura, T.; Kondo, S.; Kishimoto, S.; Miyashita, T.; Nakane, S.; Kodaka, T.; Suhara, Y.; Takayama, H.; Waku, K. Evidence that 2-arachidonoylglycerol but not N-palmitoylethanolamine or anandamide is the physiological ligand for the cannabinoid CB2 receptor Comparison of the agonistic activities of various cannabinoid receptor ligands in HL-60 cells. *Journal of Biological Chemistry* **2000**, 275, 605-612.
8. Panikashvili, D.; Simeonidou, C.; Ben-Shabat, S.; Hanuš, L.; Breuer, A.; Mechoulam, R.; Shohami, E. An endogenous cannabinoid (2-AG) is neuroprotective after brain injury. *Nature* **2001**, 413, 527-531.
9. Kirkham, T. C.; Williams, C. M.; Fezza, F.; Marzo, V. D. Endocannabinoid levels in rat limbic forebrain and hypothalamus in relation to fasting, feeding and satiation: stimulation of eating by 2-arachidonoyl glycerol. *British journal of pharmacology* **2002**, 136, 550-557.
10. Yamaguchi, T.; Hagiwara, Y.; Tanaka, H.; Sugiura, T.; Waku, K.; Shoyama, Y.; Watanabe, S.; Yamamoto, T. Endogenous cannabinoid, 2-arachidonoylglycerol, attenuates naloxone-precipitated withdrawal signs in morphine-dependent mice. *Brain research* **2001**, 909, 121-126.
11. Fowler, C. J. Monoacylglycerol lipase—a target for drug development? *British journal of pharmacology* **2012**, 166, 1568-1585.
12. Aida, J.; Fushimi, M.; Kusumoto, T.; Sugiyama, H.; Arimura, N.; Ikeda, S.; Sasaki, M.; Sogabe, S.; Aoyama, K.; Koike, T. Design, Synthesis, and Evaluation of Piperazinyl Pyrrolidin-2-ones as a Novel Series of Reversible Monoacylglycerol Lipase Inhibitors. *J Med Chem* **2018**, 61, 9205-9217.
13. Butler, C. R.; Beck, E. M.; Harris, A.; Huang, Z.; McAllister, L. A.; Am Ende, C. W.; Fennell, K.; Foley, T. L.; Fonseca, K.; Hawrylik, S. J.; Johnson, D. S.; Knafels, J. D.; Mente, S.; Noell, G. S.; Pandit, J.; Phillips, T. B.; Piro, J. R.; Rogers, B. N.; Samad, T. A.; Wang, J.;

- Wan, S.; Brodney, M. A. Azetidine and Piperidine Carbamates as Efficient, Covalent Inhibitors of Monoacylglycerol Lipase. *J Med Chem* **2017**, *60*, 9860-9873.
14. Cisar, J. S.; Weber, O. D.; Clapper, J. R.; Blankman, J. L.; Henry, C. L.; Simon, G. M.; Alexander, J. P.; Jones, T. K.; Ezekowitz, R. A. B.; O'Neill, G. P.; Grice, C. A. Identification of ABX-1431, a Selective Inhibitor of Monoacylglycerol Lipase and Clinical Candidate for Treatment of Neurological Disorders. *J Med Chem* **2018**, *61*, 9062-9084.
15. McAllister, L. A.; Butler, C. R.; Mente, S.; O'Neil, S. V.; Fonseca, K. R.; Piro, J. R.; Cianfrogna, J. A.; Foley, T. L.; Gilbert, A. M.; Harris, A. R.; Helal, C. J.; Johnson, D. S.; Montgomery, J. I.; Nason, D. M.; Noell, S.; Pandit, J.; Rogers, B. N.; Samad, T. A.; Shaffer, C. L.; da Silva, R. G.; Uccello, D. P.; Webb, D.; Brodney, M. A. Discovery of Trifluoromethyl Glycol Carbamates as Potent and Selective Covalent Monoacylglycerol Lipase (MAGL) Inhibitors for Treatment of Neuroinflammation. *J Med Chem* **2018**, *61*, 3008-3026.
16. Cao, Z.; Mulvihill, M. M.; Mukhopadhyay, P.; Xu, H.; Erdélyi, K.; Hao, E.; Holovac, E.; Haskó, G.; Cravatt, B. F.; Nomura, D. K. Monoacylglycerol lipase controls endocannabinoid and eicosanoid signaling and hepatic injury in mice. *Gastroenterology* **2013**, *144*, 808-817. e15.
17. Costola-de-Souza, C.; Ribeiro, A.; Ferraz-de-Paula, V.; Calefi, A. S.; Aloia, T. P. A.; Gimenes-Júnior, J. A.; de Almeida, V. I.; Pinheiro, M. L.; Palermo-Neto, J. Monoacylglycerol lipase (MAGL) inhibition attenuates acute lung injury in mice. *PloS one* **2013**, *8*, e77706.
18. Nomura, D. K.; Morrison, B. E.; Blankman, J. L.; Long, J. Z.; Kinsey, S. G.; Marcondes, M. C. G.; Ward, A. M.; Hahn, Y. K.; Lichtman, A. H.; Conti, B. Endocannabinoid hydrolysis generates brain prostaglandins that promote neuroinflammation. *Science* **2011**, *334*, 809-813.
19. Dajani, E.; Islam, K. Cardiovascular and gastrointestinal toxicity of selective cyclooxygenase-2 inhibitors in man. *J Physiol Pharmacol* **2008**, *59*, 117-133.
20. Kinsey, S. G.; Nomura, D. K.; O'Neal, S. T.; Long, J. Z.; Mahadevan, A.; Cravatt, B. F.; Grider, J. R.; Lichtman, A. H. Inhibition of monoacylglycerol lipase attenuates nonsteroidal anti-inflammatory drug-induced gastric hemorrhages in mice. *Journal of Pharmacology and Experimental Therapeutics* **2011**, *338*, 795-802.
21. Nomura, D. K.; Long, J. Z.; Niessen, S.; Hoover, H. S.; Ng, S. W.; Cravatt, B. F. Monoacylglycerol lipase regulates a fatty acid network that promotes cancer pathogenesis. *Cell* **2010**, *140*, 49-61.
22. Nomura, D. K.; Lombardi, D. P.; Chang, J. W.; Niessen, S.; Ward, A. M.; Long, J. Z.; Hoover, H. H.; Cravatt, B. F. Monoacylglycerol lipase exerts dual control over endocannabinoid and fatty acid pathways to support prostate cancer. *Chem Biol* **2011**, *18*, 846-56.
23. Schalk-Hihi, C.; Schubert, C.; Alexander, R.; Bayoumy, S.; Clemente, J. C.; Deckman, I.; DesJarlais, R. L.; Dzordzorme, K. C.; Flores, C. M.; Grasberger, B. Crystal structure of a soluble form of human monoglyceride lipase in complex with an inhibitor at 1.35 Å resolution. *Protein Science* **2011**, *20*, 670-683.
24. Liu, Y.; Patricelli, M. P.; Cravatt, B. F. Activity-based protein profiling: the serine hydrolases. *Proceedings of the National Academy of Sciences* **1999**, *96*, 14694-14699.
25. Niphakis, M. J.; Cravatt, B. F. Enzyme inhibitor discovery by activity-based protein profiling. *Annual review of biochemistry* **2014**, *83*, 341-377.
26. Van Esbroeck, A. C.; Janssen, A. P.; Cognetta, A. B.; Ogasawara, D.; Shpak, G.; Van Der Kroeg, M.; Kantae, V.; Baggelaar, M. P.; De Vrij, F. M.; Deng, H. Activity-based protein profiling reveals off-target proteins of the FAAH inhibitor BIA 10-2474. *Science* **2017**, *356*,

1084-1087.

27. Baggelaar, M. P.; Janssen, F. J.; van Esbroeck, A. C.; den Dulk, H.; Allarà, M.; Hoogendoorn, S.; McGuire, R.; Florea, B. I.; Meeuwenoord, N.; van den Elst, H. Development of an activity-based probe and in silico design reveal highly selective inhibitors for diacylglycerol lipase- α in brain. *Angewandte Chemie* **2013**, *125*, 12303-12307.
28. Baggelaar, M. P.; Chameau, P. J.; Kantae, V.; Hummel, J.; Hsu, K.-L.; Janssen, F.; van der Wel, T.; Soethoudt, M.; Deng, H.; den Dulk, H. Highly selective, reversible inhibitor identified by comparative chemoproteomics modulates diacylglycerol lipase activity in neurons. *Journal of the American Chemical Society* **2015**, *137*, 8851-8857.
29. Deng, H. *Chemical Tools to Modulate Endocannabinoid Biosynthesis*. Leiden University: Leiden, 2017.
30. Ye, L.; Zhang, B.; Seviour, E. G.; Tao, K.-x.; Liu, X.-h.; Ling, Y.; Chen, J.-y.; Wang, G.-b. Monoacylglycerol lipase (MAGL) knockdown inhibits tumor cells growth in colorectal cancer. *Cancer letters* **2011**, *307*, 6-17.
31. Pagano, E.; Borrelli, F.; Orlando, P.; Romano, B.; Monti, M.; Morbidelli, L.; Aviello, G.; Imperatore, R.; Capasso, R.; Piscitelli, F. Pharmacological inhibition of MAGL attenuates experimental colon carcinogenesis. *Pharmacological research* **2017**, *119*, 227-236.
32. Kabsch, W. Xds. *Acta Crystallographica Section D: Biological Crystallography* **2010**, *66*, 125-132.
33. McCoy, A. J.; Grosse-Kunstleve, R. W.; Adams, P. D.; Winn, M. D.; Storoni, L. C.; Read, R. J. Phaser crystallographic software. *Journal of applied crystallography* **2007**, *40*, 658-674.
34. Winn, M. D.; Ballard, C. C.; Cowtan, K. D.; Dodson, E. J.; Emsley, P.; Evans, P. R.; Keegan, R. M.; Krissinel, E. B.; Leslie, A. G.; McCoy, A. Overview of the CCP4 suite and current developments. *Acta Crystallographica Section D: Biological Crystallography* **2011**, *67*, 235-242.
35. Emsley, P.; Lohkamp, B.; Scott, W. G.; Cowtan, K. Features and development of Coot. *Acta Crystallographica Section D: Biological Crystallography* **2010**, *66*, 486-501.
36. Baggelaar, M. P.; Chameau, P. J.; Kantae, V.; Hummel, J.; Hsu, K. L.; Janssen, F.; van der Wel, T.; Soethoudt, M.; Deng, H.; den Dulk, H.; Allarà, M.; Florea, B. I.; Di Marzo, V.; Wadman, W. J.; Kruse, C. G.; Overkleeft, H. S.; Hankemeier, T.; Werkman, T. R.; Cravatt, B. F.; van der Stelt, M. Highly Selective, Reversible Inhibitor Identified by Comparative Chemoproteomics Modulates Diacylglycerol Lipase Activity in Neurons. *J Am Chem Soc* **2015**, *137*, 8851-7.
37. van Rooden, E. J.; Florea, B. I.; Deng, H.; Baggelaar, M. P.; van Esbroeck, A. C.; Zhou, J.; Overkleeft, H. S.; van der Stelt, M. Mapping in vivo target interaction profiles of covalent inhibitors using chemical proteomics with label-free quantification. *Nature protocols* **2018**, *13*, 752.
38. Distler, U.; Kuharev, J.; Navarro, P.; Tenzer, S. Label-free quantification in ion mobility-enhanced data-independent acquisition proteomics. *Nature protocols* **2016**, *11*, 795-812.
39. Mock, E. D.; Mustafa, M.; Gunduz-Cinar, O.; Cinar, R.; Petrie, G. N.; Kantae, V.; Di, X.; Ogasawara, D.; Varga, Z. V.; Paloczi, J. Discovery of a NAPE-PLD inhibitor that modulates emotional behavior in mice. *Nature Chemical Biology* **2020**, 1-9.

40. Mukhopadhyay, B.; Cinar, R.; Yin, S.; Liu, J.; Tam, J.; Godlewski, G.; Harvey-White, J.; Mordi, I.; Cravatt, B. F.; Lotersztajn, S. Hyperactivation of anandamide synthesis and regulation of cell-cycle progression via cannabinoid type 1 (CB1) receptors in the regenerating liver. *Proceedings of the National Academy of Sciences* **2011**, 108, 6323-6328.

Supplementary Information

Table S1. *In vitro* safety pharmacology profiling of LEI-515.

Targets	LEI-515 (μM)	% Inhibition of Control Specific Binding		
		1 st	2 nd	Mean
A _{2A} (h) (agonist radioligand)	10	8.1	15.2	11.7
α_{1A} (h) (antagonist radioligand)	10	7.3	-0.3	3.5
α_{2A} (h) (antagonist radioligand)	10	8.3	28.3	18.3
β_1 (h) (agonist radioligand)	10	0.9	12.3	6.6
β_2 (h) (antagonist radioligand)	10	25.6	28.0	26.8
BZD (central) (agonist radioligand)	10	-32.5	-13.0	-22.7
CB ₁ (h) (agonist radioligand)	10	18.7	25.8	22.3
CB ₂ (h) (agonist radioligand)	10	-8.9	-14.9	-11.9
CCK ₁ (CCKA) (h) (agonist radioligand)	10	13.3	25.8	19.5
D ₁ (h) (antagonist radioligand)	10	2.1	10.2	6.2
D _{2S} (h) (agonist radioligand)	10	-3.4	7.7	2.2
ETA(h) (agonist radioligand)	10	-5.9	-10.1	-8.0
NMDA (antagonist radioligand)	10	11.1	1.6	6.3
H ₁ (h) (antagonist radioligand)	10	12.5	3.7	8.1
H ₂ (h) (antagonist radioligand)	10	-26.7	-25.3	-26.0
MAO-A (antagonist radioligand)	10	4.9	7.4	6.1
M ₁ (h) (antagonist radioligand)	10	-25.4	-33.6	-29.5
M ₂ (h) (antagonist radioligand)	10	-6.8	-1.7	-4.2
M ₃ (h) (antagonist radioligand)	10	-24.6	-15.2	-19.9
N neuronal $\alpha_4\beta_2$ (h) (agonist radioligand)	10	-7.8	-13.2	-10.5
δ (DOP) (h) (agonist radioligand)	10	53.0	43.7	48.3
kappa (h) (KOP) (agonist radioligand)	10	62.3	56.8	59.5
kappa (h) (KOP) (agonist radioligand)	1	12.8	30.6	21.7
μ (MOP) (h) (agonist radioligand)	10	25.6	15.2	20.4
5-HT _{1A} (h) (agonist radioligand)	10	8.8	12.4	10.6

Chapter 5

5-HT _{1B} (h) (antagonist radioligand)	10	22.7	25.6	24.2
5-HT _{2A} (h) (agonist radioligand)	10	-5.5	-5.5	-5.5
5-HT _{2B} (h) (agonist radioligand)	10	30.7	24.4	27.6
5-HT ₃ (h) (antagonist radioligand)	10	-8.5	-7.8	-8.1
GR (h) (agonist radioligand)	10	29.5	30.8	30.2
AR(h) (agonist radioligand)	10	-1.1	-13.0	-7.0
V _{1a} (h) (agonist radioligand)	10	13.1	6.8	9.9
Ca ²⁺ channel (L, dihydropyridine site) (antagonist radioligand)	10	58.2	50.6	54.4
Ca ²⁺ channel (L, dihydropyridine site) (antagonist radioligand)	1	18.1	19.6	18.9
Potassium Channel hERG (human)- [3H] Dofetilide	10	8.5	3.0	5.8
KV channel (antagonist radioligand)	10	-1.2	-8.1	-4.7
Na ⁺ channel (site 2) (antagonist radioligand)	10	61.6	49.5	55.6
Na ⁺ channel (site 2) (antagonist radioligand)	1	12.6	-1.9	5.3
norepinephrine transporter(h) (antagonist radioligand)	10	24.9	25.7	25.3
dopamine transporter(h) (antagonist radioligand)	10	47.6	42.8	45.2
5-HT transporter (h) (antagonist radioligand)	10	10.3	-2.0	4.2
COX1(h)	10	13.4	-2.5	5.4
COX2(h)	10	20.3	-1.4	9.5
PDE3A (h)	10	-20.5	-33.8	-27.2
PDE4D2 (h)	10	-12.4	-20.9	-16.6
Lck kinase (h)	10	-9.2	-1.4	-5.3
acetylcholinesterase (h)	10	4.4	5.4	4.9

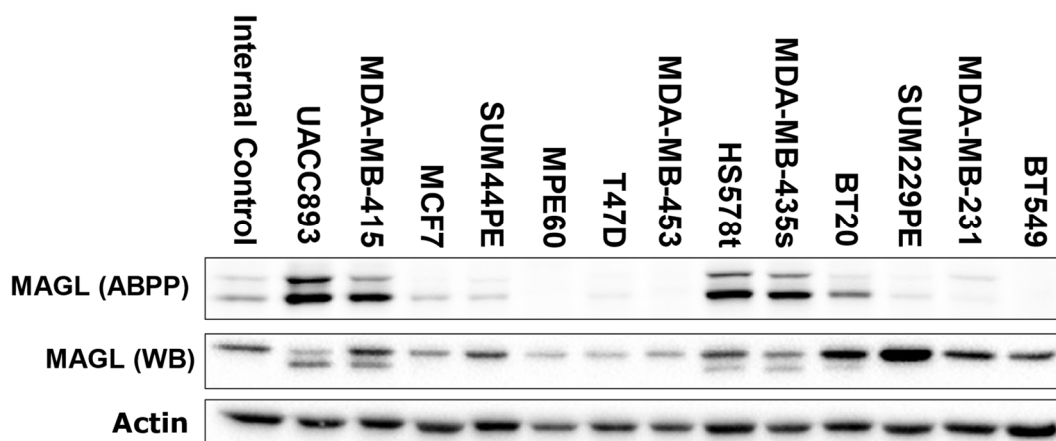


Figure S1. Profiling of MAGL activity and protein levels in a panel of 13 breast cancer cell lines.

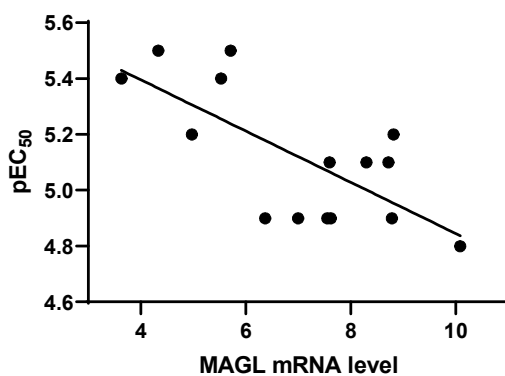


Figure S2. Plot of pEC₅₀ of LEI-515 against MAGL mRNA levels in colorectal cancer cell lines.

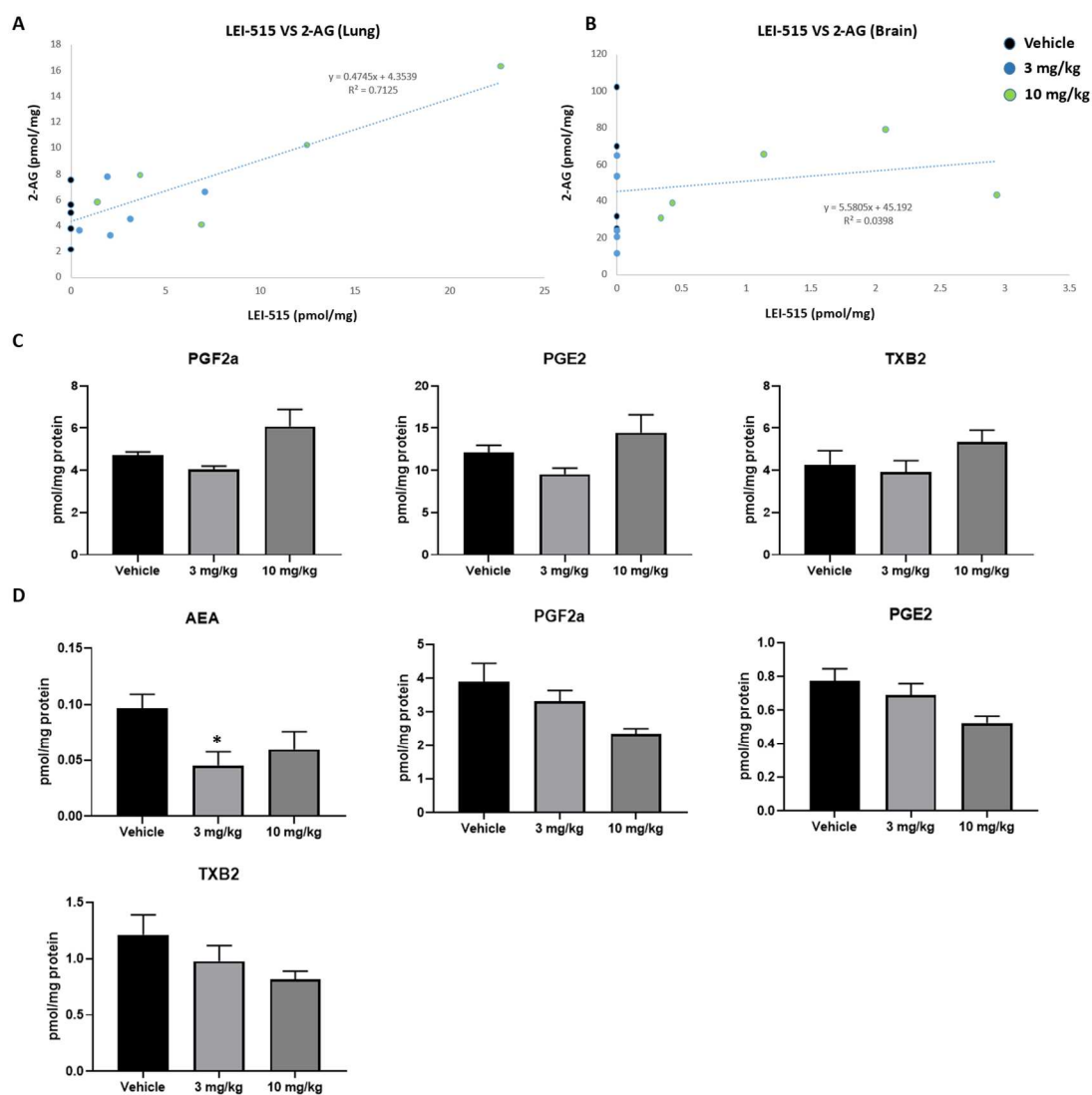


Figure S3. Plot of LEI-515 concentration versus 2-AG levels in the lung (A) and brain (B). (C) Absolute lipid levels of PGF2a, PGE2 and TXB2 in the lung (n = 5). (D) Absolute lipid levels of AEA, PGF2a, PGE2 and TXB2 in the brain (n = 5).

Chapter 6

Summary and future prospects

The aim of the research described in this thesis was to develop potent, selective and reversible monoacylglycerol lipase (MAGL) inhibitors that can be used as chemical tools to study MAGL function *in vivo* and further developed as therapeutics for the treatment of inflammation and cancer.

Chapter 1 provided an overview of the function and mode-of-action of MAGL. The enzyme is a membrane-associated protein belonging to the large family of serine hydrolases. It contains a typical α/β hydrolase fold and employs a Ser-His-Asp catalytic triad for the hydrolysis of monoacylglycerides into free fatty acid and glycerol.^{1, 2} MAGL is the key enzyme involved in the degradation of the endogenous signaling lipid 2-arachidonoylglycerol (2-AG) (Figure 1).³ 2-AG is an endocannabinoid which activates cannabinoid receptors.^{4, 5} Activation of cannabinoid receptors by endogenous ligands plays an important role in various physiological processes, such as learning and memory, pain sensation, energy balance and inflammation.⁶⁻⁸ Besides, MAGL is the predominant enzyme regulating the production of arachidonic acid (AA) in the brain, lung and liver. AA is the precursor of pro-inflammatory prostaglandins.² Therefore, MAGL inhibition is thought to have several therapeutic applications, such as anti-

inflammation, antinociception and anti-cancer. Of note, MAGL inhibitors might avoid gastrointestinal and cardiovascular side effects observed with dual cyclooxygenase 1/2 (COX1/2) and selective COX2 inhibitors because MAGL only controls eicosanoid metabolism in specific tissues.⁹⁻¹¹

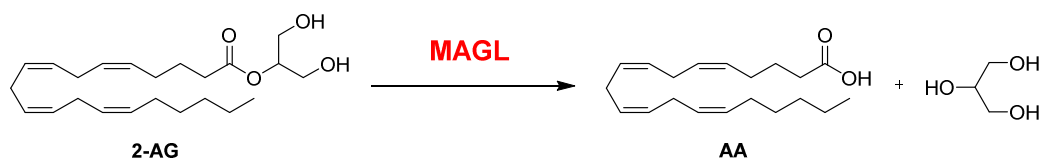


Figure 1. MAGL is the main enzyme for the hydrolysis of endocannabinoid 2-AG.

A number of drug discovery programs have been initiated to discover potent and selective MAGL inhibitors in the past two decades. Both irreversible and reversible MAGL inhibitors have been reported or patented (Figure 2).¹²⁻¹⁵ The first-in-class MAGL inhibitor ABX-1431 (**2**, Figure 2), an irreversible MAGL inhibitor, is now in clinical trial phase 1b for the treatment of posttraumatic stress disorder (NCT04597450).¹³ Irreversible inhibitors may have several advantages to act as therapeutics, like increased potency, long residence time and a less stringent pharmacokinetic profile.¹⁶ However, the irreversible mode of action may also have some drawbacks, such as reduced selectivity, idiosyncratic drug-related toxicity and, in case of MAGL inhibition, pharmacological tolerance.^{17, 18} Careful dosing or reversible inhibitors may avoid these unfavorable side-effects.¹⁹

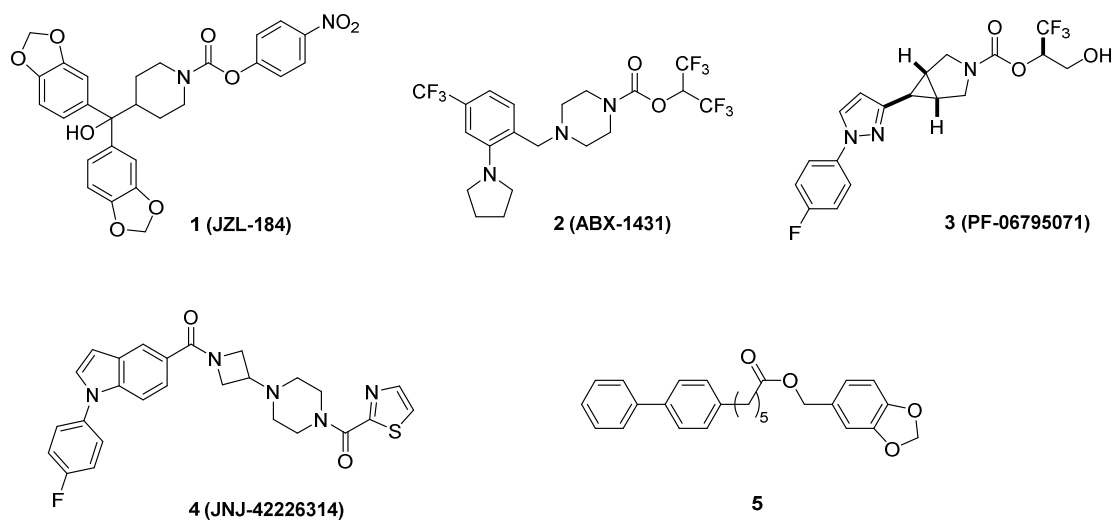


Figure 2. Chemical structures of reported MAGL inhibitors.

Previously, a high-throughput screen (HTS) was performed at the Pivot Park Screening Centre and seven compounds were validated as confirmed hits.²⁰ In **Chapter 2**, the optimization of β -sulfinyl ester-based hit **1** (Figure 1) as a novel chemotype for MAGL inhibition is described. A natural substrate-based MAGL activity assay was used to guide the hit optimization. The assay utilizes an enzymatic cascade to convert glycerol, a metabolite produced by MAGL, into a fluorescent signal.²¹ A ligand-based drug design approach was performed to improve the potency of hit **6** (Figure 3). 56 compounds were synthesized and tested. This led to the discovery of compound \pm **7** (Figure 3) as a potent MAGL inhibitor with single digit nanomolar potency ($\text{pIC}_{50} = 8.50 \pm 0.10$). The selectivity of compound \pm **7** was profiled by using activity-based protein profiling (ABPP) and it showed high selectivity against a panel of serine hydrolases, including α , β -hydrolase domain-containing protein 6 (ABHD6), ABHD12, diacylglycerol lipases (DAGLs) and fatty acid amide hydrolase (FAAH).

Compound \pm **7** contains an ester functionality, which is a metabolic liability and may act as an electrophile for the incoming catalytic serine of MAGL. To test the latter hypothesis, the replacement of the ester group with an activated ketone as reversible, covalent warhead is described in **Chapter 3**. A series of 21 α -aryl ketones was designed, synthesized and tested, which led to the discovery of compound \pm **8** (Figure 3) as a novel ketone-based MAGL inhibitor with an IC_{50} of 10 nM. This is the first alpha-keto heterocycle described as MAGL inhibitor.

In **Chapter 4**, the metabolic stability of compound \pm **7** was evaluated using a liver S9-based assay. Compound \pm **7** showed low metabolic stability as expected, because it contains a metabolically labile ester functionality. To optimize the metabolic stability of compound \pm **7**, three different strategies were employed to improve the metabolic stability: 1) reducing the lipophilicity; 2) applying steric hindrance and 3) replacing the ester group with bioisosteres. Replacing the ester group with α - CF_2 ketone group led to the discovery of **LEI-515 (9)**, (Figure 3) as a potent and metabolically stable MAGL inhibitor with subnanomolar potency.

The overall structure-activity relationship (SAR) for MAGL inhibitors developed in this thesis is displayed in Figure 3B.

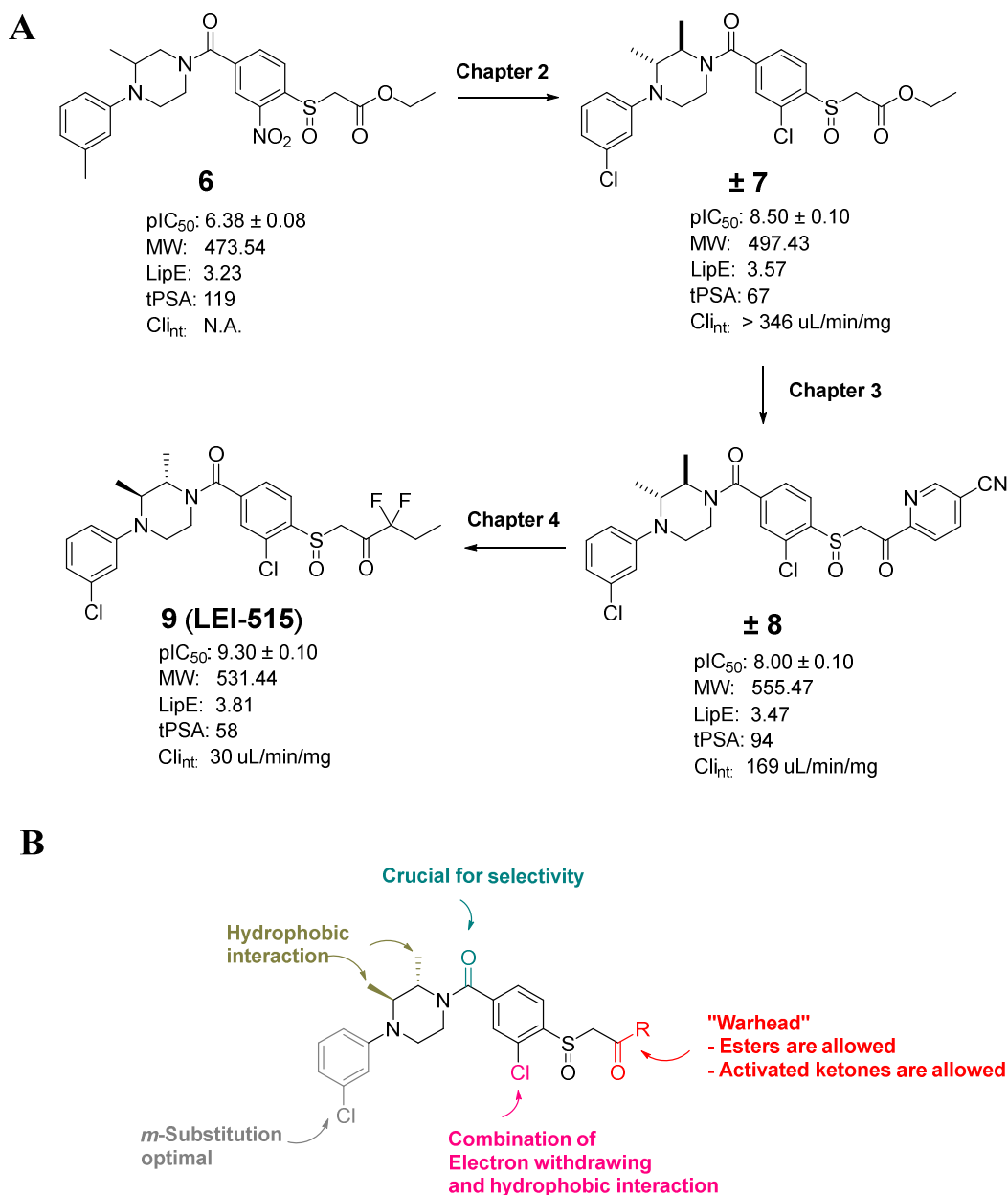


Figure 3. (A) Chemical structures, physical chemical properties and biological properties of hit compound (**6**) and analogues with improved potency (**± 7 - 9**). (B) The overall structure-activity relationship.

In **Chapter 5**, **LEI-515** was further profiled in biochemical, cellular and ADME assays as well as mouse pharmacokinetic and target engagement studies to assess its ability to act as a reversible and *in vivo* active MAGL inhibitor. Crystallography studies showed that **LEI-515** occupied the active site of MAGL and bound to the catalytic Ser122 covalently. The formed deprotonated hemiketal was stabilized by two

hydrogen-bonds with Ala51 and Met123, respectively (Figure 4). Competitive ABPP with tailor-made MAGL probe suggested that **LEI-515** is a reversible MAGL inhibitor. Activity-based protein profiling with broad-spectrum fluorophosphonate-based and β -lactone-based probes revealed that **LEI-515** was a highly selective MAGL inhibitor. **LEI-515** did not affect other enzymes involved in endocannabinoid metabolism, including ABHD6, ABHD12, DAGLs and FAAH. Hormone-sensitive lipase (LIPE) was identified as an off-target in mouse brain, liver and lung proteome. In vitro pharmacological profiling demonstrated that **LEI-515** is selective (>100 -fold selectivity) over a panel of 44 ion channels, receptors and enzymes, including the cannabinoid receptors (CB1R and CB2R), hERG channel and cyclooxygenases (COX1 and COX2). Targeted lipidomics revealed that **LEI-515** increased 2-AG levels in time- and concentration-dependent manner in human breast cancer HS578t cells. **LEI-515** also reduced the AA and AEA levels in the cells at 1 μ M. Cell viability assay showed that **LEI-515** impaired the cells growth of 15 colorectal cancer cell lines with concentration for 50% of maximal effect (EC_{50}) in the range from 2 to 20 μ M. Absorption, distribution, metabolism and excretion (ADME) profiling showed that **LEI-515** possess high stability (100 % remaining at 180 min) in both human and mouse plasma. Clearance in human microsomes (30.9 μ L/min/mg) was moderate and low in mouse microsomes (< 3.4 μ L/min/mg). **LEI-515** exhibited high protein binding (99.6% for both) in human and mouse plasma and showed negligible cell permeability in caco-2 cells ($P_{appA-B} < 0.01 \times 10^{-6}$ cm/s and $P_{appB-A} < 0.005 \times 10^{-6}$ cm/s). Pharmacokinetic study revealed excellent bioavailability and quick absorption of **LEI-515** after oral administration in mouse. Of note, **LEI-515** was found as a peripherally restricted MAGL inhibitor. Unfortunately, preliminary *in vivo* efficacy studies showed that **LEI-515** (10 mg/kg, p.o., 1h) did not increase 2-AG levels in the lung or liver, which might be due to high protein binding of the compound, too low dose and/or insufficient exposure time.

ischemia/reperfusion (I/R), lung I/R or, perhaps Covid-19 induced lung inflammation. Moreover, pharmacological and genetical inhibition of MAGL reduced tumor growth in several xenograft models, such as ovarian, melanoma, colon and prostate xenograft models.²⁵⁻²⁷ It would also be interesting to evaluate the potential application of **LEI-515** as anti-cancer agent. In summary, this thesis described the discovery and optimization of the first reversible, peripherally restricted MAGL inhibitors based on activated ketones, which can be used to validate MAGL as a potential therapeutic target for various indications.

References

1. Fowler, C. J. Monoacylglycerol lipase—a target for drug development? *British journal of pharmacology* **2012**, 166, 1568-1585.
2. Nomura, D. K.; Long, J. Z.; Niessen, S.; Hoover, H. S.; Ng, S.-W.; Cravatt, B. F. Monoacylglycerol lipase regulates a fatty acid network that promotes cancer pathogenesis. *Cell* **2010**, 140, 49-61.
3. Blankman, J. L.; Simon, G. M.; Cravatt, B. F. A comprehensive profile of brain enzymes that hydrolyze the endocannabinoid 2-arachidonoylglycerol. *Chemistry & biology* **2007**, 14, 1347-1356.
4. Savinainen, J. R.; Järvinen, T.; Laine, K.; Laitinen, J. T. Despite substantial degradation, 2-arachidonoylglycerol is a potent full efficacy agonist mediating CB1 receptor-dependent G-protein activation in rat cerebellar membranes. *British journal of pharmacology* **2001**, 134, 664-672.
5. Gonsiorek, W.; Lunn, C.; Fan, X.; Narula, S.; Lundell, D.; Hipkin, R. W. Endocannabinoid 2-arachidonyl glycerol is a full agonist through human type 2 cannabinoid receptor: antagonism by anandamide. *Molecular pharmacology* **2000**, 57, 1045-1050.
6. Di Marzo, V.; Bifulco, M.; De Petrocellis, L. The endocannabinoid system and its therapeutic exploitation. *Nature reviews Drug discovery* **2004**, 3, 771-784.
7. Lutz, B.; Marsicano, G.; Maldonado, R.; Hillard, C. J. The endocannabinoid system in guarding against fear, anxiety and stress. *Nature Reviews Neuroscience* **2015**, 16, 705-718.
8. Parsons, L. H.; Hurd, Y. L. Endocannabinoid signalling in reward and addiction. *Nature Reviews Neuroscience* **2015**, 16, 579-594.
9. Nomura, D. K.; Morrison, B. E.; Blankman, J. L.; Long, J. Z.; Kinsey, S. G.; Marcondes, M. C. G.; Ward, A. M.; Hahn, Y. K.; Lichtman, A. H.; Conti, B. Endocannabinoid hydrolysis generates brain prostaglandins that promote neuroinflammation. *Science* **2011**, 334, 809-813.
10. Dajani, E.; Islam, K. Cardiovascular and gastrointestinal toxicity of selective cyclooxygenase-2 inhibitors in man. *J Physiol Pharmacol* **2008**, 59, 117-133.
11. Kinsey, S. G.; Nomura, D. K.; O'Neal, S. T.; Long, J. Z.; Mahadevan, A.; Cravatt, B. F.; Grider, J. R.; Lichtman, A. H. Inhibition of monoacylglycerol lipase attenuates nonsteroidal anti-inflammatory drug-induced gastric hemorrhages in mice. *Journal of Pharmacology and Experimental Therapeutics* **2011**, 338, 795-802.
12. Bononi, G.; Poli, G.; Rizzolio, F.; Tuccinardi, T.; Macchia, M.; Minutolo, F.; Granchi, C. An updated patent review of monoacylglycerol lipase (MAGL) inhibitors (2018-present). *Expert Opinion on Therapeutic Patents* **2021**, 31, 153-168.
13. Cisar, J. S.; Weber, O. D.; Clapper, J. R.; Blankman, J. L.; Henry, C. L.; Simon, G. M.; Alexander, J. P.; Jones, T. K.; Ezekowitz, R. A. B.; O'Neill, G. P.; Grice, C. A. Identification of ABX-1431, a Selective Inhibitor of Monoacylglycerol Lipase and Clinical Candidate for Treatment of Neurological Disorders. *Journal of medicinal chemistry* **2018**, 61, 9062-9084.
14. Granchi, C.; Caligiuri, I.; Minutolo, F.; Rizzolio, F.; Tuccinardi, T. A patent review of Monoacylglycerol Lipase (MAGL) inhibitors (2013-2017). *Expert opinion on therapeutic patents* **2017**, 27, 1341-1351.
15. McAllister, L. A.; Butler, C. R.; Mente, S.; O'Neil, S. V.; Fonseca, K. R.; Piro, J. R.; Cianfrogna, J. A.; Foley, T. L.; Gilbert, A. M.; Harris, A. R.; Helal, C. J.; Johnson, D. S.;

- Montgomery, J. I.; Nason, D. M.; Noell, S.; Pandit, J.; Rogers, B. N.; Samad, T. A.; Shaffer, C. L.; da Silva, R. G.; Uccello, D. P.; Webb, D.; Brodney, M. A. Discovery of Trifluoromethyl Glycol Carbamates as Potent and Selective Covalent Monoacylglycerol Lipase (MAGL) Inhibitors for Treatment of Neuroinflammation. *Journal of medicinal chemistry* **2018**, 61, 3008-3026.
16. Barf, T.; Kaptein, A. Irreversible protein kinase inhibitors: balancing the benefits and risks. *Journal of medicinal chemistry* **2012**, 55, 6243-6262.
17. Singh, J.; Petter, R. C.; Baillie, T. A.; Whitty, A. The resurgence of covalent drugs. *Nature reviews Drug discovery* **2011**, 10, 307-317.
18. Schlosburg, J. E.; Blankman, J. L.; Long, J. Z.; Nomura, D. K.; Pan, B.; Kinsey, S. G.; Nguyen, P. T.; Ramesh, D.; Booker, L.; Burston, J. J. Chronic monoacylglycerol lipase blockade causes functional antagonism of the endocannabinoid system. *Nature neuroscience* **2010**, 13, 1113-1119.
19. Hernández-Torres, G.; Cipriano, M.; Hedén, E.; Björklund, E.; Canales, Á.; Zian, D.; Feliú, A.; Mecha, M.; Guaza, C.; Fowler, C. J. A reversible and selective inhibitor of monoacylglycerol lipase ameliorates multiple sclerosis. *Angewandte Chemie* **2014**, 126, 13985-13990.
20. van der Wel, T. Chemical genetic approaches for target validation. Leiden University, Leiden, 2020.
21. van der Wel, T.; Janssen, F. J.; Baggelaar, M. P.; Deng, H.; den Dulk, H.; Overkleeft, H. S.; van der Stelt, M. A natural substrate-based fluorescence assay for inhibitor screening on diacylglycerol lipase α . *Journal of lipid research* **2015**, 56, 927-935.
22. Cao, Z.; Mulvihill, M. M.; Mukhopadhyay, P.; Xu, H.; Erdélyi, K.; Hao, E.; Holovac, E.; Haskó, G.; Cravatt, B. F.; Nomura, D. K. Monoacylglycerol lipase controls endocannabinoid and eicosanoid signaling and hepatic injury in mice. *Gastroenterology* **2013**, 144, 808-817. e15.
23. Costola-de-Souza, C.; Ribeiro, A.; Ferraz-de-Paula, V.; Calefi, A. S.; Aloia, T. P. A.; Gimenes-Júnior, J. A.; de Almeida, V. I.; Pinheiro, M. L.; Palermo-Neto, J. Monoacylglycerol lipase (MAGL) inhibition attenuates acute lung injury in mice. *PloS one* **2013**, 8, e77706.
24. Xiong, Y.; Yao, H.; Cheng, Y.; Gong, D.; Liao, X.; Wang, R. Effects of monoacylglycerol lipase inhibitor URB602 on lung ischemia-reperfusion injury in mice. *Biochemical and biophysical research communications* **2018**, 506, 578-584.
25. Nomura, D. K.; Long, J. Z.; Niessen, S.; Hoover, H. S.; Ng, S. W.; Cravatt, B. F. Monoacylglycerol lipase regulates a fatty acid network that promotes cancer pathogenesis. *Cell* **2010**, 140, 49-61.
26. Pagano, E.; Borrelli, F.; Orlando, P.; Romano, B.; Monti, M.; Morbidelli, L.; Aviello, G.; Imperatore, R.; Capasso, R.; Piscitelli, F. Pharmacological inhibition of MAGL attenuates experimental colon carcinogenesis. *Pharmacological research* **2017**, 119, 227-236.
27. Nomura, D. K.; Lombardi, D. P.; Chang, J. W.; Niessen, S.; Ward, A. M.; Long, J. Z.; Hoover, H. H.; Cravatt, B. F. Monoacylglycerol lipase exerts dual control over endocannabinoid and fatty acid pathways to support prostate cancer. *Chemistry & biology* **2011**, 18, 846-856.

List of publications

Discovery of Activated Ketones as Highly Potent, Selective, Reversible and *in vivo* Active Monoacylglycerol Lipase inhibitors

M. Jiang, M. C. W. Huizenga, T. van der Wel, F. Stevens, X. Di, P. M. Gomezbarila, J. P. Medema, L. Heitman, J. Benz, M. Wittwer, U. Grether, A. Pavlovic, L. Collin, G. Zaman, B.F. Florea, R. Buijsman, H.O. Overkleeft, R. J. B. H. N.van den Berg, T. Hankemeier, C. A. A. van Boeckel, M. van der Stelt
Manuscript in preparation

Structure-Activity Relationship Studies of β -Sulfinyl Esters as Reversible Monoacylglycerol Lipase inhibitors

M. Jiang, F. Mohr, T. van der Wel, M. C. W. Huizenga, A. Amedi, A. Martella, R. J. B. H. N.van den Berg, C. A. A. van Boeckel, M. van der Stelt
Manuscript in preparation

Structure-Activity Relationship Studies of α -Ketoamides as Inhibitors of the Phospholipase A and Acyltransferase Enzyme Family

J. Zhou, E.D. Mock, K. Al Ayed, X. Di, V. Kantae, L. Burggraaff, A.F. Stevens, A. Martella, F. Mohr, M. Jiang, T. van der Wel, T.J. Wendel, T.P. Ofman, Y. Tran, N. de Koster, G.J.P. van Westen, T. Hankemeier & M. van der Stelt
Journal of Medicinal Chemistry 63, 9340-9359 (2020).

Discovery of a NAPE-PLD inhibitor that modulates emotional behavior in mice

E.D. Mock, M. Mustafa, O. Gunduz-Cinar, R. Cinar, G.N. Petrie, V. Kantae, X. Di, D. Ogasawara, Z.V. Varga, J. Paloczi, C. Miliano, G. Donvito, A.C.M. van Esbroeck, A.M.F. van der Gracht, I. Kotsogianni, J.K. Park, A. Martella, T. van der Wel, M. Soethoudt, M. Jiang, T.J. Wendel, A.P.A. Janssen, A.T. Bakker, C.M. Donovan, L.I. Castillo, B.I. Florea, J. Wat, H. van den Hurk, M. Wittwer, U. Grether, A. Holmes, C.A.A. van Boeckel, T. Hankemeier, B.F. Cravatt, M.W. Buczynski, M.N. Hill, P. Pacher, A.H. Lichtman & M. van der Stelt
Nature Chemical Biology 16, 667-675 (2020).

Endocannabinoid contributions to alcohol habits and motivation: Relevance to treatment

C.A. Gianessi, S.M. Groman, S.L. Thompson, M. Jiang, M. van der Stelt & J.R. Taylor
Addiction Biology 25, e12768 (2020).

Activity-Based Protein Profiling Delivers Selective Drug Candidate ABX-1431, a Monoacylglycerol Lipase Inhibitor, To Control Lipid Metabolism in Neurological Disorders

M. Jiang & M. van der Stelt
Journal of Medicinal Chemistry 61, 9059-9061 (2018).

Development of a Multiplexed Activity-Based Protein Profiling Assay to Evaluate Activity of Endocannabinoid Hydrolase Inhibitors

A.P.A. Janssen, D. van der Vliet, A.T. Bakker, M. Jiang, S.H. Grimm, G. Campiani, S. Butini & M. van der Stelt

ACS Chemical Biology *13*, 2406-2413 (2018).

A combined experimental and computational study of Vam3, a derivative of resveratrol, and Syk interaction

M. Jiang, R. Liu, Y. Chen, Q. Zheng, S. Fan, & P. Liu

International Journal of Molecular Sciences *15*, 17188-17203 (2014).

A combination of 3D-QSAR, molecular docking and molecular dynamics simulation studies of benzimidazole-quinolinone derivatives as iNOS inhibitors.

H. Zhang, J. Zan, G. Yu, M. Jiang, & P. Liu

International Journal of Molecular Sciences *13*, 11210-11227 (2012).

Monoacylglycerol Lipase Inhibitors

M. Jiang, F. Mohr, C. A. A. van Boeckel, M. C. W. Huizenga, A. Amedi, M. van der Stelt

EP20161029, Filing data: 04.03.20.

中文总结

单酯酰甘油酯酶可逆抑制剂的研发

本书对单酯酰甘油酯酶(MAGL)可逆抑制剂的设计、合成以及体内外生物评价进行了研究分析。

通过一系列的结构改造和体内外生物评价,发现了高活性、高选择性、作用于外周的MAGL可逆抑制剂。

第一章主要简述了MAGL的生物学功能。MAGL属于丝氨酸水解酶超家族,是内源性信号分子2-花生四烯酰甘油(2-Arachidonoylglycerol, 2-AG)代谢的关键酶。2-AG是大麻素受体的内源性完全激动剂,2-AG通过激活大麻素受体从而调控多种生理过程,例如学习与记忆、痛觉等。

除此之外,在特定的组织中,如大脑、肝和肺,MAGL是调控花生四烯酸(Arachidonic acid, AA)生物合成的主要酶,AA是促炎因子前列腺素的前体。因此,目前认为抑制MAGL的活性具有消炎,镇痛等治疗作用。值得注意的是,MAGL只调控特定组织中类十二烷酸类分子(Eicosanoid)的代谢,而不影响胃肠道中Eicosanoid的代谢,所以MAGL抑制剂或许能避免环氧合酶(Cyclooxygenase, COX)抑制剂的胃肠道副作用。

在过去的二十多年中,针对MAGL抑制剂的研发已经取得一定的进展,早期的研发主要集中于不可逆MAGL抑制剂。第一个进入临床研究的MAGL抑制剂ABX-1431目前处于临床1b阶段(NCT04597450)。ABX-1431为MAGL不可逆抑制剂。不可逆抑制剂具有某些优势,例如良好的活性、较长的保留时间和不需要严格的药代动力学性质。但同时,这种不可逆的结合模式也可能具一些劣势,例如低选择性、特异的药物相关毒性和药物耐受。可逆抑制剂或许能避免掉这些劣势。

第二章利用基于配体的结构改造策略对Hit化合物(图1)进行优化。本轮优化重点关注化合物

对 MAGL 的抑制活性，总共合成和测试了 56 个分子，最终找到了高活性的化合物 **1**。同时，利用基于活性的蛋白质表征 (Activity-based protein profiling, ABPP) 技术对化合物 **1** 的选择性进行了研究，结果发现化合物 **1** 对一系列的丝氨酸水解酶具有较好的选择性，包含脂肪酸酰胺水解酶 (Fatty acid amide hydrolase, FAAH) 和二酰基甘油酯酶 (Diacylglycerol lipases, DAGLs)。

第三章主要描述了了新颖的 α -芳基酮类型的分子作为 MAGL 共价可逆抑制剂的研究。本轮结构改造通过将化合物 **1** 的关键酯基替换成不同的 α -芳基酮从而达到维持对 MAGL 抑制活性的同时替换分子中代谢位点的目的。总共合成和测试了 21 个分子，最终找到了活性较好的化合物 **2**。

第四章主要介绍了基于代谢稳定性的结构改造。利用基于肝脏 S9 级分 (Liver S9 fractions) 的方法对化合物 **1** 的代谢稳定性进行了评价，结果发现化合物 **1** 的稳定性较差。在新一轮的优化中，主要采取以下策略进：1) 降低化合物亲酯性；2) 在酯基旁引入空间位阻和 3) 生物等排体替换酯基。研究发现，用 α -CF₂ 羰基替换酯基不仅可以提高化合物活性，同时能显著的提高代谢稳定性。经过本轮优化，最终得到化合物 **LEI-515**。

第五章主要对优化后的化合物进行了体内及体外的表征。晶体学研究揭示了 LEI-515 与 MAGL 的共价可逆的结合模式。基于广谱探针的 ABPP 研究和 Safety Panel 研究发现 LEI-515 具有良好的选择性，LEI-515 在 10 μ M 浓度下不影响内源性大麻素系统中其他蛋白的功能。细胞学研究发现 LEI-515 可以提高细胞内 2-AG 的水平，而体内研究发现 LEI-515 (10 mg/kg, p.o., 1h) 不能显著提高小鼠肝脏和肺中 2-AG 的水平，这可能由于给 LEI-515 的血浆蛋白结合率高、给药剂量低或者给药后孵育时间不足有关。

第六章对本论文的实验工作进行了总结和归纳，并对未来的研究方向进行了展望。

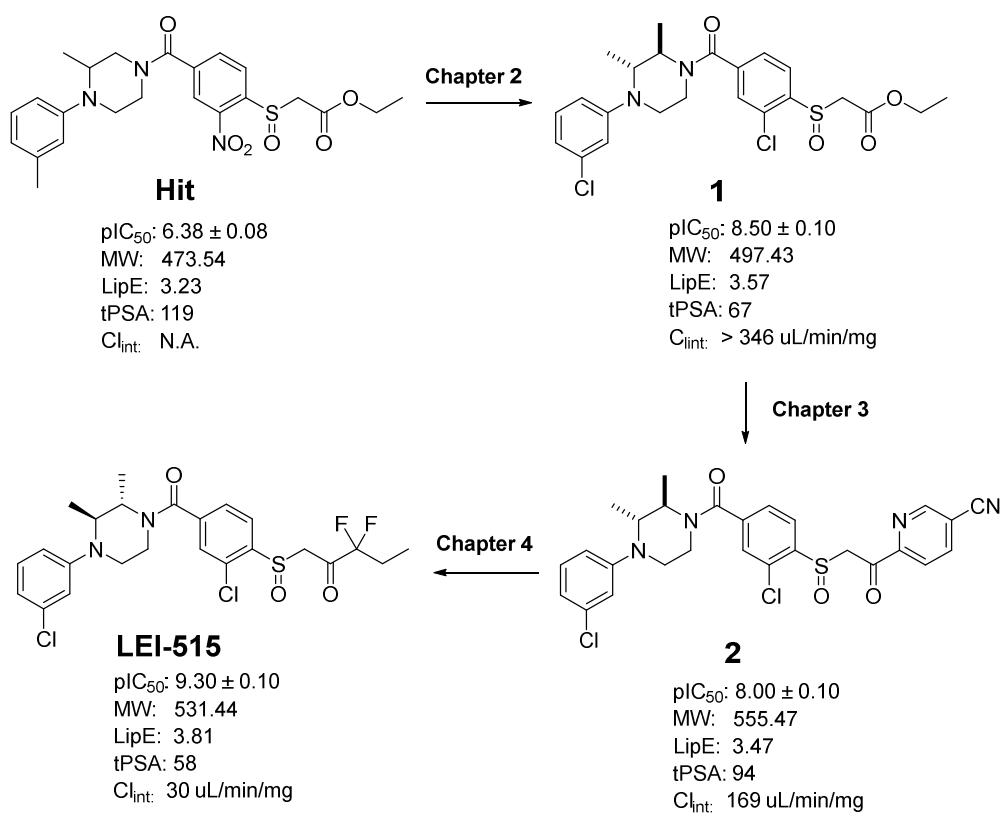


图 1. Hit 化合物和优化后的化合物的活性、化学结构、理化性质和代谢稳定性。

Curriculum Vitae

Ming Jiang was born on July 13th, 1990 in Nanchang, Jiangxi province, China. After finishing high school education in Nanchang, he started his Bachelor of Science in Huazhong University of Science and Technology with a major in pharmacy. In 2011, he obtained his Bachelor of Science and joined in Peking Union Medical College, majoring in medicinal chemistry. He did a Master research project in the group of prof. Peixun Liu, which focused on the discovery of dual iNOS and COX-2 inhibitors.

In 2015, he started as a PhD candidate in the Bio-Organic Synthesis group at Leiden Institute of Chemistry (Leiden University, The Netherlands). After one year, he continued his research in the newly created department of Molecular Physiology. He performed his research under the supervision of prof. dr. Mario van der Stelt, prof. dr. Stan van Boeckel and dr. Richard van den Berg.

Parts of the research were presented on posters at various (inter)national conferences, including CHAINS (Veldhoven, 2017) and International Cannabinoid Research Society's Conference (Leiden, 2018), of which the latter was awarded a poster prize. Oral presentation was held at CHAINS (Online, 2020).